



HAL
open science

Management of *E. coli* sister chromatid cohesion in response to genotoxic stress

Elise Vickridge

► **To cite this version:**

Elise Vickridge. Management of *E. coli* sister chromatid cohesion in response to genotoxic stress. Molecular biology. Université Paris Saclay (COMUE), 2018. English. NNT : 2018SACLS172 . tel-01827812

HAL Id: tel-01827812

<https://theses.hal.science/tel-01827812>

Submitted on 2 Jul 2018

HAL is a multi-disciplinary open access archive for the deposit and dissemination of scientific research documents, whether they are published or not. The documents may come from teaching and research institutions in France or abroad, or from public or private research centers.

L'archive ouverte pluridisciplinaire **HAL**, est destinée au dépôt et à la diffusion de documents scientifiques de niveau recherche, publiés ou non, émanant des établissements d'enseignement et de recherche français ou étrangers, des laboratoires publics ou privés.

Management of sister chromatid cohesion in response to genotoxic stress in *Escherichia coli*

Thèse de doctorat de l'Université Paris-Saclay
préparée au Collège de France

Ecole doctorale n°577 - Structure et Dynamique des Systèmes Vivants
Spécialité Sciences de la Vie et de la Santé

Thèse présentée et soutenue publiquement au Collège de France, le 22 juin 2018

Elise Vickridge

Composition du jury:

Mme Stéphanie Bury-Moné Professeure, Université Paris Sud	Présidente
Mme Mériem El Karoui Professeure, Université de Edimbourg	Rapporteure
Mr Vincent Pagès Directeur de recherche, Centre de recherche en Cancérologie, Marseille	Rapporteur
Mr Stephan Gruber Professeur, Université de Lausanne	Examineur

Title: Management of *E. coli* sister chromatid cohesion in response to genotoxic stress

Key words: *Escherichia coli* – RecN – DNA repair – topology – RecA – mitomycin C

Abstract:

Maintaining genome integrity through replication is an essential process for the cell cycle. However, many factors can compromise this replication and thus genome integrity. Mitomycin C (MMC) is a genotoxic agent that creates a covalent link between the two DNA strands. When the replication fork encounters the DNA crosslink, it breaks and creates a DNA double strand break (DSB). *Escherichia coli* (*E. coli*) is a widely used model for studying complex DNA mechanisms. When facing a DNA double strand break, *E. coli* activates the SOS response pathway. The SOS response comprises over 50 genes that are under the control of a LexA-repressed promoter. Upon a DSB induction, RecA, a central protein of the SOS response will trigger the degradation of LexA and all the SOS genes will be expressed.

We have developed a novel molecular biology tool that reveals contacts between sister chromatids that are cohesive. It has been shown (Lesterlin et al. 2012) that during a regular cell cycle, the two newly replicated sister chromatids stay in close contact for 10 to 20 min before segregating to separate cell halves thanks to the action of Topoisomerase IV. This step is called sister chromatid cohesion (SCC). We have used this molecular biology tool to study sister chromatid cohesion upon a genotoxic stress induced by (MMC). We have shown that sister chromatid cohesion is maintained and prolonged when the cell is facing a DSB. Moreover, this SCC is dependent on RecN, an SOS induced structural maintenance of chromosome-like (SMC-like) protein. In the absence of RecN, the proximity between both sister chromatids is lost and this has a deleterious effect on cell viability. By tagging the chromosome with fluorescent proteins, we have revealed that RecN can also mediate a progressive regression of two previously segregated sister chromatids. This is coordinated with a whole nucleoid compaction. Further studies showed that this genome compaction is orderly and is not the result of a random compaction in response to DNA damage.

Interestingly, inhibiting Topoisomerase IV in a *recN* mutant fully restored viability and sister chromatid cohesion, suggesting that RecN has a structural action on sister chromatid cohesion. Preserving cohesion through topological linking of the chromatids is sufficient to favor repair and cell viability even in the absence of RecN.

An RNA-seq experiment in a WT strain and a *recN* mutant revealed that the whole SOS response is downregulated in a *recN* mutant. This suggests that RecN may have an effect on the induction of the SOS response and thus RecA filament formation. This is in good agreement with the change in RecA-mcherry foci dynamics we observed. In the WT strain, RecA-mcherry forms discrete foci as described in previous work. However, in the *recN* mutant, the RecA-mcherry foci form bundle like structures. Such RecA bundles have been previously described by Lesterlin *et al.* in the particular case of a DSB occurring on a chromatid that has already been segregated from its homolog. This could mean that in the absence of *recN*, the sister chromatids segregate and RecA forms bundle like structures in order to search for the intact homologous sister chromatid.

Altogether, these results reveal that RecN is an essential protein for sister chromatid cohesion upon genotoxic stress. RecN favors sister chromatid cohesion by preventing their segregation. Through a whole nucleoid rearrangement, RecN mediates sister chromatid regression, favoring DNA repair and cell viability.

Titre : Etude de la cohésion des chromatides sœurs en réponse à un stress génotoxique chez *E. coli*

Mots clés : *Escherichia coli* – RecN – Réparation de l'ADN – topologie – RecA – mitomycine C

Résumé :

La réplication fidèle de l'ADN au cours du cycle cellulaire est essentielle au maintien de l'intégrité du génome à travers les générations. Toutefois, de nombreux éléments peuvent perturber et compromettre la réplication et donc cette intégrité. La mitomycine C (MMC) est une molécule génotoxique utilisée en chimiothérapie. Elle forme des liaisons covalentes entre les deux brins d'ADN, ce qui est un obstacle à la bonne réplication de l'ADN. La rencontre de la fourche de réplication avec une liaison covalente entre les deux brins d'ADN aboutit à une cassure double brin. *Escherichia coli* (*E. coli*) est un modèle d'étude très répandu car facile d'utilisation et permettant d'aborder des notions complexes. *E. coli* possède divers mécanismes pour réparer les cassures de l'ADN dont le régulon SOS. Le régulon SOS est un ensemble de gènes sous contrôle d'un promoteur réprimé par la protéine LexA. En réponse à des dommages à l'ADN, LexA est dégradé et les gènes du régulon sont activés.

En utilisant une technique de biologie moléculaire qui permet de quantifier l'interaction entre deux chromatides sœurs restées cohésives derrière la fourche de réplication (Lesterlin et al. 2012) (étape appelée cohésion des chromatides sœurs), nous avons montré qu'en réponse à des cassures double brin générées par la MMC, la cohésion entre les chromatides sœurs nouvellement répliquées est maintenue. Ce phénomène est dépendant de RecN, une protéine induite de façon précoce dans le régulon SOS. RecN est une protéine de type SMC (structural maintenance of chromosomes), un groupe de protéines impliquées dans la dynamique et la structure du chromosome qui est essentielle pour la survie à des stress génotoxiques de type MMC. En parallèle, des techniques de microscopie confocale et de marquage du chromosome par des protéines fluorescentes ont permis de montrer que la protéine RecN est impliquée dans une condensation globale du nucléoïde suite à un traitement par la MMC. Cette condensation du nucléoïde s'accompagne d'un rapprochement des chromatides sœurs préalablement ségrégués. Ces deux phénomènes, médiés par RecN, pourraient permettre une stabilisation globale des nucléoïdes et favoriser l'appariement des chromatides sœurs pour permettre la recombinaison homologue.

De façon intéressante, l'inhibition de Topoisomérases de Type II (Topoisomérase IV et Gyrase) permet de restaurer la perte de cohésion entre chromatides sœurs et la perte de viabilité d'un mutant *recN*. Les Topoisomérases sont des protéines impliquées dans le maintien de l'homéostasie topologique du nucléoïde. La Topoisomérase IV en particulier permet d'éliminer les liens topologiques formés entre les chromatides nouvellement répliqués. Ces liens topologiques non éliminés par les Topoisomérases pourraient permettre de garder les chromatides sœurs cohésives et favoriser la réparation par recombinaison homologue, même en l'absence de RecN.

De plus, une expérience de RNA seq (séquençage de tout le transcriptome de la bactérie) a révélé que dans un mutant *recN*, le régulon SOS est moins induit que dans les cellules sauvages. Ceci va de pair avec une déstructuration des foci de réparation RecA. Il est possible que le rapprochement des chromatides sœurs médié par RecN permette de stabiliser le filament RecA et donc l'induction de la réponse SOS.

L'ensemble de ces résultats suggère que RecN, une protéine du régulon SOS, permet de maintenir la cohésion entre les chromatides sœurs nouvellement répliquées, favorisant la réparation de cassures double brins par recombinaison homologue.

Remerciements

Je tiens tout d'abord à remercier Olivier. Olivier, tu m'as donné une chance quand je sortais d'école, après un stage chez L'Oréal, alors que je ne connaissais pas grand-chose à cette bactérie *E. coli* et la cohésion de ses chromatides. Un peu dur au début pour moi, je ne te cache pas que j'étais un peu dépassée... Mais je me suis vite mise dans le bain et le sujet s'est emparé de moi. Je pensais rester un an ou deux, puis partir dans l'industrie, décrocher un fameux CDI mais voilà que mes plans ont changé quand tu m'as proposé une thèse. J'étais hésitante mais tu as su me pousser et me donner la confiance nécessaire pour me lancer dans ce projet. Tout au long de ma thèse, tu m'as poussée à aller un peu au delà de ce que je me serais permise moi-même. Tu m'as confié l'encadrement de stagiaires, incitée à présenter à des congrès et même dernièrement dans ma recherche de post doc : tu as été le moteur dont j'avais besoin. J'imagine que je n'ai pas toujours été facile à encadrer, mais j'ai beaucoup aimé travailler avec toi, j'ai appris tellement de choses, tant d'un point de vue personnel que scientifique. Tu as toujours été disponible et enthousiaste pour discuter scientifiquement et je te remercie encore une fois pour ces 4 années passées à travailler ensemble. Je garde un excellent souvenir de mes années de thèse et je te souhaite le meilleur pour la suite.

Je tiens ensuite à remercier Vincent Pagès et Meriem El Karoui, mes deux rapporteurs, ainsi que Stephan Gruber et Stéphanie Bury-Mone, mes deux examinateurs, d'avoir accepté de participer à mon jury de thèse. C'est un réel honneur pour moi d'avoir des scientifiques de votre excellence à ma thèse et je vous remercie pour le temps que vous m'avez accordé.

Je remercie toute mon équipe (qui a évolué au cours des années !). Mes petits stagiaires, Thomas et Anna, qui m'ont donné le goût de l'encadrement et l'impression d'être chef d'une mini « Equipe Vickridge » en première année de thèse. Thomas, on se verra à Montréal ! Adrien, je sais que je n'ai pas été très présente durant ton stage mais c'est un plaisir de travailler avec toi et j'espère t'avoir transmis la fièvre RecN.

Charlie, I'm so glad you made it to the Espeli team. It was a real pleasure to have you around the lab. Your scientific and technical advice was of great value and a gossip chat was always welcome! You're far away now (I mean, come on, who works in the 15th arrondissement??) but we still get to see each other a lot, that better not change!

Brenna, comme Charlie, ton passage au cdf a été écourté mais les liens formés restent. Ce n'est pas pareil de ne pas avoir une acolyte de musique à coté de moi à qui faire découvrir des nouveaux sons... Je suis sûre qu'à Pasteur les goûts musicaux sont ...différents !

Gaëlle, on aura passé presque la même durée dans ce labo. On a vu le labo évoluer et prendre forme ensemble, mais tu es partie pour d'autres aventures. Je te remercie pour l'aide que tu as pu m'apporter durant mes années de thèse et je te souhaite plein de réussite pour ce nouveau projet !

Sylvie, je te remercie pour les discussions scientifiques et l'aide technique que tu as pu m'apporter dans mes manip. Merci pour ta générosité, tu es un peu la petite maman des filles Espeli.

Nicole, tu es arrivée récemment dans cette équipe et c'est avec plaisir que j'ai eu l'occasion d'apprendre à te connaître durant ces derniers mois. Bonne continuation dans ta nouvelle équipe 😊

Hafez, on a commencé tous les deux, les petits poussins. Tu m'as prise sous ton aile dès le premier jour et tu m'as beaucoup appris. Tu es une des personnes m'ayant réellement donné le courage de me lancer dans la thèse. Ta gentillesse et ta dévotion envers tes amis et envers moi en particulier ont permis de créer un environnement familial dans l'équipe. Quand j'étais au labo, j'étais à la maison. Je ne peux pas citer tous les délires, les rires et bons moments passés ensemble, il y en a beaucoup trop ! Te voir devenir papa a été incroyablement excitant et venir bosser le samedi semblait moins pénible quand je savais que je pourrais faire une demi-heure de Noé baby-sitting ! Encore merci d'avoir été là durant ces années et d'être encore présent aujourd'hui. We miss you here in the lab.

Victoria, les mots me manquent pour décrire notre relation. Tu es arrivée au labo dans des conditions peu évidentes et il a fallu quelques mois pour faire tomber la barrière mais une fois qu'elle fut tombée... aie aie aie ! J'ai découvert une vraie camarade de fête et de rires qui est très vite (ou très très vite... ? ^^) passée de collègue à amie. Tu as contribué à ma thèse en me soutenant, m'écoutant râler, m'accompagnant boire des bières, organisant des grosses teufs et tant d'autres. Une copine de bêtises et de potins qui rend les journées au labo excitantes. Tes avis vestimentaires tranchés, nos discussions bien (trop ?) poussées sur à peu près tous

les sujets (vraiment tous !) resteront gravés dans ma mémoire. On a embarqué Mémé et Charlène dans le sport, et ça, c'est fort. Ces moments de « pump » sont plus un plaisir qu'une souffrance grâce à vous. Tu es courageuse et déterminée, une amie fidèle, un vrai exemple à suivre. Tiens bon, la thèse c'est bientôt fini ! J'espère bien qu'on se retrouvera de l'autre côté de l'océan ☺

Charlène, je me rappelle avoir dit à Olivier « C'est elle que je veux qu'on recrute comme ingénieur » et je ne regrette tellement pas mon choix. Tu es venue me donner un coup de pouce incroyable sur mon sujet de thèse, pile au moment où j'en avais besoin. Tu es d'une rigueur scientifique et technique exceptionnelles et je n'en serais pas là aujourd'hui sans toi. Mais ce n'est pas que ça que je retiendrai de toi. Tu es quelqu'un qui a le cœur sur la main, en qui j'ai une confiance sans faille. Comme Victoria, tu es devenue une vraie amie, toujours à l'écoute, très empathique, qui sait reconforter dans les moments difficiles. Mais tu es aussi une petite fêtarde, toujours prête à aller boire un coup quand le moral est bas ou pour fêter quelque chose ! Ta présence dans l'équipe nous manque déjà.

Mélanie, j'ai dû te traquer pour que tu viennes aux soirées mais ça a fini par marcher ! Tu n'étais pas dans l'équipe Espeli, m'enfin... presque ! Ton dynamisme, tes sourires, tes éclats de rires et tes pauses répétées dans notre bureau m'ont certes parfois éloigné du « droit chemin du boulot » mais m'ont donné plein d'énergie et permis de toujours garder la pêche ! J'oublie systématiquement que tu es le petit bébé de la famille tant tes conseils et ta présence semblent être une évidence parmi nous, les « vieux ». Garde la pêche, et transmet toute cette belle énergie aux pasteuris, ils ont de la chance de t'avoir.

« Les fils », le reste de la famille quoi... Sarah, Omar, Yoyo, Reda... votre présence dans l'institut crée une réelle convivialité et donne le sentiment d'appartenance à une grande famille. Les pauses sur la terrasse, les soirées chadocs, adeli... « eh vous venez vendredi hein ??? », les dejeuners, les cocktails sur la terrasse interdite, constituent des moments inoubliables de mes années au CIRB. Plus que des collègues, vous êtes des amis et j'espère sincèrement que ça ne changera pas. Merci d'avoir été là au cours de ma thèse, vous avez fait une vraie différence et vous allez me manquer.

Tous les autres copains, Athanasia, Isma, Sonia, Camille, les potes de l'équipe Venance (Alex, Seb, Willy, Mérie, Elodie...) (et ceux qui sont partis... Pierre, Anouar, Virginie, Claudia, César)

c'est toujours un plaisir de passer du temps ensemble, que ce soit pour boire un coup, se plaindre d'une manip', ou juste papoter dans les couloirs.

Je remercie également l'équipe de la gestion et tout particulièrement Nicole et Sophie qui ont toujours été d'une grande aide. Vous êtes d'une efficacité redoutable et c'est toujours un réel plaisir de passer papoter ☺ Merci de nous avoir donné l'opportunité d'organiser la retraite des doctorants et post doctorants, c'était une expérience incroyable !

Fred, Hamid, Jean-Pierre, merci pour tout. Vous avez toujours été dévoués pour nous aider à travailler dans les meilleures conditions. Votre travail nous est précieux.

Philippe, Jeremy, Jennifer, Julien, mille mercis pour toutes les heures passées à me débloquer pour des problèmes au microscope. C'est très confortant de savoir qu'on n'est pas seule face à ces machines terrifiantes !

Je remercie ensuite mes amis, tous autant que vous êtes. Je ne peux pas citer tout le monde, Charlie, Marie, Fred, Remi, Maureen, Patou, Gaétan, Adeline, Marion, Denis, Eric, Benoit, Zynger, Flore, Thibault, Bastien, Elo, Aurélie, Quentin, Mélo, Juliette, Maxou, Julie, Mathilde... et tellement d'autres ! Merci de m'avoir encouragée dans cette aventure de thésarde, d'avoir essayé de me comprendre et d'avoir été présents dans les moments plus difficiles. Vous m'avez fait bien rire au fil de ces années, à essayer de comprendre mon sujet de thèse, ou du moins s'y intéresser un peu : « Ça se passe comment les chromos en ce moment ? », « ça va les bactos ? », « Bon, et la chromatidination de l'ADN, ça avance... ? Eu attend, c'est quoi ton sujet de thèse déjà ? », « mais elles sont cohésives ces chromatides alors ? » « RecN ?? ça fait nom de super héros, je kiffe », « J'ai appris le mot ATP par cœur pour faire intelligent : Adenosine tri phosphate ! C'est bien ça hein ? », « Bon, et tes sœurs, elles sont stressées là ? ». Certains d'entre vous ont même essayé de lire mon article : « Bon, j'ai lu l'abstract, je me suis arrêté à la 10^{ième} ligne, c'est trop dur », « ton résumé de thèse il est hardcore, je comprends rien », « Moi je l'ai lu en entier et franchement j'ai compris pas mal de trucs, c'est pas mal ». Des moments de soutien et d'encouragement à bosser « Bon, t'as intérêt à bosser demain, moi je dis à tout le monde que je connais quelqu'un qui travaille sur les chromatides alors t'as pas intérêt de te louper », « Elise, bosse, t'organiseras ce weekend quand t'auras rendu ta thèse », « Si je rendais ma thèse dans une semaine je serais pas là moi, t'es une ouf, rentres bosser franchement », « non Elise, on s'en fout pas de la thèse, il te reste 48h à tenir alors tu

vas faire un petit effort, tu vas pas voir Acid Arab et tu rentres maintenant » et beaucoup de moments de perversion pour m'écarter du droit chemin : « Allez, tu peux pas thèse, viens boire un coup », « Lâche tes mutants deux minutes, viens ! », « Tu veux rentrer pour bosser ? Mais allez, Elise, franchement, c'est quoi une thèse, comparé à de la CHOPE ? », « Tu vas pas aller au labo maintenant quand même ?? T'es clairement en gueule de bois... », « Wow, y'a Acid Arab qui passe aux Nuits Fauves, faut absolument qu'on y aille, tu feras ta thèse plus tard ». Toutes ces phrases d'encouragement et de perversion, et l'intérêt que vous avez porté à ma thèse m'ont finalement bien menée au bon endroit. Je soutiens ma thèse dans deux mois et j'espère bien que vous serez tous là, je n'y serais clairement jamais arrivé sans vous.

Benjamin, je te remercie particulièrement de m'avoir soutenue dans mon projet de thèse, d'avoir cru en moi durant tant d'années. Je ne pense pas que j'aurais commencé une thèse si tu n'avais pas été là pour m'encourager.

Je remercie mes parents, papa, tu m'as poussée, peut-être un peu brutalement, à faire une thèse mais tu as eu raison. Tu as su voir des choses que je ne voyais pas et parfois tout ce dont on a besoin est un petit coup de pouce pour se lancer. Tu m'as donné cet élan et aujourd'hui, je suis fière de devenir Docteur, comme toi ! Maman, tu as été un réel atout et ça a été un immense bonheur de t'avoir à mes côtés durant ces années. Tu m'as soutenue inconditionnellement, mis des coups de pression quand il le fallait, m'apportant parfois un peu plus de stress que nécessaire, mais toujours dans mon intérêt. J'ai eu la chance de pouvoir te voir régulièrement, au Collège de France ou à la cantine du ministère... ! Tous mes collègues te connaissent et ça me fait plaisir. Nos déjeuners improvisés, ces petits moments de partage privilégiés, vont terriblement me manquer quand je serai partie. Caroline, sista, cette dernière année a été, malgré quelques difficultés, une grande joie pour moi. Ces moments qu'on a passé ensemble nous ont incroyablement rapprochés et je les chérie beaucoup. J'adore quand tu viens squatter chez moi, faire la teuf avec toi et j'espère bien te retrouver quelque part en Colombie. Tu es quelqu'un d'exceptionnel, d'une force et d'une maturité incroyable. Tu es un roc pour moi. Tu m'as fait beaucoup de bien et j'espère pouvoir te le rendre aussi lorsque tu en auras besoin.

Pour finir, Julien... Notre histoire est complexe, ou peut-être pas après tout. Elle est évidente, elle est belle. Tu m'as suivie durant toute ma thèse et plus intensément cette dernière année.

Ta présence m'est indispensable aujourd'hui pour avancer, croire en moi et à la suite. T'avoir à mes côtés est précieux. Tes mots de réconfort, ton soutien inconditionnel, mais aussi les rires, la fête et les moments de tendresse me portent jusqu'à la ligne d'arrivée. Je te remercie pour tout et j'ai hâte de poursuivre l'aventure avec toi de l'autre côté de l'Atlantique.

Abbreviations

BER: Base Excision Repair

cSDR: Constitutive Stable DNA Replication

DPC: DNA-Protein Crosslink

DSB: Double Strand Break

Exo III: Exonuclease III

HJ: Holliday Junction

HR: Homologous Recombination

ICL: Inter-strand Crosslink

TLS: Translesion Synthesis

MMC: Mitomycin C

MMR: Mismatch Repair

NER: Nucleotide Excision Repair

Pol I: Polymerase I

Pol III: Polymerase III

RFR: Replication Fork Reversal

ROS: Reactive Oxygen Species

SCC: Sister Chromatid Cohesion

SCI: Sister Chromatid Interactions

SMC: Structural Maintenance of Proteins

SSB: Single Strand Binding Protein

ssDNA: Single Strand DNA

ssGap: Single Strand Gap

TC-NER: Transcription coupled Nucleotide excision Repair

Topo I: Topoisomerase I

Topo III: Topoisomerase III

Topo IV: Topoisomerase IV

Table of contents

I. Introduction.....	1
A. Replication.....	2
1. Replication initiation	2
2. Replication elongation.....	3
3. Replication termination.....	5
4. Origin independent replication	7
5. Avoiding over initiation: the role of SeqA	8
6. Dealing with topology during replication.....	9
a) Type I topoisomerases.....	9
i. Topoisomerase I	9
ii. Topoisomerase III	10
b) Type II topoisomerases.....	12
i. Gyrase.....	12
ii. Topoisomerase IV.....	12
B. Sister chromatid cohesion and segregation.....	13
1. Sister chromatid cohesion in Eukaryotes	13
a) Eukaryotic SMC proteins	13
b) SMC1/3, the Eukaryotic Cohesin	14
2. Sister chromatid cohesion in <i>Escherichia coli</i>	16
a) Existence of a sister chromatid colocalization before segregation.....	16
b) Role of Topoisomerase IV in sister chromatid colocalization and sister chromatid cohesion	17
c) The Snaps regions.....	19
d) Precatenane formation and removal by Topoisomerase IV.....	20
e) Other proteins involved in Sister Chromatid Cohesion during replication	21
f) Final segregation of sister chromatids: Topo IV and XerCD-dif.....	23
C. DNA damage and the DNA damage response pathways in <i>Escherichia coli</i>	25
1. Avoiding replication errors during a regular cell cycle: Mismatch repair (MMR).....	25
2. DNA damage lesions.....	27
a) Modified bases	27
i. Spontaneous base deamination.....	27
ii. Abasic sites	27

b)	DNA adducts	29
c)	DNA protein crosslinks	30
d)	Oxidative DNA damage.....	31
e)	Inter-strand and intra-strand crosslinks.....	32
3.	Management of DNA lesions.....	33
a)	Base excision repair (BER)	33
b)	Nucleotide excision repair (NER).....	35
c)	Transcription-coupled Nucleotide excision repair	38
4.	Formation of DNA breaks by unrepaired lesions: single strand Gaps (SSG), Single strand Breaks (SSBs) and double strand breaks (DSBs).....	39
a)	Single Strand Gaps.....	39
i.	Replication lesion bypass	39
ii.	Chain terminators: The example of AZT	40
iii.	Nucleotide depletion: the example of Hydroxyurea (HU).....	42
b)	Single strand Breaks	42
c)	Double strand Breaks	42
i.	Arrested replication forks lead to double strand breaks	43
ii.	Double strand breaks induced by Replication Fork Reversal	43
iii.	Overview of MMC-induced double strand breaks	47
5.	Repair of single strand gaps, single strand breaks and double strand breaks	48
a)	General overview of the the SOS response.....	48
b)	LexA, the SOS repressor	49
c)	RecA, the central protein of the SOS response	50
i.	RecA's general function.....	50
ii.	RecA loading	51
iii.	Formation of RecA nucleofilament	55
iv.	RecA mediated induction of the SOS response.....	58
v.	Homology search and strand invasion	59
vi.	Branch migration and resolution.....	62
vii.	Induction of translesion polymerases and translesion synthesis.....	64
viii.	Mutants of RecA activity	65
d)	Characteristics of various SOS response proteins	66
i.	Proteins of unknown function.....	66
ii.	Other SOS induced proteins	67

iii.	RecN protein.....	67
D.	Sister chromatid cohesion and DNA repair	72
1.	Eukaryotic Cohesins are essential for survival to DNA damage	72
2.	Sister chromatid cohesion and DNA repair in <i>E. coli</i>	73
E.	Thesis Objectives	74
II.	Results	76
A.	Published results	76
B.	Complementary results	96
1.	Implication and role of Topoisomerases in sister chromatid cohesion in response to genotoxic stress.....	96
a)	Inhibition of Gyrase compensates the loss of viability and sister chromatid interactions of a <i>recN</i> mutant.....	96
b)	Topoisomerase III acts at ssGaps created by AZT but not HU.....	100
2.	RecN influences nucleoid dynamics	103
3.	The mobility of fluorescent foci is increased in a <i>recN</i> mutant.....	105
4.	FRAP microscopy reveals RecN's influence on the diffusion of a DNA binding protein	107
5.	The hunt for RecN's partner(s): Identifying other proteins involved in SCC.....	110
a)	RecN co-immunoprecipitation reveals possible proteins interacting with RecN.....	110
b)	The SOS response is downregulated in a <i>recN</i> mutant	115
c)	Characterization of genes involved in a back-up pathway for RecN.....	118
d)	iPOND reveals protein profile at undamaged and damaged forks	123
III.	Discussion.....	126
A.	Sister chromatid cohesion and homology search	126
1.	Importance of RecN for homology search	127
2.	RecN's influence on RecA filament formation	128
B.	RecN's influence on chromosome dynamics.....	129
1.	RecN induces a whole nucleoid compaction.....	129
2.	Could the MMC-induced genome compaction favour protein diffusion?	132
3.	RecN's influence on damaged DNA mobility.....	134
C.	Interplay between RecN and the Nucleotide Excision Repair pathway.....	135
D.	Impact of the supercoiling density on DNA repair	137
E.	Is transcription repressed by cohesion?.....	140
1.	What mechanisms are responsible for transcription repression?	140
2.	Why is there a transcription repression?	142

F.	Concluding remarks.....	143
IV.	Material & Methods.....	144
A.	Strains.....	144
B.	Ori/ter quantification by qPCR assay on <i>dnaA</i> ts strains	148
C.	Cell viability assay.....	148
D.	Construction of microscopy strains.....	148
E.	FRAP (Fluorescence Recovery After Photobleaching).....	148
F.	Foci dynamics	149
G.	RNAseq	149
H.	RecN Co-immunoprecipitation.....	150
I.	iPond.....	151
J.	Gene overexpression bank.....	152
K.	Construction of <i>recA-mcherry</i> fusion	152
L.	Construction of LoxP strains.....	153
M.	LoxP recombination assays	153
N.	Published article in Methods in Molecular Biology: The Bacterial Nucleoid	154
V.	Résumé de thèse en français.....	163
VI.	Bibliography.....	168
VII.	Annex.....	189

Table of figures

Figure 1. Schematic representation of <i>E. coli</i> replisome	4
Figure 2. Schematic of chromosomal positioning of <i>ter</i> sites on the <i>E. coli</i> chromosome	6
Figure 3. Formation of precatenanes and catenanes.....	11
Figure 4. Schematic representation of a Eukaryotic SMC protein	15
Figure 5. Schematic description of the <i>loxP</i> recombination assay principle.....	18
Figure 6. Representation of sister chromatid cohesion mediated by precatenanes in <i>E. coli</i>	21
Figure 7. Schematic model for SeqA binding	23
Figure 8. Mismatch repair pathway in <i>E. coli</i>	26
Figure 9. Modified bases	28
Figure 10. DNA adduct formation	29
Figure 11. Schematic representation of a frozen Topoisomerase Type II	31
Figure 12. Base Excision Repair (BER) pathway.....	34
Figure 13. Nucleotide excision repair (NER) pathway.....	36
Figure 14. Two models for replication lesion bypass	40
Figure 15. Formation of single strand Gaps by AZT incorporation.....	41
Figure 16. Replication fork encounter with a DNA lesion may lead to replication fork reversal.....	44
Figure 17. Formation of a double strand break upon replication fork reversal.....	46
Figure 18. MMC-induced double strand breaks.....	47
Figure 19. Simple representation of the induction of the SOS response in <i>E. coli</i>	49
Figure 20. Structure of RecA presynaptic nucleofilament	51
Figure 21. RecA loading through the RecFOR pathway.....	53
Figure 22. RecA loading through the RecBCD pathway	55
Figure 23. Regulation of RecA nucleoprotein filament formation	58
Figure 24. Model for homology search by short 1D sliding and 3D hoping.....	60
Figure 25. Mechanism for homology recognition by RecA	61
Figure 26. Homologous Recombination reaction in <i>E. coli</i>	63
Figure 27. Translesion Synthesis (TLS) pathway.....	65
Figure 28. Architecture of Full-length RecN.....	70
Figure 29. Inhibition of Gyrase activity compensates the loss of SCIs and viability of a <i>recN</i> mutant .	99
Figure 30. Topo III acts at ssGaps induced by AZT but not by HU	102
Figure 31. Influence of <i>sulA</i> deletion on nucleoid compaction and cell filamentation	104
Figure 32. Effect of MMC on MSD slopes of fluorescent foci in a WT strain and <i>recN</i> mutant.....	106

Figure 33. RecN influences the diffusion dynamics of HU protein.....	109
Figure 34. Co-immunoprecipitation with RecN reveals possible partners or interacting proteins	113
Figure 35. Expression of SOS response genes is downregulated in a recN mutant	117
Figure 36. Genetic screen reveals possible RecN partners	121
Figure 37. Immunoprecipitation of EdU crosslinked proteins	125
Figure 38. Model for RecN action on sister chromatid cohesion and nucleoid merging.....	126
Figure 39. Model for RecA bundle formation in the absence of RecN	128
Figure 40. Model for DSB recognition in D.radiodurans	130
Figure 41. Model for RecN binding at sites of NER induced double strand breaks	131
Figure 42. An ordered chromosomal structure may facilitate homology search	134
Figure 43. Putative viability and SCC pathway for recN and uvrA mutants	137
Figure 44. Excessive catenation may impede branch migration.....	139
Figure 45. Model for transcription repression behind the replication fork.....	141

I. Introduction

In every cell, DNA carries the genetic information making all life forms possible. Maintaining genome integrity is therefore essential to ensure faithful transmission of the genetic information to the next generation. Replication allows the duplication of one DNA molecule into two identical DNA molecules before cell division. However, DNA is constantly threatened by intracellular and extracellular factors that are a menace to the faithful replication of the genome. Indeed, when DNA is compromised during replication, various DNA lesions may occur. Single strand gaps and double strand breaks are highly deleterious. If they remain unrepaired, they can lead to a loss of genetic information, which in turn, can provoke cell death or trigger genetic mutations, often involved in cancer. To limit these threats, every cell has developed a large repertoire of proteins dedicated to the removal of DNA lesions and the repair of broken DNA. These proteins work coordinately in specific pathways for each type of lesion.

Cancers are frequently caused or facilitated by mutations in genes involved in DNA repair pathways (P53, BCRA-2, FANC-A ...) (Chae et al., 2016). Some chemotherapy and radiotherapy treatments aim at weakening cancer cells by inducing DNA damage. However, different repair pathways help ensure highly efficient repair of DNA damage and efficient replication often at the cost of genome integrity. Although essential for genome maintenance, DNA damage repair pathways render chemotherapy less efficient. By studying and understanding the DNA repair mechanisms that are triggered by chemotherapeutic drugs, researchers hope to optimize chemotherapy treatment and decrease the strong side effects linked to the lack of specificity of action of the drugs.

In this bibliographic introduction, I will start by describing the fundamentals of genome duplication in the model organism, the *Escherichia coli* bacterium. I will focus on DNA replication, segregation and particularly on sister chromatid cohesion: What is sister chromatid cohesion? How is sister chromatid cohesion formed? What purpose may it have? I will then extensively guide you through the different forms of DNA damage and DNA damage response (DDR) pathways. Finally, I will address the potential importance of sister chromatid

cohesion for DNA repair, and give you a state of the art of the knowledge on the promising role that the SOS-induced RecN protein may have in this step.

A. Replication

Escherichia coli (*E. coli*) is a single cell micro-organism. It has a unique circular chromosome. The genome of K12 MG1655 *E. coli* is 4.6 Mbp long, but some pathogenic strains have a genome going up to 5 Mbp long. Once stretched out, it is equivalent to 1.6 mm, approximately 1000 times longer than the size of an average *E. coli* cell. The duplication time of an *E. coli* cell can be very short, ~30 min in a rich medium and at an optimal temperature (O'Donnell et al., 2013). It is therefore crucial that *E. coli* replicates its chromosome with a high efficiency and at a maximum speed (~1kb/sec). However, as mentioned previously, replication is a key step to guarding the genome's integrity, and although replication must occur with a high processivity, it must also remain highly accurate. This accuracy of replication is partly due to mechanisms that immediately remove mis-incorporated nucleotides (this is called proofreading). Cells also present mechanisms that detect and eliminate lesions that are present on the DNA. Moreover, cells use mechanisms that repair DNA after a breakage of continuity. Among them, homologous recombination (HR) uses the intact sister chromatid to copy the information and repair.

The whole process of DNA replication is divided into three phases: Initiation, elongation and termination.

1. Replication initiation

In *E. coli*, *oriC* is the unique site of replication initiation. DnaA, the initiator protein at *oriC*, binds to a nine base pair sequence called a DnaA box. Five different DnaA boxes are in the *oriC* region, and DnaA has a different affinity for each box. DnaA oligomerizes by binding to these DnaA boxes, and induces a local unwinding of the adjacent AT-rich region of the double helix, by using ATP-hydrolysis. DnaA then recruits DnaB, a processive DNA helicase, which is loaded

onto the single stranded DNA by DnaC, the helicase loader (Jameson and Wilkinson, 2017; Kaguni, 2011).

Once DnaB is loaded on the single stranded DNA, DnaC must dissociate so that DnaB can unwind the duplex DNA. DnaB helicase also recruits DnaG, the DNA primase. The interaction of these two proteins leads to primer formation. DnaG synthesizes a ~12 RNA nucleotide, which will serve as a primer for Polymerase III (Pol III). The interaction of DnaB and DnaG induces a conformational change, leading to the dissociation of DnaC from DnaB and marking the switch from initiation to elongation (Makowska-Grzyska and Kaguni, 2010).

2. Replication elongation

Once DNA polymerases and helicases are loaded, the helicase can move bidirectionally towards the left and the right arms of the chromosome. The replication machinery is generally referred to as the “replisome”. It consists of four DNA polymerase complexes, the DNA helicase, the DNA primase, a clamp loader and the DNA Polymerase I. DnaB helicase is at the head of the replication fork, and moves on the lagging strand in the 5' to 3' direction, thus unwinding and separating the two DNA strands in an ATP-dependent manner (Jameson and Wilkinson, 2017). DnaB having separated the two DNA strands, Single Strand Binding Protein (SSB), coats and polymerizes on the single strand DNA (ssDNA), protecting them from the action of nucleases.

Replication of the leading strand is continuous. Pol III moves continuously in the 3' to 5' direction, extending the RNA primer synthesized by DnaG. Pol III is composed of three subunits, α , ϵ and θ . Pol III moves forward, interacting with DnaN, also known as the β -clamp. DnaN sits behind Pol III and enhances its processivity (Jameson and Wilkinson, 2017). DNA polymerases only synthesize DNA in the 5' to 3' direction. Therefore, on the lagging strand, DnaG forms a complex with DnaB, and synthesizes an RNA primer once DnaB has exposed enough ssDNA. This new RNA primer, called an Okazaki fragment, is around 1200 nucleotides long and serves as a starting point for synthesis by Pol III (Balakrishnan and Bambara, 2013). Pol III polymerizes a new segment of DNA until it reaches the adjacent Okazaki fragment. At that point, DNA Polymerase I (Pol I) replaces Pol III. Pol I removes the RNA primer thanks to

its 5' to 3' exonuclease activity and fills in the gap by synthesizing DNA. DNA ligase will then ligate the two adjacent DNA fragments (figure 1).

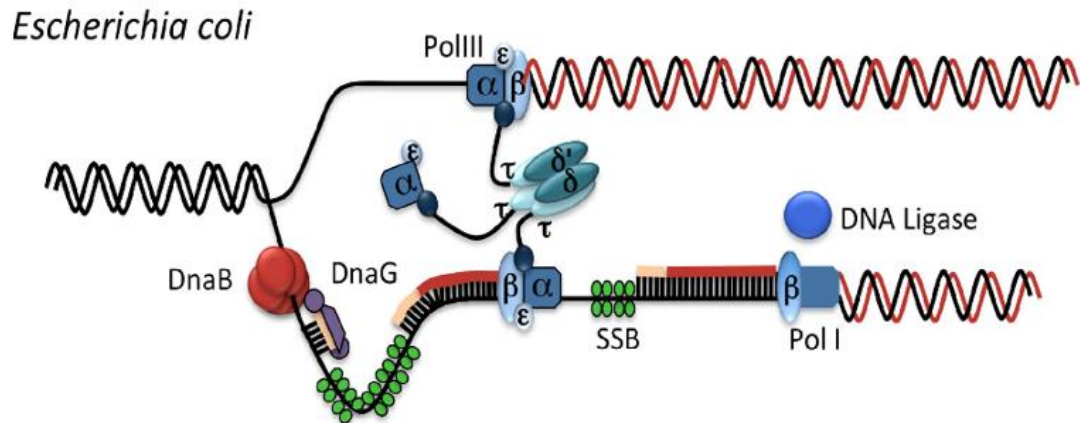


Figure 1. Schematic representation of *E. coli* replisome

Replication is carried out by DnaB helicase, DnaG primase, DNA Pol III, the β -clamp, the clamp loader and lagging strand Pol I and DNA ligase.

Figure from Jameson & Wilkinson, 2017

It was recently shown that an active *E. coli* replisome is formed of three Pol III polymerases, but only two are active at a given time. Two of these polymerases may be dedicated to lagging strand synthesis, and the third one is the processive leading strand polymerase (Reyes-Lamothe et al., 2010). It seems quite obvious that processing of the leading strand and lagging strand must occur in a coordinated manner to avoid gaps in DNA replication on the lagging strand (which could lead to breaks), and insure that replication is completed simultaneously on both strands. Interestingly though, very recent work has shown that the DNA polymerases of the lagging strand and the leading strand have discontinuous rates, and exhibit random pauses. The helicase somehow senses these pauses and can reduce its speed by 80%, allowing for a recoupling of the helicase and the polymerase. This suggests that replication can process without such a tight coordination of the lagging strand and leading strand (Graham et al., 2017).

- DNA polymerase proofreading

Considering the high processivity with which the replisome synthesizes new DNA, the error rate in *E. coli* is very low 10^{-10} (Drake et al., 1998). This high rate of fidelity is partly due to the polymerase's proofreading activity, which enhances fidelity by around 200 fold (Fersht and Knill-Jones, 1983). Brutlag & Kornberg showed in 1972, that DNA polymerase exhibits 3' to 5' exonuclease activity that serves as a proofreading of correct DNA replication. Incorporation of a mispaired nucleotide will inhibit incorporation of a new nucleotide and the mispaired nucleotide will be removed before replication can move on (Brutlag and Kornberg, 1972; Loeb and Kunkel, 1982).

The DNA polymerase holoenzyme has seven subunits. The α subunit encoded by *dnaE*, the ϵ subunit encoded by *dnaQ*, and the θ subunit form the Polymerase III core (McHenry and Crow, 1979). The α subunit harbours the polymerase activity and the ϵ subunit contains the proofreading activity (Maki et al., 1985; Scheuermann et al., 1983).

3. Replication termination

Moving bidirectionally, the replisomes of both the left arm and the right arm simultaneously reach the terminus region, opposite to *oriC*, called *Ter*. Bird *et al.* first described the concept of a replication terminus in 1972 (Bird et al., 1972). It has been shown that this terminus region of *E. coli* is composed of several *ter* sites (23 pb sequences, named *terA* to *terJ*) bound by a Tus protein, that arrest replication from one direction only, creating a trap for both replisomes in the Ter region (Neylon et al., 2005) (figure 2).

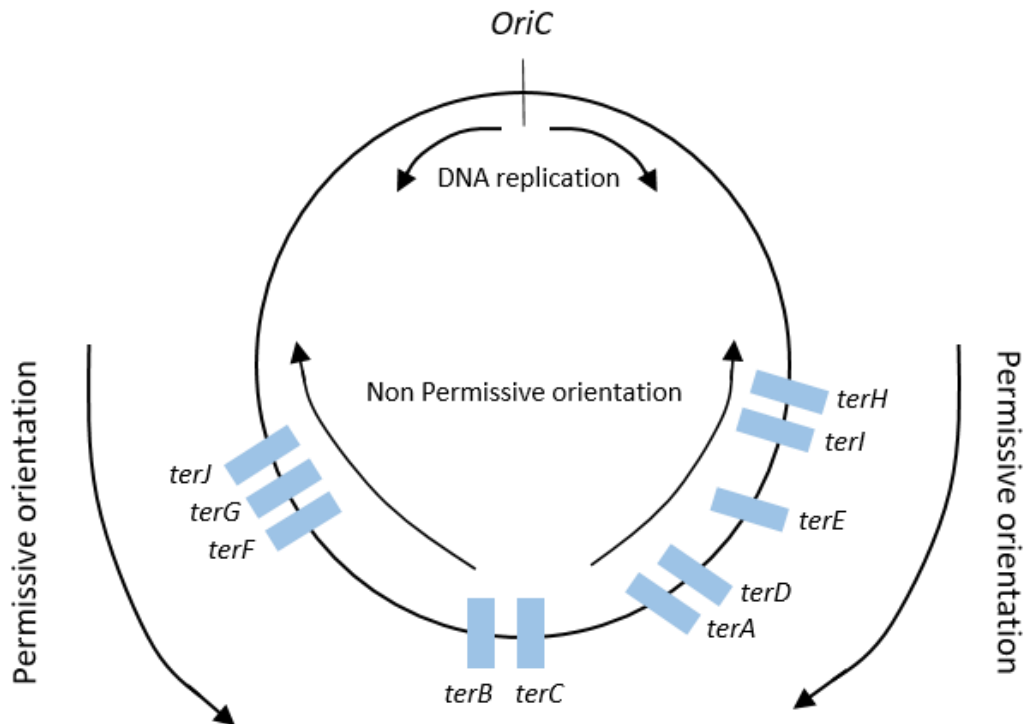


Figure 2. Schematic of chromosomal positioning of *ter* sites on the *E. coli* chromosome

terC to *terH* allow replication from the right replichore to proceed. Replication from the left replichore is arrested because it is coming from the wrong direction. *terB* to *terJ* allow replication from the left replichore to proceed but replication coming from the opposite direction is arrested.

For a long time, it has been unclear how a Tus-*ter* complex can block a replisome coming from one direction but not the other. The replisome can replicate past the first 5 Tus-*ter* complexes it encounters when it is coming from the correct direction, but will be blocked at the following 5 Tus-*ter* complexes because it will be considered coming from the wrong direction (Hill, 1992). Several studies have given new insight into this matter and three distinct models are currently discussed. One model suggests that the helicase DnaB physically interacts with one side of the Tus-*ter* complex, rendering its processing permissive when it encounters it from one side and non-permissive when it encounters it from the other side (Hill et al., 1987). The second model suggests that a difference in binding between the Tus protein and the two ends of the *ter* sequence. Binding of Tus with the different ends of the *ter* sequence induces a different blocking efficiency, letting the helicase move forward in one case but not the other

(Kamada et al., 1996). Finally, the third model, called the mouse trap model suggests that when DnaB encounters the Tus-*ter* complex from one side, it induces some sort of conformational change, that reorients the specific C(6) base into a cytosine binding pocket in the Tus protein, ultimately causing an arrest of the helicase (Berghuis et al., 2018; Pandey et al., 2015). Today, although the two first models are not excluded, an extended, multistep and more complex mouse trap model seems to be favored (Berghuis et al., 2018). Once the replisomes are arrested in the Ter region, final segregation of the two new sister chromatids in the Ter domain can occur. This is a complex step of DNA replication, which I will discuss in another section.

4. Origin independent replication

Unlike Eukaryotic cells that fire replication at many origins all over the chromosome, replication is initiated at a single position called *oriC* in *E. coli*. Therefore, if a replication fork of one of the replisomes is blocked during replication, before reaching the terminus region, the remaining portion of that replicore will not be replicated while the opposite fork is still ongoing. This can create a delay in cell cycle completion, segregation defects or even worse, cell death. To circumvent these deleterious events, several mechanisms promoting replication fork rescue and replication restart exist.

It has been well characterized that in particular conditions replication can initiate at chromosomal sites that are far from *oriC*. This replication has been called constitutive stable DNA replication (cSDR). In cells replicating by cSDR, DNA-RNA hybrids (called R-loops) serve as primers for replication initiation. *rnase HI* or *recG* mutants, that are involved in eliminating R-loops, exhibit DNA synthesis even in the absence of *oriC* and DnaA (Kogoma, 1997). It has been suggested that the mechanism by which cSDR carries out replication in the *rnaseHI* mutant and the *recG* mutant differs (Rudolph et al., 2013). Indeed, it is proposed that cSDR arising in *recG* mutants is the consequence of unresolved fork collisions in the Ter region. In *recG* mutants, replication initiated at the terminus can be suppressed by mutating *priA* or deleting the *priB* gene. These proteins are involved in DnaB loading at stalled replication forks, suggesting that a substrate for PriA loading and replisome assembly is formed. It was suggested that replication fork collisions may trigger the formation of 3' ssDNA flaps, providing

a substrate for PriA-dependent replication fork assembly (Rudolph et al., 2009) (the rescue of stalled replication forks will be discussed in section C). *recG dnaA* mutants exhibit replication firing in both directions from the *Ter*, but the extent is limited since it is restricted by the *Tus/ter* boundaries. Moreover, destabilizing the transcription complexes with an *rpoB*35* mutation also allows further extension of replication. Combining these mutations enables cells to grow and form colonies in the absence of *oriC* initiation. Interestingly, in a *recG rpoB*35 tus/ter dnaA* mutant, when *oriC* is moved from its original locus, the forks meet opposite to the ectopic *oriC* and replication is initiated in this new artificial *Ter* region (Rudolph et al., 2013). DnaA independent replication is further increased in *recG* mutants treated with UV-irradiation. UV irradiation may favor the assembly of new replication forks linked to the repair of such lesions, provoking more fork collisions (Rudolph et al., 2009).

5. Avoiding over initiation: the role of SeqA

SeqA is a protein that is involved in preventing re-initiation of replication at *oriC* immediately after it has been replicated. SeqA protein binds to hemimethylated DNA at *OriC* and by doing so, prevents DnaA binding and prevents *dnaA* transcription since *dnaA* gene is one of the first transcribed genes (Jameson and Wilkinson, 2017). Campbell *et al.* showed that although methylation by Dam methylase occurs right after replication over the chromosome, the *OriC* region remains hemimethylated for a short period before dam methylase fully methylates it (Campbell and Kleckner, 1990). Moreover, the *dnaA* promoter contains a GATC site that undergoes the same sequestration phenomenon, thus reducing its transcription and lowering its amount in the cell, which is essential for replication initiation (Slater et al., 1995). By binding the GATC hemimethylated sequences at *oriC* and in the *dnaA* promoter, SeqA sequesters the origin of replication for up to one third of the cell cycle. A combination of SeqA dissociation and methylation of the hemimethylated DNA will lead to a release of the sequestered origin and allow a new round of replication (Jameson and Wilkinson, 2017).

There exists other systems to repress over-initiation events, for instance, the *datA* locus contains five DnaA boxes that favor binding of many DnaA proteins, thus decreasing the amount of free DnaA proteins available for *oriC* initiation events (Kitagawa et al., 1998).

6. Dealing with topology during replication

Replication of the *E. coli* chromosome is a topological challenge. Indeed, the processing of the replisome on a circular chromosome creates topological tension, called supercoiling, ahead of the replication fork and behind the replication fork (Postow et al., 1999). These supercoils need to be dealt with to avoid chromosome breakage. However, many biological processes such as transcription, initiation of replication, enzyme activity or even site-specific recombination require a certain degree of supercoiling, rendering it essential for cell survival. It is therefore very important to maintain a steady state level of topological tension on the DNA throughout the cell cycle (Postow et al., 1999; Zechiedrich et al., 2000).

A group of enzymes called topoisomerases is responsible for managing this supercoiled homeostasis of the chromosome. Topoisomerases have the ability to change the supercoiling state of the DNA by introducing or removing knots. They can be divided into two types (Type I and Type II) depending on whether their activity involves the breakage of one or two strands of DNA.

a) *Type I topoisomerases*

i. Topoisomerase I

Topoisomerase I (Topo I) is a Type I topoisomerase that catalyzes the cleavage on a single strand of DNA allowing for the relaxation of negative supercoiling. It is mainly dedicated to topological homeostasis during transcription and recent studies have actually suggested a direct interaction between Topo I and the RNA polymerase (Banda et al., 2017; Tiwari et al., 2016). Topo I mutants are synthetically lethal with *rnaseH* null mutants, due to overproduction of R-loops suggesting a role for Topo I in R-loop (DNA-RNA hybrids) removal during transcription (Drolet et al., 1995). It has been shown that Topo I actually inhibits R-loop formation during transcription by relieving the negative supercoils accumulated by the RNA polymerase. Indeed, unremoved negative supercoils behind the RNA polymerase may leave place for reannealing of RNA to DNA and promote R-loop formation. In cells lacking Topo I, R-loop mediated cSDR is increased (Martel et al., 2015) and the overexpression of RnaseH

partially restores a Topo I deficient mutant (Drolet et al., 1995; Massé and Drolet, 1999). Besides removing R-loops, Topoisomerase I does not seem to be crucial in the replication cell cycle.

ii. Topoisomerase III

Although Topoisomerase I and Topoisomerase III have the same mode of action (i.e. relaxing negatively supercoiled DNA by cleaving a single strand of DNA), their roles differ greatly. To better understand the role of Topoisomerase III (Topo III), it is important to explain what precatenanes are and how they form.

During replication, as mentioned in the previous section, topological tension accumulates on the chromosome. As the replication fork moves forward, it creates an excess of positive supercoils. Gyrase deals with these positive supercoils ahead of the replisome, but Champoux & Been suggested that these positive supercoils may also diffuse behind the replication fork as the replisome swivels and create precatenanes. Precatenanes are topological links, formed between the two newly replicated sister chromatids. The name precatenane comes from the term catenane, because precatenanes, if unresolved lead to catenated chromosomes at the end of replication (Champoux et al., 1979) (figure 3).

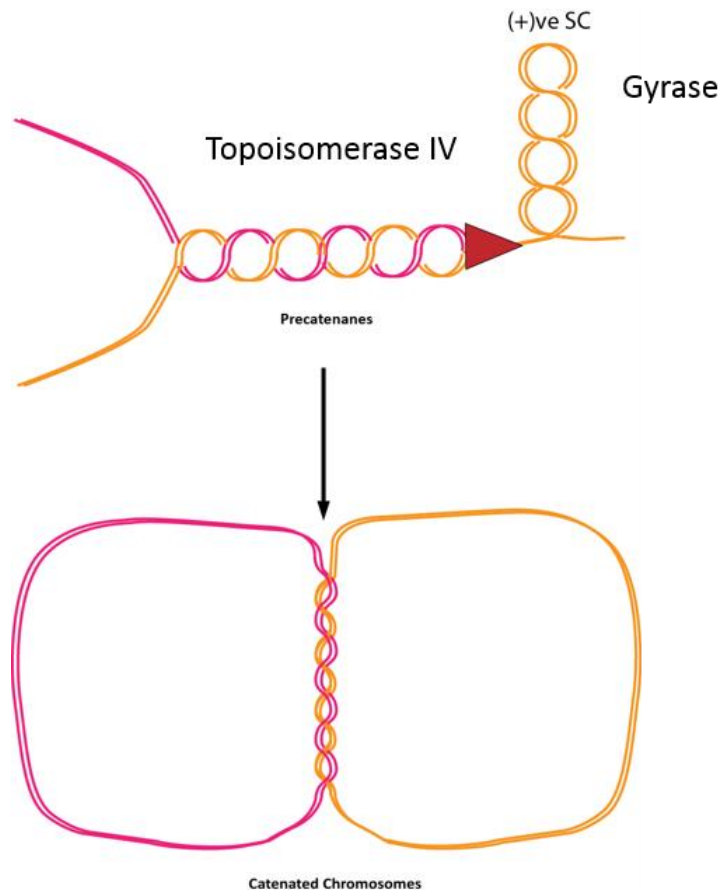


Figure 3. Formation of precatenanes and catenanes

Positive supercoils ahead of the fork are eliminated by Gyrase. Precatenanes formed behind the replication fork are removed by Topoisomerase IV. Unresolved precatenanes may lead to the formation of catenated chromosomes at the end of replication.

Adapted from Reyes-Lamothe et al. 2012

No obvious phenotype for *topB* (the gene encoding Topo III) mutants has been observed but a Topo III overexpression in a temperature sensitive mutant of Topoisomerase IV (the main precatenane removing enzyme, see section B) can restore viability and restore chromosome segregation. This means that Topo III can act as a decatenase during replication by removing precatenanes, although a single strand gap is required as a substrate (Nurse et al., 2003).

Other interesting activities have been described for Topoisomerase III. *Zhu et al.* described in 2001 that Topo III and RecQ can act together to resolve recombination intermediates such as Holliday Junctions (HJ) before chromosome segregation (Zhu et al., 2001). It was later shown that RecQ and Topo III act together to resolve stalled converging replication forks. Their action is mediated by SSB protein. These two different functions of the RecQ-Topo III pair results

from a different activity of RecQ in both reactions. The former being linked to RecQ's branch migration activity and the latter to its DNA unwinding activity (Suski and Mariani, 2008). The overexpression of RuvABC (a resolvase of recombination intermediates) rescued a double Topo IV/Topo III mutant. These Topo IV/Topo III double mutants are barely viable, even at the permissive temperature. They grow very slowly and have segregation defects. The rescue of this mutant by overexpression of RuvABC confirms a possible role for Topo III in managing recombination intermediates (Lopez et al., 2005).

b) Type II topoisomerases

i. Gyrase

As the replication fork moves forward, topological tension accumulates ahead of the fork. These positive supercoils are mainly dealt with by Gyrase. Gyrase is a specific topoisomerase that only exists in bacteria. It is the only topoisomerase that has the ability to introduce negative supercoils, in an ATP-dependent manner (Gellert et al., 1976). Gyrase is composed of two subunits, GyrA and GyrB. GyrA has the DNA binding motif and GyrB exhibits the ATP-hydrolysis activity. Gyrase's ATP-hydrolytic activity allows the introduction of negative supercoils ahead of the replication fork, thus acting against the natural accumulation of positive supercoils created by replication. The introduction of negative supercoils is essential to let the DNA polymerase move forward.

ii. Topoisomerase IV

Topoisomerase IV is a type II topoisomerase formed of two subunits, ParE and ParC. It is the main decatenase in E.coli (Zechiedrich et al., 1997). Topoisomerase IV can act behind the replication fork to relieve topological links called precatenanes (Lesterlin et al., 2012; Wang et al., 2008). However, Topoisomerase IV is mainly required at the end of replication for the resolution of catenation links that have persisted after replication (Espeli et al., 2003).

The role and action of Topoisomerase IV will be further discussed in section B.2.

B. Sister chromatid cohesion and segregation

1. Sister chromatid cohesion in Eukaryotes

During replication in Eukaryotic cells, the newly replicated sister chromatids stay cohesive during the subsequent gap (G_2) phase and during early mitosis, prophase, prometaphase, and metaphase. This physical connection between sister chromatids is called Sister Chromatid Cohesion (SCC). This step is crucial to avoid premature sister chromatid separation and thus ensure proper chromosome segregation. It has been proposed that this SCC step is essential for proper bi-orientation of the chromosomes on the mitotic spindle (Tanaka et al., 2000). Moreover, SCC creates tension by resisting the forces of the microtubules which is highly important for the correct segregation of the chromatids (Nasmyth and Schleiffer, 2004). A defect in SCC can be very detrimental for the cell and several human diseases have been linked to an inappropriate segregation of chromosomes. For instance, cohesion defects and subsequent chromosome instability are associated to Hodgkins lymphoma (Sajesh et al., 2013).

a) *Eukaryotic SMC proteins*

In Eukaryotes, sister chromatid cohesion is mediated by Cohesin. Cohesin is a multiproteic complex, formed of several subunits that are part of the SMC protein family (originally, SMC stood for stability of mini-chromosomes, but it is also referred to as structural maintenance of chromosomes). There exist at least six SMC proteins, SMC1 to SMC6, which have different roles in chromosome dynamics, cohesion, condensation and even gene expression. SMC proteins are typically between 150-170 kb and each SMC dimer has an amino- and a carboxy-terminal globular domain, also called head domain, carrying the Walker A motif at the amino terminal and a DA box (resembling the Walker B box) at the carboxy-terminal. These motifs are highly conserved structures involved in ATP binding and hydrolysis (figure 4A) (for review, (Cobbe and Heck, 2000)). The two head domains associate by folding of the hinge domains, forming a coiled coil (figure 4A).

In Eukaryotic cells, SMC proteins associate by the hinge domain to form heterodimers. SMC1 associates with SMC3, SMC2 with SMC4 and SMC5 associates with SMC6. SMC2/4 forms the Condensin complex, responsible for chromosome compaction during metaphase. The SMC5/6 heterocomplex is involved in DNA repair and homologous recombination although other genome maintenance functions may be attributed to the SMC5/6 complex (Kegel and Sjögren, 2010). This particular SMC complex will further be discussed in section D).

b) SMC1/3, the Eukaryotic Cohesin

The SMC1/3 complex is the Eukaryotic Cohesin. SMC1 and SMC3 bind together through their hinge domain. The association of their globular heads forms a nucleotide binding domain (NBD) that is connected by the kleisin protein Scc1 (Michaelis et al., 1997). The association of these three proteins forms a tripartite ring-like structure that may entrap the sister chromatids. A fourth subunit, (Scc3 in yeast or SA in higher Eukaryotes) binds Scc1 and is essential for sister chromatid cohesion (Gruber et al., 2003; Haering et al., 2002). Other proteins, such as Wapl/Rad61, Pds5, and Sororin can bind to Scc1 or Scc3 and influence cohesion. These kleisins or other kleisin-associated subunits can vary depending on the organism (figure 4B).

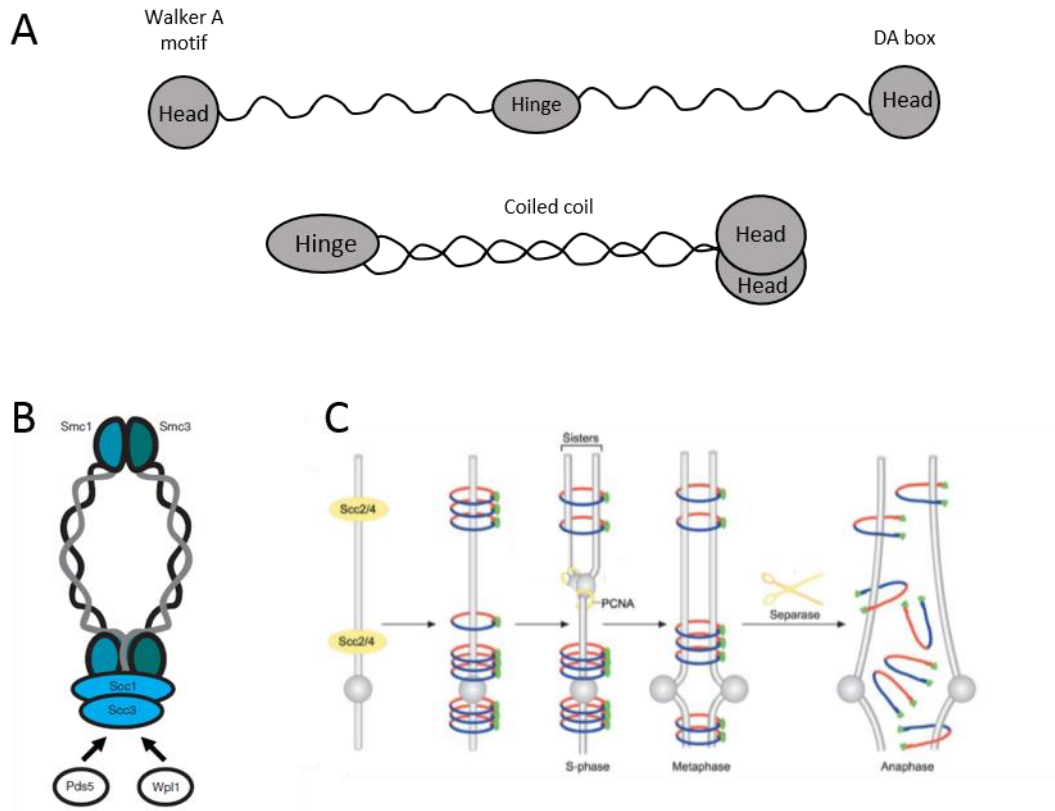


Figure 4. Schematic representation of a Eukaryotic SMC protein

A- Schematic representation of an SMC protein. The protein is folded at the hinge domain forming a long coiled coil domain bringing the two globular heads together. B- Schematic representation of the Cohesin complex. The names of the subunits are the yeast names. SMC1 and SMC3 are associated by the Scc1 kleisin and kleisin-associated proteins. C- Cohesin cycle in yeast. Scc2 and Scc4 load Cohesin onto chromosomes. Cohesion is established between sister chromatids. Cohesion leads to tension at the centromeres and biopolar orientation is achieved. Separase cleaves Scc1 subunit and Cohesin dissociates from the chromosomes allowing segregation.

Adapted from Kegel & Sjogren, 2010 and Nasmyth & Haering, 2005

Cohesin is associated to chromosomes during S phase and its loading is dependent on Scc2 and Scc4 proteins, the two subunits of the Adherin complex (Ciosk et al., 2000). Cohesin can be loaded onto chromosomes throughout the cell cycle but cohesion will only be established during replication (Uhlmann and Nasmyth, 1998) (figure 4C).. It has been proposed that DNA entry into the Cohesin ring requires a transient dissociation of the hinge domains of SMC1 and SMC3 (Gruber et al., 2006). Interestingly, ChIP experiments in *Saccharomyces cerevisiae* have revealed that Adherin complexes and Cohesin are bound at different sites on the chromosome. It has been proposed that Cohesins may be loaded onto DNA at the Adherin

sites and that they translocate and slide to other chromosomal regions. More specifically, it was shown that Cohesin accumulates between genes of converging transcription, meaning that Cohesin binding is rather defined by transcription than the recognition of a specific DNA sequence. These observations, coupled to experiments suggesting that Cohesin can slip off small linearized chromosomes lead to the proposal that Cohesin can move laterally along DNA (Ivanov and Nasmyth, 2005). Cohesin binding sites expanded over approximately 4 kb and the distance between two neighboring binding sites varied between 2 to 35 kb (Lengronne et al., 2004). Once bound to sister chromatids, Cohesin keeps the sister chromatids connected until the onset of division in anaphase. Cleavage of Scc1 by Separase releases Cohesin from the sister chromatids, abolishing SCC and allowing segregation (Uhlmann et al., 2000).

2. Sister chromatid cohesion in *Escherichia coli*

a) *Existence of a sister chromatid colocalization before segregation*

In *E. coli*, cohesion of sister chromatids as described in Eukaryotes does not exist because they lack Cohesin proteins. However, experiments have shown that there exists a lag between the replication and the segregation of a given locus. Fluorescence *in situ* hybridization (FISH) microscopy in synchronized cells showed that a chromosomal locus situated near *oriC* had only one single fluorescent focus for approximately 35 min, before exhibiting two distinct fluorescent foci suggesting that although the locus is replicated, there is an extensive lag before it segregates. These observations were confirmed for other *loci* in the origin proximal half of the chromosome. A possible role for MukBEF complex (an *E. coli* SMC protein) but not Dam methylase in these events was described (Sunako Yumi et al., 2002). Later, Bates and Kleckner proposed that the splitting of the sister chromatids could occur simultaneously over a large portion of the nucleoid (except for the Ori and Ter regions that behave differently) and that it is followed by a chromosome reorganization that leads to chromosome segregation at the onset of cell division (Bates and Kleckner, 2005). Using live cell microscopy and fluorescent labelling of chromosomal *loci*, Espeli *et al.* showed that the dynamics and mobility of chromosomal *loci* actually vary depending on the macrodomain they belong to. These

experiments further revealed the segregation pattern of the various macrodomains. The Ori macrodomain and the non-structured regions segregate first, followed by the left and right macrodomains. *Loci* in the non-structured regions appear to be less constrained than foci in the left or right macrodomains. Interestingly, foci in the macrodomains segregate progressively, following the genetic map, but foci in the non-structured regions present irregular and unpredictable segregation timings. This suggests that the colocalization step following replication depends on its chromosomal position and thus its belonging to a given macrodomain or non-structured region (Espeli et al., 2008).

b) Role of Topoisomerase IV in sister chromatid colocalization and sister chromatid cohesion

Topoisomerase IV is a Type II topoisomerase that removes positive supercoils and catenanes. It is formed of two subunits, ParE and ParC. Topo IV mutants are not viable and ParE or ParC temperature sensitive mutants exhibit a long elongated cell phenotype with a nucleoid partitioning defect when placed at a non-permissive temperature (Kato et al., 1990).

An original DNA microarray experiment, based on gene copy number and the relative abundance of replicated DNA over non-replicated DNA, allowed to measure fork progression in conditions where Topoisomerase IV was inhibited or not. This revealed that Topoisomerase IV promotes fork progression by relieving positive supercoils ahead of the replication fork at 1/3 of the rate provided by Gyrase (Khodursky et al., 2000). But the main activity of Topo IV appears to be DNA ring decatenation (Zechiedrich et al., 1997).

Topoisomerase IV is essential to decatenate *E. coli* chromosomes (Kato et al., 1990). It was later shown that inhibition of Topo IV prevents locus segregation, and conversely, overexpression of Topo IV dramatically reduces the time of sister chromatid cohesion. Interestingly, inhibition of Topo IV did not prevent ongoing replication, but did prevent segregation of sister loci (Wang et al., 2008).

A site-specific recombination assay, based on *loxP* recombination, revealed that sister chromatids stay cohesive for a tightly controlled period of time before segregating and confirmed that their segregation relies on Topo IV activity. This site specific recombination

assay detects contacts between sister chromatids at a molecular level rather than probing sister chromatid colocalization as described in the previous studies (Bates and Kleckner, 2005; Espeli et al., 2008; Sunako Yumi et al., 2002) (figure 5).

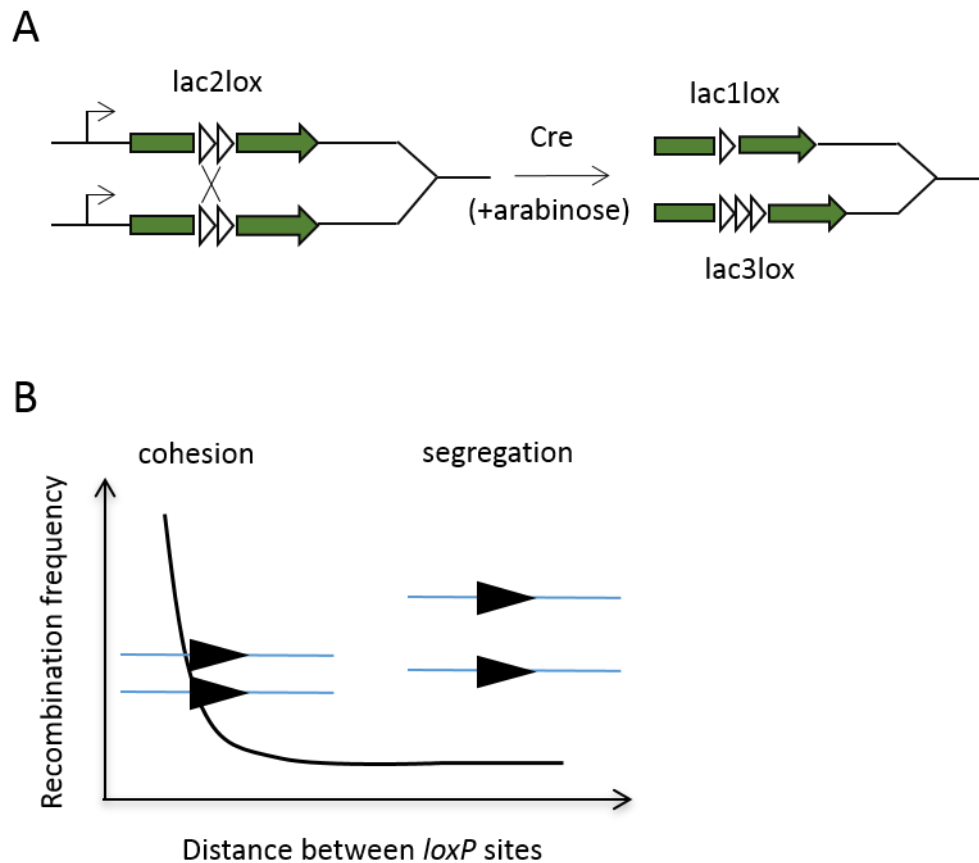


Figure 5. Schematic description of the *loxP* recombination assay principle

A- Principle of the *loxP* site specific recombination assay. Upon Cre induction the two consecutive *loxP* sites can only recombine with the *loxP* sites carried by the sister chromatid. Recombination gives rise to the recombination products: 1/*loxP* site on one chromatid and 3/*loxP* sites on the other chromatid (Adapted from Lesterlin et al. 2012). B- Illustration of the amount of *loxP* recombination as a function of distance between *loxP* sites (and hence, sister chromatids).

This assay revealed that recombination occurred more frequently between homologous sequences, meaning that the sister chromatids are tightly and physically bound (enough for *loxP* recombination to occur between homologous chromatids), and not just colocalized, which could have been the case with conclusions solely inferred from fluorescence microscopy experiments. It was further estimated that the region of cohesion behind the replication fork varies between 400 kb and 1M bp, corresponding to a time frame of 10 to 30 min after replication (Lesterlin et al., 2012). This observation is consistent with the work of Bates & Kleckner and Espeli *et al.* and could also be explained by the existence of particular chromosomal regions called SNAPS (Joshi et al., 2011).

c) *The Snaps regions*

Although the loss of interactions between sister loci has been described as progressive and coordinated with replication (Lesterlin et al., 2012), imaging of individual loci revealed regions with delayed segregation. Two regions near the origin of replication, defined as SNAPS, exhibit late splitting. These two regions, that are about 150 kb long, are both situated on the right replichore. Loci situated in both SNAP regions segregate concomitantly and are linked to the appearance of the bilobed form of the nucleoid (Joshi et al., 2011). Sites such as *gln*, or *psd* and *fecR* that are in two different SNAP regions, separate at the same time although they are over 150 kb apart on the genetic map. Moreover, these two regions exhibit prolonged cohesion even though the flanking regions have already segregated. The *gln* locus in one of the SNAP regions also presented an increased frequency of sister loci interactions in the *loxP* recombination assay compared to other loci (Lesterlin et al., 2012). Although “the raison” d’être of such regions is not quite clear, it is proposed that internal forces and accumulation of segregation tension in these SNAP regions, may be of high relevance for proper sister chromatid segregation and partitioning to opposite cell halves.

d) *Precatenane formation and removal by Topoisomerase IV*

As previously mentioned, during replication, unwinding of the duplex DNA by helicases causes overwinding ahead of the replisome. Gyrase and Topoisomerase IV manage the positive supercoils accumulated ahead of the fork, but these supercoils can also diffuse behind the replication fork due to a rotation of the replisome, and form what are called precatenanes (Cebrián et al., 2015; Peter et al., 1998).

Precatenanes were originally described on plasmids (Postow et al., 1999). If left unresolved, these precatenanes may lead to catenanes that topologically link the chromosomes at the end of replication (Champoux et al., 1979). In 2008, Wang and coworkers showed that segregation of newly replicated loci was impaired when Topoisomerase IV is inhibited and accelerated when Topo IV was increased (Wang et al., 2008). Later, Lesterlin *et al.* linked sister chromatid cohesion to the formation of putative precatenanes. Indeed, using the site specific *loxP* recombination assay, they showed that the recombination frequency was drastically increased when the activity of Topo IV is impaired in a *parE^{ts}* or *parC^{ts}* mutant, suggesting that sister chromatids stay tightly bound together when Topo IV activity is inhibited. These observations lead to a model where precatenanes form behind the replication fork, interlocking the newly replicated sister chromatids, keeping them cohesive for a period of time before the action of Topoisomerase IV allows their segregation. This step is defined as the sister chromatid cohesion period in *E. coli* (Bermejo et al., 2008; Lesterlin et al., 2012) (figure 6). Recently, similar topological links have been directly observed in yeast suggesting that precatenanes do form on the chromosome (Mariezcurrana and Uhlmann, 2017).

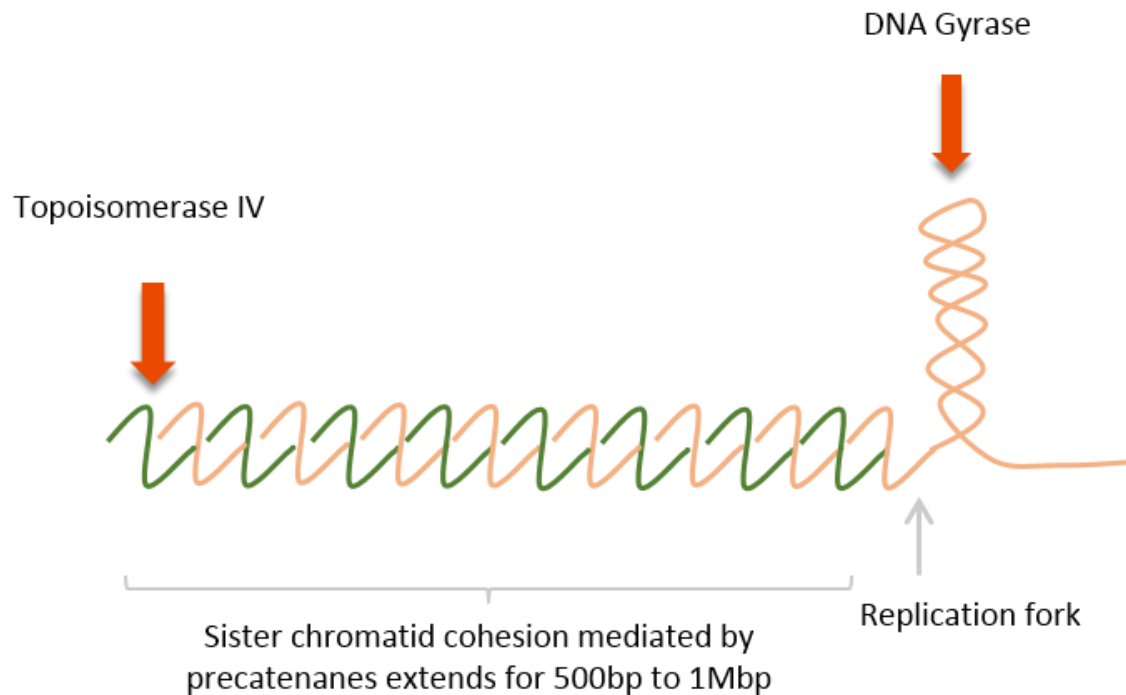


Figure 6. Representation of sister chromatid cohesion mediated by precatenanes in *E. coli*

Gyrase relieves positive supercoils ahead of the replication fork. Topoisomerase IV removes precatenanes behind the replication fork.

Adapted from Lesterlin et al. 2012

e) Other proteins involved in sister chromatid cohesion during replication

Although Topoisomerase IV seems to be the main factor directly involved in precatenane removal, other proteins may be indirectly influencing precatenane removal and sister chromatid cohesion. Indeed, the rate of precatenane formation is much slower than the rate of Topo IV decatenation activity, suggesting that Topo IV activity may be negatively regulated, in order to maintain a steady state of precatenanes behind the fork and keep sister chromatids cohesive (Lesterlin et al., 2012). Lesterlin *et al.* in 2012 and Joshi *et al.* in 2013 tested several candidate proteins for their possible action on sister chromatid cohesion (Joshi et al., 2013; Lesterlin et al., 2012). Using the site specific *loxP* recombination assay, Lesterlin *et al.* tested

the effect of MukB (an SMC-like protein) and MatP (Ter macrodomain organizing protein) on sister chromatid interactions, and showed that neither of these proteins significantly influenced specific homologous sister chromatid interactions. Using fluorescence microscopy, *Joshi et al.* tested various candidate proteins: MukB and RecN (SMC like proteins), HNS, IHF and Fis (nucleoid associated proteins), and SeqA (replication fork tracking protein) as well as its regulator, Dam (Adenine DNA methylase). Of these tested proteins, only SeqA and Dam had an effect on sister chromatid cohesion during replication. They observed that in a *seqA* mutant, the cohesion period of the *gln* locus dropped from 30 min to 12 min. They propose that SeqA binds immediately behind the replication fork, on hemimethylated DNA, and specifically on GATC sites, thus delaying precatenane removal by Topo IV. Interestingly, they found that SNAP regions had a high frequency of GATC sequences, and that SeqA binding, revealed by Chip-qPCR experiments was over 10 times stronger in these regions, shedding light on the particular cohesion pattern observed in these regions. Naturally, *dam*- mutants exhibited a similar cohesion phenotype to that observed in a *seqA* mutant (figure 7). It was later shown that there was an increased spacing of GATC sites around the Topo IV cleavage sites. This could be linked to SeqA binding at GATC, creating a barrier to Topo IV cleavage. Interestingly, Topo IV cleavage sites are rare in the SNAPs regions. However, no effect of *seqA* deletion was observed on Topo IV cleavage at two sites outside of the SNAPs, suggesting that the effect of SeqA might be limited to regions with a high density of GATC (El Sayyed et al., 2016).

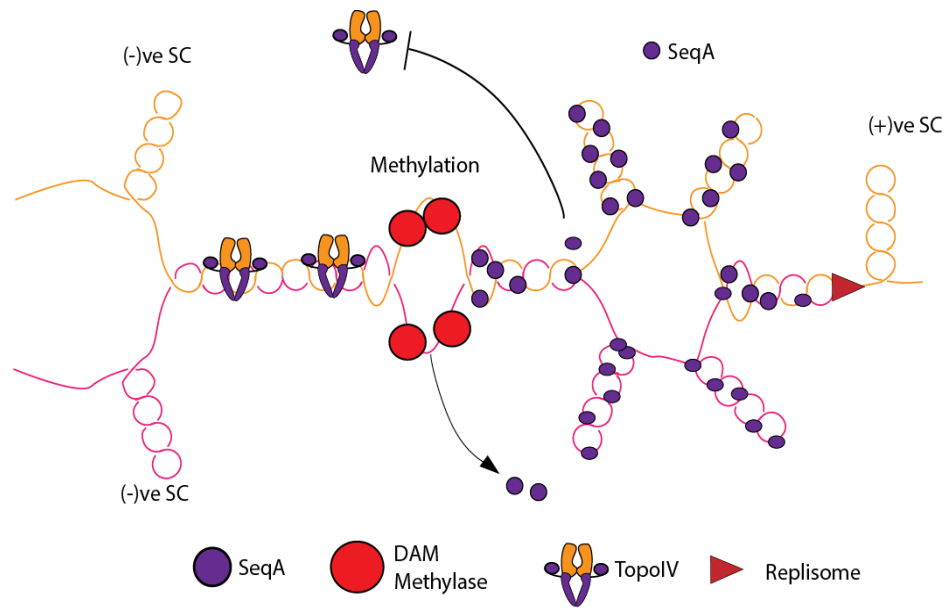


Figure 7. Schematic model for SeqA binding

SeqA binds hemi-methylated DNA behind the replication fork. SeqA binding may prevent access of the hemi-methylated region to Topoisomerase IV and thus prevent Topoisomerase IV action and subsequent segregation. Upon methylation of the second strand of DNA, SeqA is removed and Topoisomerase IV may bind and eliminate precatenanes.

f) Final segregation of sister chromatids: Topo IV and XerCD-dif

We have extensively discussed the segregation of sister chromatids, which is concomitant with replication. However, although most of the sister chromatids have migrated into different cell halves during replication, they remain bound in the terminus region, where they need to be decatenated. Topoisomerase IV plays a crucial role in precatenane removal but most of its activity is detected late in G2 phase, presumably for the final decatenation step of fully replicated chromosomes (Espeli et al., 2003).

In fact, the terminus region follows an original pattern of segregation. The sister *loci* of the Ter macrodomain do not segregate until the onset of cell division. This extended colocalization period is partly due to MatP, the Ter macrodomain organizing protein. MatP binds specifically to the 23 *matS* sites spread throughout the terminus region. In the absence of either MatP protein, or the *matS* sites, the Ter region presented an early segregation pattern (Mercier et

al., 2008). Interestingly, although deleting *matP* had an effect on late sister chromatid segregation and co-localization, it did not have a strong effect on sister chromatid interactions revealed by site-specific *loxP* interactions. This confirms MatP's role as a global Ter macrodomain organizer, that does not necessarily favor contacts between homologous regions of sister chromatids, as is the case with precatenanes (Lesterlin et al., 2012).

MatP plays many roles in chromosome segregation. First, its association with ZapB, a septal ring protein, forces the colocalization of the two newly replicated Ter regions at mid-cell forming a colocalization focus (Espeli et al., 2012). Second, MatP stimulates the dissociation of MukB with the Ter regions. MukB binds transiently to *matS* sites and is rapidly ejected by MatP that catalyses the ATP hydrolysis of MukB (Nolivos et al., 2016). This activity creates a large region around *dif* where MukB influence on chromosome folding differs from the rest of the chromosome (Lioy et al., 2018). MukB displacement from this region is necessary to form clusters at Ori (Nicolas et al., 2014; Nolivos et al., 2016). These MukB clusters are required for correct positioning of the origin of replication to the quarter position of the cell, which is important for chromosome partitioning. This differential positioning of MukB influences Topo IV decatenation activities and seems important for the formation of Topo IV clusters near the origin, although direct effect of *mukB* deletion on Topo IV cleavage in the Ter or another strong cleavage site has not been observed. However, Topo IV binding analyzed by ChIP-seq follows an *oriC*–*dif* gradient that might be compatible with MukB depletion in the Ter domain by MatP (El Sayyed et al., 2016).

In the final step of segregation, FtsK, a DNA translocase acts to release MatP-mediated cohesion. It then actively segregates the terminus region of sister chromatids by translocating DNA following the orientation of the polar KOPS motifs (Stouf et al., 2013).

When there is an uneven number of recombination events during replication, the two new chromosomes may form chromosome dimers that need to be resolved for proper segregation. The resolution of these dimers is performed at *dif*, thanks to the action of XerC and XerD recombinases. El Sayyed *et al.* showed that Topo IV activity was strongest at *dif*, the site of catenane resolution. This activity was dependent on XerC binding and the *xerC* box but not XerD. MatP is also required for Topo IV loading at the *dif* site for the faithful decatenation of fully replicated chromosomes (Sayyed et al., 2016).

C. DNA damage and the DNA damage response pathways in *Escherichia coli*

1. Avoiding replication errors during a regular cell cycle: Mismatch repair (MMR)

Although the proofreading activity of the DNA holoenzyme Pol III is very efficient, some errors persist once the replication fork has passed. These mis-paired bases need to be dealt with because they can lead to mutations and thus disease or cancer.

In 1976, Wagner and Meselson showed that mismatches introduced into *E. coli* triggered repair reactions. They also hypothesized that this mismatch repair reaction could serve to correct mis-paired bases incorporated during replication (Wagner and Meselson, 2005). One of the critical steps of the Mismatch Repair (MMR) pathway is to identify which of the two strands has incorporated the wrong base. In *E. coli*, the detection of the incorrect strand relies on DNA methylation. Since MMR is a post-replicative DNA damage response, the newly synthesized strand is not yet methylated. The DNA is in a hemi-methylated state, targeting correction to the un-methylated strand (Lu et al., 1983; Pukkila et al., 1983). Mismatch recognition may differ depending on the species. For instance, in *B. subtilis*, the β -clamp directs MutS to the DNA for mismatch recognition (Simmons et al., 2008). In *E. coli*, MutS recognizes and binds the mismatch (Su and Modrich, 1986). Interaction of MutS and MutL activates MutH, an endonuclease that recognizes and cleaves the strand carrying the mis-paired base, at an unmethylated GATC site (Au et al., 1992). UvrD helicase uses the incision made by MutH to initiate unwinding of the nascent strand and goes beyond the mis-paired base (Grilley et al., 1993). Through a direct interaction, MutL enhances UvrD helicase activity more than 10 fold (Yamaguchi et al., 1998) and UvrD thus unwinds DNA, exposing a single strand, which is the substrate for MMR exonucleases. SSB binds to the parental DNA, protecting it from exonuclease activity (Ramilo et al., 2002). Whether the un-methylated sequence, dGATC that will direct repair of the mismatch is situated 3' or 5' to the mismatch, different exonucleases are recruited. When the dGATC sequence is 5' to the mismatch, Exonuclease VII or RecJ, exhibiting a 5' to 3' exonucleolytic activity are required, whereas

Exonuclease I is recruited for 5' to 3' exonuclease activity (Cooper et al., 1993). Regardless of the orientation of the mismatch, excision by the exonucleases (for both directions), was shown not to exceed 100 nucleotides beyond the mis paired base. DNA Pol III then fills the gap and ligase seals it (Lahue et al., 1989) (figure 8).

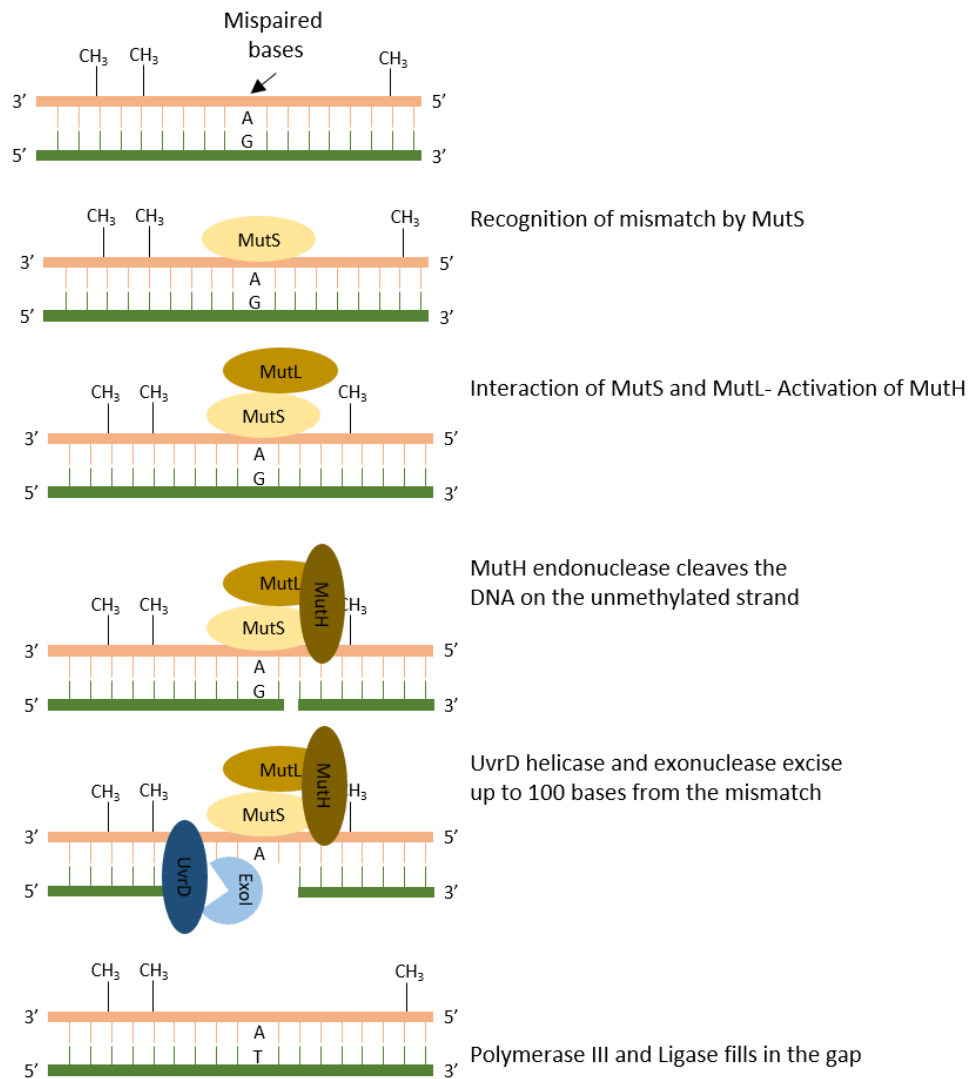


Figure 8. Mismatch repair pathway in *E. coli*

MutS recognizes and binds the mismatch. MutS and MutL interact and activate MutH. MutH recognizes the mispaired base thanks to the hemimethylated state of the DNA and incises the DNA. UvrD helicase unwinds the DNA and the appropriate exonuclease degrades up to 100 nucleotides on the strand carrying the mismatch. Pol III fills in the gap and ligase reseals it.

2. DNA damage lesions

Extracellular and intracellular events compromise DNA and create various types of DNA lesions. These lesions can be dealt with through different repair pathways, and in the most detrimental situations, lead to DNA double strand breaks (DSBs). Some DNA lesions change the structure and nature of the DNA. They modify the bases, create covalent links or even change the chemistry of the bases.

a) Modified bases

i. Spontaneous base deamination

Deamination is a frequent source of spontaneous mutagenesis. It is a reaction where cytosine, adenine, guanine and 5-methyl cytosine have their amine group replaced by an oxygen atom to become uracil, hypoxanthine, xanthine and thymine respectively (Chatterjee and Walker, 2017). Deaminated cytosines are rapidly removed by uracil DNA glycosylase, but thymine for instance, resulting from the deamination of 5-methyl cytosine, is poorly removed. Indeed, thymine, that is naturally part of DNA is more difficultly recognized, making it one of the major sources of single site genetic diseases (Cooper and Youssoufian, 1988). These highly mutagenic lesions are dealt with through the Base Excision Repair (BER) pathway (figure 9A).

ii. Abasic sites

An abasic site appears on duplex DNA when the N-glycosyl bond between a nucleobase and the deoxyribose is hydrolysed. This reaction can occur spontaneously but also arises as an intermediate of the Base Excision Repair (BER) pathway. Indeed, the removal of uracil by uracil DNA glycosylase creates a transient abasic site, also called apurinic or apyrimidinic site (AP site), that is managed by the BER pathway. In humans, a defect in the BER pathway leaves AP sites unattended and leads to genetic mutations or cancer (figure 9B).

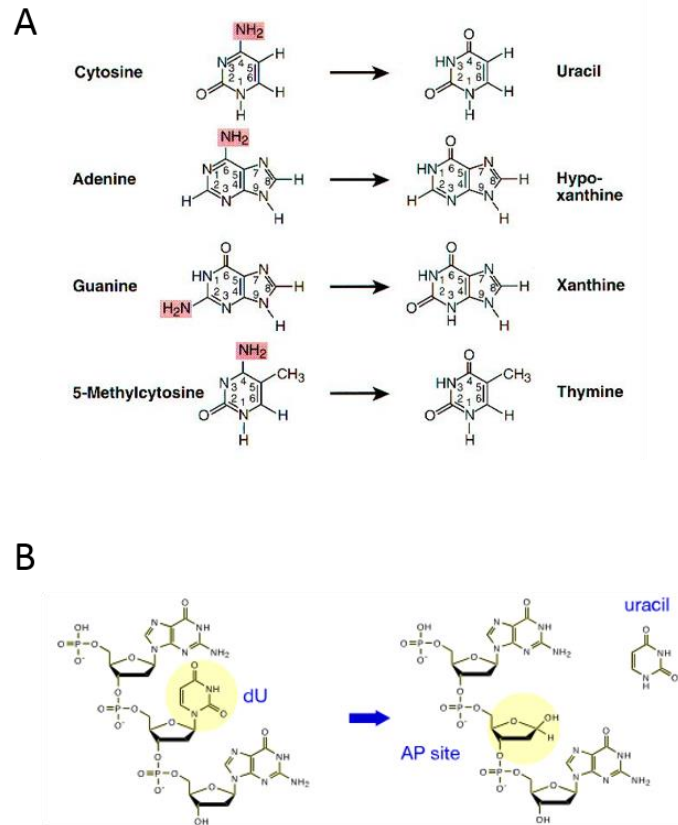


Figure 9. Modified bases

A- Spontaneous deamination of a base results from the replacement of the NH_2 group by an oxygen atom. B- An abasic site appears when the N-glycosylic bond between the deoxyribose and the base is cleaved. Depending on whether the cleaved base is a purine or a pyrimidine, the abasic site may be called an apurinic or an apyrimidinic site (AP site).

Recent studies in *E. coli* have shown the surprising role of GAPDH in the BER pathway and the repair of spontaneous or drug induced abasic sites (Ferreira et al., 2015). In *E.coli* GAPDH catalyzes the oxidative phosphorylation of glyceraldehyde 3-phosphate (G3P) to 1,3-bisphosphoglycerate (BPG) using the cofactor NAD and phosphate during glycolysis and gluconeogenesis in *E. coli*.

Using pull down assays, Ferreira *et al.* showed that GAPDH most likely interacts with Endonuclease IV and the uracil DNA glycosylase. However, the actual role of GAPDH in DNA repair and the BER pathway remains unknown.

b) DNA adducts

DNA adducts result from the covalent attachment of a chemical to a DNA base in a reaction called alkylation and are highly mutagenic if not removed (figure 10).

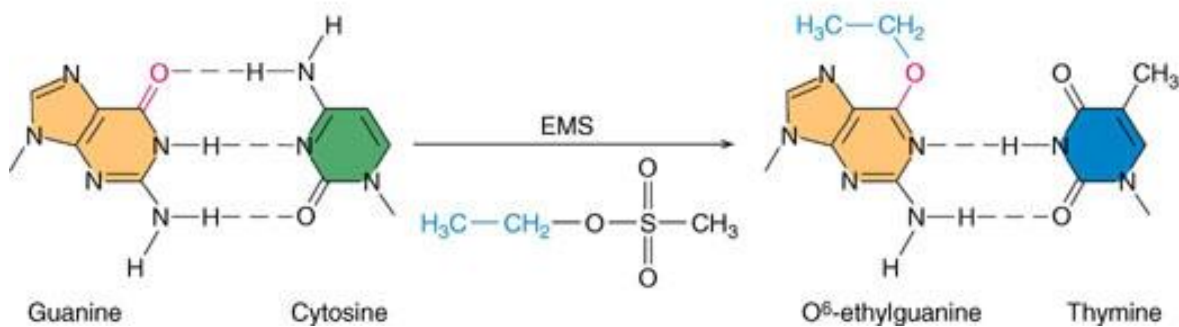


Figure 10. DNA adduct formation

DNA adducts result from the formation of a covalent link called alkylation between a chemical and a nucleobase. Here is the illustration of an adduct between Guanine and Cytosine formed by EMS (Ethyl methanesulfonate).

Although a wide variety of different types of adducts exist, they all rely on the reaction between the electrophile alkylating agent and the nucleophilic DNA.

There are different alkylating agents, such as Méthyl-methanesulfonate (MMS) or N-methyl-N'-nitro-N-nitrosoguanidine (MNNG) that can be used in chemotherapy, but a large variety of alkylating agents derive from food, cigarette smoke or pesticides (Chatterjee and Walker, 2017). Initially un-harmful, these agents are modified during cellular metabolism and give rise to toxic molecules such as nitrosamines, aflatoxins, aromatic amines, and polycyclic aromatic hydrocarbons.

Interestingly, certain DNA adducts arise from molecules contained in food or beverages. For instance, high temperature cooked meat has been shown to be carcinogenic in rat prostate, possibly due to the formation of DNA adducts by 2-amino-1-methyl-6-phenylimidazol [4,5-b] pyridine (PhIP), one of the most abundant heterocyclic amines contained in high temperature cooked meat (Nakai et al., 2007). On the other hand, red wine (and other beverages such as

beer or coffee) diminish PhIP mutagenicity by altering its metabolism. Resveratrol, an antioxidant present in red wine, may inhibit PhIP-DNA adduct formation (Dubuisson et al., 2002; Rybicki et al., 2011). *So if you're eating well cooked meat, make sure to sip on some red wine!*

c) *DNA protein crosslinks*

DNA protein crosslinks (DPCs) result from a covalent link between a protein and a DNA nucleotide. They can form through various ways, including environmental factors (UV light, radiation...), and therapeutic drugs or treatments (ionizing radiation, cisplatin, nitrogen mustards...). A large amount of DPCs arises from endogenous non-enzymatic and enzymatic activity (Barker et al., 2005).

Reactive aldehydes are formed through non-enzymatic cellular metabolism such as amino acid metabolism. They can form a stable covalent bond between an arginine or a lysine residue of a protein, thus creating a DPC. Acetaldehyde and formaldehyde are also DPC inducing aldehydes. Formaldehyde is a well-known lab chemical, but it is also formed *in vivo* as a byproduct of methyl group removal from DNA (Trewick et al., 2002).

DPCs also form during enzymatic reactions involving proteins that transiently form a covalent link with the DNA. A common and widely studied example of enzymatically induced DPCs is frozen topoisomerases. As described previously in this introduction, Type II topoisomerases covalently link to DNA and cut the DNA, creating a transient double strand break through which a second DNA strand may pass. Many chemotherapeutic drugs target Type II topoisomerases, while they are linked to DNA, in the cutting conformation (figure 11).

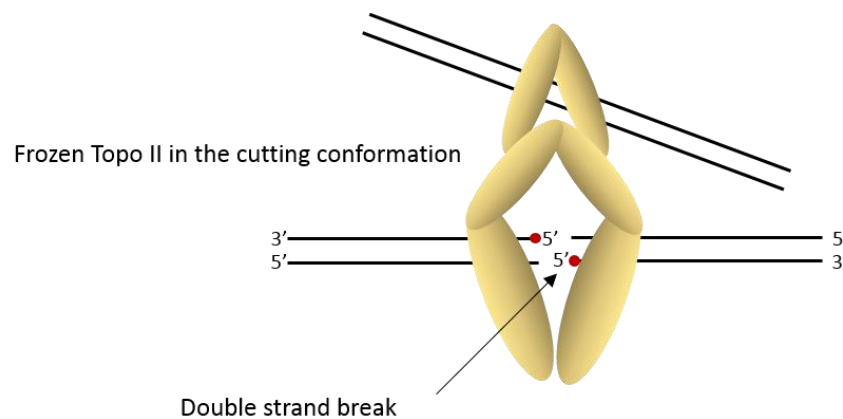


Figure 11. Schematic representation of a frozen Topoisomerase Type II

Chemical drugs can covalently link to topoisomerases while they are in the cutting conformation creating an exposed double strand break.

An interesting study showed that inhibiting Topoisomerase II at a semi-sensitive temperature maintained viability but conferred resistance to anti-Topoisomerase II drugs, suggesting that the action of anti-Topo II drugs was indeed linked to the activity of the enzyme rather than its transcription or protein amount in the cell (Nitiss et al., 1993). These anti-topoisomerase drugs trap the enzyme when it is covalently bound to DNA, exposing a double strand break. However, this complex is reversible and work from different teams has shown that it is the collision of Helicase (Howard et al., 1994) or the replication fork (Hiasa et al., 1996) with the complex that renders it toxic for the cell. Conversely, Hiasa *et al.* showed that the encounter of the replication fork with a frozen topoisomerase that was not in the cutting conformation did not create a double strand break, and it is only during the denaturation step, to remove the frozen topoisomerase that the double strand break occurred (Hiasa et al., 1996).

d) Oxidative DNA damage

Reactive oxygen species (ROS) are formed in many cellular processes such as cellular respiration (in Eukaryotes) but also anabolic processes or peroxisomal metabolism (Henle and Linn, 1997). The most common and abundant ROS are hydrogen peroxide (H_2O_2), superoxide

ion (O_2^-) and hydroxyl radical ($OH\cdot$). OH radicals are the most deleterious form of ROS. They can react with lipids, proteins and DNA. When reacting with DNA bases, they can cause a wide variety of DNA damage, amongst which adding a double bond, subtracting hydrogen atoms from their methyl groups, attacking the sugar residue, and even double strand breaks (Breen and Murphy, 1995).

The repair of such ROS induced DNA damage is mainly done by Base Excision Repair (BER), but it has been shown in *Saccharomyces cerevisiae* that nucleotide excision repair (NER) and homologous recombination (HR) can also be involved in the repair of such lesions (Swanson et al., 1999). In *E. coli*, ROS can lead to DNA damage, stalled replication forks and subsequent SOS induction. *dinF*, a protein induced by the SOS response, protects against ROS induced DNA damage possibly by reducing protein carbonylation and reducing intracellular levels of ROS (Rodríguez-Beltrán et al., 2012).

Other species, such as *Coxiella Burnettii* have the ability to fight against ROS in their host human cells by expressing specific repair genes and enzymes capable of destroying the ROS (Mertens and Samuel, 2012).

e) *Inter-strand and intra-strand crosslinks*

Inter-strand crosslinks (ICLs) arise when a chemical compound creates a covalent bond between the two DNA strands. An intra-strand crosslink results from the same mechanisms but covalently binds two bases from the same DNA strand. Crosslinking agents involve damage on both DNA strands, which makes them the most deleterious form of genotoxic agents (Mendelsohn et al., 1992). They have been shown to cause large chromosomal rearrangements and promote sister chromatid exchanges, probably due to a high rate of homologous recombination (Noll et al., 2006). Widely spread crosslinking agents are psoralen, nitrogen mustard, platinum compounds, or Mitomycin C (MMC). Mitomycin C is the genotoxic crosslinking agent that is mainly used in our laboratory. It is a product of the mold *Streptomyces caespitosus* and a common chemotherapeutic drug used for treating cancer. MMC reacts with the guanine residue of a 3'-CG-5' sequence. Through a series of complicated chemical reactions, MMC first forms a mono-adduct with the guanine from one strand and

ultimately forms a crosslink with a guanine on the opposite strand (Noll et al., 2006). MMC actually crosslinks in the minor groove, thus hardly perturbing the structure and bending of the DNA. This particularity of MMC can be important when considering its detection in DNA.

If left unattended, crosslinks can be highly toxic because they lead to double strand breaks. Inter-strand crosslinks have been the focuses of many studies and many uncertainties still remain on their repair. Unlike other forms of DNA damage, ICLs involve many different repair pathways. The error-prone translesion synthesis (TLS) pathway is involved but homologous recombination (HR) and NER (that ultimately ends by HR) seem to be the main repair pathways of ICLs (Noll et al., 2006). In fact, a commonly accepted model suggests a combination of NER and HR for the repair of ICLs (Cole, 1973). This will be further detailed in the next section.

3. Management of DNA lesions

DNA is constantly under exogenous or endogenous attacks, under many forms and leading to very different types of damage as discussed in the section above. The cell possesses a variety of DNA damage response pathways, whose role is to avoid the occurrence of a single strand or double strand break.

a) Base excision repair (BER)

Base excision repair (BER) corrects DNA lesions that do not significantly change the structure of the DNA. Such lesions result from deamination, base oxidation, alkylation...

In 1974, Thomas Lindahl found that the uracil DNA glycosylase can cleave uracil from DNA, leaving an apyrimidinic site (AP site). He showed that this uracil DNA glycosylase specifically cleaved uracil from double stranded or single stranded DNA, and not RNA, dUMP or uridine (Lindahl, 1974). This was one of the first steps in unravelling the BER pathway. BER pathway is thus initiated by the removal of a damaged base by one of the several DNA glycosylases (Nth or FpG in *E. coli* for instance). Once the damaged base has been removed, an apurinic or

apyrimidinic endonuclease catalyzes the cleavage of a 5' phosphodiester bond to the AP site. *E. coli* has two AP endonucleases, Endonuclease IV and Exonuclease III, which in spite of its name, exhibits mainly an AP endonuclease activity (Cunningham et al., 1986). The remaining sugar phosphate residue is then removed by RecJ and DNA Polymerase I then fills in the one nucleotide gap and a DNA ligase rejoins the ends. However, an alternative pathway exists, resulting in the replacement of several nucleotides rather than the single damaged base (Dianov and Lindahl, 1994). The initial steps, involving the DNA glycosylase and the AP endonuclease remain unchanged, but the next step is carried out by Pol I rather than RecJ. Pol I creates a strand displacement coupled to resynthesis of the displaced bases creating a 2 to 5 nucleotide overhang. This overhang is then cleaved by the 5' nuclease activity of Pol I (figure 12).

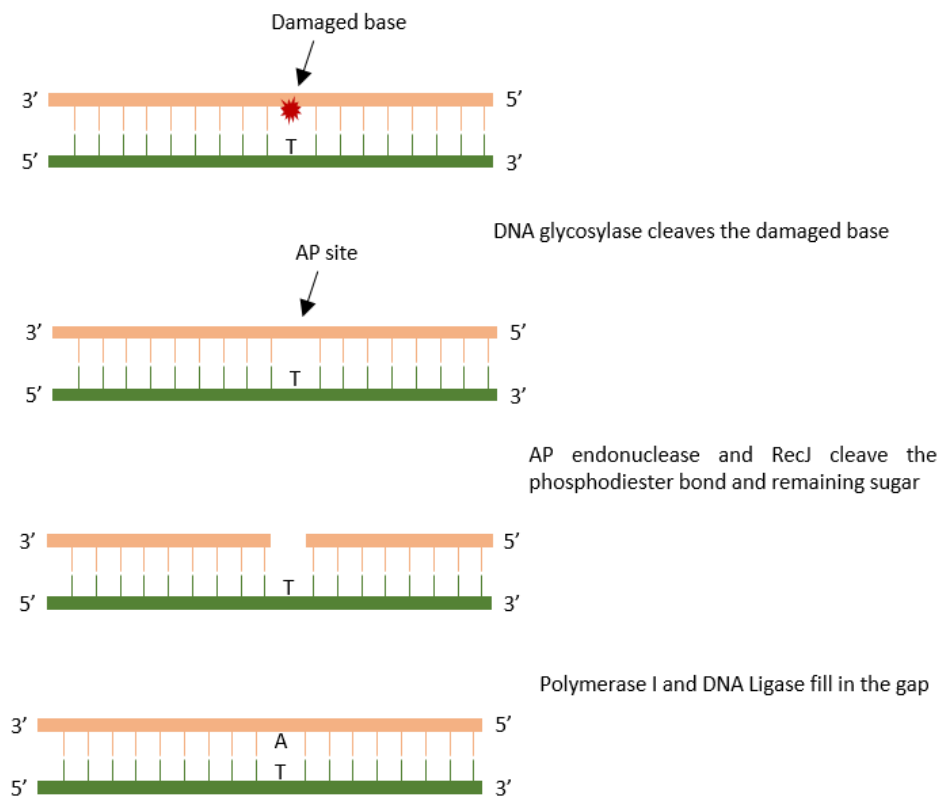


Figure 12. Base Excision Repair (BER) pathway

DNA glycosylase cleaves the damaged site creating an AP site. An AP endonuclease cleaves the phosphodiester bond and RecJ removes the remaining sugar phosphate; Polymerase I fills in the gap.

b) Nucleotide excision repair (NER)

Unlike BER, Nucleotide Excision Repair (NER) targets larger DNA adducts (called bulky adducts), that have introduced a conformational change in the DNA structure. Two of the most common bulky adducts that are repaired by NER are pyrimidine dimers, and 6,4 photoproducts, induced by ultraviolet light (UV light). However, a number of adducts induced by crosslinking agents, such as Mitomycin C or psoralen are also partly repaired via the NER pathway (Wood, 2010). In 1964, Setlow and Carrier first described the removal of pyrimidine dimers induced by UV light, and showed that this was a prerequisite for DNA synthesis to resume after being blocked by the adduct (Setlow and Carrier, 1964). Further work was done by Sancar and Rupp on the identification of UvrA, UvrB and UvrC, the three central proteins of the NER pathway (Sancar et al., 1981a, 1981b, 1981c).

The first step of NER is the recognition of the lesion. This primarily happens by recognition of a structural distortion of the double helix induced by the chemical adduct. UvrA is a DNA-binding protein that has a higher affinity for damaged DNA than non-damaged DNA. UvrA is considered as the DNA damage recognition enzyme of the triplet UvrABC exinuclease (for excision endonuclease). UvrA dimerizes, forming UvrA₂, and binds UvrB to form the (UvrA₂)(UvrB₁) complex. Under this protein-complex conformation, UvrA delivers UvrB to the damaged DNA. Once UvrB has been delivered, UvrA dissociates, leaving a stable UvrB-DNA complex (Orren and Sancar, 1989). It has been suggested that UvrB also dimerizes, forming a (UvrA₂)(UvrB₂) complex that binds DNA. Once the (UvrA₂)(UvrB₂) complex is bound to a possible site of damage, DNA wraps around one of the UvrB monomers which probes one strand for DNA damage. If the lesion is not recognized on this strand by the first UvrB monomer, the DNA wraps around the second UvrB protein that will probe the other strand for damage (Verhoeven et al., 2002). UvrA may facilitate wrapping of the DNA around UvrB (Wang et al., 2009). This UvrB recognition step involves a β -hairpin insertion between the two strands of DNA, thus confirming damage recognition and determining which DNA strand carries the lesion (Truglio et al., 2006). The efficiency with which the UvrA and UvrB proteins recognize the lesion can depend on the type of adduct and the extent of structural distortion, but overall, the Uvr proteins can sense a wide variety of DNA lesions (Jia et al., 2009; Truglio et al., 2006). Recent experiments using photoactivated localization microscopy (PALM) have

demonstrated that UvrA binds first, scanning the genome for damage and then recruits UvrB once the damage is detected, without forming a complex prior to DNA binding. These new observations are in opposition to the previous models described above and will undoubtedly lead to further investigations (Stracy et al., 2016).

Actual incision of the bulky adduct is carried out by UvrC after it binds the UvrB-DNA complex (Orren and Sancar, 1989) (figure 13).

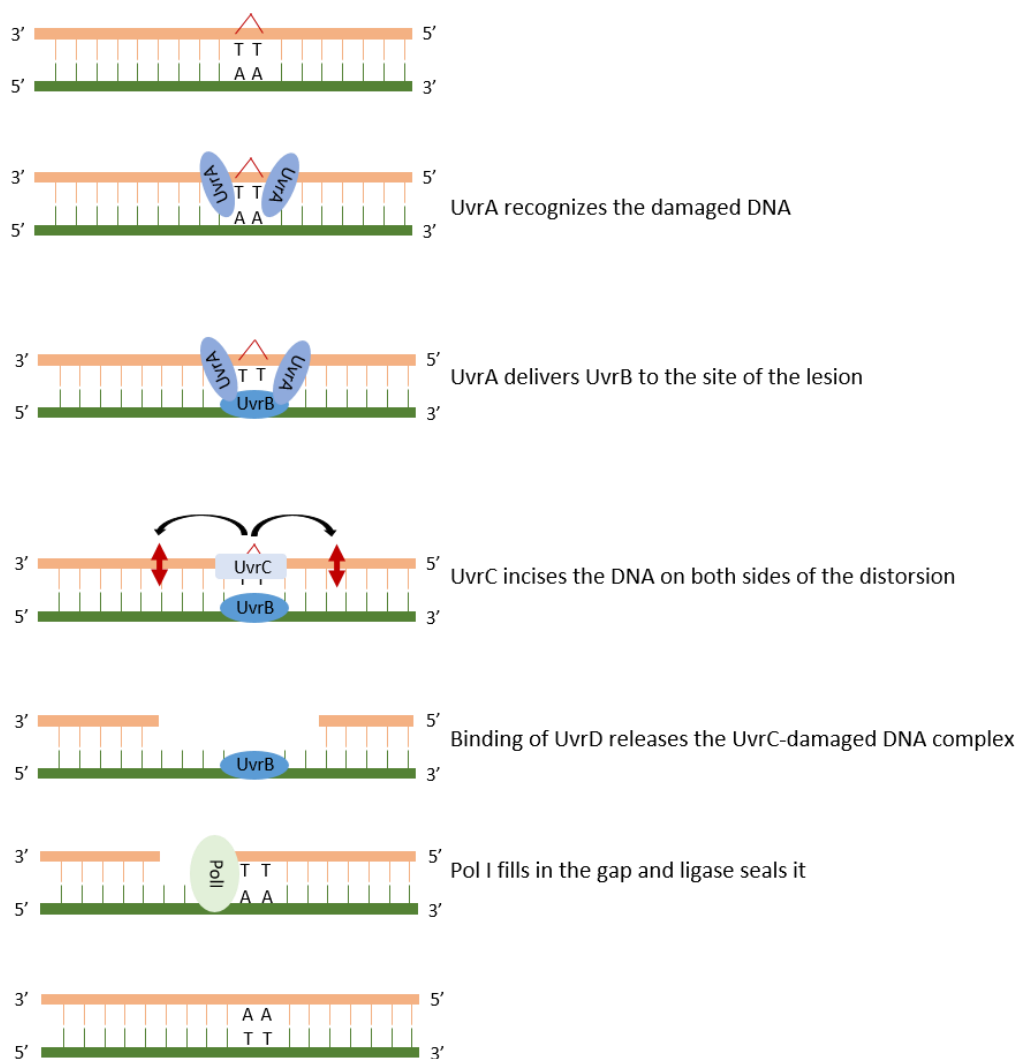


Figure 13. Nucleotide excision repair (NER) pathway

UvrA recognizes the damaged nucleotides and targets UvrB to the site. UvrC cleaves both sides of the damaged nucleotide. UvrD helicase releases UvrC and excises the damaged nucleotide. Polymerase I fills in the gap and ligase seals it.

The UvrC protein contains two distinct catalytic sites. The N-terminal half of the protein carries the catalytic activity for cleavage of the 3' side and the C-terminal half of the protein is responsible for incision on the 5' side of the lesion (Lin and Sancar, 1992; Verhoeven et al., 2000). UvrC thus hydrolyses the 4th or 5th phosphodiester bond on the 3' side of the lesion, and immediately after, hydrolyses the 8th phosphodiester bond on the 5' side. A truncated N-terminal UvrC protein is capable of incising the 5' if the substrate is prenicked in 3', meaning that the C-terminal side of the protein is autonomous for 5' incision (Verhoeven et al., 2000).

An UvrC homolog, Cho (UvrC homolog), has also been described as part of the NER pathway. Unlike UvrA, UvrB and UvrC, Cho is poorly conserved and is only present in a few Prokaryote branches. Cho, like UvrA and UvrB, but unlike UvrC, is SOS induced (Courcelle et al., 2001; Moolenaar et al., 1987). Cho is capable of incising DNA at the 3' side of the lesion but not the 5' side. The incision made by Cho is 4 nucleotides further away from the adduct, probably because Cho binds to a different domain of UvrB than UvrC does. Depending on the type of damage, Cho's 3' incision efficiency can be higher than that of UvrC, meaning that the activity of Cho or UvrC can be better suited depending of the type of damaged substrate. However, Cho's activity is limited to the 3' incision and UvrC is strictly required for the subsequent 5' incision (Moolenaar et al., 2002; Van Houten et al., 2002).

Once the UvrABC proteins have carried out recognition and incision of the lesion, UvrD helicase (also called helicase II) excises the damaged oligonucleotide. Orren *et al.* showed in 1992 that once UvrC (and/or Cho) have performed incision, UvrB-UvrC and the damaged DNA stayed bound together, forming a post-incision complex. Binding of UvrD releases UvrC and the damaged oligonucleotide, and UvrB stays bound to the single strand gap until Polymerase I binds and promotes its removal (Orren et al., 1992). Polymerase I fills the gap by synthesizing the new oligonucleotide and DNA ligase seals the ends.

Because the main drug we are using in the laboratory is Mitomycin C (MMC), I will briefly resume state of the art knowledge on MMC-induced NER.

As previously mentioned, MMC is an inter-strand crosslinking agent which most usually leads to DSBs, dealt with by homologous recombination. It has been shown that the NER pathway is involved in the repair of MMC ICLs but various models, all leading to a DSB, are proposed.

In 1973, Cole proposed a first model involving sequential NER and HR steps. The ICL is first incised on each side. A nuclease widens the gap and this allows for strand exchange between homologous sisters. One of the DNA strands still carries the ICL adduct, which is then excised by NER enzymes in a final step (Cole, 1973).

In Eukaryotes, a different nonexclusive model exists. Replication forks may stall at an ICL and wait for endonucleases to process the ICL and create a double strand break, further processed by HR (Hanada et al., 2006; Kuraoka et al., 2000).

Another model, proposed by Weng and coworkers proposes that the UvrABC proteins can make a dual incision on both strands of the ICL, creating a double strand break and generating DNA fragments corresponding to the liberated DNA inter-strand crosslink (Weng et al., 2010). The group of Greenberg confirmed this model. They showed *in vitro*, that 15% of the ICLs created by C4'-oxidized abasic site (C4-AP) lead to a toxic double strand break. However, this type of ICL is particular because it is adjacent to a nick (Sczepanski et al., 2009). Soon after, they showed that in the case of an inter-strand crosslink produced by DNA radicals or radical ions arising from gamma-radiation, double strand breaks occur in 25-29% of the incision events. They propose that these double strand breaks are the result of a double incision by UvrC occurring on both strands. The hypothesis of a double incision is favored rather than a re-association of the protein after a first round of incision because UvrABC is not expected to bind the ternary complex created following the initial incision (Peng et al., 2010).

c) *Transcription-coupled Nucleotide excision repair*

Transcription coupled NER (TC-NER) is a specific NER pathway that removes lesions of the transcribed strand of expressed genes. TC-NER initiates when the RNA polymerase stalls at a lesion in the DNA template. It was first shown that removal of pyrimidine dimers on the transcribed strand is much quicker than that of the non-transcribed strand (Mellon and Hanawalt, 1989). This bias is the result of Mfd (mutation frequency decline) protein activity. Mfd, also called transcription repair coupling factor, dislodges the stalled RNA polymerase and enhances NER repair by promoting rapid recruitment of UvrA to the lesion (Selby and Sancar, 1993, 1995). The downstream events are analogous to NER as described above.

4. Formation of DNA breaks by unrepaired lesions: single strand Gaps (SSG), Single strand Breaks (SSBs) and double strand breaks (DSBs)

a) Single Strand Gaps

Single strand gaps are stretches of DNA where one of the DNA strands carries a gap of nucleotides. Such gaps can occur naturally during replication, which distinguishes them from single strand breaks.

i. Replication lesion bypass

MMR, BER and NER repair pathways are very efficient at eliminating DNA lesions. However, some lesions remain unresolved. It was originally described that when the replication fork encounters a DNA lesion, it stalls, but the DnaB helicase keeps unwinding, creating a single strand gap opposite the lesion. Pol III may dissociate and resume replication downstream of the lesion (Rupp and Howard-Flanders, 1968). Later, work from Yeeles and Marians revealed that upon encounter with a lesion, the replication fork does not dissociate from the DNA, it “skips” the lesion, and resumes replication downstream of the damage in a DnaG-dependant leading strand re-priming manner (Yeeles and Marians, 2011). Another model suggests that the replisome may dissociate, allowing replication to continue on the lagging strand, and creating subsequent single strand DNA regions on the leading strand (figure 14) (Heller and Marians, 2006). Such replication lesion bypasses give rise to single stranded gaps that will be further processed by Translesion Synthesis (TLS) or Homologous Recombination (Fujii et al., 2006).

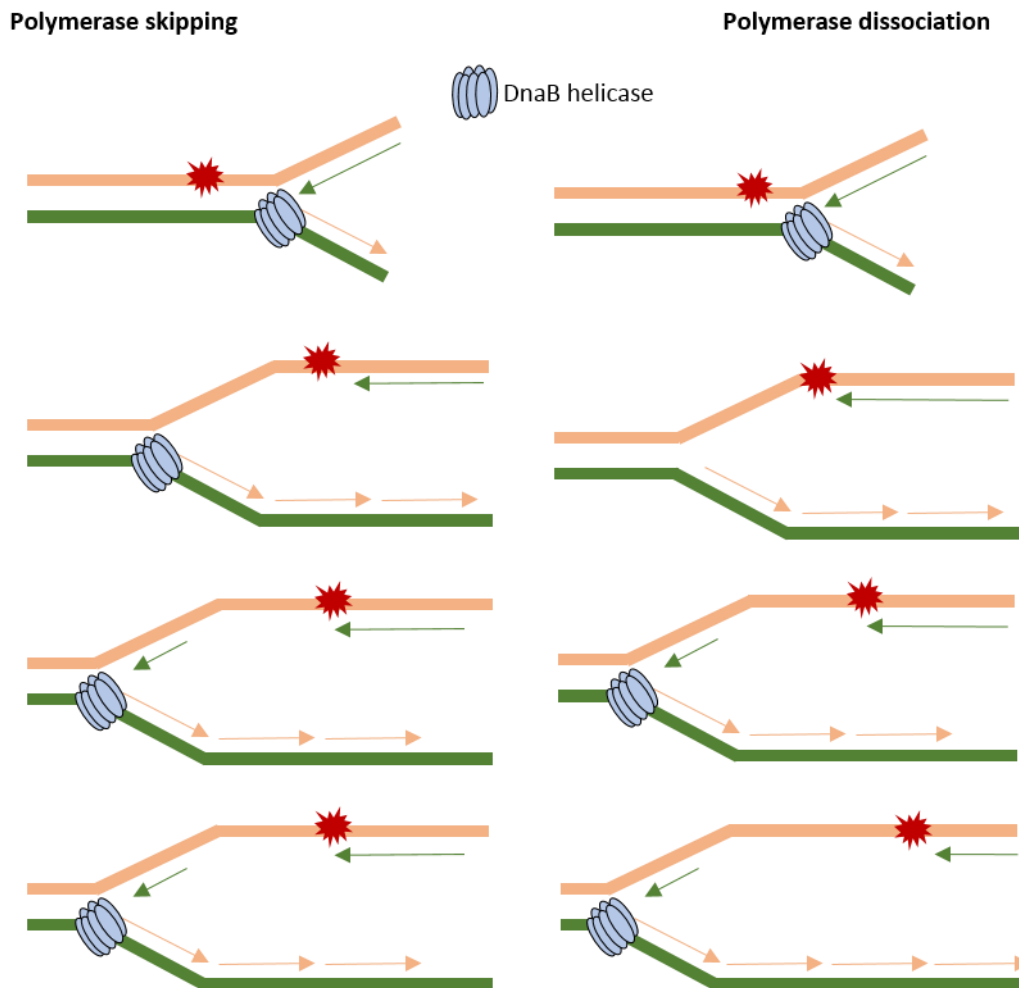


Figure 14. Two models for replication lesion bypass

In the Polymerase skipping model, the Polymerase does not dissociate from the DNA. It skips the lesion and resumes replication after the lesion. In the Polymerase dissociation model, the polymerase dissociates. DnaB helicase keeps unwinding and the Polymerase then reassociates downstream of the lesion.

ii. Chain terminators: The example of AZT

Chain terminators act by stalling replication forks rather than damaging the DNA itself. Various chemicals act as chain terminators (stavudine D4T, didanosine ddi...), but one of the most commonly used is 3'-Azidothymidine (AZT).

AZT is used to treat HIV by preventing reverse transcription of the viral RNA to DNA. The azido group replaces the 3'OH of thymidine and blocks replication (Cooper et al. 2011). AZT has been shown to be highly genotoxic for cells and induces the SOS response (Mamber et al., 1990). By blocking replication of the bacterial DNA, AZT leads to the formation of large single strand gaps (ssGaps) (figure 15).

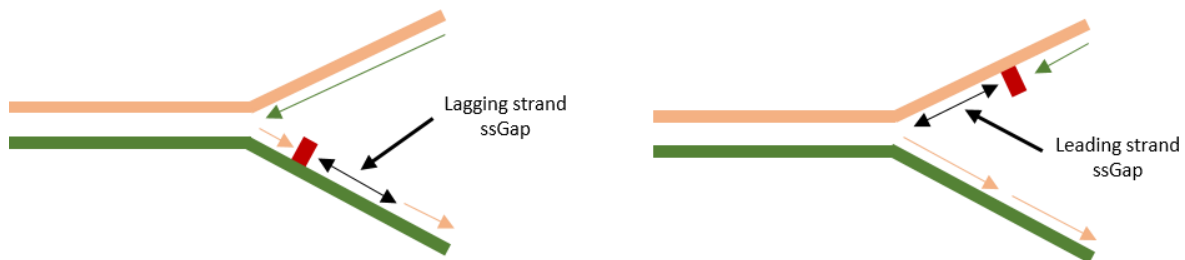


Figure 15. Formation of single strand Gaps by AZT incorporation

AZT is incorporated in replicating DNA and halts replication. This forms large single stranded gaps on the lagging or leading strand.

RecFOR proteins are involved in the repair of ssGaps by homologous recombination. Sensitivity of RecFOR mutants to AZT suggests that Recombination is initiated by these SSGaps. Interestingly, RecBCD mutants (repair of DSBs by homologous recombination) are also highly sensitive, meaning that a large amount of these single strand gaps may be converted to double strand breaks, repaired by HR. This hypothesis is strengthened by the sensitivity of RuvABC mutants, involved in the resolution of Holliday Junction HR-intermediates (Cooper and Lovett, 2011). The sensitivity of Exonuclease III (Exo III) mutants suggests that Exo III (also involved in the excision of damaged bases in BER) is required to remove the residual AZT from DNA.

iii. Nucleotide depletion: the example of Hydroxyurea (HU)

HU is an inhibitor of ribonucleotide reductase (RNR), the enzyme responsible for dNTP synthesis, thereby reducing the cellular levels of deoxynucleotide precursors for DNA replication (Timson, 1975). HU has been shown to reduce the dNTP pool in a variety of mammalian cells and in *E. coli* (Sneeden and Loeb, 2004), thereby provoking DNA damage independent stalling. Translesion polymerases, Pol IV and Pol V play a role in the processing of DNA damage independent replication stalling (Godoy et al., 2006). Pol IV and Pol V affinity for dNTPs is much lower than that of Pol III, which could explain why they can function in nucleotide-depleted cells. Surprisingly, wild type cells still manage to replicate upon HU treatment, albeit at a slower rate. This could be due to a cycling of translesion synthesis polymerase recruitment and subsequent handoff to the replicative Pol III (Godoy et al., 2006). HU treatment induces the SOS response. Indeed, a micro array experiment revealed that SOS genes such as SulA, RecN, RuvA and UvrB were overexpressed in HU treated cells suggesting that various repair pathways may be involved in the HU stress response (Davies et al., 2009).

b) *Single strand Breaks*

The main sources of single strand breaks (SSBs) are frozen Topoisomerase I, oxidative damage or spontaneous disintegration of deoxyribose (Hegde et al., 2008; Wang, 2002). But SSBs also arise from failure to complete repair mechanisms such as BER and NER (Uphoff et al., 2013).

c) *Double strand Breaks*

Crosslinking agents, DNA adducts or thymidine dimers induced by UV light can ultimately provoke DSBs if not correctly removed and repaired. Indeed, these unattended lesions can provoke single strand breaks that, upon encounter with the replication fork will create a double strand break (Kuzminov, 2001). Another less common, but highly damageable double strand break inducing factor is ionizing radiations (Schulte-Frohlinde, 1994).

i. Arrested replication forks lead to double strand breaks

It has been quite extensively documented that Double Strand Breaks (DSBs) can arise during replication (Kuzminov, 1995; Michel et al., 1997). Such DSBs can result from the encounter of the replication fork with a nick or a gap in the template DNA (Kuzminov, 1995), but compelling evidence shows that these DSBs may be the result of arrested replication forks. Indeed, homologous recombination seems to be essential for viability in certain DNA helicase mutants such as *rep* and *dnaB*, meaning that replication defects cause DNA damage that needs HR for repair (Michel et al., 1997, 2001).

Ligase and Pol I mutants require RecBCD and RecA for viability (Kuzminov, 1995), probably due to small nicks and gaps in the lagging strand, resulting from unsealed Okazaki fragments.

hold (subunit of the Pol III clamp loader) mutants require RecBCD for viability. These mutants undergo frequent replication arrest, suggesting that lesions induced by replication fork arrest require recombinational proteins (Flores et al., 2001).

ii. Double strand breaks induced by Replication Fork Reversal

Replication forks can also be arrested by blocking lesions (resulting from UV irradiation for example), or *bona fide* replication blocks such as the Tus/Ter complex (Horiuchi et al., 1994). When such replication forks are arrested, they undergo a specific reaction called replication fork reversal (RFR), transforming the blocked replication fork into a recombination substrate (figure 16).

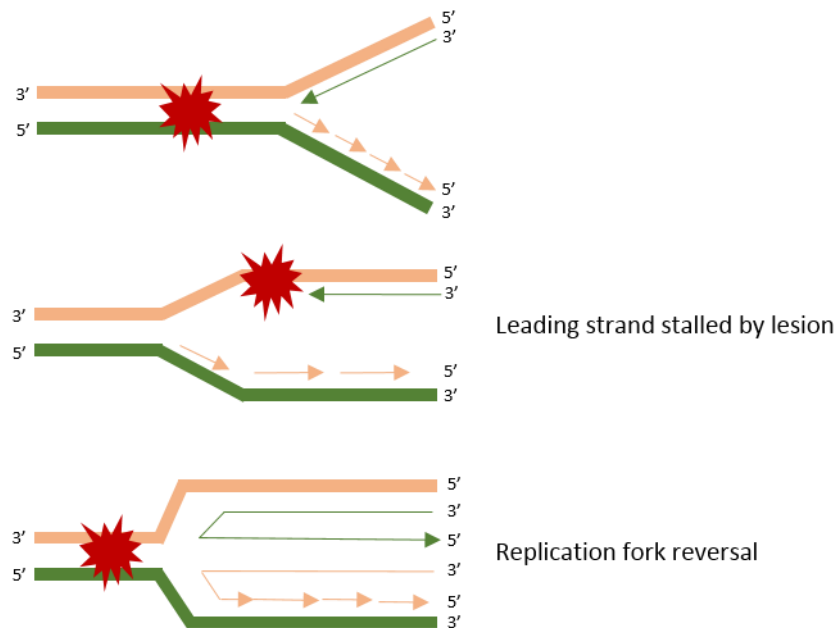


Figure 16. Replication fork encounter with a DNA lesion may lead to replication fork reversal

Upon encounter of the replication fork with a lesion, the two newly synthesized strands can re-anneal and form a recombination substrate.

Indeed, double strand breaks formed by stalled replication forks in *rep recB^{ts} recC^{ts}* mutants are suppressed by inactivating RuvA or RuvB (Seigneur et al., 1998). RuvA and RuvB are two proteins belonging to the RuvAB operon. They are involved in the late steps of Holliday Junction resolution (Lloyd et al., 1984). Seigneur *et al.* propose that a Holliday Junction recombination intermediate is formed at blocked replication forks and that the action of RecBCD and RuvAB rescues these blocked forks, avoiding the formation of DSBs and allowing the reconstitution of a new replication fork. RuvAB may bind to the arrested replication fork, favoring the formation of a Holliday Junction. Once formed, the junction migrates, either toward the terminus or toward the replication origin, creating a double strand tail, a substrate for RecBCD helicase. RecBCD then resects up to the RuvAB-DNA complex, allowing the assembly of a new replication fork and PriA dependent replication restart, without creating a chromosome break (Seigneur et al., 2000).

An alternative yet not incompatible model, suggests that RecG is involved in the processing of stalled replication forks by reversing the fork. In 2000, McGlynn and Lloyd demonstrated that

RuvAB does not catalyze the actual formation of Holliday Junctions although these proteins can be involved in their resolution. They rather propose that RecG acts on stalled replication forks to form a Holliday Junction that does not require subsequent cleavage for replication resumption. This particular feature circumvents the creation of a possibly deleterious double strand break (McGlynn and Lloyd, 2000). A year later, they showed that RecG can unwind the leading and lagging strands *in vitro* (McGlynn and Lloyd, 2001).

Interestingly, it was proposed that UvrD, the NER helicase, may also be acting at stalled replication forks. Flores and coworkers constructed different genetic backgrounds prone to replication fork reversal: a *DnaN^{ts}* mutant (thermosensitive allele of the β -lamp loader) and a *DnaE^{ts}* mutant (Catalytic subunit of the Pol III holoenzyme). They combined these mutations with inactivation of RecBC to measure the amount of linear DNA in the presence or absence of UvrD. In these mutants, the Holliday Junctions formed by the subsequent fork reversal are processed by RuvAB independently of DSB end processing by RecBC.

In a *DnaN^{ts} RecBC^{ts} uvrD* mutant, the amount of linear DNA is decreased suggesting that less DSBs are formed. This observation gives rise to a role for UvrD in the formation of reversed forks. These UvrD formed reversed forks would be toxic and lead to DSBs (i.e linear DNA) in a *DnaN^{ts} RecBC^{ts}* mutant. The same phenotype was observed for a *DnaE^{ts} RecBC^{ts} uvrD* mutant. They propose that UvrD could act to unwind the leading and/or lagging strand, maybe with another protein. An alternate model could be that UvrD removes proteins that are bound to the blocked fork, allowing another protein to catalyze fork reversal *per se* (Flores et al., 2004) (figure 17). PriA then directs the reestablishment of the replisome and replication resumption (Marians, 2000). Once the fork is recovered, the lesion can be repaired (Singleton et al., 2001).

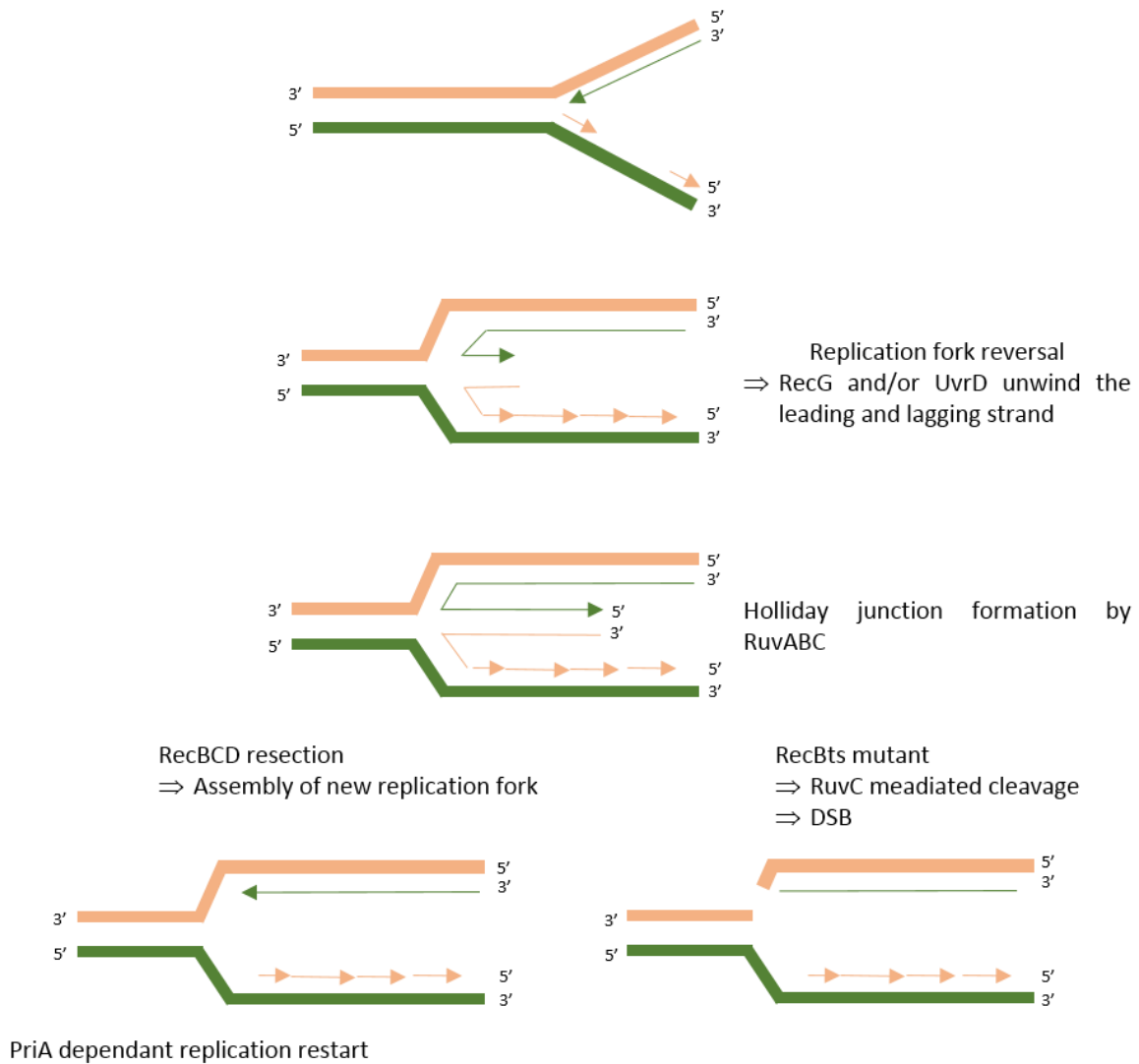


Figure 17. Formation of a double strand break upon replication fork reversal

RecG and/or UvrD unwind the leading and lagging strand. RuvABC forms a Holliday Junction. In WT cells, RecBCD resects the reversed fork and allows for the assembly of a new fork. In *RecB^{ts}* mutants, RuvC cleaves the HJ intermediate leading to a DSB.

iii. Overview of MMC-induced double strand breaks

Since MMC is the main genotoxic agent I used for my experiments, I have summarized the main causes of MMC-induced double strand breaks in (figure 18). However, this is not an exclusive summary as other pathways may lead to MMC-induced double strand breaks. It is interesting to note that the DSBs seem to arise in the case of pathogenic or poorly processed repair pathways.

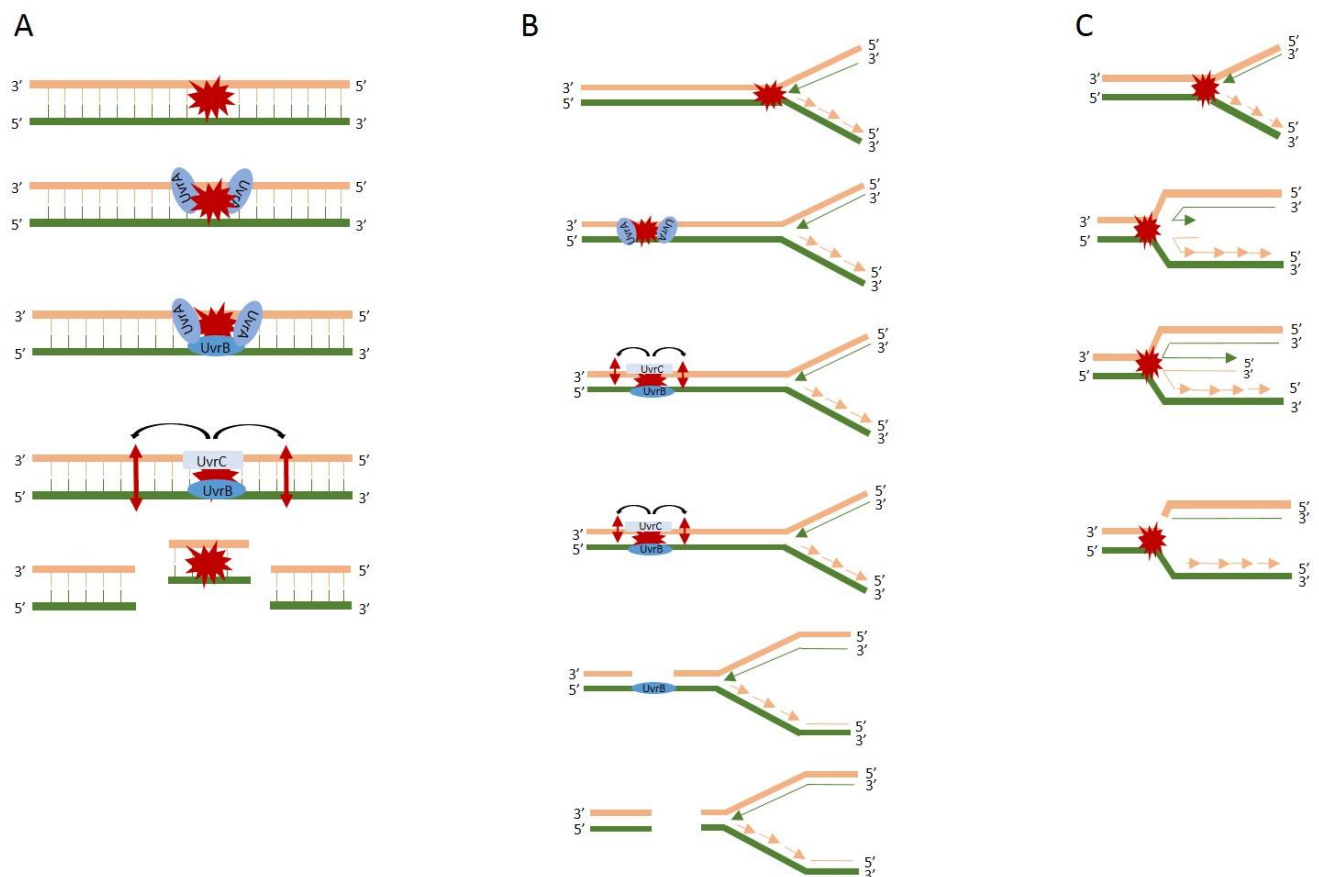


Figure 18. MMC-induced double strand breaks

Various pathways can lead to MMC-induced double strand breaks. A) During the NER management of an MMC-ICL, UvrC can perform a double incision leading to a double strand break and liberate the ICL associated DNA fragment. B) During the NER pathway, UvrC performs a single incision creating a single strand gap. If this single strand gap is not correctly processed by polymerase I and Ligase, the subsequent encounter with the replication fork may lead to a DSB. C) The encounter of a replication fork with an MMC induced ICL may lead to replication fork reversal. Such RFR can lead to a DSB if it not correctly processed.

5. Repair of single strand gaps, single strand breaks and double strand breaks

a) General overview of the the SOS response

In 1974, Miroslav Radman first described the existence of a pathway induced upon DNA damage in *E. coli*: the SOS response (Radman, 1975). Other Prokaryote species also have similar DNA damage inducible responses but to date, the *E. coli* SOS response has been the most extensively characterized. Two main proteins, LexA and RecA regulate the SOS response. In the absence of DNA damage, LexA forms a dimer that binds to a 20 bp palindromic sequence called a *lexA box*. These *lexA boxes* are in the promoter region of the SOS genes. When LexA dimer is bound to the *lexA boxes*, the expression of the genes is repressed. Although LexA and RecA are constitutively expressed, they are also under the control of a *lexA box* (Brent and Ptashne, 1981). When DNA is damaged, single strand DNA regions are bound by RecA, which polymerizes along the ssDNA, in an ATP-dependent manner, forming a nucleoprotein filament. Under this polymerized form, RecA's coprotease activity is activated, triggering the auto-cleavage of LexA. When LexA is cleaved, it cannot bind the *lexA boxes*, and the repressed genes can thus be transcribed. Over 100 genes are regulated by *lexA boxes*, involved in different functions of DNA repair (Courcelle et al., 2001) (figure 19).

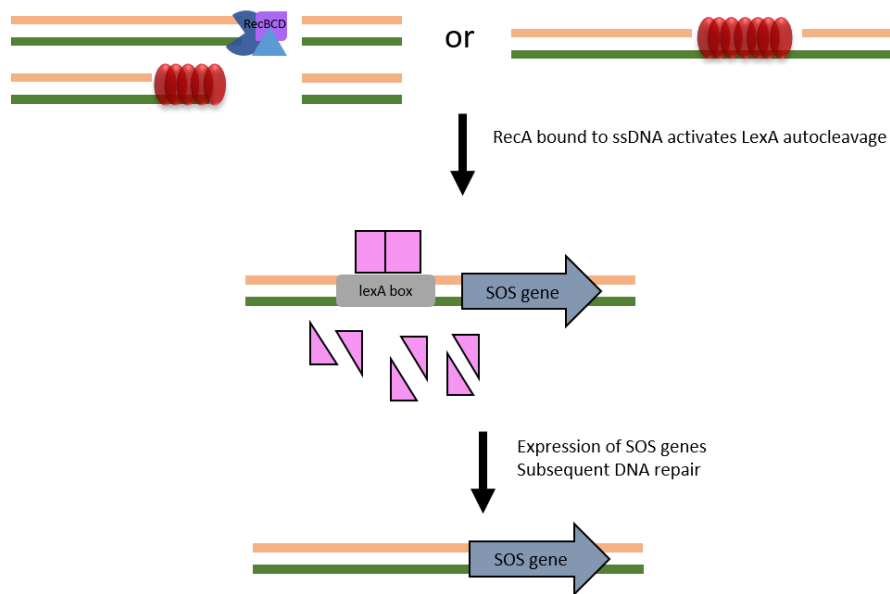


Figure 19. Simple representation of the induction of the SOS response in *E. coli*

RecA binds to ssDNA which activates autocleavage of LexA, the repressor of SOS genes. Once LexA is cleaved, expression of the SOS response genes is permitted. When the break is repaired, ssDNA decreases, RecA does not bind ssDNA and cleavage of LexA is repressed.

When damage has been repaired, the availability of ssDNA decreases, RecA filament decreases and LexA can dimerize and bind the *lexA boxes*, thus repressing the SOS genes (Walker, 1984). In the next section, I will describe the various induction steps and responses of the SOS pathway, emphasizing on the regulation and activity of the key players, LexA and RecA.

b) *LexA, the SOS repressor*

LexA protein (locus for x-ray sensitivity A) is encoded by the *lexA* gene. LexA protein has two major domains: the N-terminal domain which is important for dimerization and the C-terminal domain which is important for auto-cleavage. Serine 119 and lysine 156 are the two essential residues for LexA auto-cleavage (Slilaty and Little, 1987). Actual cleavage of the protein occurs at a specific site between Ala84 and Gly85 (Horii et al., 1981).

In 1980, Little *et al.* showed that RecA specifically catalyzed this cleavage reaction (Little et al., 1980). Later, it was shown that in the absence of RecA, cleavage of LexA could also be stimulated by alkaline pH, notably by Co^{2+} , Ca^{2+} or Mg^{2+} . This observation led to the hypothesis that RecA was not cleaving LexA in a direct reaction, as a protease would, but could rather be an allosteric effector of the protein or act by lowering the pK of a critical LexA lysine residue. The term “co-protease” rather than protease was thus proposed, to emphasize RecA’s indirect role in LexA cleavage (Little, 1984, 1991).

The mechanism by which RecA stimulates LexA cleavage has been extensively studied but remains unclear. The resolution of crystal structures of LexA revealed that LexA can adopt different conformations, one that is compatible with cleavage and the other that isn’t (Luo et al., 2001). Giese and coworkers showed in 2008 that RecA can bind LexA in its non-cleavable form and promote the conversion to its cleavable form through an allosteric mechanism (Giese et al., 2008). The fragments produced by the auto-cleavage of LexA are further degraded by ClpXP protease. ClpXP specifically recognizes the cleaved peptides of LexA and not the full length of LexA protein, ensuring that ClpXP degrades LexA once RecA has catalyzed the auto-cleavage of LexA and allowed induction of the SOS response and not in the absence of DNA damage. Lon Protease has also been shown to degrade LexA peptides (Neher et al., 2006). Various mutants of LexA have been characterized. The most commonly used are the *lexA ind-* (*lexA3*) and the *lexA null* mutants that I have both used during my thesis. The *lexA ind-* mutant is non cleavable. Mutations around the cleavage site (Ala84-Gly85) or near the Ser 119 and Lys 156 residues, which are important for the cleavage reaction, lead to the *lexA ind-* phenotype (Lin and Little, 1988). A *lexA deficient* mutant allows constitutive SOS induction, but its mutation must be combined to a mutation in the *sulA* gene that induces excessive cell filamentation if not repressed (Mount, 1977; O’Reilly and Kreuzer, 2004).

c) *RecA, the central protein of the SOS response*

i. RecA’s general function

RecA is undoubtedly the key protein of the SOS response. It belongs to the family of DNA strand exchange proteins comprising RecA and Rad51 protein family that are essential for

homologous recombination (Lin et al., 2006). The protein has three main functions in the cell: Pairing and strand exchange of homologous DNA molecules; Induction of the SOS response and the activation of Polymerase V for Translesion Synthesis.

ii. RecA loading

The structure of RecA was first described in 1992 by Story and Steitz. One RecA monomer binds three nucleotides, thus polymerizing nonspecifically on ssDNA (and to a lesser extent, dsDNA) in an ATP-ase dependent manner. RecA bound to ssDNA forms a helical nucleofilament, which is the active form of the protein for DNA strand exchange and LexA cleavage (Story and Steitz, 1992). RecA is a polypeptide containing 352 amino acid residues and has a molecular mass of 38 kDa, that is basally expressed at a level of approximately 1000 monomers per cell (figure 20).



Figure 20. Structure of RecA presynaptic nucleofilament

Construction of the filament results from fusion of 6 RecA genes in tandem spaced with linkers between them. DNA binding, DNA-dependent ATPase and strand-exchange activities of the RecA5 and RecA6 are comparable to those of monomeric RecA. The 6 RecA protomers are numbered from the N-terminal of the RecA fusion protein. DNA backbone is in red.

Two distinct pathways serve to load RecA, the RecFOR pathway and the RecBCD pathway.

- RecFOR mediated loading of RecA

The RecF pathway has been described to manage the repair of single strand gaps (ssGaps) (Horii and Clark, 1973). A mutant protein of RecA, RecA803 gave further insight into the possible role of RecFOR on RecA loading. This RecA mutant is a suppressor of RecF, RecO and RecR mutations (Volkert and Hartke, 1984; Wang and Smith, 1986). RecA803 can displace SSB protein from single stranded DNA with a higher efficiency than the wild type RecA. It was thus hypothesized that RecF, RecO and RecR are involved in RecA loading on single stranded DNA (Sawitzke and Stahl, 1992). It was further demonstrated that it is the combined action of the three proteins that is required for loading of RecA specifically onto SSB coated ssGaps. RecF recognizes the 5' end of dsDNA at the junction between ssDNA and dsDNA. RecO and RecR then bind RecF and help load RecA onto the SSB-coated ssDNA. Moreover, RecFOR provides a stabilizing function for RecA filament formation against the competitive effect of SSB protein, but only on ssGaps (Morimatsu and Kowalczykowski, 2003). It is further suggested that in the RecFOR pathway, a mediator protein may be required for targeting of RecFOR to the dsDNA-ssDNA junction at the end of a DNA gap (Sakai and Cox, 2009) (figure 21A).

In 2009, Sakai and Cox showed that RecOR can define a distinct pathway from RecFOR for RecA loading onto ssDNA. When no duplex DNA is adjacent to the loading site, RecOR is more efficient for RecA loading. This pathway depends on the interaction of RecO with the C-terminus region of SSB (Sakai and Cox, 2009). RecO may displace SSB protein from the ssDNA, but RecA does not load until RecR has bound RecO (Inoue et al., 2008) (figure 21B).

Interestingly, in the RecFOR pathway, the interaction of RecO with SSB is not required. Instead, RecO may serve to load RecR rings onto the DNA, thus helping RecR as a RecA loader.

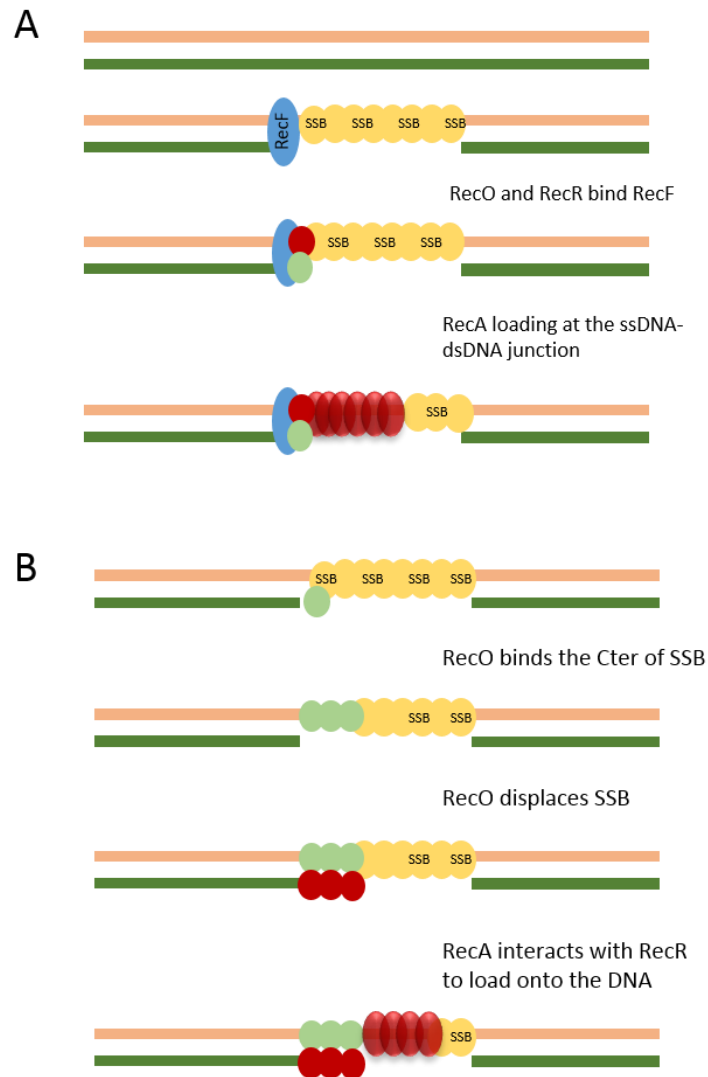


Figure 21. RecA loading through the RecFOR pathway

A) RecFOR loading of RecA. RecF recognizes the 5' end of the ssDNA-dsDNA junction. RecO (green) and RecR (red) bind RecF and help RecA displace SSB. B) RecOR loading of RecA. RecO interacts with the C-terminus of SSB and may displace it. RecR binds RecO and helps loading of RecA.

- RecBCD mediated loading of RecA

In the case of a double strand break rather than a single strand gap, RecBCD enzyme activity is necessary for RecA binding. RecBCD substrate is a free double strand DNA nearly blunt end (no more than 25 nucleotides offset between the 3' and 5' end) (Taylor and Smith, 1985).

RecBCD is a helicase-nuclease, where RecB and RecD are helicases that exhibit different processivity, travelling in the same direction but opposite polarities (Dillingham et al., 2003). RecBC unwinds while simultaneously degrading the DNA (Taylor & Smith, 1985). RecD helicase is faster than RecB helicase, resulting in the formation of a loop ahead of RecB (Taylor and Smith, 2003). As RecBCD translocates along the dsDNA, the 3' terminated strand is passed through a *chi* recognition site in the RecC protein (Handa et al., 2012). In *E. coli*, *chi* (Crossover Hotspot Instigator) is an octamer sequence (5'-GCTGGTGG-3'). Interaction of RecBCD with the *chi* site induces a switch in the nuclease polarity activity. The 3' to 5' nuclease activity is attenuated and the 5' to 3' activity is enhanced (Anderson and Kowalczykowski, 1997), creating a dsDNA with a ssDNA tail, terminated at its 3' end. RecBCD's end resection activity has recently been observed with the use of a fluorescent reporter *in vivo*. RecBCD resection is very fast (approx. 1.6kb/sec) and processive (approx. 1kb). It can even resect as far as 250kb from the break on the Ori-distal side of the break. Interestingly, degradation is not symmetrical on both sides of the break. The Ori-distal region is more extensively degraded than the Ori-proximal end of the break. This can be simply explained by the amount of *chi* sites that is higher near the origin in order to better protect it from degradation (Wiktor et al., 2018).

RecBCD further enables RecA loading onto the single strand tail created by RecBCD activity (figure 22). Loading of RecA onto the *chi* containing strand results from the combined activity of RecA and RecBCD, alleviating the inhibitory effect of SSB (Anderson and Kowalczykowski, 1997). More specifically, it was proposed that it is the RecBC enzyme that loads RecA onto the ssDNA. RecD subunit may act to block RecA loading, until the encounter with the *chi* site (Churchill et al., 1999).

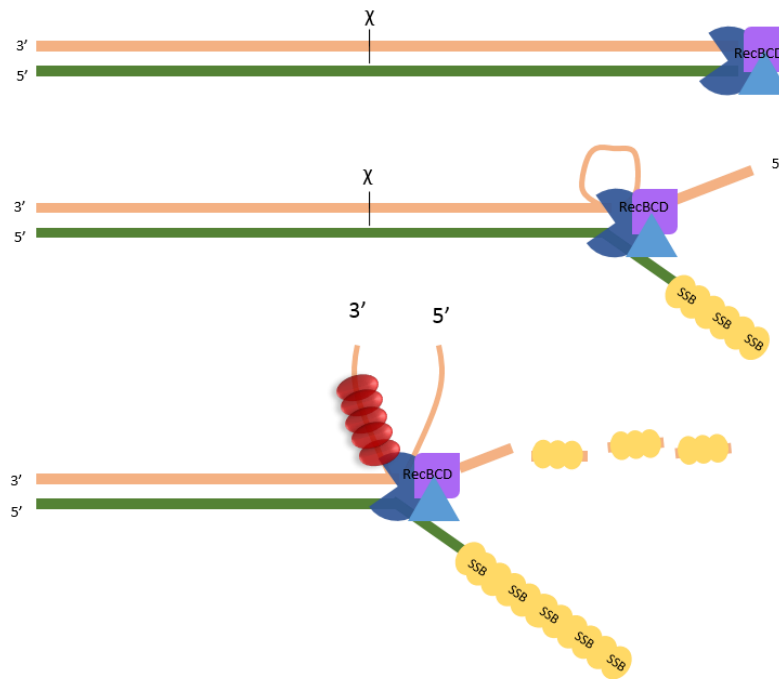


Figure 22. RecA loading through the RecBCD pathway

RecBCD resects the DNA until it encounters a χ site. Upon encounter with the χ sequence, RecBCD's activity is altered creating a single strand DNA extension. RecBCD then helps RecA to load onto the ssDNA by displacing SSB.

iii. Formation of RecA nucleofilament

RecA assembly on ssDNA occurs in the 5' to 3' direction, and preferentially nucleates at ssDNA-dsDNA junctions containing 5' termini (Register and Griffith, 1985). The direct observation of filament assembly on double stranded DNA, using fluorescently labeled RecA, revealed that filament growth rates range from 3 to 10 nm.sec⁻¹ (Galletto et al., 2006). DNA entrapped in the RecA nucleofilament is relaxed 1.5 times compared to unbound DNA (Nishinaka et al., 1997).

Binding of RecA on double stranded DNA has been described but is not the major substrate for RecA polymerization (Pugh and Cox, 1987). Nucleation rates on ssDNA are much higher than on dsDNA at a neutral pH. When RecA nucleation occurs on ssGaps (rather than a single stranded overhang), it may nucleate out of the gap and polymerize on the contiguous dsDNA (Shan and Cox, 1997). On a ssDNA substrate, it was shown that one RecA monomer binds

approximately 3 nucleotides and has a helical pitch of 6 monomers per turn. The bound RecA subunits were shown to be arranged in order to expose RecA-bound DNA, enabling contact with dsDNA, probably to facilitate homology search (Egelman and Stasiak, 1986).

As described above, RecA binding onto ssDNA in the absence of DNA damage is inhibited by preferential binding of SSB. Binding of ssDNA by SSB is important to protect ssDNA from nucleolytic activity but also to avoid the formation of non-necessary secondary structures and homologous recombination. Thus, there exists a competition between SSB and RecA for ssDNA binding. SSB-ssDNA prevents RecA filament assembly. In the presence of DNA damage, RecFOR helps RecA displace SSB and bind to ssDNA.

Recently, a direct interaction between RecA and SSB was proposed using a single molecule tethered particle motion (TPM) technique (Wu et al., 2017). Using monitored amounts of SSB, a RecA filament assembly involving a RecA-SSB interaction was shown. RecOR stimulates RecA binding onto SSB-ssDNA. They propose that RecOR stimulation reveals the required RecA binding domain for SSB interaction. This interaction however, is weak as it was not identified by pull down assays. Moreover, a strong interaction would maintain SSB bound to RecA, leading to inefficient RecA filament formation (Wu et al., 2017).

Regulation of the RecA nucleoprotein filament is crucial since RecA filament directs SOS induction, homology search and drives homologous recombination. Poor regulation of RecA nucleofilament could therefore affect these steps of the DNA damage response and compromise efficient DNA repair. Many proteins are thus involved in the regulation of RecA filament formation and stabilization. RecX, DinI, PsiB, RdgC and possibly other uncharacterized proteins participate in RecA filament dynamics.

RecX is a 19.4 kDa protein that is necessary to overcome deleterious effects of RecA overexpression (De Mot et al., 1994). *In vitro*, RecX inhibits the ATPase strand exchange activity of RecA. RecX is therefore a negative regulator of RecA protein activities. Drees & coworkers showed that RecX's function is to block RecA filament assembly. Through a direct RecA-RecX interaction, RecX caps the assembly ends of the filaments and limits its extension. (Drees et al., 2004). *In vitro*, independently of RecX, dissociation of RecA subunits requires ATP-hydrolysis and proceeds at approximately 70 monomers per minute per filament end

(Arenson et al., 1999). Monomers disassemble primarily at the end opposite to which assembly occurred.

In vivo, the ***DinI*** protein stabilizes RecA filament formation. DinI acts to prevent disassembly of RecA filaments but does not enhance its formation. Interestingly, at high concentrations, DinI destabilizes the RecA filaments. At very high concentrations, DinI has a very deleterious effect on RecA filaments, and most RecA activities are inhibited (Lusetti et al., 2004; Yasuda et al., 1998).

The concerted action of DinI and RecX seems essential for proper RecA filament assembly and stabilization. In fact, there may be some sort of competition between RecX and DinI. RecX can bind at the end of the RecA filament, preventing filament extension, but also along the filament length. Binding of RecX along the filament competes directly with DinI binding, and slow dissociation of one protein allows binding of the other protein. Thus, these two proteins exhibit mutually exclusive and opposite activities that are key modulators for RecA activity and the SOS response (Lusetti et al., 2004).

Another regulator of RecA is ***RdgC***. RdgC is a DNA binding protein that binds ssDNA and dsDNA aspecifically. It was proposed that RdgC may bind DNA and inhibit RecA binding and filament formation (Moore et al., 2003). RdgC was later shown to inhibit RecA activities (LexA cleavage, strand exchange at RecA's ATPase activity). RdgC and SSB have additive effects, and a high concentration of RdgC in SSB expressing cells can suppress RecA filament formation. It is therefore suggested that RdgC, somewhat like SSB, inhibits RecA filament formation by competing with RecA for ssDNA (Drees et al., 2006).

PsiB protein has also been shown to inhibit RecA activity. Unlike the other described genes, *psiB* is carried by the R6-5 plasmid, near the origin of conjugational transfer. Induction of the SOS response triggered by the entry of a conjugational plasmid in the cell may be highly deleterious due to division arrest or the induction of translesion synthesis polymerases. PsiB may inhibit SOS induction by inhibiting RecA function, thus protecting the conjugational plasmid and the host cell from the detrimental effects of an unwanted SOS induction (Bailone et al., 1988). PsiB protein actually binds RecA directly, when it is free from DNA, sequestering it, and preventing it from binding its ssDNA substrate (Petrova et al., 2009). If RecA cannot

bind DNA the amount of RecA available for ssDNA binding is reduced and so is the SOS induction (figure 23).

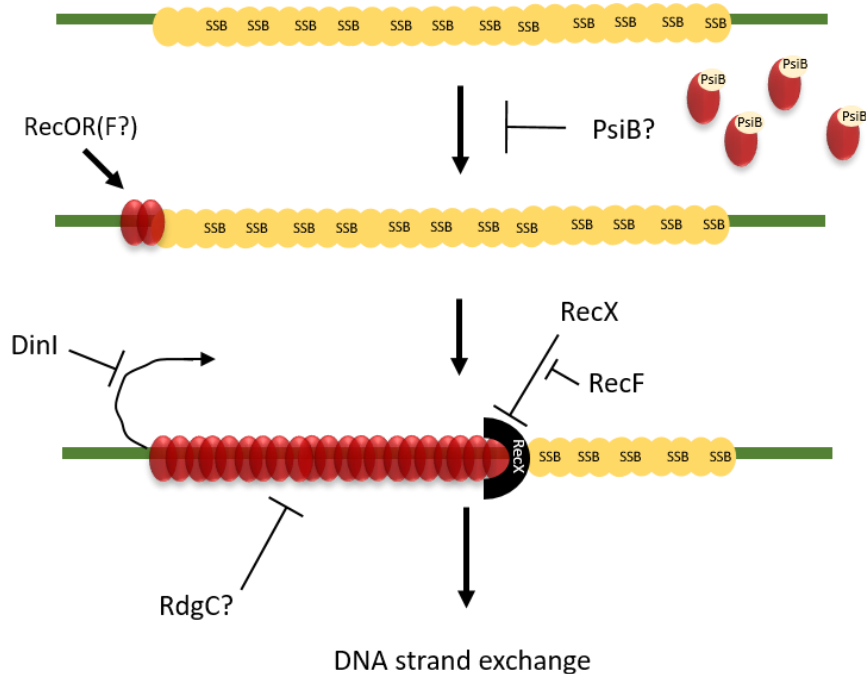


Figure 23. Regulation of RecA nucleoprotein filament formation

PsiB may bind free RecA, preventing it from binding ssDNA. RecFOR helps RecA binding on ssGaps. RecX caps the filament end and prevents its extensive propagation. On the other hand, DinI stabilizes RecA filament by interacting with its C-terminal end. RdgC may inhibit RecA binding by competing for ssDNA.

iv. RecA mediated induction of the SOS response

As mentioned above, one of the main functions of RecA is to induce the autocleavage of LexA, the SOS regulon repressor. Once bound to single stranded DNA, RecA mediates the cleavage of LexA repressor, which will allow the induction of SOS genes.

v. Homology search and strand invasion

Undoubtedly, the most fascinating yet poorly understood function of RecA is its ability to perform homology search. This function of RecA protein has been extensively studied, however it remains quite unclear how RecA, bound to ssDNA, can find the homologous sequence out of a 4.6 Mbp nucleoid.

- Homology search

The method by which ssDNA-RecA samples the dsDNA is controversial and may be the combination of various events. Previous *in vitro* studies revealed a possible 1D sliding of the RecA nucleoprotein filament on short DNA sequences. RecA diffuses along the dsDNA, sampling several hundred base pairs for homology, before dissociating when homology is not found (Ragunathan et al., 2012). The same year, Forget & Kowalczykowski proposed a “3D inter-segmental contact sampling model”. They showed that RecA could bind non-specifically and simultaneously distant dsDNA segments. This sampling is dependent on the 3D conformation and the length of the nucleoprotein filament (Forget and Kowalczykowski, 2012). Indeed, the coiled structure of the dsDNA is crucial for proper homology search. As coiling of the dsDNA is increased, the local concentration of DNA is higher. This enhances the probability of the RecA nucleoprotein filament to encounter multiple segments of dsDNA at a time. A recent paper shows that the RecA-mediated homology search occurs in various steps and time scales and could be the combination of both 1D sliding and 3D inter segmental transfers. Using Atomic Force Microscopy (AFM) they showed that multiple RecA-ssDNA nucleoprotein filaments associate with dsDNA, occupying nearly 20% of the target sequence space. Then, the sequences having found homology stay tightly bound, while the other sequences dissociate (Lee et al., 2017) (figure 24).

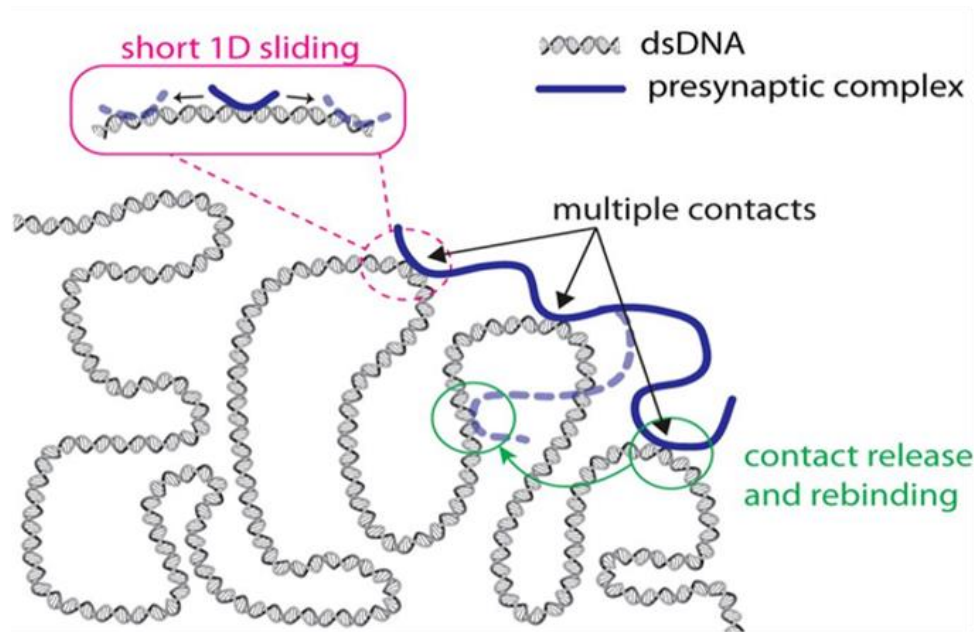


Figure 24. Model for homology search by short 1D sliding and 3D hopping

RecA can perform long range 3D hopping and short range 1D sliding along the chromosome.

From Forget and Kowalczykowski, 2012

In 2013, Lesterlin *et al.* published a non-exclusive model, describing the formation of “RecA bundles”, when a double strand break occurs on a sister chromatid previously segregated and distant from its homolog (i.e. a DSB induced by the I-sceI endonuclease). They propose that RecA bundles can promote the pairing of distant sister homologs, subsequently leading to the RecA-mediated strand invasion. The cut locus moves towards the uncut homologous locus, on the other side of the cell, irrespective of whether the homolog is present or not. If homology is found, pairing is observed. Super-resolution three-dimensional structured illumination microscopy (3D-SIM) and live cell time-lapse imaging gave some insight on the structure of these RecA bundles: RecA-bundles contain about 70% of the total amount of RecA protein, and are mainly DNA-free (Lesterlin *et al.*, 2014).

- Homology recognition

RecA has two DNA binding sites. The first DNA site binds the initial ssDNA and the secondary binding site can bind ssDNA or dsDNA (Müller et al., 1990). Mazin *et al.* later suggested that the secondary site can bind dsDNA first, allowing for homology search. Once the homologous sequence is found, it binds the ssDNA with a higher affinity than dsDNA (Mazin and Kowalczykowski, 1996). Considering RecA ATP-hydrolysis is not required for homologous recombination and strand exchange, it was hypothesized that it is not an active process.

The ssDNA bound by RecA is globally stretched but locally maintains a B-form structure. Binding of the dsDNA in the secondary site may induce a conformational change and stretch of the dsDNA (Chen et al., 2008). The bases of this locally disrupted dsDNA may rotate out of their hydrogen bond and sample the incoming ssDNA by forming a new, transient hydrogen bond (De Vlaminck et al., 2012). A minimum of 8 bp is required for stable homology pairing. In this case, the complex is highly stable and strand exchange can occur (figure 25).

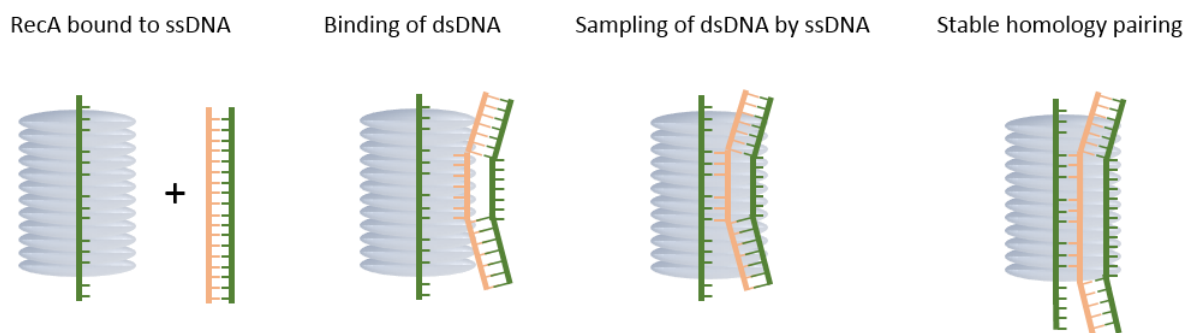


Figure 25. Mechanism for homology recognition by RecA

ssDNA is sampled by incoming dsDNA. Homology recognition is achieved when both DNA strands of the incoming dsDNA are bound to the ssDNA binding sites of the RecA filament. Homology pairing requires 8 bp for a stable complex to form and strand exchange to occur.

Adapted from De Vlaminck et al. 2012

When homology is found by correct recognition between the ssDNA and the dsDNA, the bond becomes stable and RecA can proceed with strand invasion. Strand invasion by RecA forms a D-loop structure, independently of ATP hydrolysis (Menetski et al., 1990).

vi. Branch migration and resolution

After D-loop formation, the original DNA strand from the dsDNA homolog is displaced and the ssDNA from the RecA nucleoprotein filament replaces it, forming a Holliday Junction (HJ). RecA then drives branch migration. ATP-hydrolysis renders polymerization unidirectional, in the 5' to 3' direction with respect to single stranded DNA. Rossi *et al.* showed that this ATP-hydrolysis dependency is the result of an association/ dissociation mechanism of RecA which is itself, dependent on ATP-hydrolysis (Rossi et al., 2011). In the presence of ATP-hydrolysis, the extent of branch migration is dependent on the length of available homology. In the absence of ATP hydrolysis, branch migration does not extend over a few kbs (Jain et al., 1994). The branch migration is capable of overcoming mismatches and various deletions or modified bases (Livneh and Lehman, 1982).

Branch migration is further processed by RuvA and RuvB. RuvA and RuvB stimulate strand exchange by RecA by acting upon the recombination intermediates formed by RecA. RuvA provides specificity by directly binding the HJ intermediate and RuvB acts as a motor for branch migration by ATP hydrolysis (Tsaneva et al., 1992).

RuvC nuclease, cleaves the Holliday Junction intermediate, at preferred sequences (Bennett et al., 1993) giving rise to a nicked DNA duplex that can be repaired by ligase. PriA helps load DnaB helicase to reassemble a functional replisome and allow replication restart (Kogoma et al., 1996) (figure 26).

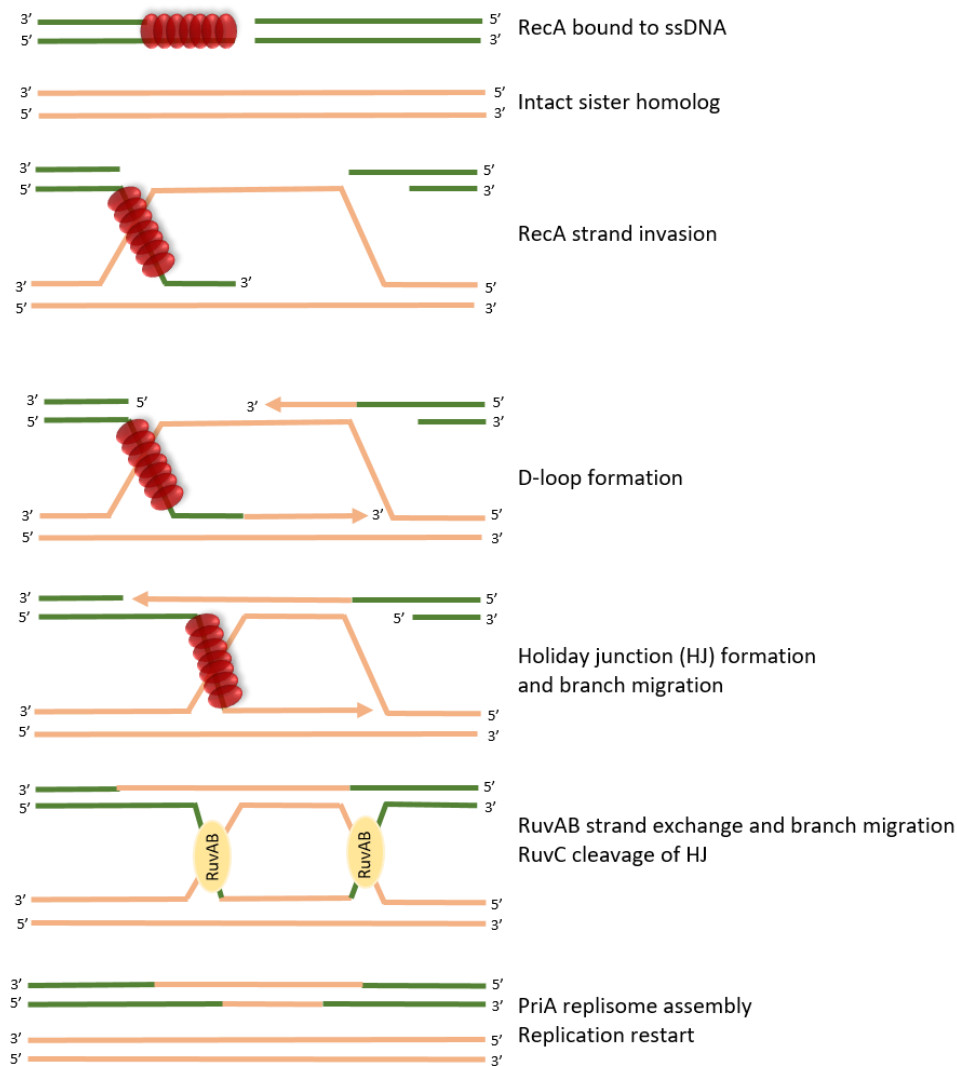


Figure 26. Homologous Recombination reaction in *E. coli*

RecA bound to the ssDNA catalyzes strand invasion and forms a Holliday Junction. RecA then drives branch migration. RuvAB catalyzes strand exchange and RuvC cleaves the HJ. PriA helps DnaB loading and replisome assembly for replication restart.

Interestingly, *in vitro*, RecG protein seems to have overlapping activities with RuvA and RuvB but not RuvC. However, a slight deficiency in recombination of each single mutant suggests that their activities are not fully interchangeable and are somewhat complementary. RecG is an ATPase that can bind Holliday Junctions and catalyze branch migration, but no evidence has been found that RecG can actually cleave the junctions (Lloyd and Sharples, 1993).

Another protein, RadA has been described to exhibit redundant activities with those of RuvAB and RecG. A *radA* deletion was strongly synergistic with a *recG* mutation and triple *radA*, *ruvAB*, *recG* mutants showed comparable sensitivity to *recA* mutants when treated with UV, AZT or Ciprofloxacin. Moreover, the sensitivity of a *radA recG* mutant can be suppressed by deleting *recA*, suggesting that toxic recombination intermediates accumulate in *radA recG* mutants, possibly because they remain unresolved (Beam et al., 2002). It was later shown *in vitro*, that RadA can stimulate RecA's branch migration activity and thus RecA-mediated recombination. Interestingly, they showed that RadA can promote branch migration, even in the absence of RecA (Cooper and Lovett, 2016).

The efficiency of homologous recombination (HR) controls the pathway choice between HR and the error prone DNA damage bypass pathway, Translesion Synthesis (TLS). Indeed, in RecA mutants that are incapable of performing D-loops, homologous recombination is downregulated and translesion synthesis is increased (Naiman et al., 2016).

vii. Induction of translesion polymerases and translesion synthesis

As mentioned above, RecA bound to single stranded DNA induces the SOS response. If RecA is unable to perform D-loops and strand invasion, the SOS induction signal persists. This signal mediates cleavage of UmuD, a translesion polymerase thus activating it for its function in translesion synthesis (TLS).

The TLS pathway allows replication over the lesion, without prior repair and without leaving a single strand gap. Although DNA breakage is avoided, the process is highly error-prone. RecA bound to the single stranded DNA resulting from the gap created by replication bypass induces the SOS response, which will in turn activate Polymerase V by autocleavage of UmuD into UmuD'. Pol V (umuD'₂C) is one of the two TLS polymerases in *E. coli*. The *dinB* gene encodes the other polymerase, Polymerase IV. Both TLS polymerases are SOS induced. They fill in the gap by insertion of nucleotides opposite the lesion (Fuchs, 2016; Fuchs and Fujii, 2013). Lesions persisting in the daughter cells should be processed before the second round of replication (Bichara et al., 2011) (figure 27).

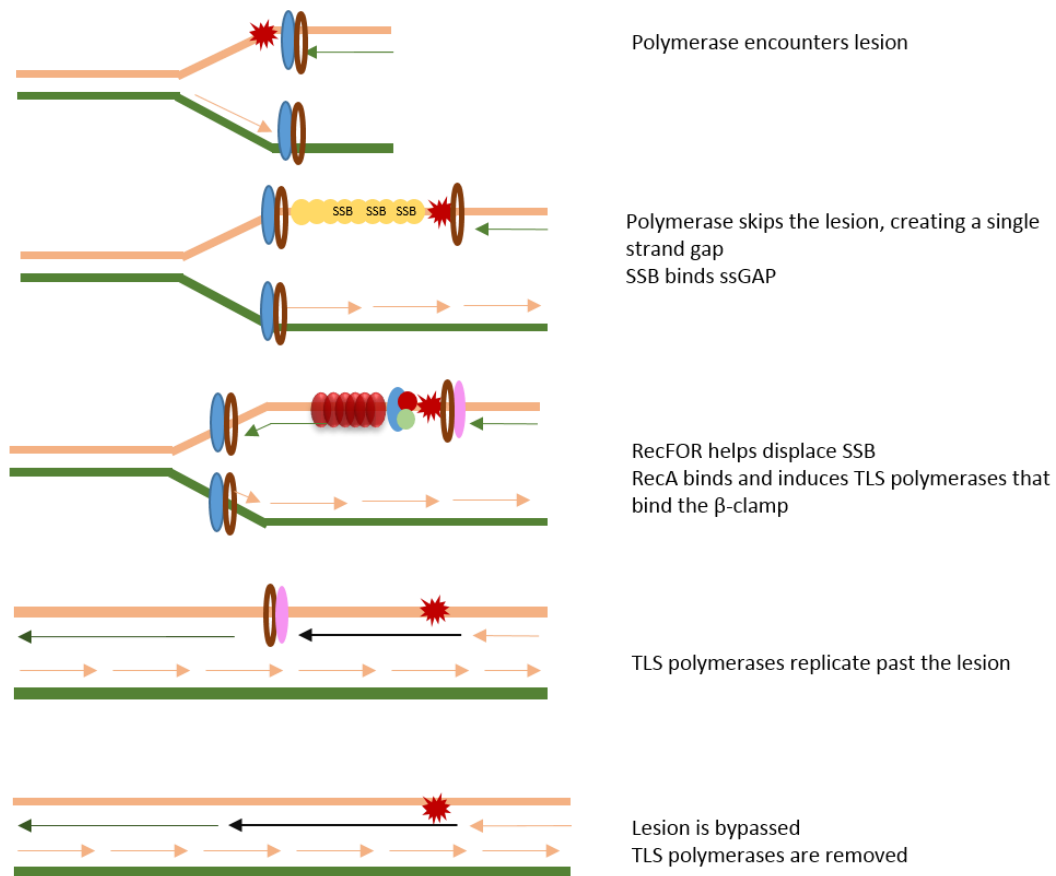


Figure 27. Translesion Synthesis (TLS) pathway

The polymerase encounters the DNA lesion and skips it creating a single strand gap. RecA bound to the ssDNA induces TLS polymerases that are bind to the β -clamp and they replicate past the gap.

viii. Mutants of RecA activity

Certain alleles of RecA that constitutively induce the SOS response, even in the absence of DNA damage, were isolated. These alleles had a higher affinity for single stranded DNA than SSB, favoring RecA binding on ssDNA at the replication fork for instance, thus explaining the constitutive SOS induction (Knight et al., 1984).<

d) *Characteristics of various SOS response proteins*

As mentioned above, the SOS response comprises over 100 proteins. The belonging of a given protein to the SOS response depends on its regulation by LexA. LexA binds to a consensus sequence 5'-TACTG(TA)₅CAGTA-3'. Based on a mathematical formula developed by Berg & Von Hippel, Lewis *et al.* defined a Heterology Index (HI index) that indicates the deviation of a given LexA binding sequence from the palindromic consensus. Sequences having a low HI are closer to the LexA binding consensus sequence (Berg and von Hippel, 1988; Lewis et al., 1994). Computational approaches using the LexA binding consensus sequence allowed the identification of over 60 genes with a potential LexA site (Henestrosa et al., 2000). At the same period, Courcelle and coworkers identified several dozen proteins that were upregulated in a LexA-dependent manner upon UV light exposure (Courcelle et al., 2001). Other stresses such as oxidative stress (Baharoglu and Mazel, 2014; Rodríguez-Beltrán et al., 2012), γ irradiation (Kozubek et al., 1990) or even high pressure (Aertsen et al., 2004) can trigger the induction of the LexA regulated proteins. Among these genes, some remain of unknown function but most of them are known and related to DNA repair (RecA, RuvABC, UvrAB...), replication (Umu proteins...), mutagenesis or even metabolism.

i. *Proteins of unknown function*

Many proteins have been described to be regulated by LexA but their actual function in the DNA damage response remains unknown. For instance, such proteins are:

- YdjM, which has been described as an inner membrane protein (Henestrosa et al., 2000).
- RmuC, which has been poorly described, but seems to be involved in DNA rearrangements and inversions (Slupska et al., 2000).
- DinQ, which seems to be able to modulate membrane-dependent functions such as membrane polarization or intracellular ATP concentrations (Weel-Sneve et al., 2013).

ii. Other SOS induced proteins

- SulA (also called SfiA) inhibits cell division (Huisman et al., 1984). SulA blocks the septal ring formation by inhibiting Z ring formation by FtsZ (Mukherjee et al., 1998). Preventing cell division when DNA is compromised prevents segregation of damaged DNA to the daughter cells.
- DinF's function in the SOS response is poorly characterized. However, recent work has described DinF's role in protection against oxidative damage. DinF possibly detoxifies the cell from high intracellular levels of Reactive Oxygen Species (ROS) (Rodríguez-Beltrán et al., 2012)
- RecJ is a single strand DNA exonuclease that degrades substrates in the 5' to 3' direction (Lovett and Kolodner, 1989). It was identified for its role in a RecBC-independent repair pathway (Lovett and Clark, 1984) and has been shown to mediate the excision step of mismatch repair after UvrD unwinding.
- DinD is highly expressed upon UV-light exposure and has recently been shown to inhibit RecA during strand exchange *in vitro*. DinD appears to be able to halt the progression of DNA pairing by promoting the disassembly of RecA (Uranga et al., 2011).
- TisB is a LexA regulated toxic peptide, which is part of the toxin/antitoxin system IstR/TisB. Induction of TisB leads to cell growth inhibition (Unoson and Wagner, 2008).

iii. RecN protein

RecN protein is an SMC-like protein (Rostas et al., 1987) that was first described in 1984 by Robert Lloyd. He showed that the *recN* gene product (originally called *radB* (Sargentini and Smith, 1983)) was important for cell survival to MMC and ionizing radiation but not UV exposure (Picksley et al., 1984). It was soon demonstrated that RecN is rapidly induced after MMC treatment, through an SOS dependent pathway (Finch et al., 1985).

A few years later, viability tests on double mutants suggested that RecJ and RecN act in two different pathways. RecN seems to act in the RecBC DSB repair pathway while RecJ is mainly involved in the daughter strand gap repair pathway (Wang and Smith, 1988).

Little is known about the actual function of RecN protein in DNA repair despite various studies over the years. In 2004, Kosa *et al.* observed a strong requirement of RecN for survival to bleomycin treatment, a drug creating double strand breaks (Kosa *et al.*, 2004). In good agreement with the apparently specific requirement of RecN for DSB repair, it was shown that RecN is essential when cells are challenged with more than one iScel double strand break (Meddows *et al.*, 2005). Interestingly, they showed that SOS induction in a *recN* mutant was increased nearly two-fold. In the same study, a genetic screen for mutations increasing sensitivity to Mitomycin C highlighted *DksA*'s role in survival to MMC. Combining a *recN* and *dksA* knock down increased sensitivity of each single mutant, showing a synergistic action of both proteins. However, the synergism between *dksA* and *recN* is more likely due to the effect of *DksA* on transcription than to a direct role for *DksA* in DNA repair *per se*, although they showed that the levels of RecA, RecB, RecG or Ruv expression were not altered in the absence of RecN. Another possible explanation is that *DksA* destabilizes the RNAP and transcription complexes, clearing the way for repair proteins and replication fork reassembly (Meddows *et al.*, 2005).

Microscopy experiments using a RecN-GFP fusion protein demonstrated that RecN forms aggregates at the pole and on the nucleoid when it is damaged. A genetic screen for RecA mutants that mimic a *recN* phenotype (sensitive to MMC, but resistant to UV) led to the isolation of a RecA mutant, RecA^{Q300R}. In this mutant, RecN-GFP does not form nucleoid associated foci. All RecN-GFP foci are located at the poles, strongly suggesting that RecN requires RecA for proper loading. A RecN mutant deficient for ATPase activity, RecN^{K35A} is capable of forming foci but is not released from damaged DNA, meaning that ATP hydrolysis is not required for binding but necessary for the release of RecN (Keyamura *et al.*, 2013). Once RecN is released from the break, it is degraded by the ClpXP protease. Its removal is essential for recovery after DNA repair since accumulation of RecN aggregates in the cytoplasm are toxic for the cell (Nagashima *et al.*, 2006).

Interestingly, RecN promotes a nucleoid compaction after a UV irradiation of 3 J.m⁻². This DNA compaction is transient, and lasts for approximately 15-20 min before decompacting. In the absence of RecN, no compaction, nor decompaction is observed (Odsbu and Skarstad, 2014). The observation of such a strong phenotype for RecN in UV irradiated cells is surprising considering *recN* mutants are not sensitive to UV light exposure (Picksley *et al.*, 1984). It is

possible that RecN mediates this nucleoid compaction in response to all DNA damage, regardless of whether it is necessary or not for the repair of a given lesion.

RecN is a highly conserved protein, present in almost all Prokaryotes. It has been shown to be involved in survival to gamma rays in *D. radiodurans* (Funayama et al., 1999), homologous recombination dependent repair in *Neisseria gonorrhoeae* (Skaar et al., 2002) and DNA repair in *B.subtilis* (Kidane et al., 2004). Work on RecN in *E. coli* has been limited due the difficulty of purifying it. However, thanks to its highly conserved structure, it is possible to infer some of its functions from *in vitro* work done in *D.radiodurans* or *B.subtilis*, although the repair mechanisms of these two species differs from that of *E. coli*.

In *Bacillus subtilis*, *in vitro* and *in vivo* studies revealed that RecN may bind 3'ssDNA ends of DSBs, in an ATP dependent manner, before RecA binds (Sanchez and Alonso, 2005). In fact, the same group later showed that RecN is one of the first proteins to recognize and be recruited to the break (Kidane et al., 2004; Sanchez et al., 2006). RecN may tether the 3'ss DNA ends together, concentrating all the DNA ends into what is termed a repair center, and facilitating the access of the broken DNA to RecA (Sanchez et al., 2008).

The function of RecN in *B. subtilis* and *E. coli* may be very different though. Indeed, the SOS response system differs between both species. In *B.subtilis*, the SOS response is induced at a basal level and SOS induction is not required for survival to ionizing radiation in WT cells (Simmons et al., 2009). A basal induction of the SOS proteins (and thus, RecN) make it possible for RecN to act before RecA binding to ssDNA. In *E. coli*, RecN is expressed by SOS induction, in a RecA dependent manner rendering it difficult to imagine that RecN would act before RecA. RecN-YFP forms a single focus localized at the break as is the case in *B.subtilis* (Sanchez et al., 2006), although RecN expression is also increased upon the induction of a double strand break (Cardenas et al., 2014).

In *Caulobacter crescentus*, RecN is involved in nucleoid dynamics when one break occurs on a chromatid previously segregated from its homolog. It was proposed that RecN may structure the DNA in a way that is important for the repair dynamics without actually moving the DNA *per se* (Badrinarayanan et al., 2015; Wang and Maier, 2008).

In vitro RecN from *D. radiodurans* can stimulate intermolecular ligation of linear DNA in the presence of ATP. ATP hydrolysis by RecN is stimulated by duplex DNA but not ssDNA and is dependent on the concentration of RecN protein suggesting that RecN-RecN interactions may be required (Reyes et al., 2010). Pieces of *D. radiodurans* RecN have also been crystallized shedding light on a putative structure of the full protein. The head domain (with the C and N ter ends) was expressed and purified allowing a partial structural analysis. This domain forms a globular head by interaction of the N- and C- terminal ends of RecN protein. The coiled-coil domain was later purified allowing its structural analysis. These partial structures permitted a full representation of RecN structure by Pellegrino and coworkers. RecN resembles a Structural Maintenance of Chromosome (SMC) – like protein, adopting a conformation similar to other SMC proteins (figure 28).

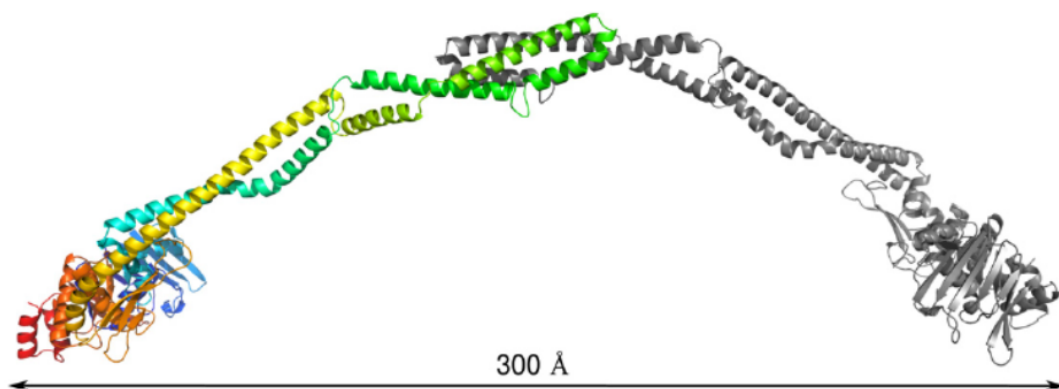


Figure 28. Architecture of Full-length RecN

Structure is predicted from purification of pieces of RecN from *D. radiodurans*
 From Pellegrino et al. 2012

However its coiled coils are much shorter than other known SMC proteins, suggesting it may act in a different manner (Graumann and Knust, 2009). The structural analysis and biochemical experiments led to a model where RecN, as one of the first actors to the break, may bind and

tether the DNA ends, polymerize along the double stranded damaged DNA and encircle the two DNA molecules (Pellegrino et al., 2012).

Very recently, an interesting article by the team of Shelley Lusetti described a functional interaction between RecA and RecN from *D. radiodurans in vitro*, consistent with previously published data in *E. coli* (Keyamura et al., 2013). They further showed that RecN stimulates strand invasion by RecA, thus acting pre-synaptically. This D-loop stimulation is dependent on the ATPase activity of RecN, and incubating RecA bound to DNA can actually stimulate RecN's ATPase activity up to 20 fold. Interestingly, the order with which the different partners are added influences the rapidity of the reaction, suggesting that a defined order is important for the reaction: RecA binds DNA, recruiting RecN, that will then stimulate D-loop formation and dissociate following ATP hydrolysis (Keyamura et al., 2013; Uranga et al., 2017).

D. Sister chromatid cohesion and DNA repair

Many DNA repair pathways involve the presence of an intact homolog to serve as a template for repair of the broken sister, in order to avoid losing genetic information. Intuitively, the presence of an intact sister homolog near a DSB occurring on the other sister should be beneficial for homologous recombination and DNA repair, possibly by helping homology search. Indeed, in Eukaryotes, the cohesin complex is required for efficient double strand break repair after γ -irradiation (Sjögren and Nasmyth, 2001).

1. Eukaryotic Cohesins are essential for survival to DNA damage

Eukaryotes have at least six Structural of Maintenance of Chromosome (SMC) proteins. The SMC1/SMC3 complex (Cohesin) is the most characterized complex. It mediates sister chromatid cohesion during replication and controls chromosome dynamics, meiosis and mitosis. The SMC2/SMC4 complex forms Condensin, necessary for chromosome condensation, chromosome assembly and segregation. The SMC5/SMC6 complex has been shown to be involved in DNA repair, although it also has a role in the maintenance of non-damaged chromosomes (See Section B).

Cohesin complexes are recruited during normal DNA replication, but *de novo* recruitment of Cohesins is induced upon DNA double strand breaks. Cohesin complexes are recruited to the damaged and undamaged sister chromatids. In unbroken chromosomes, Cohesins can load during G2/M phase but cannot generate cohesion. They only generate cohesion during the S phase. However, in the presence of a DSB, cohesion can be generated genome wide (on the broken and unbroken chromosomes) even during G2/M phase (Ström and Sjögren, 2007; Unal et al., 2007). Interestingly, it was shown that it is the cohesion between sister chromatids that is required for repair rather than the Cohesin protein complex *per se* (Sjögren and Nasmyth, 2001).

Although SMC5/SMC6 has been shown to be involved in various pathways and functions, growing evidence shows that the complex is strongly recruited during DNA damage. The SMC5/6 complex associates with several non-SMC proteins (Nse proteins), including Nse1-6.

In undamaged cells, ChIP on ChIP experiments revealed that SMC5/6 binds to the chromosomes as soon as they are replicated. These experiments further revealed a specific role for the SMC5/6 complex in the maintenance of long chromosomes and that SMC5/6 requires Cohesin (directly or indirectly) for proper localization on chromosomes. Overall, in undamaged cells, the chromosomal binding pattern of SMC5/6 is similar to the binding pattern of SMC1/3 although SMC1/3 seems to prevent early segregation of chromosomes and SMC5/6 favors their partitioning (Lindroos et al., 2006).

SMC5/6 mutants are sensitive to DNA damaging agents (Lehmann et al., 1995). A study in human cells showed that SMC5/6 is recruited to DSBs and recruits the SMC1/3 complex to the break to favor cohesion and homologous recombination (Potts et al., 2006). Although the Cohesin complex favors HR and DNA repair by merely keeping the sister chromatids in close contact (Ström et al., 2004), the SMC5/6 complex, associated at the sites of DSBs but also at collapsed replication forks, may be involved in repair induced replication or correct management of the sister chromatids during repair (Lindroos et al., 2006).

SMC5/6 has also been shown to be crucial for meiosis since Nse1 mutants show severe meiotic segregation defects and impaired homologous recombination (Pebernard et al., 2004).

2. Sister chromatid cohesion and DNA repair in *E. coli*

As described in the previous sections, sister chromatid cohesion in *E. coli* is mediated by topological links such as precatenanes rather than Cohesins. To date, very little work has been done on the putative role of precatenanes in DNA repair and no Cohesins have been characterized in *E. coli*.

E. Thesis Objectives

My PhD project focuses on this particular sister chromatid cohesion step in response to DNA damage and its possible relevance for DNA repair and homologous recombination. The role of cohesion in DNA repair has been studied in Eukaryotes but the molecular mechanisms underlying it are far from being characterized. *E. coli* has a high experimental potential allowing complex questions. Using *E. coli* as a model, my PhD project aimed at addressing the following questions:

- i) Is sister chromatid cohesion modified in response to DNA damage?
- ii) What is the impact of different drugs (and thus, different DNA breaks) on sister chromatid cohesion?
- iii) Is this process dependent on the SOS response? If so, what proteins of the SOS response are involved?
- iv) What role may Topoisomerases have in DNA damage mediated SCC?

To answer these questions, I used a site-specific recombination assay that reveals direct interactions between homologous chromosomes. I combined this with cell biology methods such as live cell fluorescence imaging and microfluidics. In order to identify different proteins involved in DNA damage mediated SCC, I performed high throughput experiments such as RNAseq, Co-immunoprecipitation and iPOND.

I showed that sister chromatid interactions are maintained during the repair of a DSB induced by genotoxic stress (such as Mitomycin C treatment). The preservation of sister chromatid interactions (SCIs) upon genotoxic stress is fully dependent on the SOS response. Indeed, in a *lexA* non inducible mutant, most SCIs are lost upon MMC treatment. More specifically, I have shown that the RecN protein, belonging to the SOS response, is an essential protein for double strand break induced SCIs. We observed that the loss of SCIs observed in a *recN* mutant can be fully rescued by the inhibition of Topoisomerase IV activity, suggesting that the main activity of RecN is to maintain sister chromatids in close proximity during the repair of a DSB. The rescue of SCIs by Topoisomerase IV alteration is coupled with a rescue in viability, directly linking sister chromatid cohesion and cell viability in response to genotoxic stress.

Among the SOS proteins that we tested, only RecN and RecA (because it contributes to RecN induction and loading) had an effect on SCI preservation.

Another interesting feature of the RecN protein that we discovered is its capability to promote the merging of previously segregated sister chromatids. This specific merging of sister loci is coordinated with a large, whole nucleoid merging and compaction. This RecN-dependent DNA compaction is transient. We rapidly observe a decompaction of nucleoids accompanied by cell filamentation. Moreover, I observed that the RecA foci dynamics is strongly altered in a *recN* mutant, suggesting that RecN may interact with RecA. This hypothesis was confirmed by co-immunoprecipitation experiments that revealed a direct interaction between RecN and RecA. These results are the object of a publication in Nature Communications (Vickridge et al., 2017). However, other experiments and questions arose during my PhD that I will present in the Complementary Results Chapter

.

II. Results

A. Published results

ARTICLE

Received 1 Oct 2016 | Accepted 13 Jan 2017 | Published 6 Mar 2017

DOI: 10.1038/ncomms14618

OPEN

Management of *E. coli* sister chromatid cohesion in response to genotoxic stress

Elise Vickridge^{1,2,3}, Charlene Planchenault¹, Charlotte Cockram¹, Isabel Garcia Junceda¹ & Olivier Espéli¹

Aberrant DNA replication is a major source of the mutations and chromosomal rearrangements associated with pathological disorders. In bacteria, several different DNA lesions are repaired by homologous recombination, a process that involves sister chromatid pairing. Previous work in *Escherichia coli* has demonstrated that sister chromatid interactions (SCIs) mediated by topological links termed precatenanes, are controlled by topoisomerase IV. In the present work, we demonstrate that during the repair of mitomycin C-induced lesions, topological links are rapidly substituted by an SOS-induced sister chromatid cohesion process involving the RecN protein. The loss of SCIs and viability defects observed in the absence of RecN were compensated by alterations in topoisomerase IV, suggesting that the main role of RecN during DNA repair is to promote contacts between sister chromatids. RecN also modulates whole chromosome organization and RecA dynamics suggesting that SCIs significantly contribute to the repair of DNA double-strand breaks (DSBs).

¹Center for Interdisciplinary Research in Biology (CIRB), Collège de France, UMR CNRS-7241, INSERM U1050, PSL Research University, 11 place Marcelin Berthelot, 75005 Paris, France. ²Université Paris-Saclay, 91400 Orsay, France. ³Ligue Nationale Contre le Cancer, 75013 Paris, France. Correspondence and requests for materials should be addressed to O.E. (email: olivier.espeli@college-de-france.fr).

All cells must accurately copy and maintain the integrity of their DNA to ensure faithful transmission of their genetic material to the next generation. DNA double-strand breaks (DSBs), single-stranded gaps (SSGs) and DNA adducts such as interstrand crosslinks (ICLs) are serious lesions that, if left unrepaired, are potentially lethal to the cell. DSBs, SSGs and DNA adduct repair involve homologous recombination (HR) pathways^{1,2}. On the basis of current models, there are two major pathways for recombinational repair and homologous recombination in *Escherichia coli*³. The daughter strand gap repair pathway requires RecFOR, RecA and RuvABC gene products and the DSB-repair pathway requires RecBCD, RecA and RuvABC gene products⁴. The initial step of DNA damage repair by HR requires RecA loading on single-stranded DNA (ssDNA). It is achieved either by RecFOR on SS gaps, or DNA resection up to a *chi* site, by RecBCD on a DSB. RecA loading and strand invasion are essential for homologous pairing and regeneration of replication fork structures⁵. RecA protein bound to ssDNA triggers the autoproteolysis of LexA and the induction of many genes from the SOS regulon^{6–8}.

The DSB-repair pathway strongly relies on RecA-mediated pairing of the damaged DNA molecule with an undamaged copy serving as a template during the repair process, presumably the sister chromatid. In eukaryotes, during replication, cohesins keep the newly replicated sister chromatids together before segregation⁹. Cohesins have been shown to be important for DSB repair in G2 phase and post-replicative recruitment of cohesins has been observed at the site of the DSB^{10–12}. However, the DSB-induced cohesion is not limited to broken chromosomes but occurs also on unbroken chromosomes, suggesting that cohesion provides genome-wide protection of chromosome integrity^{13,14}.

In bacteria, following replication, sister loci do not immediately segregate, and the duration of cohesion is controlled by the activity of topoisomerase IV (Topo IV)^{15–17}. The role of Topo IV in the segregation of sister chromatids has led to a well-accepted, but yet undemonstrated model, involving precatenane links as the major post-replicative cohesion factor in *E. coli*. Using a site-specific recombination assay, we demonstrated that interactions and genetic exchanges between sister loci (sister chromatid interactions (SCIs)) are favored for a 10–20 min period following replication¹⁶. These SCIs rapidly decrease when replication is arrested but persist if Topo IV activity is impeded, suggesting that post-replicative topological links enhance genetic exchange between homologous regions.

Previously, the absence of identified cohesins and the progressive segregation of bacterial sister chromosomes following replication have suggested that homologous recombination in bacteria requires a genome-wide homology search. Recent studies have demonstrated that a site-specific DSB can be efficiently repaired using distant sister homology¹⁸. These processes correlate with the formation of a RecA bundle and the merging of sister foci. In another study, DSB formation by a replication fork encountering a frozen topoisomerase provokes the rapid association of large regions of the previously segregated sister chromatids¹⁹.

The SOS-inducible *recN* gene, which encodes an SMC (structural maintenance of chromosomes)-like protein, was identified over 20 years ago^{20,21}. Expression of the *recN* gene is regulated by the LexA repressor, and following derepression, the RecN protein is one of the most abundantly expressed proteins in response to DNA damage^{7,22}. RecN is also involved in the RecBCD-dependent DSB repair pathway^{21,23,24}. *recN* mutants are sensitive to ionizing radiation, I-SceI cleavage and mitomycin C (MMC)^{24,25} but do not exhibit extensive DNA degradation following DSB²⁵. *In vitro* assays have been developed with RecN from *Deinococcus radiodurans*. *D. radiodurans* RecN enhances ligation of linear DNA fragments suggesting DNA end bridging

or cohesin-like activities^{26,27}. In addition, *Bacillus subtilis* RecN, which is among the first actors to the site of a DSB, promotes the ordered recruitment of repair proteins to the site of a lesion^{28,29}. Interestingly, a different activity has been observed for RecN in *Caulobacter crescentus* and *E. coli*. It has been reported that RecN in this system is implicated in nucleoid dynamics following DSB repair^{30,31}.

Considering the sister chromatid cohesion and segregation mechanism in *E. coli* and the intriguing but unclear role of the SOS protein, RecN, we sought to investigate the importance of DNA precatenane-mediated sister chromatid cohesion in DNA repair. In this study, we used genotoxic agents to evaluate the role of topological links between sister chromatids in the repair of DNA damage. Our results demonstrate that SCIs are preserved upon treatment with MMC. Upon MMC treatment, SCIs become dependent on the induction of the *recN* gene product by the SOS response. Interestingly, a *recN* deletion can be fully rescued by a thermosensitive mutation in Topoisomerase IV, suggesting that the main function of RecN during DNA repair is to maintain SCIs, as precatenanes do under normal conditions. The loading of RecN onto sister chromatids is dependent on the presence of DSBs processed by RecA. Therefore, RecN can be considered as a DSB-specific cohesion factor. Because the presence of RecN accelerates growth resumption following genotoxic stress and affects the shape and dynamics of RecA repair structures, we propose that RecN-mediated preservation of SCIs is a key element in the repair of DSBs.

Results

SCIs are preserved in MMC-treated cells. SCIs are essential for genomic stability. During the bacterial cell cycle, SCIs are determined by the balance between the rates of chromosomal replication and segregation¹⁶ (Fig. 1a). We have previously developed a system that detects and accurately measures sister chromatid cohesion *in vivo*¹⁶. This *LacloxP* assay is based on the Cre-*loxP* site-specific recombination systems of bacteriophage P1. We engineered a cassette containing two adjacent *loxP* sites that can only recombine when Cre encounters the homologous region on the sister chromatid. The frequency of Cre recombination events is therefore dependent on the proximity between sister loci¹⁶. *LoxP* recombination was used in this study to monitor the organization and dynamics of sister chromatids following DNA damage induced by MMC. MMC is a potent antibiotic that inhibits DNA synthesis by reacting with guanines of complementary DNA at CpG sequences creating interstrand-crosslinks³². MMC treatment (i) promotes the formation of replicative lesions: SSGs³³ and DSBs³⁴), (ii) induces the SOS response³⁵, (iii) blocks the completion of *oriC*-dependent chromosome replication (Supplementary Fig. 1A) and (iv) rapidly halts DNA replication (Fig. 1b,c). We placed the *loxP* cassette at the *ori-3* locus (positioned 450 kb from *oriC*) and used this assay to measure SCIs in the presence and absence of MMC. To stimulate recombination, 20 min pulses of Cre induction were performed before MMC addition, immediately after MMC addition (0–20 min), 20 min after MMC addition (20–40 min) or 40 min after MMC addition (40–60 min). The recombination frequency slightly increased after MMC addition (Fig. 1d). This observation is in sharp contrast with the abrupt drop of the recombination frequency observed in a *dnaC* allele (*dnaCts*) when initiation of replication is blocked at a non-permissive temperature (40 °C; Fig. 1d). Interestingly, in the presence of MMC, SCIs also persist in the *dnaCts* strain at a non-permissive temperature (Fig. 1d). These observations suggest that MMC impedes sister chromatid segregation and renders SCIs independent of replication.

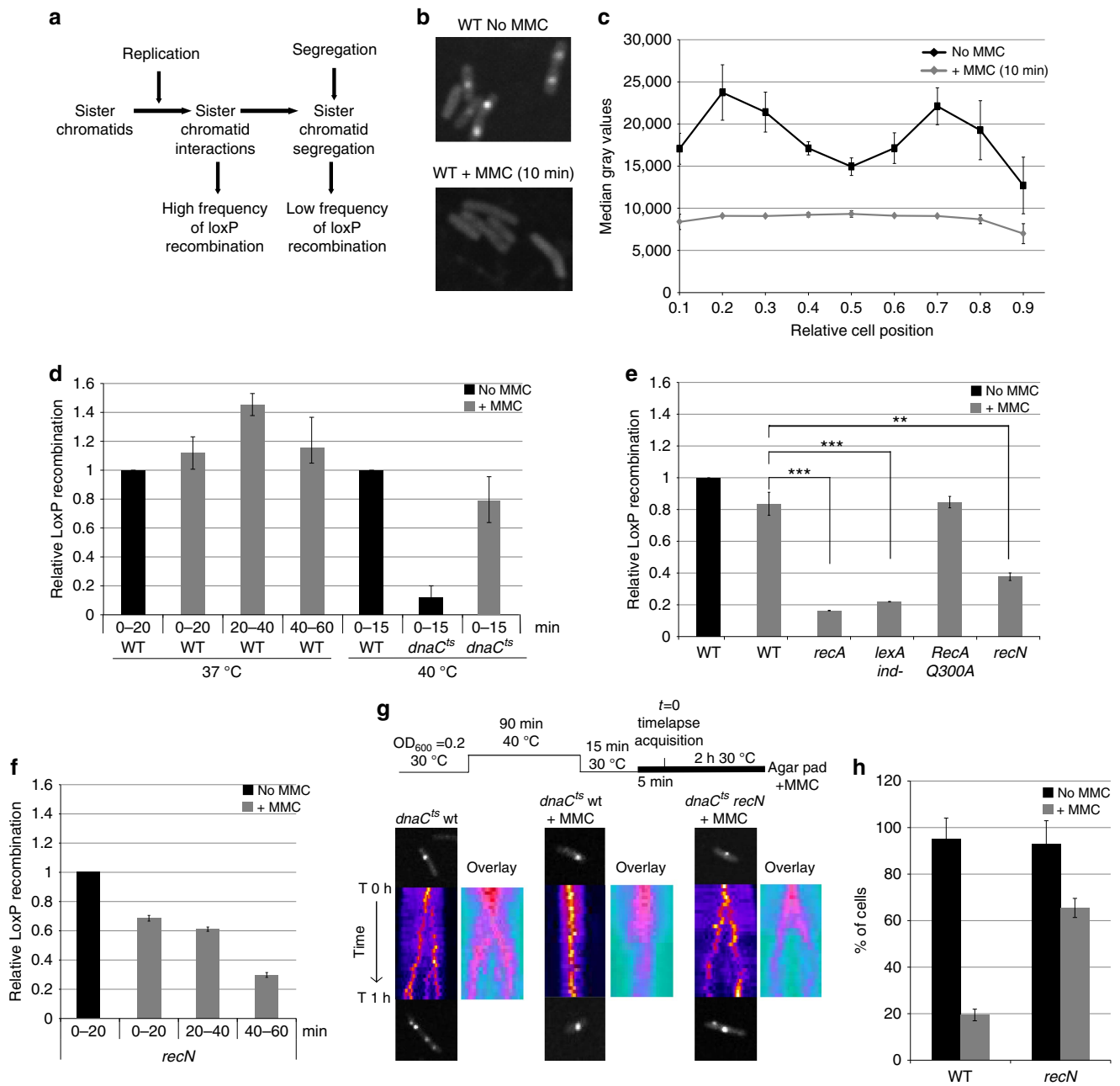


Figure 1 | SCIs are preserved in the presence of MMC via a RecN-dependent pathway. (a) The number of SCIs is under the control of replication that produces cohesive sister chromatids and segregation that separates them. (b) MMC causes rapid replication arrest. An MG1655 wild-type strain was used to monitor EdU incorporation in the presence and absence of MMC ($10 \mu\text{g ml}^{-1}$) for 10 min. (c) Quantification of a 10 min EdU incorporation pulse in WT cells treated or not with MMC. (d) SCIs were estimated at different time points after replication arrest in WT and *dnaC^{ts}* cells treated or not with MMC. SCIs were measured in WT and *dnaC^{ts}* strains by adding arabinose during 20 min pulses after MMC addition. In the *dnaC^{ts}* strain initiation of replication was arrested at 40 °C. (e) Upon MMC treatment, SCIs are dependent on RecA, LexA and RecN. SCIs were estimated using the frequency of *loxP*/Cre recombination at the *ori-3* locus. The results at 40 min are presented; the results at 10, 20 and 30 min are presented in Supplementary Fig. 1. The results are expressed as the relative *loxP* recombination normalized to the untreated WT strain. Statistical comparisons of histological data were performed using Student's *t*-test. *P* values are considered to be significant for $\alpha = 0.05$. **P* < 0.05, ***P* < 0.01, ****P* < 0.001. (f) SCIs are not maintained in a *recN* mutant. MMC was added and SCIs were measured as described in d. (g) MMC prevents sister chromatid segregation in synchronized cells. *dnaC^{ts}* and *dnaC^{ts} recN* cells tagged with a *parSP^{MT1}*/ParB-GFP system at *ori-3* were synchronized for 90 min at 40 °C, and replication was re-initiated at 30 °C for 10 min. Cells were then placed on an agar pad, with or without MMC, and a time course analysis was performed. The images represent kymographs of a single-cell (fire colour map) and an overlay of about 20 cells (ice colour map). (h) Quantification of segregation events in *dnaC^{ts}* WT and *recN* strains (100 cells were analysed for each strain). Cells were treated as described in g. Error bars are s.d. of four experiments.

SCIs are dependent on RecA and RecN in the presence of MMC. We sought to determine the role of HR and the SOS response in SCIs. Indeed, HR and more particularly the repair intermediates such as holliday junctions could promote SCIs. We observed that

the degree of SCIs in the presence of MMC was strongly reduced in the absence of RecA (Fig. 1e, Supplementary Fig. 1B). This observation could suggest that RecA is required for preserving these interactions or that DNA degradation happening in the *recA*

mutant could more dramatically affect sister chromatids that are interacting (that is, the closest to the replication fork) than segregated sister chromatids. We used EdU incorporation to monitor DNA degradation. A brief incorporation of EdU before addition of MMC allowed us to measure degradation of the newly replicated DNA regions. We estimate that EdU labelling extended over 500 kb during the pulse, a distance that corresponds to the region involved in SCIs. In the WT strain, EdU foci were present in every cell for more than 3 h after MMC addition (Supplementary Fig. 1C,D) and the average fluorescence intensity of EdU labelling slowly decreased over the 3 h time course (Supplementary Fig. 1E). In some cells fluorescence intensity of EdU labelling increased at later time points (2 and 3 h). This increasing intensity is correlated with a reduction in the number of foci and a compaction of the nucleoids (Supplementary Fig. 1C). In the absence of RecA, the reduction of EdU intensity and the number of cells presenting EdU foci is only manifest after 1 h of treatment (Supplementary Fig. 1D,E). However, since DNA degradation was not significant during the first hour after MMC addition it was not correlated with the SCIs reduction observed in the first 40 min following MMC. Interestingly, in a mutant that is unable to induce the SOS response (*lexA ind-*)³⁶, we also observed a reduction of SCIs and loss of viability (Fig. 1e, Supplementary Fig. 1B,F). In order to test the relationship between the defects in SCIs and the ability of a strain to perform HR, we measured SCIs in the *recA*^{Q300A} mutant. This mutant is strongly deficient in HR (<10% of the activity of a WT strain) but exhibits WT levels of LexA cleavage activity and SOS upregulation³⁷. We observed that, despite a dramatic drop in the viability upon MMC treatment (Supplementary Fig. 1G), SCIs were maintained at a high level in the *recA*^{Q300A} mutant compared to the *recA* mutant (Fig. 1e). Altogether, these observations indicate that completion of DNA repair and efficient HR are not required for the preservation of SCIs. Therefore we considered that a member of the SOS regulon may be responsible for SCI preservation upon MMC treatment.

To identify the SOS proteins responsible for maintaining SCIs, we analysed 15 mutants of SOS-inducible genes whose functions have not been clearly established, for their ability to preserve SCIs after DNA damage. We observed that of the 15 mutants tested, only a *recN* mutation significantly reduced SCIs in the presence of MMC (Fig. 1e, Supplementary Fig. 1H). In good agreement with a low basal level of expression (Supplementary Fig. 2A,B), a *recN* deletion had no effect on SCIs under normal growth conditions (Supplementary Fig. 1B). We measured the persistence of SCIs in the absence of RecN using pulses of Cre induction, as described in Fig. 1d. *LoxP* recombination progressively decreased during the 60 min following MMC addition (Fig. 1f), suggesting that SCIs disappear in the absence of RecN. In good agreement with the fact that RecN is only expressed after RecA loading on ssDNA, the *recN* mutant did not present any DNA degradation phenotype upon I-SceI cleavage²⁵ or MMC treatment (Supplementary Fig. 1C–E). In the *recN* mutant, EdU foci degradation was comparable to WT cells even at the latest time points. Therefore the decrease of *loxP* recombination observed in the *recN* strain is not the consequence of DNA degradation. We favour the hypotheses that RecN is either involved in preserving SCIs or in the formation of *de novo* SCIs in the presence of MMC. Interestingly, the level of SCIs in the absence of RecN was significantly higher than in the *recA* or *lexA ind-* mutants, suggesting that other processes are altered in these mutants and perhaps an additional, yet-unidentified, SOS-induced protein participates in maintaining SCIs.

RecN impedes segregation of damaged sister chromatids. Our observations suggest that in the presence of MMC, RecN is required to maintain SCIs. To examine whether RecN is directly

capable of preventing segregation of sister chromatids, we performed live cell imaging of sister chromatid dynamics. We utilized strains containing a *dnaCts* allele to synchronize the replication cycle and treated the cells with or without MMC 5 min after the estimated replication of a *parS/ParB-GFP* tag at the *ori-3* locus. Replication synchrony and timing were measured by marker frequency analysis³⁸. In the absence of MMC, both WT cells and *recN* mutant cells presented a reproducible segregation pattern in the 20 min following replication (Fig. 1g,h). In the presence of MMC, segregation was only observed in 20% of WT cells, the remaining cells contained either a single focus for the entire time course or brief alternating cycles of duplication and merging back of sister foci. In contrast, the majority (65%) of *recN* mutant cells presented a separation of the initial focus into two foci. These observations demonstrated that RecN is able to limit segregation of sister chromatids in the presence of MMC and therefore functions as a DNA damaged-induced cohesion factor in *E. coli*.

The lack of RecN is compensated by extensive precatenation. It has previously been demonstrated that sister chromatids stay cohesive behind the replication fork, forming structures known as precatenanes¹⁶. The type II Topoisomerase IV is responsible for the decatenation of these structures and ensures the correct segregation of both sister chromatids. We used a Topo IV thermosensitive mutant (*parEts*), in both WT and *recN* backgrounds, to test whether preventing the removal of precatenanes can maintain SCIs and restore viability in the presence of different DNA damaging agents. In untreated conditions, we observed an increase in post-replicative SCIs when the *parEts* mutant was shifted to a non-permissive temperature¹⁶. Following treatment with MMC, the frequency of SCIs decreased in the *parEts* cells but remained at a greater level than that observed in WT cells. Interestingly, the level of SCIs following MMC treatment was unaffected by either a *recA* or *recN* deletion in the *parEts* mutant (Fig. 2a, Supplementary Fig. 3A–F). This suggests that, in this context, maintaining precatenanes behind the replication fork can compensate for the absence of RecN, and that more generally; in spite of a DSB most precatenane links do not immediately disappear.

Preservation of SCIs is linked to MMC-treated cell survival. To assess whether the preservation of SCIs observed in the *parEts recN* mutant facilitates efficient DNA repair and cell survival upon MMC treatment, we performed CFU measurements in WT, *recN*, *recA*, *parEts*, *parEts recN* and *parEts recA* strains in the presence of MMC (Fig. 2b). Following a brief period at a non-permissive temperature, the *recA* and *recN* cells were strongly sensitive to MMC but the *parEts* cells were only slightly sensitive when compared to WT cells. Interestingly, the double *recN parEts* mutant presented a similar viability to the *parEts* mutant, suggesting that the decrease in viability in the *recN* mutant can be compensated by an increase in topological linking between sister chromatids during replication. On the other hand, inhibiting TopoIV in a *recA* mutant did not rescue viability, suggesting a specific role for RecN in the maintenance of SCIs (Fig. 2b and Supplementary Fig. 3G). We also measured the CFU in a *parEts lexA ind-* strain where the SOS response is down but RecA is present in basal levels (Supplementary Fig. 3H). The inhibition of TopoIV in a *lexA ind-* strain did not rescue the loss of viability of the *lexA ind-* strain. These observations strengthen the hypothesis that topological links, when they are artificially maintained, specifically compensate for a lack of RecN and therefore suggest that RecN is playing a structural role by maintaining sister chromatids close together.

RecN requires DSBs and RecA to load on DNA. To test whether the overproduction of RecN in a wild-type strain could affect SCIs, we constructed a vector containing RecN under control of a leaky promoter (pZARecN). Overexpressing RecN in the *recN* mutant restored viability and preserved SCIs following MMC

treatment (Fig. 2c, Supplementary Fig. 4A–D). However, RecN overexpression did not modify SCIs in untreated WT cells, in contrast to the Topo IV *parEts* mutation. These observations suggest that RecN is inactive in the absence of DNA lesions. To determine whether RecA itself or another SOS-inducible protein is responsible for RecN activation, we constructed an SOS constitutive strain (*sfiA lexA51*) in which *recA* is deleted but the SOS induction is maintained³⁹. The *sfiA lexA51 recA* strain presented strong sensitivity to MMC (Supplementary Fig. 4E). In the *sfiA lexA51 recA*, we observed a low frequency of recombination, suggesting that DNA damage-induced SCIs are directly dependent on RecA (Supplementary Fig. 4F). We performed co-immunoprecipitation experiments in WT strains expressing RecN-Flag. In the presence of MMC, RecN was robustly co-immunoprecipitated with an anti RecA antibody. Co-immunoprecipitation of RecA with an anti Flag antibody was less specific. Nevertheless in the presence of MMC and RecN-Flag induction the amount of co-immunoprecipitated RecA significantly increased (Supplementary Fig. 5). These observations demonstrate an interaction between RecA and RecN and that perhaps RecA serves as a loader for RecN. Interestingly, immunoprecipitation experiments revealed that a small amount of RecN was present even in the absence of MMC (Supplementary Fig. 5). We cannot distinguish if it corresponds to a basal level of RecN in all cells or to a fraction of cells inducing RecN through SOS in response to spontaneous damages. Considering the first hypothesis, this would suggest that RecN could intervene very early following DNA damage. To test whether RecA bound to SS DNA was sufficient to observe RecN-mediated SCIs, we used Azidothymidine (AZT) which is a DNA chain terminator. RecA is loaded on SS gaps in the presence of AZT; however, we observed no requirement of RecN on viability or SCIs in these conditions (Fig. 2d,e). SCIs disappeared rapidly in the presence of AZT in WT strain but were kept at high level when Topo IV was inhibited. This suggests that in these conditions precatenanes are rapidly removed and that RecN does not participate to SCI near SS gaps.

RecN promotes the regression of segregated chromosomes. Our data have demonstrated that RecN can prevent the segregation of newly replicated sister chromatids. However, it has recently been reported in *C. crescentus*, that RecN participates in DNA dynamics following the regression of segregated loci in response to an I-SceI-induced DSB³⁰. We used time-lapse microscopy to evaluate RecN's putative role in sister chromatid dynamics following an MMC-induced DSB. We used a *parB^{pmT1}*-YFP fusion that binds to a *parS* site inserted at the *ori-3* locus

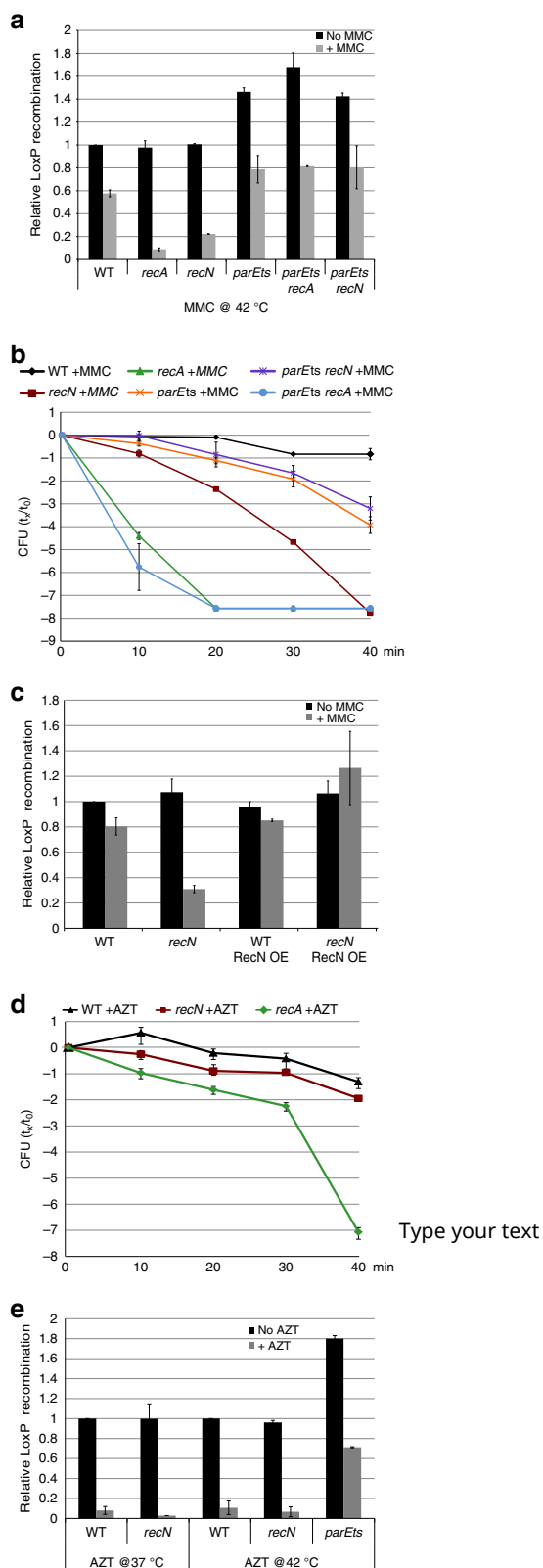


Figure 2 | RecN-mediated SCIs are specifically established in response to DSBs. (a) Measurements of SCIs following Topo IV alteration in the presence of MMC. *LoxP* assays were performed at 10, 20, 30 and 40 min after the addition of MMC. The results at 30 min are presented; the results at 10, 20 and 40 min are presented in Supplementary Fig. 3. The results are expressed as the relative *loxP* recombination, with MMC normalized to untreated WT. Cells were incubated for 25 min at 42 °C before the addition of 0.1% arabinose and MMC. (b) Influence of Topo IV alteration on WT, *recN* and *recA* mutant viability in the presence of MMC. The cell viability assay was performed at non-permissive temperature of 42 °C. (c) Influence of RecN overexpression on SCIs. The plasmid pZA31 carries *recN* under the control of a leaky promoter. The results are expressed as the relative *loxP* recombination of the MMC-treated sample normalized to the untreated WT. (d) Viability of WT, *recN* and *recA* mutants in the presence of SS gaps formed by AZT. (e) Measurement of SCIs in the presence of SS gaps. *LoxP* assays were performed as described in A. Error bars are s.d. of four experiments.

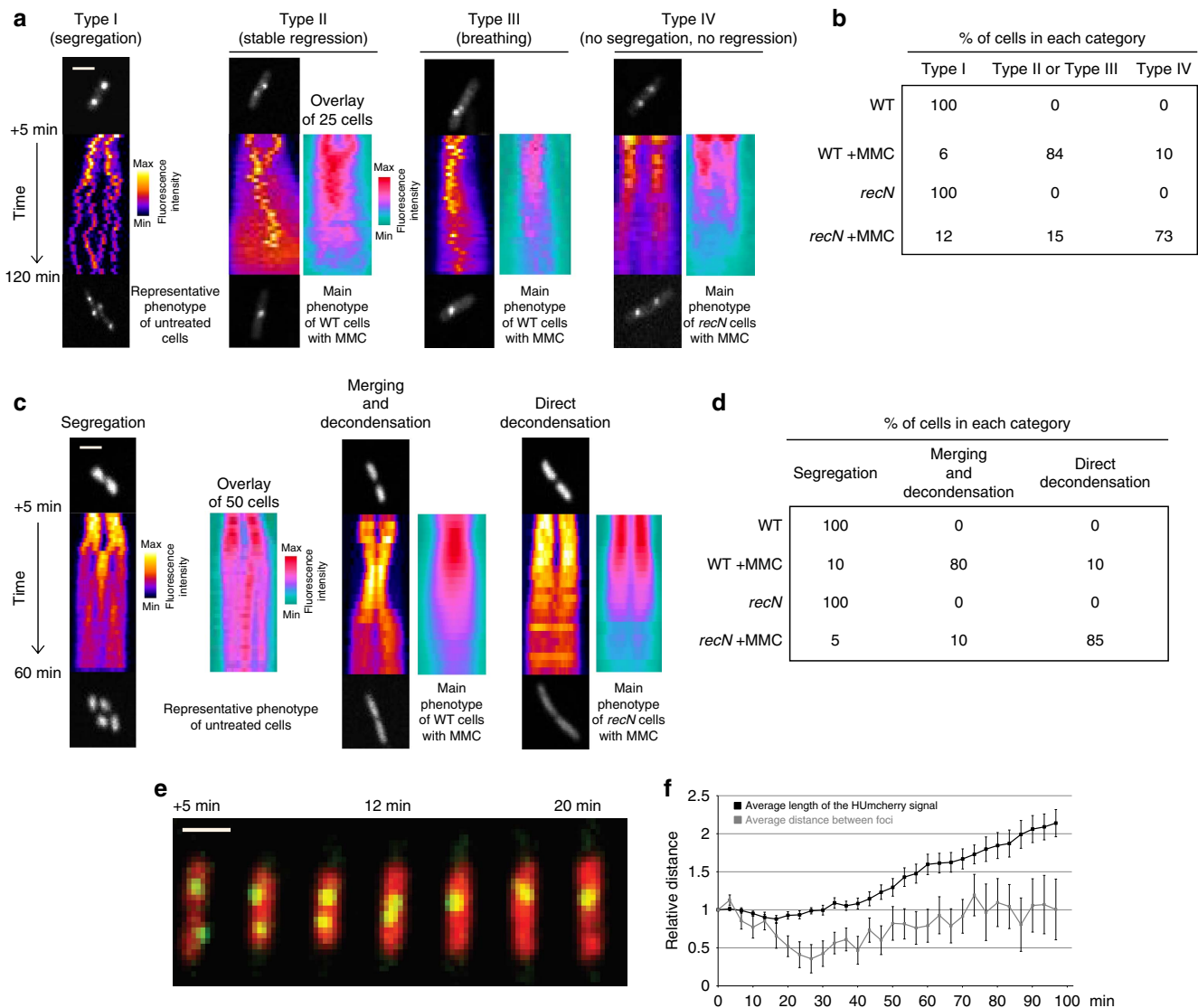


Figure 3 | *RecN* participates in sister locus re-pairing and nucleoid rearrangement in response to DSBs. (a) Representative kymographs of sister focus dynamics in the absence or presence of MMC. Kymographs were constructed along the long axis of the cell. Time-lapse imaging starts 5 min after the initial contact with MMC. Images were acquired every 3 min for 2 h. The fire lookup kymographs represent a single cell. The Ice lookup kymographs are an overlay of kymographs. (b) Frequency of the different types of sister focus dynamics was measured in the presence of MMC. Results are expressed as a percentage. About 100 cells were observed. (c) Representative kymographs of nucleoid (HU-mCherry) dynamics in the absence or presence of MMC. (d) The frequency of the different types of nucleoid dynamics was measured in the presence of MMC for the WT strain and the *recN* mutant. Results are expressed as a percentage. About 100 cells were observed. (e) Dynamics of sister foci and nucleoids in the presence of MMC. A time course was performed in a strain tagged with a *parS^{MTI}*/ParB tag at *ori-3* and labelled with HU-mCherry. (f) The distance between nucleoid edges and the distance between sister foci were recorded at each time point of the experiment presented on e. Distances were normalized to 1 for the time +5 min after MMC addition and are an average of 50 cells. Error bars are standard deviations of 50 cells. Scale bars are 1 μ m.

(450 kb from *oriC*). In the absence of MMC, at time 0, more than 80% of WT cells contained two foci and we observed the segregation of the two foci into four foci immediately before cell division, each daughter cell containing two new foci (Fig. 3a, Type I and Fig. 3b). The presence of MMC significantly altered focus segregation. In most cases, bacteria with two foci at time point 0 failed to produce four foci, and eventually, the two segregated foci regressed back into one central focus that either persisted in this state for an extended period of time (Type II, 45% of the population) or regressed transiently into one focus (Type III, 39%; Fig. 3a,b and Supplementary Movie 1). This phenotype was strongly dependent on *RecN* (Fig. 3a,b and Supplementary Movie 2). We observed the beginning of regression between 12 and 47 min after MMC treatment. We tagged additional loci on

the chromosome to evaluate *RecN*'s influence at various distances from the replication fork and thus the DSB. Focus regression occurred at a high frequency near to *oriC* (100 and 450 kb away from *oriC*), less frequently in the middle of the left replicore (1,300 kb) and very infrequently near the terminus (2,300 kb from *oriC*). This suggests that *RecN* can mediate merging of sister foci upstream from a replication fork but is not able to re-anneal fully segregated chromosomes.

To observe the whole nucleoid dynamics associated with the foci merging, we used cells containing the HU protein fused to mCherry. HU is a histone-like protein that binds ubiquitously to the whole nucleoid. We detected the merging of segregating nucleoids in response to MMC treatment (Fig. 3c,d). This phenomenon was observed 10 ± 10 min after MMC addition and,

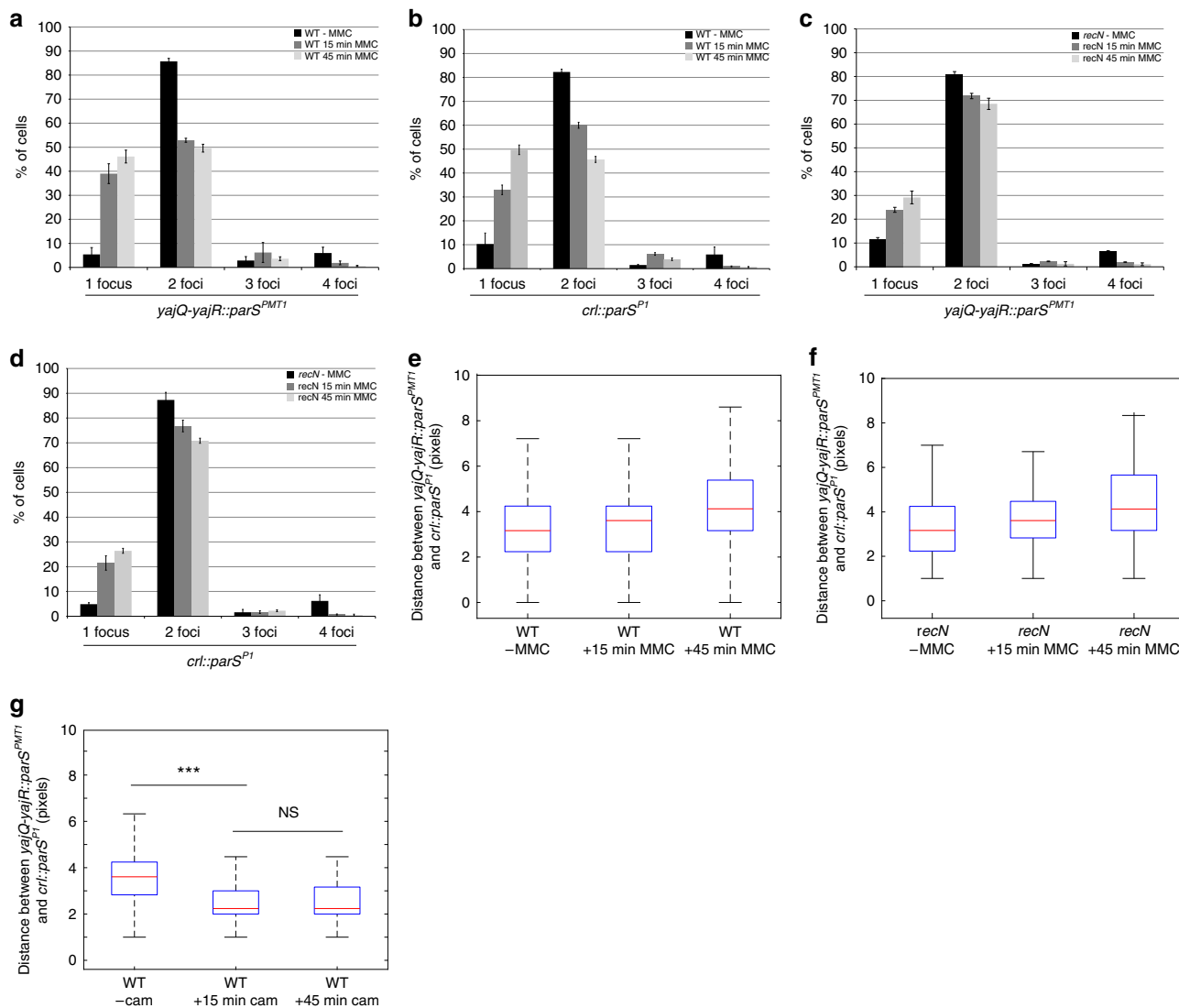


Figure 4 | RecN influences SCC but not DNA condensation. (a) The number of foci per cell at the *yajR-yajQ::parS^{PMT1}* site was counted in cells treated with MMC for 0, 15 or 45 min. (b) The number of foci per cell at the *cri::parS^{P1}* site was counted in cells treated with MMC for 0, 15 or 45 min. (c) Same as a, but performed in the *recN* mutant. (d) Same as b, but performed in the *recN* mutant. In a–d, error bars represent standard deviations of 300 cells. (e) The distance between two loci on the same replichore of the chromosome, spaced by 188 kb and tagged with a *parS^{P1}* or a *parS^{PMT1}* site (*cri::parS^{P1}* and *yajQ-yajR::parS^{PMT1}*, respectively), was measured after treatment with 10 μg ml⁻¹ MMC for 0, 15 or 45 min. The results are shown as a box plot representing the median, first and fourth quartiles (N = 300). (f) Same as e, but performed in the *recN* mutant. (g) The distance between two loci on the same replichore of the chromosome, spaced by 188 kb and tagged with a *parS^{P1}* or a *parS^{PMT1}* site (*cri::parS^{P1}* and *yajQ-yajR::parS^{PMT1}*, respectively), was measured after treatment with 30 μg ml⁻¹ of chloramphenicol for 0, 15 or 45 min. (t-test ***P < 10⁻³⁰, NS (not significant) P > 10⁻⁵).

as previously described, was dependent on both the RecA and RecN proteins³¹. Regression of sister foci was observed a few minutes following nucleoid merging (Fig. 3e,f and Supplementary Movie 3). These observations suggest that RecN-mediated preservation of SCIs, regression of segregated sister loci and nucleoid merging are coordinated steps in the repair process of DSBs.

RecN do not promote nucleoid condensation. The merging of nucleoids observed following MMC treatment may result from two distinct phenomena: a global DNA compaction, mediated by RecN and favoring the random encounter of sister homologues, or an ordered re-zipping that realigns homologous regions of the nucleoid. To distinguish between these two hypotheses, we measured the distance between two loci tagged with *parS^{PMT1}* and *parS^{P1}* sites spaced 188 kb apart on the same replichore

(975 kb from *oriC* and 1,163 kb from *oriC*). When cells were treated for 15 min with MMC (at this moment most bi-lobbed cells have merged their nucleoids), the number of foci per cell decreased substantially in the WT strain (1.4 foci per cell on average in the presence of MMC compared to 1.7 in regular conditions, Fig. 4a,b). By contrast, this number remained constant in the absence of RecN (1.65 foci per cell in the presence of MMC compared to 1.7 in regular conditions, Fig. 4c,d). In spite of the reduction of the number of foci, the distance between the tagged loci was unchanged, even though the nucleoids were merged at this time point (Fig. 4e and Supplementary Table 1). After 45 min of MMC application, the distance between the loci increased significantly, reflecting the nucleoid decondensation observed with HU-mCherry and cell filamentation. Importantly, the distance between the two tagged foci was independent on RecN (Fig. 4f). To check that a chromosomal condensation can indeed be observed with our experimental set-up, we performed

the same experiment in the presence of chloramphenicol, an antibiotic that is known to strongly condense the chromosome⁴⁰. The interfocal distance was decreased in the presence of chloramphenicol when compared to untreated cells (Fig. 4g). These observations demonstrate that RecN does not participate in nucleoid condensation and that nucleoid merging is ordered and only leads to encounters between homologous loci. We thus propose that RecN is a cohesion factor that promotes strict realignment of an extensive part of the nucleoid initiating at the site of a damaged replication fork.

RecN stimulates cell cycle restart after genotoxic stress. To evaluate the influence of RecN and SCIs on DNA repair efficiency, we analysed cell cycle restart after MMC treatment at the single-cell level on a microfluidic platform. WT and *recN* cells were grown in the microfluidic chamber for 20 min, $10 \mu\text{g ml}^{-1}$ MMC was injected for 10 min and immediately washed out with fresh medium. In these conditions, the WT and *recN* strains show almost similar viability to the untreated cells. We can thus observe the impact of RecN on the efficiency of repair rather than viability. Cell division and nucleoid dynamics were followed for 3 hours after washing (Fig. 5a,b and Supplementary Movies 4 and 5). In the presence of RecN, 70% of the bacteria recovered from the MMC treatment and underwent one (9%), two (50%) or three divisions (41%) in the ensuing 2 h. In the absence of RecN, only 36% of the cells recovered and performed one (16%), two (59%) or three divisions (25%). The number of filamenting cells at the end of the time course was also strongly reduced in the presence of RecN (15% in WT cells compared to 56% in the *recN* mutant). Altogether, these results suggest that RecN activity contributes to accelerate the repair process and thus allows a rapid return to normal growth.

The absence of RecN modifies RecA dynamics. It has been proposed that RecA contributes to RecN loading onto nucleoids via a direct RecA–RecN interaction²³, and our results suggest that RecN favors the rapid repair of MMC-induced lesions. We therefore sought to determine whether RecN influences RecA-mediated homology search and RecA-mediated DNA repair by preserving SCIs. RecA forms repair foci in the cell in the presence of DNA damage⁴¹, and the presence of Rad51 or 52 repair foci in eukaryotic cells is considered a good reporter of ongoing DNA repair⁴². Thus, we performed time-lapse fluorescence microscopy in the presence of MMC in strains containing an ectopic *recA*-mCherry fusion in addition to the wild-type *recA* gene. RecA-mCherry formed large aggregated foci at the pole as well as small dynamic foci that likely correspond to repair foci (Fig. 5c). The repair foci were very dynamic, and their fluorescence was weak. In the continuous presence of MMC, these foci only persisted at a given position for 10–20 min (Fig. 5e). In the absence of RecN, RecA formed foci and elongated dynamic structures (Fig. 5d–f). Elongated structures were observed in 21% of *recN* cells at any given time point (Fig. 5g), but almost every cell presented one at some point during the 90 min time course. They persisted for 30 ± 10 min. Such structures, called RecA bundles, have been described following sister chromatid cleavage by I-SceI, although their role in recombination repair is not yet understood⁴⁸. However, in contrast with this previous report, we observed very few bundles in WT cells after MMC treatment, suggesting that bundles form preferentially when the broken sister is far from its intact homologue.

Discussion

Repair of DNA damage by homologous recombination requires the presence of an undamaged sister homologue. In *E. coli*, during

a regular cell cycle, sister chromatids are kept in close contact by topological links called precatenanes^{16,17,43}. They allow for perfect alignment of sister chromatids and thus promote site-specific recombination between sister loci¹⁶. SCIs are thought to favour homologous recombination and could thus accelerate the repair process. However, because topological structures diffuse extensively on DNA, topological cuffing of sister chromatids might not persist if DNA is broken. In the present work, we unravel a role for SCIs in DNA damage repair induced by MMC. Furthermore, their preservation in the presence of MMC requires induction of the SOS response. We demonstrate here that RecN is a central protein for the preservation of SCIs (Fig. 1). The lack of *recN* is not as detrimental as *recA* or *lexA ind-* mutants for SCIs preservation, suggesting that another yet unknown factor may also participate in the process.

RecN is a well-conserved bacterial SMC protein, and its involvement in the repair of DSBs has been known for some time. In *E. coli*, RecN expression is repressed under regular growth conditions but is strongly expressed by the SOS regulon in the presence of MMC, ultraviolet, quinolone drugs or oxidative stress^{7,44}. Based on research in *D. radiodurans* and *B. subtilis*, two different functions have been proposed for RecN: a cohesion function²⁷ and an end-joining function^{26,28}. Recent work has suggested that RecN loading onto DSBs requires interaction with RecA²³. In our study, we demonstrate that RecN induction allows for preservation of SCIs and abolishes segregation of newly replicated loci (Fig. 1). In theory, preservation of SCIs may be possible if the binding of RecN to DNA ends prevents precatenane diffusion through the DSB. Importantly, because the absence of RecN can be rescued by a mutation that affects Topoisomerase IV function, we propose that RecN bridges sister chromatids in a manner similar to cohesins (Fig. 6). We cannot exclude that RecN participates in DSB end joining in *E. coli*, however our observations demonstrate that end joining is not the only function of RecN in *E. coli*. This is in good agreement with the huge amount of RecN produced upon SOS induction^{7,22}. ChIP-seq experiments demonstrated that RecA filaments extend over 20 kb from a double-strand break, this is much less than the extent of the genome affected by RecN activity (SCI preservation and the regression of segregated sister foci) suggesting that even if RecA directly interacts with RecN near the DSB, RecN should be able to escape and propagate on the genome (Fig. 6). Such a process is reminiscent with what has been observed for other bacterial SMC proteins, such as MukB and SMC (*B. subtilis* or *C. crescentus*) that are respectively loaded by MatP⁴⁵ and ParB^{46–49}. The mechanism by which RecN promotes cohesion is not yet understood. As *E. coli* RecN is a small SMC protein ($\sim 1/3$ of SMC3), it is unlikely that a dimer alone could form a ring that entraps two DNA double strands. Multimers of of *D. radiodurans* RecN have been observed, therefore, we can postulate that head-to-tail RecN multimerization can favour long stretches of sister chromatid pairing (Fig. 6).

Theoretically, replication-dependent precatenanes could facilitate repair via homologous recombination by increasing SCIs. However, the observations that RecN is required to preserve SCIs in the presence of MMC suggest that precatenanes are not sufficient to maintain SCIs under these conditions. We observed that Topo IV alteration, which prevents the removal of post-replicative precatenanes, can fully compensate for the absence of RecN in the presence of MMC. This means that when post-replicative precatenanes are not efficiently removed by Topo IV, they facilitate homology search and homologous recombination. It has been proposed that precatenanes do not accumulate homogeneously along the chromosome^{15,16}, some regions called SNAPs tend to remain colocalized, presumably because SeqA bound to these regions inhibits Topo IV activity⁴³. SCIs are

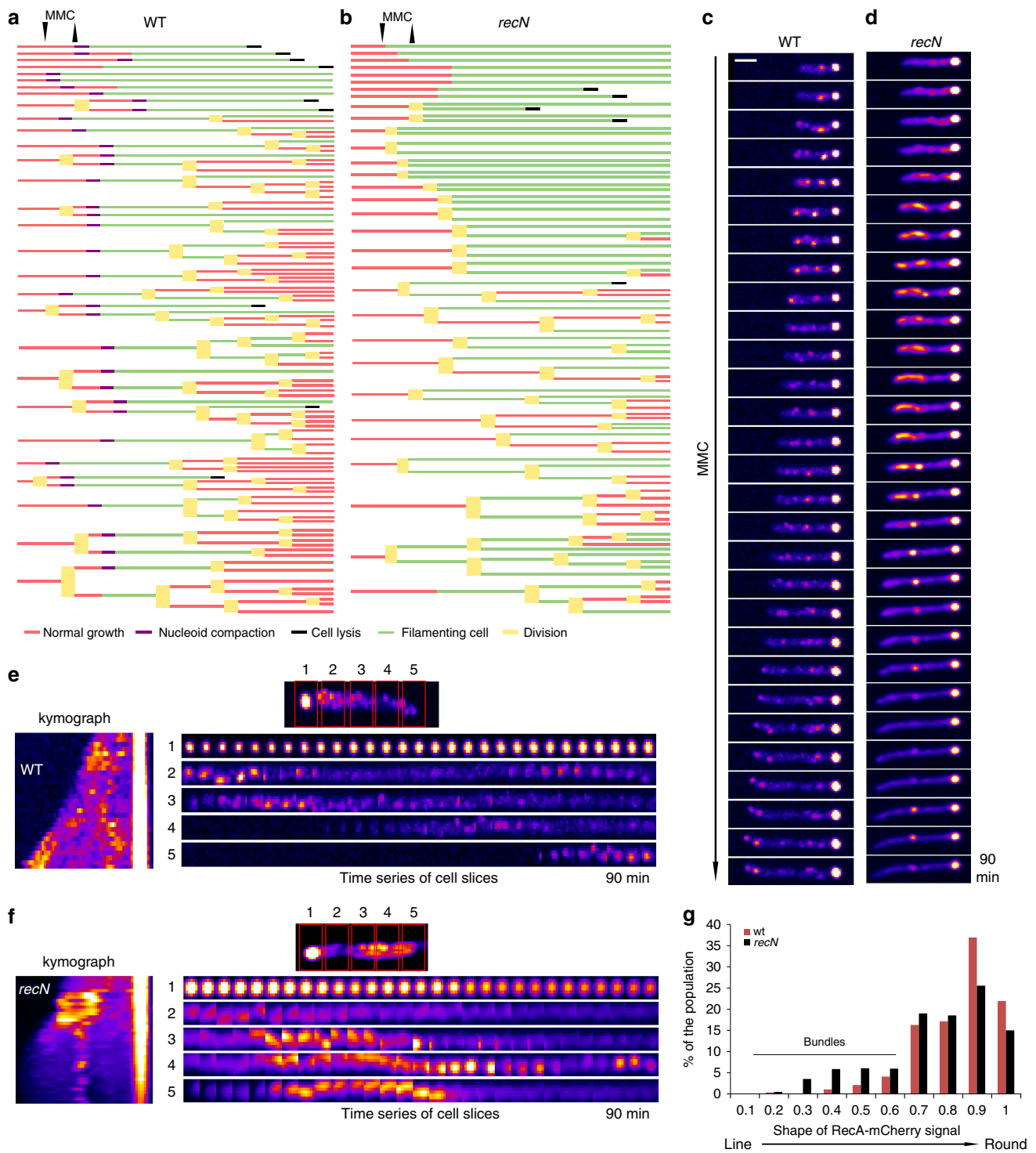


Figure 5 | *recN* mutant has altered homology search and delayed cell cycle restart. (a) Cell cycle restart pattern after a brief MMC treatment using a microfluidic platform. WT cells were introduced into the chambers, and fresh minimal medium A was perfused for 20 min; $10 \mu\text{g ml}^{-1}$ MMC was then perfused for 10 min and immediately washed with clean medium, and incubation and imaging were continued for over 3.5 h. Cell lineage was measured for 100 cells; each colour corresponds to a given state of the cell. (b) The same experiment as described in a was performed in the *recN* mutant, which exhibits delayed cell cycle restart. (c) Representative time-lapse microscopy of RecA-mCherry focus dynamics in the presence of MMC in the WT strain. Time-lapse imaging starts at 5 min after initial contact with MMC. Pictures were acquired every 3 min for 2 h on an agarose pad with MMC. (d) RecA-mCherry focus dynamics in the presence of MMC in the *recN* mutant. Experiments were performed as described in c. (e) Analysis of RecA foci dynamics. Kymograph and time series of cell slices for RecA-mCherry WT. The experiment was performed as described in c. (f) Analysis of RecA foci dynamics in the *recN* mutant. The experiment was performed as described in d. (g) The frequency of bundles was estimated as a function of the shape of the RecA mCherry signal in WT and the *recN* mutant. The WT and *recN* distribution are significantly different (t -test $P = 10^{-30}$). Scale bar is $1 \mu\text{m}$.

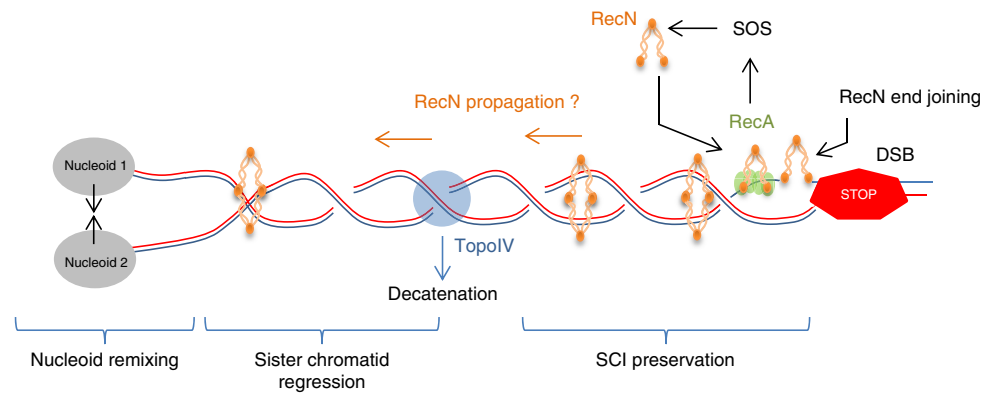


Figure 6 | Roles of RecN during repair of an induced DSB. Our observations suggest that when a replicative DSB occurs, RecA (Green) is responsible for RecN (orange) expression (through the SOS response) and RecN loading onto the sister chromatids. RecN loading prevents the complete removal of SCIs by Topo IV (blue) and may participate in DNA end joining. In a second step, RecN may propagate on the newly replicated chromatids to mediate regression of the segregated sister chromatids and re-mixing of brother nucleoids.

preserved in SNAPS, and it would be interesting to ascertain whether this corresponds to improved homologous recombination at these sites.

In addition to preserving SCIs, MMC provokes regression of segregated sister foci. Similar observations have been previously reported for I-SceI^{18,19,31}. This regression of sister chromatids over a large distance is correlated with the re-merging of segregating nucleoids. SCI preservation, sister regression and nucleoid merging are dependent on the RecA and RecN proteins. The fluorescent labelling of two loci spaced 188 kb apart on the same replicore revealed that MMC induces RecN-dependent realignment of the nucleoids rather than random condensation. Our observations suggest that inhibition of sister segregation is the first activity of RecN when recruited to the DSB by RecA and that segregated loci regression is a secondary step. However, we do not yet understand the mechanism promoting this or the purpose of such a profound chromosomal reorganization.

Bacteria experience a large number of stresses in the environment or in their host, many of which induce DSBs. To survive DSBs, *E. coli* induces the SOS response, which blocks cell division and suspends the bacterial cell cycle. Following genotoxic stress, it is essential for damaged bacteria to restart growth as quickly as possible. Therefore, SOS induction could be essential for survival in an environment in which competition among bacterial species is high. Our observations demonstrate that growth recovery is significantly accelerated in the presence of RecN (Fig. 5a,b), and this capacity of RecN to accelerate repair might be responsible for its high conservation among bacteria. In this way, RecN can be viewed as an ancestor of the SMC5/6 complex that maintains stalled replication forks in a recombination-competent conformation^{50,51}.

Methods

Strains. The strains and plasmids used in this study are described in Supplementary Table 1. All strains are derived from wild-type MG1655 or MG1656 (Δ lac MluI). Strains containing *loxP* sites were constructed by λ red recombination using the plasmid pGBK Δ lax as matrix¹⁶. The strains used for microscopy were constructed by λ red recombination using the plasmid pGBK Δ parS-pMT1 as matrix⁵². Details of the construction are presented in the Supplementary Methods. The RecA-mCherry fusion is a gift from Bénédicte Michel; its construction is described in the Supplementary Methods.

LoxP assays. Every experiment is performed in the same conditions. An overnight culture was diluted 1:200 in Minimum Media A supplemented with 0.2% glycerol and 0.2% casamino acids. Three to five biological replicates were performed for each sample. The cells were grown at the indicated temperature to an OD_{600nm} of ~0.2. In these conditions, generation time at 37 °C is 65 min. Cre expression was induced by the addition arabinose (0.1%) to growth media. Genotoxic stress was

induced by the addition of 10 μ g ml⁻¹ MMC to the growth media at time point 0. At each time point, 1.5 ml of cells was flash frozen in liquid nitrogen. Genomic DNA was extracted using the Pure Link Genomic DNA Mini Kit (Life Technologies) and quantified using a Nanodrop spectrophotometer (Thermo Scientific). Genomic DNA was diluted to 2 ng ml⁻¹, and PCR was performed using ExTaq polymerase (Takara). The amplified DNA was analysed using the DNA 1000 Assay on a Bioanalyzer (Agilent). The frequency of recombination was measured as follows: (amount of *1loxP* DNA + amount of *2loxP* DNA)/(total amount of *loxP* DNA).

Colony forming unit measurement. At an OD_{600nm} of 0.2, 10 μ g ml⁻¹ MMC or 1 μ g ml⁻¹ AZT was added to the culture. Cell viability was followed every 10 min for 40 min. At each time point, cells were serially diluted in LB (10⁰–10⁻⁶) and plated on LB agar plates. Plates were incubated for 16 h at 37 °C, and colonies were counted.

EdU staining. At an OD_{600nm} of 0.2, the cells were either incubated with 10 μ g ml⁻¹ of MMC for 10 min and then incubated with an equal amount of 2X EdU (Click-IT Assay Kit, Thermo Fisher Scientific) (to monitor DNA replication) or first incubated with an equal amount of 2X EdU for 10 min and then MMC (to monitor DNA degradation). Cells were then fixed with Formaldehyde mix (5% Formaldehyde, 0.05% Glutaraldehyde and 1 \times PBS) for 10 min at room temperature and 50 min on ice. Cells were washed three times with 1 \times PBS and resuspended in 98 μ l of fresh GTE buffer (50 mM glucose, 20 mM Tris pH 8, 10 mM EDTA). Cells can be left ON at 4 °C. Following this step, 2 μ l of freshly prepared 500 μ g ml⁻¹ lysozyme were added to each sample and the sample was then immediately transferred onto a poly-lysine-coated slide and left for 3 min at room temperature. The slide was rinsed twice with 1 \times PBS, and 150 μ l Click-IT Cocktail (prepared according to manufacturer's instructions) was added; the sample was then incubated in the dark at room temperature for 30 min. The slides were rinsed two times with 1 \times PBS + DAPI (1 μ g ml⁻¹). The slides were then rinsed 10 times with 1 \times PBS and left to dry at room temperature. Finally, 10 μ l of SlowFade (Thermo Fisher Scientific) were added to the slide. The slides were stored at 4 °C for one hour before imaging.

Microscopy. An overnight culture was diluted 1:200 in Minimum Media A supplemented with 0.2% casamino acids and 0.25% glucose (to limit overexpression of ParB protein glucose is used instead of glycerol for microscopy experiments). In these conditions, generation time at 37 °C is 50 min. The cells were grown to an OD_{600nm} = 0.2 at 37 °C, pelleted and resuspended in 50 μ l of fresh medium. One per cent Agarose pad slides were prepared within a gene frame (VWR)⁵³. Genotoxic stress was induced by the addition of 10 μ g ml⁻¹ MMC or 1 μ g ml⁻¹ AZT to the agarose pad. Time-lapse microscopy was performed using a confocal spinning disk (X1 Yokogawa) on a Nikon Ti microscope at 100 \times magnification controlled by Metamorph (Molecular Imaging) and an EMCCD camera (Roper). Definite focus (Nikon) was used for each time point. Images were acquired every 3 min for 2 h at 30 °C. Five positions were observed simultaneously for each experiment, with 20–50 cells per position. Snapshot experiments for focus counting and inter-foci distance measurements were performed as previously described⁵³.

Microfluidic experiments. An overnight culture was diluted 1:200 in Minimum Media A supplemented with 0.2% casamino acids and 0.25% glucose. The cells were grown to an OD_{600nm} of approximately 0.2. A microfluidic plate was set-up according to the Merck Millipore protocol for bacteria. Medium changes were

controlled by the Onyx system from Merck Millipore. Fresh minimum medium A was perfused for 20 min at 37 °C; 10 µg ml⁻¹ MMC was perfused for 10 min and fresh medium was perfused for 3 h. Images were acquired every 3 min using a confocal spinning disk (Yokogawa W1) on a Zeiss Axio imager microscope at a × 63 magnification with an Orca Flash 4 camera (Hamamatsu). Time-lapse images were acquired using Metamorph (Molecular Imaging) and analysed with ImageJ software.

Data availability. All relevant data, material and methods are available from the authors.

References

- Pâques, F. & Haber, J. E. Multiple pathways of recombination induced by double-strand breaks in *Saccharomyces cerevisiae*. *Microbiol. Mol. Biol. Rev.* **63**, 349–404 (1999).
- Zdraveski, Z. Z., Mello, J. A., Marinus, M. G. & Essigmann, J. M. Multiple pathways of recombination define cellular responses to cisplatin. *Chem. Biol.* **7**, 39–50 (2000).
- Kuzminov, A. Recombinational repair of DNA damage in *Escherichia coli* and bacteriophage lambda. *Microbiol. Mol. Biol. Rev.* **63**, 751–813 (1999).
- Michel, B., Boubakri, H., Baharoglu, Z., LeMasson, M. & Lestini, R. Recombination proteins and rescue of arrested replication forks. *DNA Repair (Amst.)* **6**, 967–980 (2007).
- Sassanfar, M. & Roberts, J. W. Nature of the SOS-inducing signal in *Escherichia coli*. The involvement of DNA replication. *J. Mol. Biol.* **212**, 79–96 (1990).
- Kreuzer, K. N. DNA damage responses in prokaryotes: regulating gene expression, modulating growth patterns, and manipulating replication forks. *Cold Spring Harb. Perspect. Biol.* **5**, a012674 (2013).
- Courcelle, J., Khodursky, A., Peter, B., Brown, P. O. & Hanawalt, P. C. Comparative gene expression profiles following UV exposure in wild-type and SOS-deficient *Escherichia coli*. *Genetics* **158**, 41–64 (2001).
- Kenyon, C. J. & Walker, G. C. DNA-damaging agents stimulate gene expression at specific loci in *Escherichia coli*. *Proc. Natl Acad. Sci. USA* **77**, 2819–2823 (1980).
- Nasmyth, K. & Haering, C. H. Cohesin: its roles and mechanisms. *Annu. Rev. Genet.* **43**, 525–558 (2009).
- Sjögren, C. & Nasmyth, K. Sister chromatid cohesion is required for postreplicative double-strand break repair in *Saccharomyces cerevisiae*. *Curr. Biol.* **11**, 991–995 (2001).
- Ström, L., Lindroos, H. B., Shirahige, K. & Sjögren, C. Postreplicative recruitment of cohesin to double-strand breaks is required for DNA repair. *Mol. Cell* **16**, 1003–1015 (2004).
- Unal, E. *et al.* DNA damage response pathway uses histone modification to assemble a double-strand break-specific cohesin domain. *Mol. Cell* **16**, 991–1002 (2004).
- Ström, L. *et al.* Postreplicative formation of cohesin is required for repair and induced by a single DNA break. *Science* **317**, 242–245 (2007).
- Unal, E., Heidinger-Pauli, J. M. & Koshland, D. DNA double-strand breaks trigger genome-wide sister-chromatid cohesion through Eco1 (Ctf7). *Science* **317**, 245–248 (2007).
- Joshi, M. C. *et al.* *Escherichia coli* sister chromosome separation includes an abrupt global transition with concomitant release of late-splitting intersister snaps. *Proc. Natl Acad. Sci. USA* **108**, 2765–2770 (2011).
- Lesterlin, C., Gigant, E., Boccard, F. & Espéli, O. Sister chromatid interactions in bacteria revealed by a site-specific recombination assay. *EMBO J.* **31**, 3468–3479 (2012).
- Wang, X., Reyes-Lamothe, R. & Sherratt, D. J. Modulation of *Escherichia coli* sister chromosome cohesion by topoisomerase IV. *Genes Dev.* **22**, 2426–2433 (2008).
- Lesterlin, C., Ball, G., Schermelleh, L. & Sherratt, D. J. RecA bundles mediate homology pairing between distant sisters during DNA break repair. *Nature* **506**, 249–253 (2014).
- Shechter, N. *et al.* Stress-induced condensation of bacterial genomes results in re-pairing of sister chromosomes: implications for double strand DNA break repair. *J. Biol. Chem.* **288**, 25659–25667 (2013).
- Lloyd, R. G., Picksley, S. M. & Prescott, C. Inducible expression of a gene specific to the RecF pathway for recombination in *Escherichia coli* K12. *Mol. Gen. Genet.* **190**, 162–167 (1983).
- Sargentini, N. J. & Smith, K. C. Characterization of an *Escherichia coli* mutant (radB101) sensitive to gamma and UV radiation, and methyl methanesulfonate. *Radiat. Res.* **93**, 461–478 (1983).
- Finch, P. W., Chambers, P. & Emmerson, P. T. Identification of the *Escherichia coli* recN gene product as a major SOS protein. *J. Bacteriol.* **164**, 653–658 (1985).
- Keyamura, K., Sakaguchi, C., Kubota, Y., Niki, H. & Hishida, T. RecA protein recruits structural maintenance of chromosomes (SMC)-like RecN protein to DNA double-strand breaks. *J. Biol. Chem.* **288**, 29229–29237 (2013).
- Picksley, S. M., Attfield, P. V. & Lloyd, R. G. Repair of DNA double-strand breaks in *Escherichia coli* K12 requires a functional recN product. *Mol. Gen. Genet.* **195**, 267–274 (1984).
- Meddows, T. R., Savory, A. P., Grove, J. I., Moore, T. & Lloyd, R. G. RecN protein and transcription factor DksA combine to promote faithful recombinational repair of DNA double-strand breaks. *Mol. Microbiol.* **57**, 97–110 (2005).
- Pellegrino, S. *et al.* Structural and functional characterization of an SMC-like protein RecN: new insights into double-strand break repair. *Structure* **20**, 2076–2089 (2012).
- Reyes, E. D., Patidar, P. L., Uranga, L. A., Bortoletto, A. S. & Lusetti, S. L. RecN is a cohesin-like protein that stimulates intermolecular DNA interactions *in vitro*. *J. Biol. Chem.* **285**, 16521–16529 (2010).
- Ayora, S. *et al.* Double-strand break repair in bacteria: a view from *Bacillus subtilis*. *FEMS Microbiol. Rev.* **35**, 1055–1081 (2011).
- Sanchez, H. & Alonso, J. C. *Bacillus subtilis* RecN binds and protects 3'-single-stranded DNA extensions in the presence of ATP. *Nucleic Acids Res.* **33**, 2343–2350 (2005).
- Badrinarayanan, A., Le, T. B. K. & Laub, M. T. Rapid pairing and re-segregation of distant homologous loci enables double-strand break repair in bacteria. *J. Cell Biol.* **210**, 385–400 (2015).
- Odsbu, I. & Skarstad, K. DNA compaction in the early part of the SOS response is dependent on RecN and RecA. *Microbiology* **160**, 872–882 (2014).
- Weng, M. *et al.* Repair of mitomycin C mono- and interstrand cross-linked DNA adducts by UvrABC: a new model. *Nucleic Acids Res.* **38**, 6976–6984 (2010).
- Otsuji, N. & Murayama, I. Deoxyribonucleic acid damage by monofunctional mitomycins and its repair in *Escherichia coli*. *J. Bacteriol.* **109**, 475–483 (1972).
- Kogoma, T., Cadwell, G. W., Barnard, K. G. & Asai, T. The DNA replication priming protein, PriA, is required for homologous recombination and double-strand break repair. *J. Bacteriol.* **178**, 1258–1264 (1996).
- Kogoma, T., Torrey, T. A. & Connaughton, M. J. Induction of UV-resistant DNA replication in *Escherichia coli*: induced stable DNA replication as an SOS function. *Mol. Gen. Genet.* **176**, 1–9 (1979).
- Lin, L. L. & Little, J. W. Isolation and characterization of noncleavable (Ind-) mutants of the LexA repressor of *Escherichia coli* K-12. *J. Bacteriol.* **170**, 2163–2173 (1988).
- Adikesavan, A. K. *et al.* Separation of recombination and SOS response in *Escherichia coli* RecA suggests LexA interaction sites. *PLoS Genet.* **7**, e1002244 (2011).
- El Sayyed, H. *et al.* Mapping topoisomerase IV binding and activity sites on the *E. coli* genome. *PLoS Genet.* **12**, e1006025 (2016).
- Bridges, B. A. & Woodgate, R. Mutagenic repair in *Escherichia coli*: products of the recA gene and of the umuD and umuC genes act at different steps in UV-induced mutagenesis. *Proc. Natl Acad. Sci. USA* **82**, 4193–4197 (1985).
- Zusman, D. R., Carbonell, A. & Haga, J. Y. Nucleoid condensation and cell division in *Escherichia coli* MX74T2 ts52 after inhibition of protein synthesis. *J. Bacteriol.* **115**, 1167–1178 (1973).
- Renzette, N. *et al.* Localization of RecA in *Escherichia coli* K-12 using RecA-GFP. *Mol. Microbiol.* **57**, 1074–1085 (2005).
- Lisby, M., Barlow, J. H., Burgess, R. C. & Rothstein, R. Choreography of the DNA damage response: spatiotemporal relationships among checkpoint and repair proteins. *Cell* **118**, 699–713 (2004).
- Joshi, M. C. *et al.* Regulation of sister chromosome cohesion by the replication fork tracking protein SeqA. *PLoS Genet.* **9**, e1003673 (2013).
- Jeong, K. S., Ahn, J. & Khodursky, A. B. Spatial patterns of transcriptional activity in the chromosome of *Escherichia coli*. *Genome Biol.* **5**, R86 (2004).
- Nolivos, S. *et al.* MatP regulates the coordinated action of topoisomerase IV and MukBEF in chromosome segregation. *Nat. Commun.* **7**, 10466 (2016).
- Gruber, S. & Errington, J. Recruitment of condensin to replication origin regions by ParB/SpoOJ promotes chromosome segregation in *B. subtilis*. *Cell* **137**, 685–696 (2009).
- Marbouty, M. *et al.* Condensin- and replication-mediated bacterial chromosome folding and origin condensation revealed by Hi-C and super-resolution Imaging. *Mol. Cell* **59**, 588–602 (2015).
- Sullivan, N. L., Marquis, K. A. & Rudner, D. Z. Recruitment of SMC by ParB-parS organizes the origin region and promotes efficient chromosome segregation. *Cell* **137**, 697–707 (2009).
- Wang, X. *et al.* Condensin promotes the juxtaposition of DNA flanking its loading site in *Bacillus subtilis*. *Genes Dev.* **29**, 1661–1675 (2015).
- Irmisch, A., Ampatzidou, E., Mizuno, K., O'Connell, M. J. & Murray, J. M. Smc5/6 maintains stalled replication forks in a recombination-competent conformation. *EMBO J.* **28**, 144–155 (2009).
- Lindroos, H. B. *et al.* Chromosomal association of the Smc5/6 complex reveals that it functions in differently regulated pathways. *Mol. Cell* **22**, 755–767 (2006).
- Espéli, O. *et al.* A MatP-divisome interaction coordinates chromosome segregation with cell division in *E. coli*. *EMBO J.* **31**, 3198–3211 (2012).
- Espeli, O., Mercier, R. & Boccard, F. DNA dynamics vary according to macromolecule topography in the *E. coli* chromosome. *Mol. Microbiol.* **68**, 1418–1427 (2008).

Acknowledgements

We thank Bénédicte Michel and Michele Valens for the gift of the strains. We also thank Bénédicte Michel for scientific advice and careful reading of the manuscript. We thank Anouar Khayachi for his help on the Co-Immunoprecipitation experiments. We thank Avradip Chatterjee and Kenneth Mariani for RecN antibody. We thank Angela Taddei for helping us with the Onix Cell microfluidics system. This work was supported by ANR (grants ANR-14-CE10-0007 MAGISBAC and ANR-15-CE11-0023-01 HIRESBACS), Fondation ARC, Ligue contre le Cancer and Fondation pour la Recherche Médicale.

Author contributions

E.V., C.P., I.G.J., C.C. designed, performed and analysed experiments; O.E. designed and analysed experiments. E.V., C.C. and O.E. wrote the manuscript.

Additional information

Supplementary Information accompanies this paper at <http://www.nature.com/naturecommunications>

Competing financial interests: The authors declare no competing financial interests.

Reprints and permission information is available online at <http://npg.nature.com/reprintsandpermissions/>

How to cite this article: Vickridge, E. *et al.* Management of *E. coli* sister chromatid cohesion in response to genotoxic stress. *Nat. Commun.* **8**, 14618 doi: 10.1038/ncomms14618 (2017).

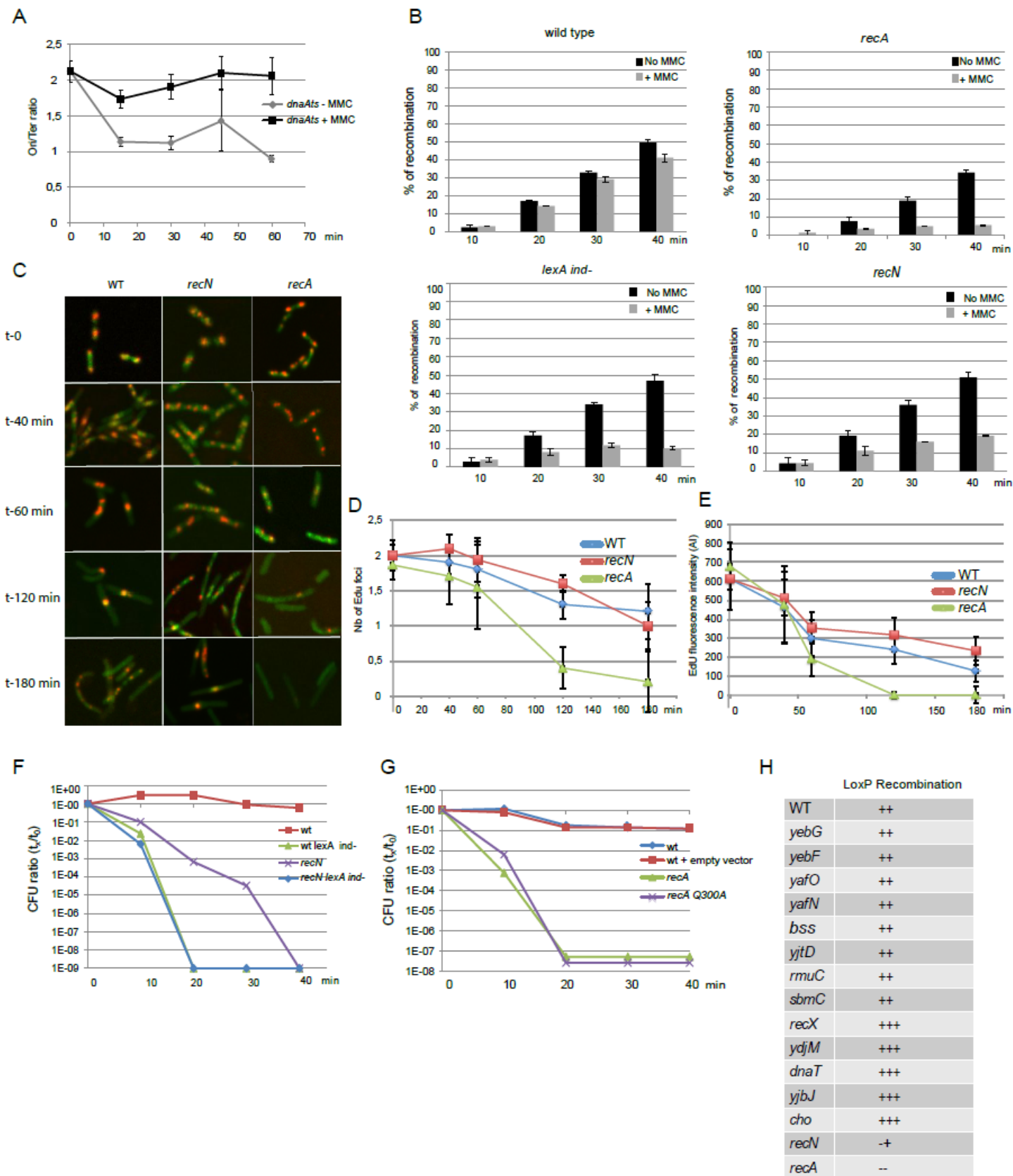
Publisher's note: Springer Nature remains neutral with regard to jurisdictional claims in published maps and institutional affiliations.



This work is licensed under a Creative Commons Attribution 4.0 International License. The images or other third party material in this article are included in the article's Creative Commons license, unless indicated otherwise in the credit line; if the material is not included under the Creative Commons license, users will need to obtain permission from the license holder to reproduce the material. To view a copy of this license, visit <http://creativecommons.org/licenses/by/4.0/>

© The Author(s) 2017

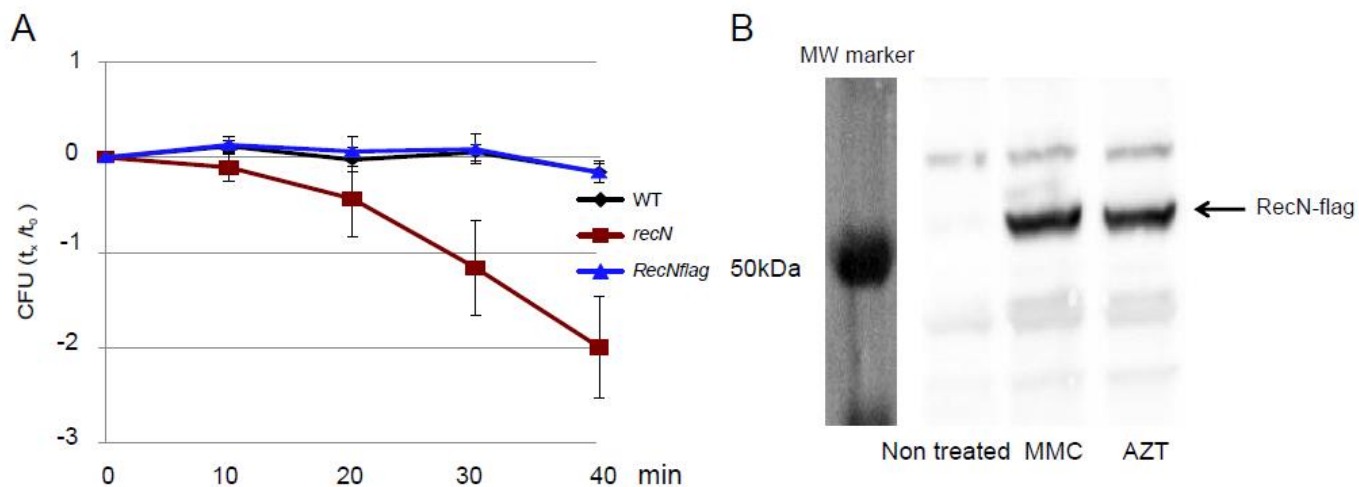
Supplementary Fig. 1 brings supplementary data regarding Figure 1 of the manuscript. Experiments on RecN's role on DNA degradation and the preservation of SCIs.



Supplementary Figure 1

A) MMC provokes a rapid replication arrest. We used a strain with a *dnaAts* allele to block the initiation of replication when placed at 40°C. The *ori/ter* ratio was monitored by qPCR. In the repressive condition the progression of replication provokes an increase of the amount of terminus region. In the presence of MMC the *ori/ter* ratio is constant, suggesting replication arrest. **B)** Frequency of *loxP*/Cre recombination at the *ori-3* locus for various mutants. *LoxP* assays were performed 10, 20, 30 and 40 min after addition of 10µg/ml MMC. *LoxP* recombination frequency was monitored in the WT, *recA*, *lexA ind-* Supplementary Fig. 1 brings supplementary data regarding Figure 1 of the manuscript. Experiments on RecN's role on DNA degradation and the preservation of SCIs. (SOS down) and *recN* mutants treated with MMC (10µg/ml) or not. The frequency of recombination products (1 +3 *loxP*) compared to non recombined products (2 *loxP*) was measured by PCR and bioanalyzer detection. Results are expressed as the *loxP* recombination frequency at each timepoint $(1+3loxP)/(1+2+3loxP)$. Error bars are standard deviation of 4 experiments. **C)** Monitoring degradation of newly replicated DNA in the WT, *recN* and *recA* mutants. EdU was incorporated for 10 min before addition of MMC, at the indicated time-point, after addition of MMC, the cells were washed, fixed and immuno-stained (red), DNA was stained with DAPI (green). **D)** Quantification of the average number of EdU foci per nucleoids of the cells presented in panel C. **E)** Quantification of the average intensity of EdU fluorescence in the cells presented in panel C. **F)** Cell viability in response to MMC (10µg/ml) for the indicated mutants. Bacteria were treated for the indicated amount of time with MMC then washed and plated on LB plates. The data are plotted as a ratio between the number of colonies formed in the absence of MMC and the number of colonies formed in the presence of MMC. Error bars are standard deviation of 200 cells. **G)** Cell viability in response to MMC (10µg/ml) for the indicated mutants. Experiments were performed as in Fig S1G. **H)** *loxP* recombination in response to 10µg/ml MMC treatment for various SOS mutants. Mutants were treated for 40 min with 10µg/ml MMC or not. Results are expressed as the mutant recombination frequency with MMC over the wild type recombination frequency with MMC.

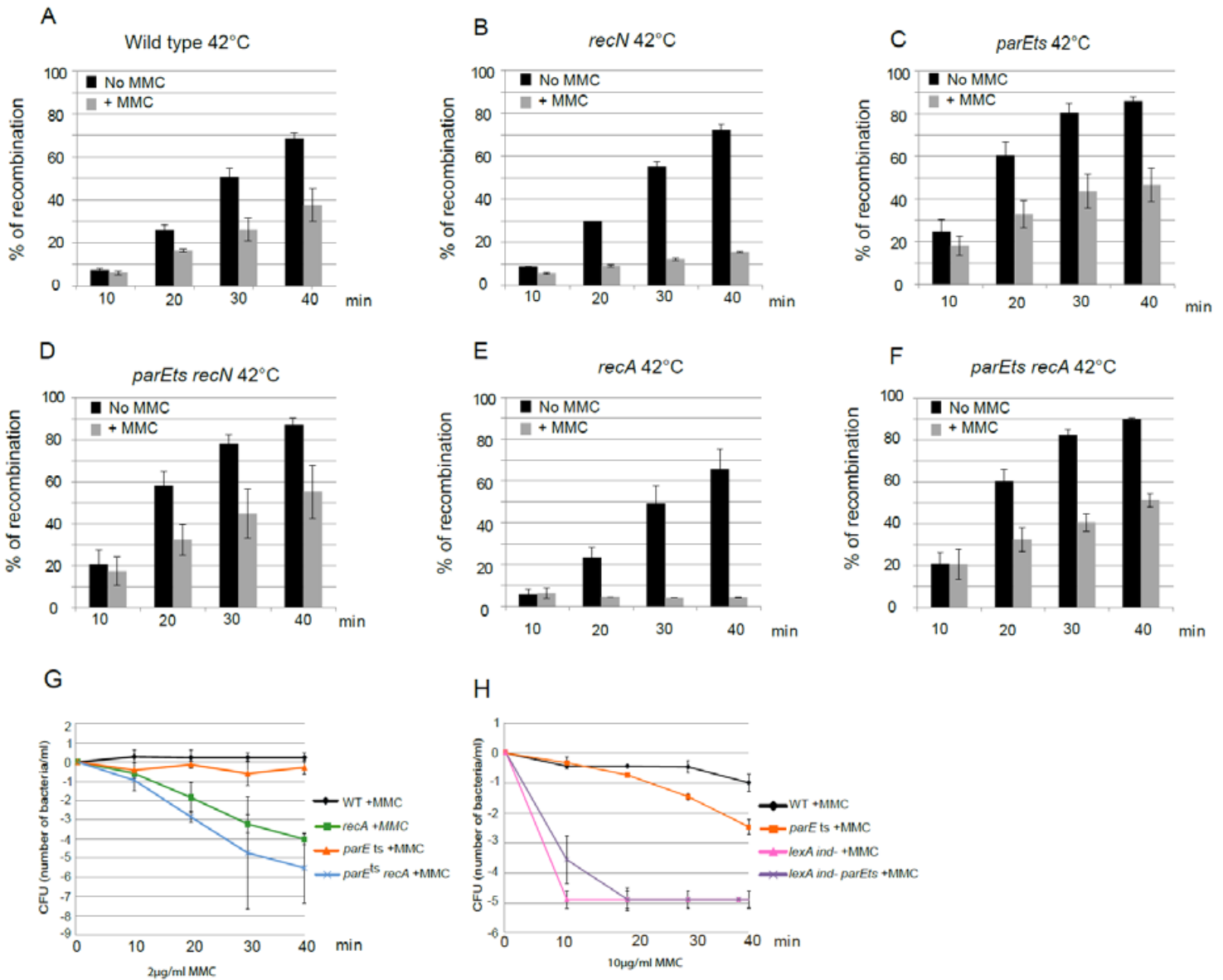
Supplementary Fig. 2 brings supplementary data regarding Figure 2 of the manuscript. Experiments show viability curves and a WB of the induction of the RecN-flag construction



Supplementary Figure 2

A) Cell viability of the RecN flag-tagged strain compared to the WT and *recN* strains. Cells were treated for 10, 20, 30 or 40 min with 10 μ g/ml MMC. Cell viability was assessed for each time point. Error bars are standard deviation of 3 experiments. **B)** RecN protein is expressed in cells treated with 10 μ g/ml MMC or 1 μ g/ml AZT. Western blot analysis on a RecN-flag protein reveals that RecN protein is induced in response to a 40 min MMC treatment or a 40 min AZT treatment. RecN is strongly repressed in the absence of DNA damage. Secondary antibody coupled with Horse radish peroxidase was used to reveal RecN-flag protein. The MW marker lane was acquired using bright field light.

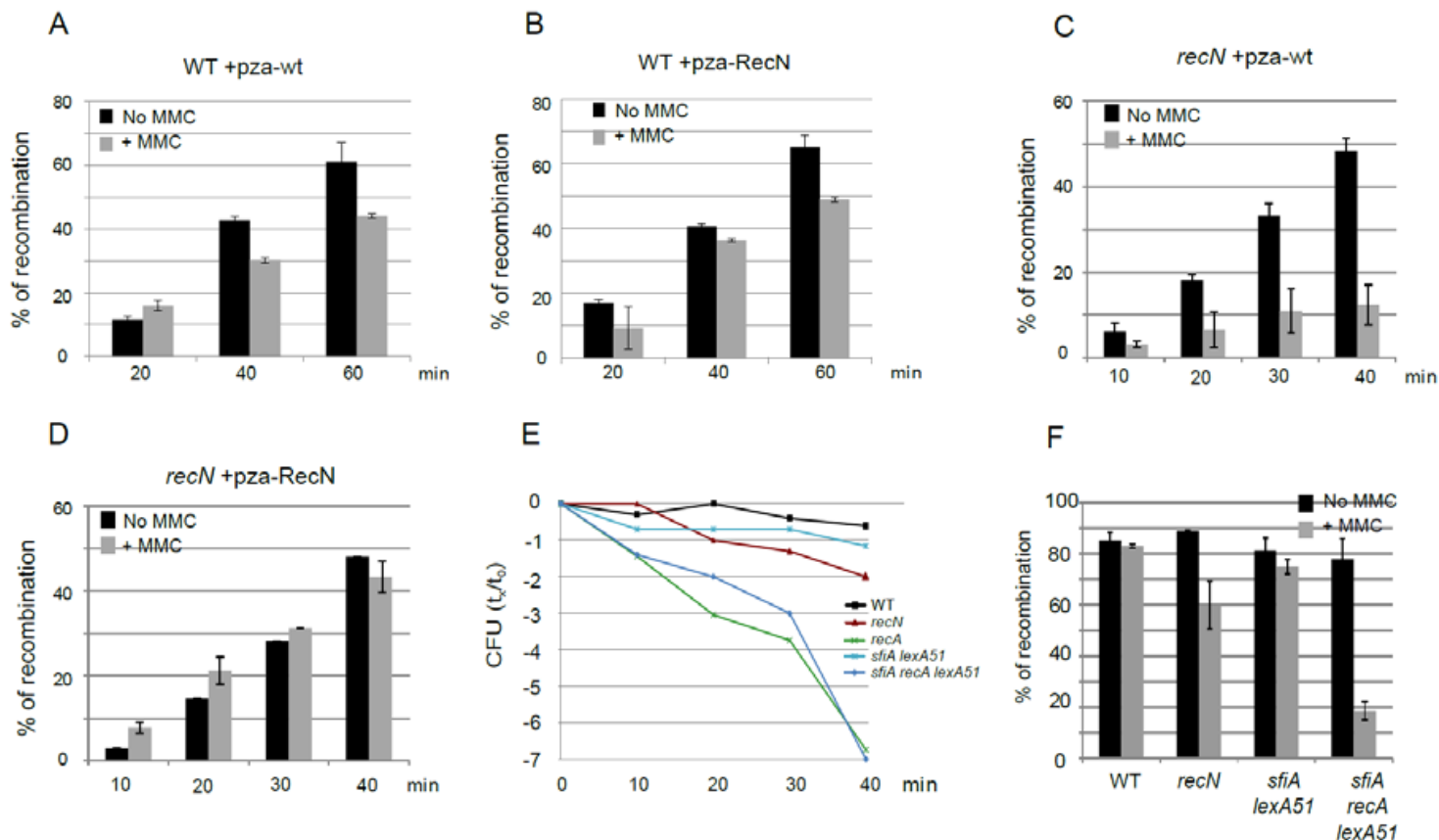
Supplementary Fig. 3 brings supplementary data regarding Figure 3 of the manuscript. Experiments show the effect of Topoisomerase IV inhibition on SCIs and viability in a WT, a *recN* and a *recA* background



Supplementary Figure 3

A-F) Measure of SCIs following Topo IV alterations in the presence of MMC. *loxP* assays were performed 10, 20, 30 and 40 min after addition of 10µg/ml MMC. Results are expressed as the *loxP* recombination frequency for each timepoint. The cells were incubated 25min at 42°C prior to addition of arabinose (for Cre induction) and MMC (10µg/ml). Error bars are standard deviation of 3 experiments. **G)** Cell viability in response to MMC (2µg/ml) for the indicated mutants. **H)** Cell viability in response to MMC (10µg/ml) for the indicated mutants. Error bars are standard deviation of 3 experiments.

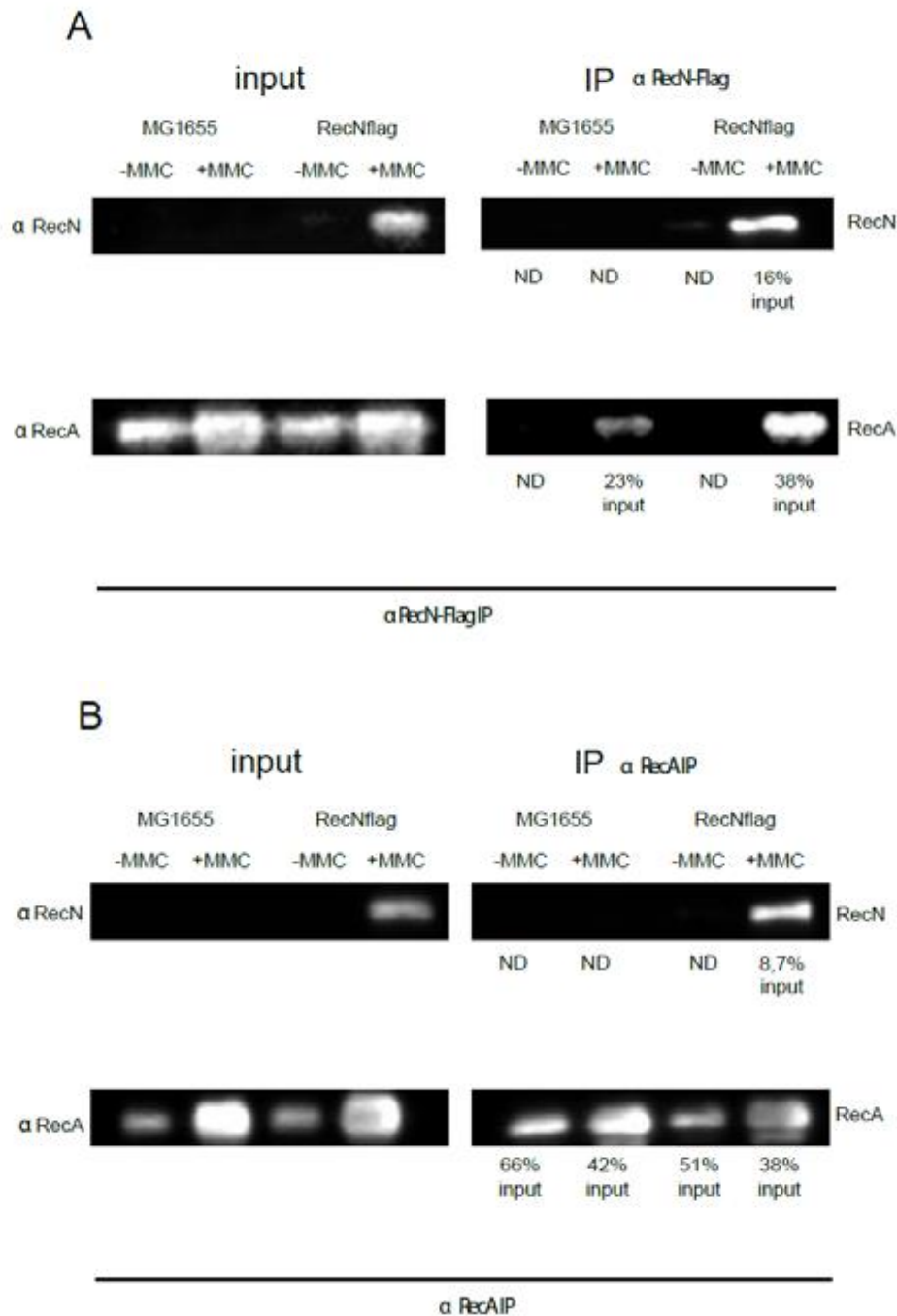
Supplementary Fig. 4 brings supplementary data regarding Figure 4 of the manuscript. Experiments show the effect of RecN overexpression on SCIs and the effect of constitutive *lexA* induction on SCIs and viability



Supplementary Figure 4

A-D) Influence of *RecN* overexpression on SCIs. *recN* was cloned onto a plasmid with a leaky promoter. *loxP* recombination frequency was measured at 10, 20, 30 and 40min. Results are expressed as the percentage of *loxP* recombination at each time point. **E)** Cell viability of constitutively induced SOS strains. Cells were treated for 10, 20, 30 or 40min with 10µg/ml MMC. Cell viability was assessed for each time point. **F)** SCIs of constitutively induced SOS strains. Cells were treated for 40min with 10 µg/ml of MMC. Due to poor growth conditions in minimum medium, the assay was performed in LB. Results are expressed as the percentage of *loxP* recombination at each time point. Error bars are standard deviation of 3 experiments.

Supplementary Fig. 5 brings supplementary data regarding Figure 5 of the manuscript. Experiments show WB revelation of a RecN IP blotted by anti-RecN and anti-RecA and a RecA IP blotted by anti-RecN and anti-RecA



Supplementary Figure 5

A) RecA co-immunoprecipitates with RecN. Immunoprecipitation with an anti-flag antibody was done on the RecN protein tagged with a flag peptide and a WT MG1655 strain. Samples were blotted with an anti-flag antibody (top panel) or an anti-RecA antibody (bottom panel) revealing an interaction between RecN and RecA. **B)** RecN co-immunoprecipitates with RecA. Immunoprecipitation with an anti-RecA antibody was performed on the WT MG1655 strain and the strain carrying the RecN-flag protein. Samples were blotted with an anti-flag antibody (top panel) or an anti-RecA antibody (bottom panel) revealing an interaction between RecN and RecA. The percentage of IP signal compared to Input signal is indicated.

Supplementary Table. 1 brings supplementary data regarding Figure 4 of the manuscript. The table shows statistical significance of the inter-focal distances measured between two foci spaced by 188 kb in the WT strain and *recN* mutant.

	WT	WT + 15 min MMC	WT + 45 min MMC	<i>recN</i>	<i>recN</i> + 15 min MMC	<i>recN</i> + 45 min MMC
WT		0.204	4.10^{-37}	0.219	0.008	3.10^{-44}
WT + 15 min MMC			9.10^{-25}	0.019	0.23	2.10^{-30}
WT + 45 min MMC				5.10^{-42}	6.10^{-19}	0.12
<i>recN</i>					2.10^{-4}	5.10^{-48}
<i>recN</i> + 15 min MMC						3.10^{-23}
<i>recN</i> + 45 min MMC						

Supplementary Table 1

Statistical significance (t-test) of the difference between inter-focal distances measured in the WT and *recN* mutant in Fig 4E and 4F.

B. Complementary results

In this paragraph are presented complementary results to the work that led to the article published in Nature Communications (Vickridge et al., 2017) and also new results that I obtained after the publication of the article and a few very recent results obtained by Adrien Camus, a master student under my supervision. These results bring a complementary view on RecN interplay with Topoisomerases, sister chromatid cohesion in the presence of drugs leading to single strand gaps, and chromosome and chromatin dynamics in the presence of DSBs.

1. Implication and role of Topoisomerases in sister chromatid cohesion in response to genotoxic stress

a) Inhibition of Gyrase compensates the loss of viability and sister chromatid interactions of a recN mutant

It has been demonstrated that the inhibition of Topoisomerase IV leads to an increase of sister chromatid interactions during replication, due to inhibition of precatenane removal (Lesterlin et al., 2012).

As described in Vickridge *et al.*, the loss of SCIs observed in a *recN* mutant can be compensated by an inhibition of Topoisomerase IV. Inhibiting Topoisomerase IV in a *recN* mutant also compensates the loss of viability of *recN* (Vickridge et al., 2017). Considering these intriguing results, I thought to test the possible involvement of other Topoisomerases in sister chromatid cohesion (SCC) during DNA damage. Gyrase is a Type II Topoisomerase that can compensate for the overwinding generated by the replication fork on the unreplicated region, ahead of the replication fork. When Gyrase's activity is insufficient, the positive supercoils ahead of the fork may also diffuse behind the replication fork, creating topological links called precatenanes, which are further relieved by the action of Topoisomerase IV. Gyrase is 100 fold less efficient than Topoisomerase IV for decatenation, it is therefore postulated that its activity is very limited on precatenanes. Gyrase activity is essential to promote replication at an optimum

speed (Khodursky et al., 2000) but also to maintain topological homeostasis during transcription.

To test the impact of the inhibition of Gyrase on sister chromatid interactions (SCIs) in the presence of DSBs, I used a Gyrase thermosensitive mutation in the B subunit of Gyrase called *GyrB^{ts}*. At 30°C, Gyrase is active and cells are viable. At 40°C, Gyrase is inactive and cells cannot form colonies. I tested the inhibition of Gyrase on viability and SCIs in a WT and *recN* background.

As observed in a *Topo IV^{ts}* mutant, inhibition of Gyrase at a non-permissive temperature in untreated cells lead to an increase of SCIs (1.3x). This is in good agreement with an increase of the catenation of sister chromatids. In the presence of MMC, I observed an increase of SCIs in the *GyrB^{ts}* mutant compared to the WT strain and a slight decrease of SCIs relative to the untreated *GyrB^{ts}* sample. These results suggest that when topological tension increases because of a Gyrase inhibition, the *Topo IV* molecules present in the cell are not able to globally increase their activity to deal with the excess of links between sister chromatids. Interestingly, deleting *recN* in the *GyrB^{ts}* mutant did not significantly decrease the level of SCIs. These observations are comparable to the ones observed in the *Topo IV^{ts} recN* mutant (figure 29A). We can hypothesize that the effect seen in the Gyrase mutant which is similar to the effect of the *Topo IV^{ts}* mutant, is the consequence of the supercoils accumulated ahead of the fork and diffusing behind the replication fork.

To test whether these high levels of SCIs were also favorable to viability and could compensate for the loss of viability of the *recN* mutant, I performed a CFU experiment (figure 29B). The inhibition of Gyrase rescued a portion of the viability of the *recN* mutant. However, the results differ from what was observed with *Topo IV^{ts}* where the rescue was total. These observations confirm that DNA topology management is an important aspect of DSB repair and that *RecN* is really at the interface between DNA repair and DNA topology or DNA organization. Interestingly, unlike the *Topo IV^{ts}* mutant, the *GyrB^{ts}* mutant alone was not sensitive to MMC. It has been shown that replication is slow in a Gyrase mutant (Khodursky et al., 2000) while it progresses at full speed in *Topo IV^{ts}* mutant (Wang et al., 2008). This could explain that the Gyrase mutant was less sensitive to MMC than the *Topo IV^{ts}* mutant even if topological problems are comparable. These observations give rise to several questions that remain

unanswered. If Gyrase is inhibited and the precatenanes are diffused behind the fork, why isn't Topo IV action enough to release the topological links causing SCIs? Could there be an excess of precatenanes that Topo IV is unable to handle? Are these precatenanes partly involved in the rescue of the *recN* viability?

We can hypothesize that replication may be only partly arrested, moving gradually forward as the supercoils ahead of the fork diffuse behind. The *GyrB^{ts}* mutant alone would therefore be less sensitive than the *Topo IV^{ts}* mutant because it encounters less frequently an ICL. Moreover, replication being decreased in the *Gyrase^{ts}* mutant, the NER pathway may have more time to excise the ICLs before the replication fork encounters a crosslink leading to a DSB. Interestingly, the viability of the *Topo IV^{ts}* and *Gyrase^{ts}* mutant differed, but the amount of SCIs was equivalent suggesting that the sensitivity of the *Topo IV^{ts}* mutant may be specific to its action on precatenanes or may be linked to another of its function's, maybe during decatenation. These points will be addressed in the discussion section.

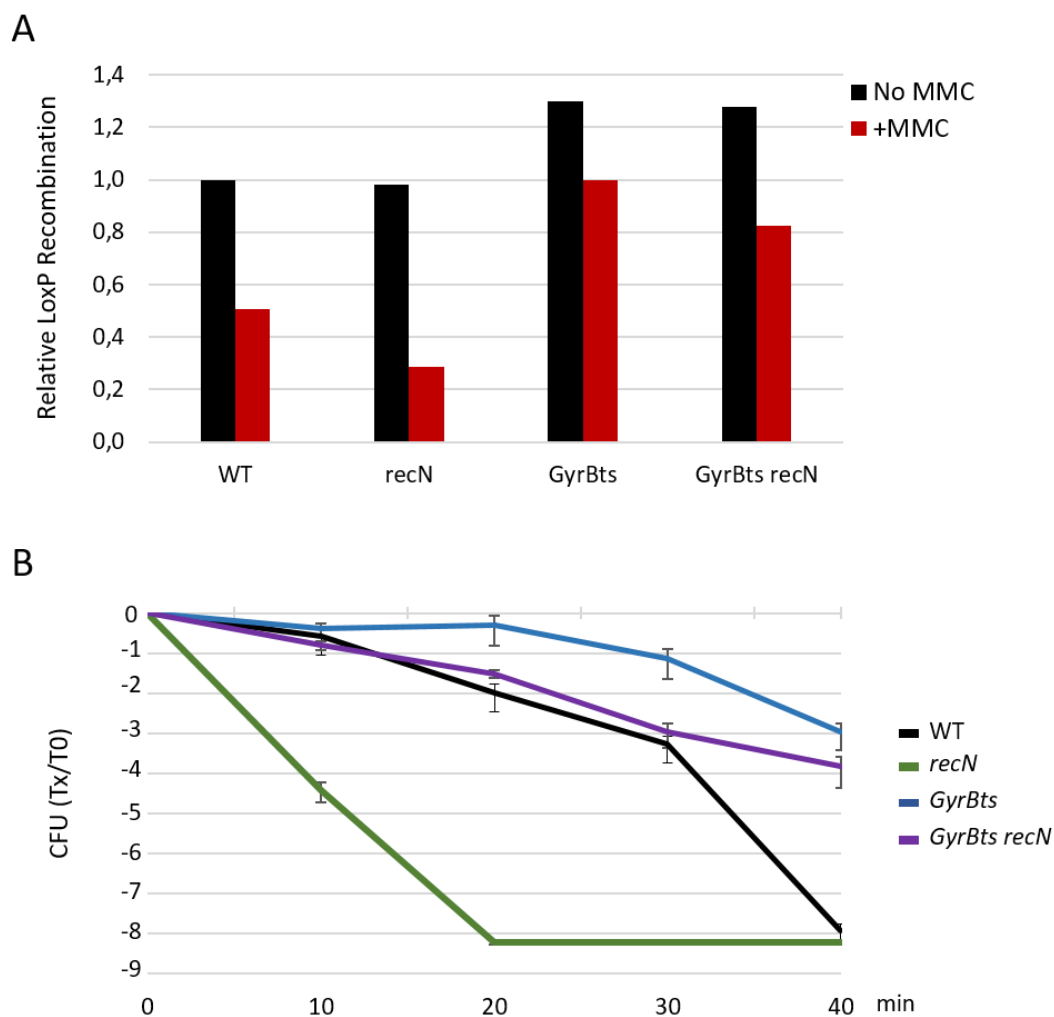


Figure 29. Inhibition of Gyrase activity compensates the loss of SCIs and viability of a *recN* mutant

A- Measurement of SCIs following Gyrase alteration in the presence of 10 $\mu\text{g/ml}$ MMC. Results after a 30 min of MMC treatment are presented. Results are expressed as a relative *loxP* recombination, normalized to the untreated WT. Cells were incubated at 40°C for 20 min prior to addition of 10 $\mu\text{g/ml}$ MMC and 0.1% arabinose. B- Measurement of cell viability following Gyrase alteration in the presence of 15 $\mu\text{g/ml}$ MMC. Cells were incubated at 40°C for 20 min prior to MMC addition and plated in serial dilutions at 10, 20, 30, and 40 min after MMC addition.

b) *Topoisomerase III acts at ssGaps created by AZT but not HU*

Topoisomerase III is a Type I Topoisomerase. It was shown that overexpression of Topo III can compensate for the loss of viability of a Topo IV^{ts} mutant, suggesting that it can act to release precatenanes (Nurse et al., 2003). Its potential role in the resolution of Holliday Junctions (HJs) during Homologous Recombination (HR), described by Zhu *et al.* in 2001 was also an interesting observation that lead to testing Topo III's possible implication in MMC mediated SCC (Zhu et al., 2001). Deleting *topB* (the Topo III gene) in a WT or a *recN* background did not alter the SCI profile in the absence or presence of MMC treatment (figure 30A). When using a *recA* mutant that is ineffective for HR, we showed that the SCIs observed in response to MMC treatment were not the result of HR intermediates (Vickridge et al., 2017). Considering that Topo III may act to resolve Holliday Junctions during HR, it is possible that there is no effect on SCIs linked to this property of Topo III. An interesting experiment would be to overexpress Topo III in a Topo IV^{ts} mutant to see if it reverts the compensation of the *recN* mutant by Topo IV inhibition thanks to its capacity to remove precatenanes.

We tested the deletion of Topo III on sister chromatid cohesion in response to AZT or Hydroxyurea (HU) treatment. AZT is a chain terminator creating single strand gaps, which may lead to DSBs if they are not repaired before an encounter with the next replication fork. Hydroxyurea treatment reduces the pool of nucleotides, resulting in a rapid replication arrest and creating single strand gaps.

When cells were treated with AZT, the frequency of inter sister chromatid *loxP*/Cre recombination is drastically reduced (figure 30B). This was also observed when cells were treated with HU (figure 30C). I used an intra-molecular recombination cassette to test if Cre expression or activity could have been reduced because of AZT or HU treatment (figure 30D). Intra-molecular recombination was not altered in the presence of AZT or HU suggesting that the loss of SCIs is not due to poor Cre induction. The substantial loss of inter-molecular SCIs in response to AZT or HU was very puzzling. Our first interpretation was that replication was arrested and Topoisomerase IV very efficiently removed the remaining topological links. In this case, RecN might not be able to intervene on sister chromatids. When replication is inhibited in a DnaC^{ts} mutant, we observe a gradual drop of SCIs. In this mutant, Ori-dependant initiation is prevented at the origin but ongoing rounds of replication can carry on. In cells

treated by HU or AZT, replication forks are arrested at any genomic location by incorporation of AZT, a chain terminator, or by nucleotide pool depletion (HU treatment) and no ongoing replication can continue. This may explain the discrepancy observed between both experiments. Interestingly, deleting Topo III lead to a slight increase of SCIs when treated with AZT. This increase was independent of RecN, suggesting that Topo III may partially act at ssGAPs to remove the topological links. These topological links are not suitable substrates for RecN cohesion activity since deleting *recN* in the Topo III mutant had no effect on SCIs when treated with AZT (figure 29B). Topo III deletion did not enhance SCIs in cells treated with HU, suggesting that the replication arrest and the ssGaps created by HU may not be analogous to AZT formed ssGaps and are not a suitable substrates for the action of Topo III (figure 29C).

These observations are interesting because the role of Topo III remains mysterious. Here we observed for the first time a direct, but modest, topological role of Topo III in a wild type genetic context.

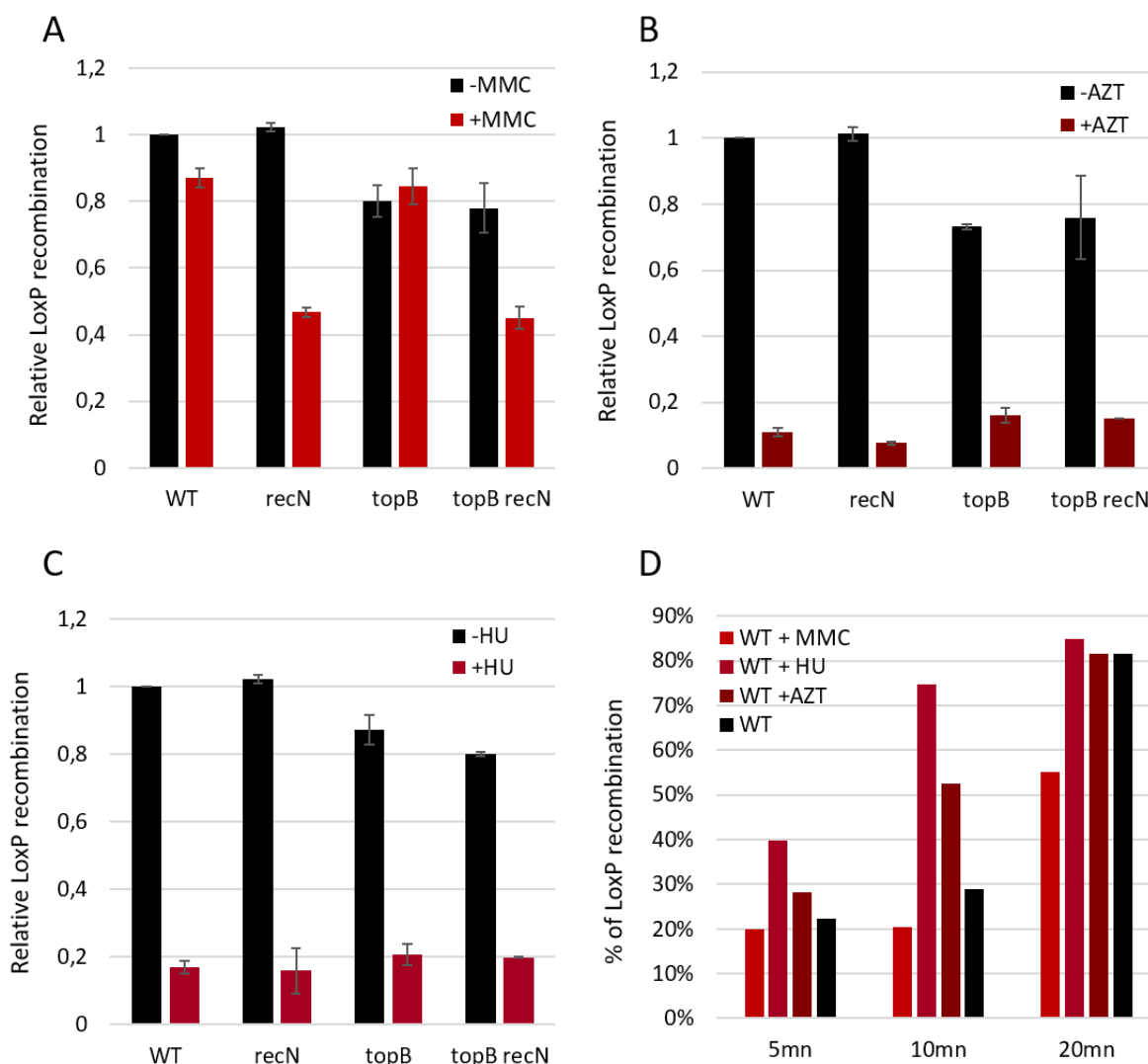


Figure 30. Topo III acts at ssGaps induced by AZT but not by HU

A- Measurement of SCIs in a *topB* mutant in the presence of 10 $\mu\text{g/ml}$ MMC. Results after a 30 min MMC treatment are presented. Results are expressed as a relative *loxP* recombination, normalized to the untreated WT. B- Measurement of SCIs in a *topB* mutant in the presence of 1 $\mu\text{g/ml}$ AZT. Results after a 30 min AZT treatment are presented. Results are expressed as a relative *loxP* recombination, normalized to the untreated WT. C- Measurement of SCIs in a *topB* mutant in the presence of 10X Hydroxy Urea. Results after a 30 min HU treatment are presented. Results are expressed as a relative *loxP* recombination, normalized to the untreated WT. D- Intramolecular recombination of 2 *loxP* sites inserted on either side of a rifampicine resistance gene was measured at 5, 10 and 20 min after arabinose addition in the presence of AZT, HU or MMC. Results are expressed as a percentage of recombination.

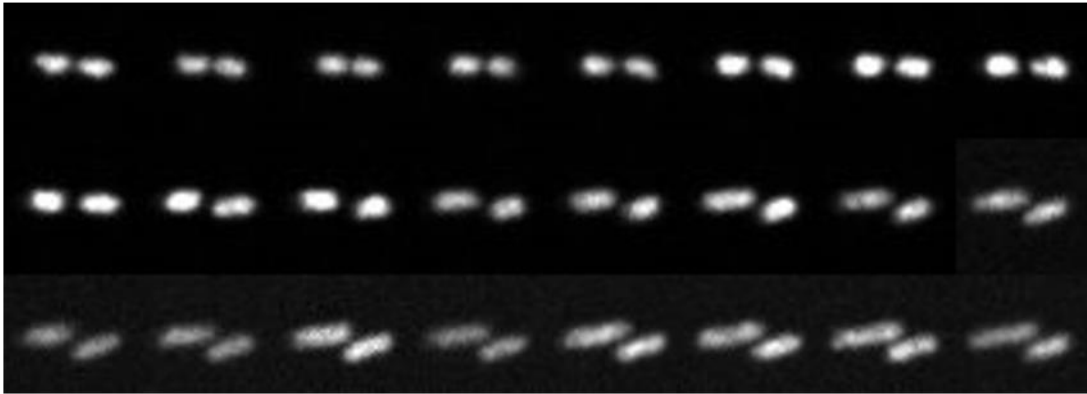
2. RecN influences nucleoid dynamics

As published in Vickridge *et al.*, timelapse experiments with an HU-mcherry fluorescent protein in a WT and *recN* mutant revealed an unexpected function of RecN for nucleoid dynamics when the cells were treated with MMC. Indeed, upon MMC addition, the nucleoids merge transiently in a process that is dependent on RecN. When MMC is maintained in the medium, the nucleoids decondense after a ~10min compaction period, as the cells filament. Microfluidics experiments revealed that when MMC is washed after 10 minutes, the nucleoids also decondense as the cells filament.

The shortness of the compaction period was surprising. How can such a brief phenomenon be sufficient to promote repair? A hypothesis for this brief nucleoid merging is that filamentation of the cells changes the physical constraint on the nucleoids, and the decondensation observed results from a passive nucleoid expansion due to cell volume increase. To test this hypothesis, I observed nucleoid merging and decondensation in a *sulA* mutant. Sula is a highly induced SOS protein that inhibits cell division in response to DNA damage. I performed timelapse experiments in the presence of MMC and observed cell division with phase contrast acquisitions. I also observed the nucleoids with HU-mcherry labelling. Interestingly, I observed two different phenotypes. 42 % of cells divided once after MMC addition, as we could expect in a *sulA* mutant, but 58% of cells did not divide, as the WT would. In the cells that were capable of dividing, DNA was not at the septum (two nucleoids already separated in the two daughter cells). They divided after a brief compaction of each nucleoid, but the nucleoids remained in distinct cells halves, the septum ring may have already been formed. After division, the cells filamented, as observed in WT strains and the nucleoids decondensed as the cells filamented (figure 31A). I observed that the cells that did not divide at all may have had DNA at their septum (nucleoids were not clearly distinct), suggesting the action of another cell division inhibition process, maybe SImA. SImA is another checkpoint protein which is SOS independent and prevents cell division when DNA is detected at the septum (Bernhardt and de Boer, 2005) (figure 31B). Unfortunately, I did not find conditions where I observed nucleoid merging in the absence of subsequent cell filamentation. In all conditions, the cells ended up filamenting, and the nucleoids decondensed. It could have been relevant to test a *sImA sulA* mutant to fully impede cell filamentation. In order to address the question of space constraint

on nucleoid compaction and decondensation, we could also make the cells filament first, with cephalixin for instance, and then treat the cells with MMC and measure the compaction volume or measure whether the time of compaction is shorter when the cell is bigger.

A



B

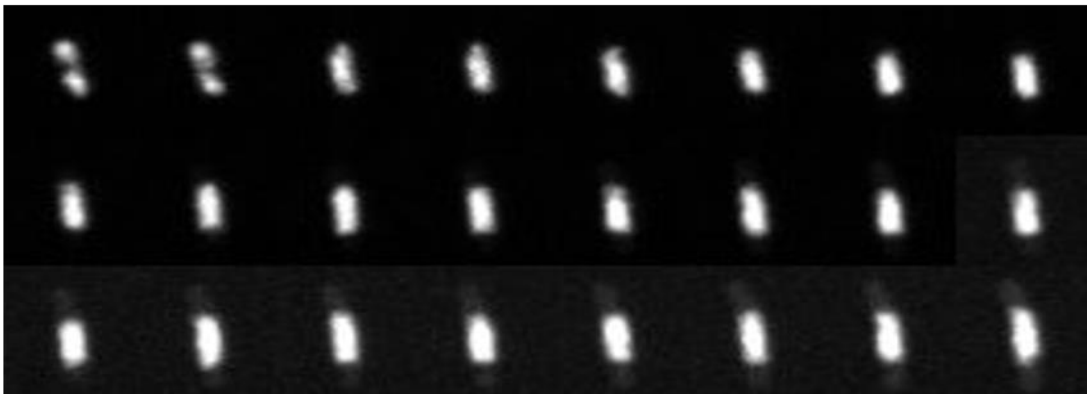


Figure 31. Influence of *sulA* deletion on nucleoid compaction and cell filamentation

Images were taken every three minutes for 80 min. A- Image montage of the HU-mcherry signal of a cell that divides and then filaments. B- Image montage of the HU-mcherry signal of a cell that does not divide but filaments.

3. The mobility of fluorescent foci is increased in a *recN* mutant

An article published in 2012 by the team of Rodney Rothstein revealed that the mobility of fluorescently marked loci was increased when the chromosome is damaged in yeast. They suggested that a higher mobility favored homology search, allowing the broken DNA end to explore a larger portion of the chromosome (Miné-Hattab and Rothstein, 2012). Similar observations were made by Dion and coworkers in 2012. Later, Strecker *et al.* confirmed these observations and showed the impact of centromere tethering on DSB induced foci mobility. In the absence of DNA damage, centromeres constrain chromatin mobility. Upon induction of a DSB, this constraint is counteracted by various proteins, allowing an increase of mobility of the broken DNA ends (Dion et al., 2012; Strecker et al., 2016) .

One of the hypothesis for the role of RecN in the repair process is that it could enhance homology search and therefore may influence DNA mobility. To investigate whether RecN could be involved in such a process in *E. coli*, I tagged a given locus near the origin, with a fluorescent protein and measured the mobility of the foci in a WT strain or a *recN* mutant after DNA damage induced by MMC, during a timelapse experiment. The mobility of the foci was measured for 10 min with 10 sec intervals, approximately 10 min after MMC induction. I used the mosaic plugin on imageJ to analyze the movement of the foci. Here are represented the mean square displacement slopes which are characteristic of a subdiffusive movement ($MSD = c (\Delta t^\alpha)$, $\alpha = MSD \text{ slope}$), for each focus over the course of the timelapse. The mean square displacement gives the average distance (here in pixels, 1 pixel = 100nm) that a particle travels in a given time (here, 10 seconds). After MMC addition, we calculated the mean MSD slope of hundreds of fluorescent foci. The MSD slope was increased in the WT strain ($\alpha = 0.52 \pm 0.13$) relative to the MSD slope in untreated cells ($\alpha = 0.46 \pm 0.11$). This is in good agreement with the work of R. Rothstein (figure 32A). In the *recN* mutant, MSD slopes was not increased when treated with MMC ($\alpha = 0.43 \pm 0.11$) (figure 32B and 32C). Complementary analyses are required to characterize these changes and confirm the eventual influence of RecN in the process.

Although RecN acts to keep sister chromatids cohesive in response to DNA damage, possibly reducing the mobility of the whole chromatids, it may, at a local level, favor the mobility of

the DNA and favor homology search or protein diffusion. Moreover, Rothstein's work describes that the increase of DNA dynamics is dependent on early the steps of HR. This RecN-dependent increase of mobility could therefore be the indirect consequence of RecN's involvement in early steps of HR, maybe via its interaction with RecA. In the absence of RecN, HR may be decreased and associated loci mobility too.

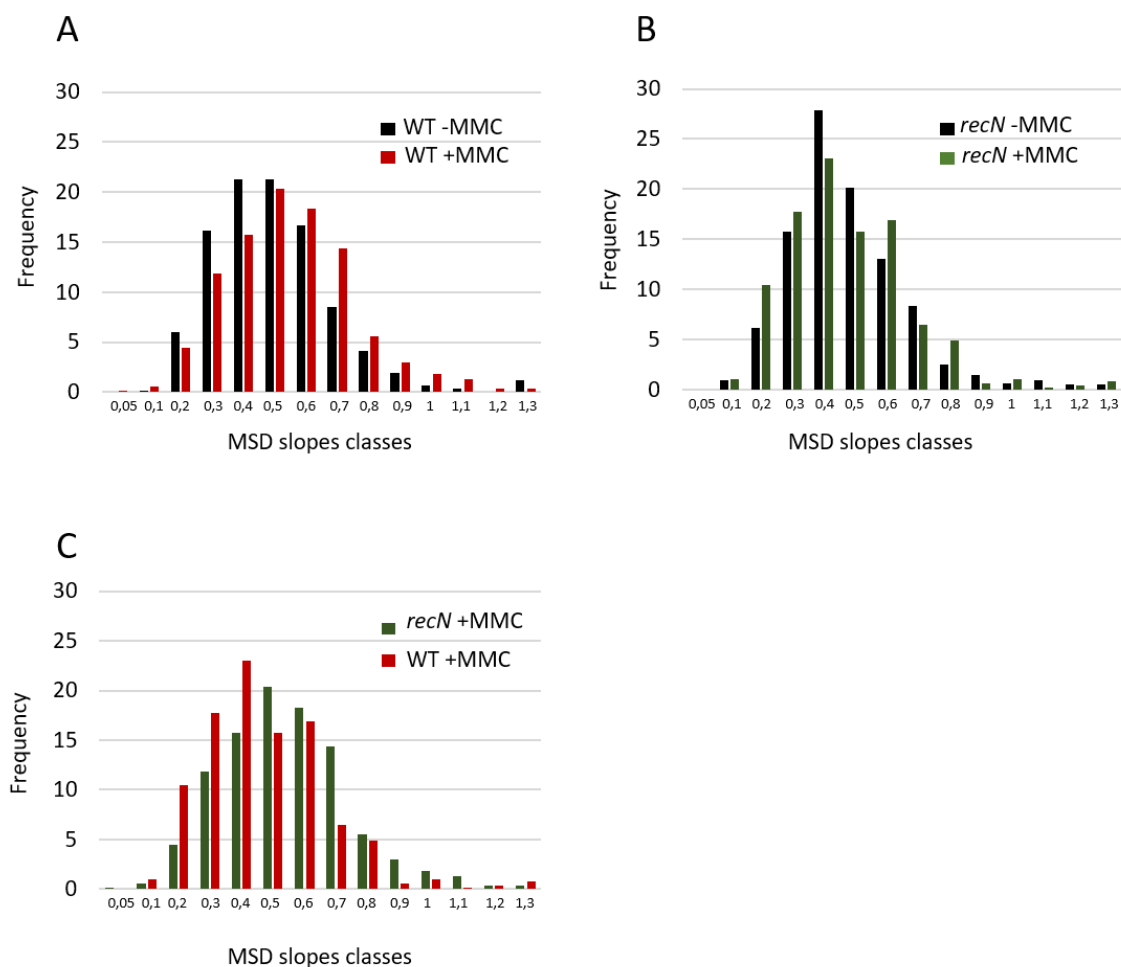


Figure 32. Effect of MMC on MSD slopes of fluorescent foci in a WT strain and *recN* mutant

A fluorescent tag was inserted near the origin in the WT strain and the *recN* mutant. A timelapse was performed in the presence or absence of MMC. The mean square displacement slope (MSD slope) was measured for each fluorescent focus. A- Comparison of MSD slopes in the WT strain treated with MMC versus the untreated WT. B- Comparison of MSD slopes in the *recN* mutant treated with MMC versus the untreated *recN* C- Comparison of MSD slopes in the *recN* mutant treated with MMC versus the WT strain treated with MMC.

4. FRAP microscopy reveals RecN's influence on the diffusion of a DNA binding protein

To further understand and characterize the observation on foci dynamics and the whole nucleoid compaction observed in MMC treated cells, I performed FRAP experiments on HU-GFP stained nucleoids of a WT strain and a *recN* mutant. FRAP (Fluorescence Recovery After Photobleaching) is a method used in microscopy to measure the diffusion rate of proteins through cells. As a reporter of chromatin dynamics, I used an HU-GFP fluorescent protein in the WT and *recN* mutant and photobleached a region corresponding to approximately half the nucleoid. The intention was to infer a diffusion coefficient of the DNA, attached by HU-GFP protein. However, the diffusion rate was short, suggesting that we might actually be measuring the diffusion rate of HU-GFP protein on the nucleoid rather than movement of the nucleoid itself.




Considering the nucleoids undergo different conformations when treated with MMC (compacted, decompacted), I performed FRAP on nucleoids in the different stages of nucleoid dynamics in the WT strain and *recN* mutant. Phase 1 corresponds to timepoint 0 after MMC addition. Phase 2 corresponds to 10-15 min after MMC addition, the nucleoids are in a compacted form, and phase 3 corresponds to 25-30 min after MMC addition when the nucleoids have decompacted and the cells are filamenting. Regardless of the stage the nucleoid was in, we observed that the diffusion rate of HU was much shorter in the WT than in the *recN* mutant. When performing FRAP on the nucleoids before they underwent compaction (phase1), the half-life of fluorescence regeneration was 1.37sec in the WT strain and 2.33 seconds in the *recN* mutant, suggesting that even before the compaction is visible, structural reorganization may be happening. In the second phase, when WT nucleoids were compacted and *recN* nucleoids weren't (phase2), the half-life of fluorescence regeneration was substantially different: 0.19 sec in the WT compacted nucleoids and 1.38 sec in the *recN* mutant. Interestingly, the half-life also decreased in the *recN* mutant, although to a much lesser extent than in the WT. Finally, in the last phase, corresponding to decondensed nucleoids (phase 3), the half-life of fluorescence recovery decreased, although very slightly, in the WT and the *recN* mutant (figure 33A, 33B and 33C). This observation is quite surprising since one could expect the half-life to increase when the nucleoids are decondensed. It is

possible that at this stage, the cells are dying or the DNA is highly damaged, maybe fragmented, favoring quick movement of the HU-GFP protein.




Altogether, these results suggest that protein diffusion may be decreased in a *recN* mutant, due to a different state of structure of the nucleoid. By promoting a whole nucleoid compaction, RecN may favor the diffusion and recruitment of the proteins to the break.

Interestingly, these results match the foci mobility and nucleoid dynamics experiments. Indeed, RecN favors nucleoid compaction and protein diffusion along the damaged nucleoid, consistent with an increased mobility of broken loci. Altogether, these results suggest that RecN strongly alters chromosome dynamics, protein diffusion and nucleoid mobility during DNA damage.

A

Wild type	Phase1 	Phase2 	Phase3 
Medium half life (in seconds)	1.37 (+/- 0.86)	0.19 (+/- 0.04)	0.17 (+/- 0.059)

B

<i>recN</i> mutant	Phase1 	Phase2 	Phase3 
Medium half life (in seconds)	2.33 (+/- 1.07)	1.38 (+/- 0.34)	1.13 (+/- 0.209)

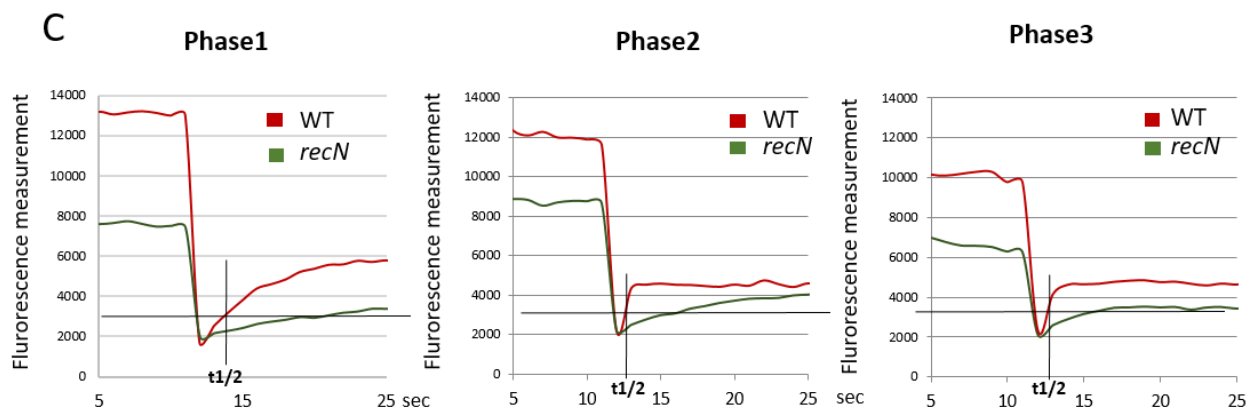


Figure 33. *RecN* influences the diffusion dynamics of HU protein

A- Measurement of the medium half-life of fluorescence recovery after photobleaching in a WT strain. FRAP photobleaching was performed in WT cells marked with an HU-GFP fusion, treated with 10 μ g/ml MMC. Photobleaching was carried out on nucleoids in three different phases. Phase1: Nucleoids before DNA compaction. Phase2: Nucleoids during DNA compaction. Phase3: Nucleoids after DNA compaction. For each phase, the medium half-life of fluorescence recovery was measured in seconds. B- Measurement of the medium half-life of fluorescence recovery after photobleaching in a *recN* mutant. C- Characteristic curve of fluorescence during photobleaching and fluorescence recovery in the WT strain and the *recN* mutant for the three phases.

5. The hunt for RecN's partner(s): Identifying other proteins involved in SCC

Eukaryotic Cohesins are large multi-proteic complexes that usually comprise several proteins. In 2002, Schleiffer defined a superfamily of proteins forming Ring-like structures with SMC proteins in Eukaryotes and Prokaryotes, called kleisins. Such proteins are Scc1 for the SMC1/3 complex, Nse4, Nse1 and Nse3 for the SMC5/6 complex or ScpA for *B.subtilis* SMC (Schleiffer et al., 2003) . They form a tripartite complex capable of entrapping the two DNA molecules, generating cohesion. Mutations affecting the interaction of kleisins with SMC proteins also affect the association of Cohesins with DNA (Gligoris et al., 2014). Later, Palecek and Gruber described another set of SMC partners, the kite proteins. They associate with kleisins and are essential elements of the SMC complex. Such kite proteins are ScpB for *B.subtilis* SMC or MukE for the *E.coli* MukBEF protein for instance. Interestingly, the Eukaryotic SMC5/6 complex possesses a kite protein, Nse1 or Nse3 but Cohesin and Condensin don't (Palecek and Gruber, 2015).

Considering RecN has an SMC-like structure, we thought to look for a possible partner, maybe a kleisin-like or kite-like protein.

a) RecN co-immunoprecipitation reveals possible proteins interacting with RecN

Co-immunoprecipitation experiments, performed with a Flag tagged version of RecN, coupled to a western blot with an anti-RecA antibody revealed a direct interaction between RecN and RecA. To further test if the RecN Co-immunoprecipitation could reveal other proteins possibly interacting with RecN, we used Mass Spectrometry analysis of the immune precipitated samples. The MG1655 strain carrying wild type untagged RecN was treated with 10 µg/ml MMC for 20 min, and a strain carrying a RecN-FLAG protein was treated, or not, with 10 µg/ml MMC for 20 min. Immunoprecipitation was carried out with an anti-FLAG antibody and the three samples were analyzed by mass spectrometry. Over a hundred proteins were identified in each IP sample. Among them, a large quantity of highly expressed membrane and ribosomal

proteins were pulled down, suggesting that a large amount of unspecific proteins were sequenced. Increasing the stringency of the washing procedure did not significantly change the protein repertoire in the samples. We decided to use a normalized peptide count measurement to compare the samples and obtain a semi-quantitative estimation of protein enrichment in each sample. To establish the specificity of the identified proteins in the RecN-FLAG strain treated with MMC, all peptide counts were normalized to the total amount of reads for each sample. We then subtracted the number of reads in the untreated sample from the number of reads in the MMC treated sample (figure 34A). With this procedure, RecN itself had a score of 25 and RecA had a score of 11. The distribution went from 45 to -35, and we considered all scores above 5 to be possibly interesting. To test if the method was pertinent to identify RecN partners, I focused on proteins of the SOS response or proteins with a known function in DNA repair that had a high score. Of these proteins, UvrA had a score of 11, pinpointing the NER pathway. Also, RadA had a score of 5,5 making it an interesting candidate to test.

UvrA is part of the UvrABC complex and is a central protein of the Nucleotide Excision Repair (NER) pathway. It is the first protein to bind DNA and recognize the damaged region, before UvrB actually recognizes the nucleotides to incise and UvrC carries out the incision. If a dual incision by UvrC is made on both sides of the ICL, a double strand break may be formed (Peng et al., 2010; Weng et al., 2010).

RadA protein has been less extensively characterized in *E. coli*. However, increasing evidence suggests that RadA may have a role in branch migration or the resolution of intermediate recombination structures (Cooper et al., 2015). Combination of a *radA* mutation with a *recG* mutant conferred extreme sensitivity to MMC and UV light. This genetic redundancy with *recG* confirms RadA's possible implication in the stabilization of branched molecules or recombination intermediates (Beam et al., 2002).

To further test UvrA and RadA's possible implication in SCIs and their putative interaction with RecN, we constructed *uvrA* and *radA* mutants that we combined or not with the *recN* deletion. We first tested the viability of these mutants when treated with MMC. The *uvrA* mutant alone was very sensitive to MMC, as was the *recN* mutant. Combining both mutations had a strong additive effect, suggesting that both proteins may be acting in alternative pathways allowing

survival to ICL lesions (figure 34B). Quite surprisingly, the SCI profile did not match the interpretation of the viability curves. In the *uvrA* mutant when cells were treated with MMC, SCIs dropped suggesting that in the absence of *uvrA*, RecN mediated SCIs cannot be conserved. When the *uvrA* mutation was combined with *recN*, SCIs were at approximately the same level as the single *uvrA* mutant (figure 34C). This phenotype is similar to a *recA* deletion. These results indicate that UvrA action, or a subsequent DNA repair intermediate may be required for RecN loading or action and SCI conservation upon MMC treatment.

Interestingly, the *radA* mutant phenotype was quite different. Viability assays revealed that *radA* mutant alone was not sensitive to MMC. However, combining the *recN* and *radA* deletions lead to complete cell death after a 40 min MMC treatment (figure 34B). This synergistic effect between both mutations suggests that in the absence of RecN the pathway involving RadA becomes essential for survival, while its role is minor in the presence of RecN. SCI analysis revealed that *radA* mutant alone did not exhibit a loss in SCIs. When combined with a *recN* deletion SCIs dropped to the same level as the *recN* mutant alone. This means that the synergistic effect observed on viability is not the result of RadA's action on sister chromatid interactions (figure 34C).

The results obtained with UvrABC and RadA suggest that the Co-IP approach could be interesting to find proteins that collaborate with RecN. However, the large amount of proteins recovered with the actual protocol, limits our chance to identify them. These results need to be repeated and further experiments need to be carried out. We have recently obtained a strain expressing a functional 3X FLAG tagged RecN. This strain opens the possibility to enhancing IP efficiency. We will also use isobaric labeling (iTRAQ) to enhance our ability to compare samples with mass spectrometry.

A

PNTA_ECOLI	10,7	YDGA_ECOLI	6,4	MSCK_ECOLI	41,5
SECY_ECO57 (+2)	10,0	AG43_ECOLI	6,3	RECN_ECOLI	26,0
BLC_ECO57 (+1)	10,0	ODP1_ECO57 (+1)	6,3	SYA_ECODH [2]	25,1
DPO1_ECOLI	10,0	PYRD_ECO24 (+13)	6,3	ACRB_ECOLI	25,0
EMRA_ECOLI	9,7	NAGC_ECO57 (+2)	6,3	RPOC_ECO24 [8]	21,0
EPTC_ECOLI	9,7	HFLL_ECO57 (+2)	6,3	SYM_ECO24 (+10)	19,1
HELD_ECOLI	9,7	GUAA_ECOBW (+2)	6,3	LON_ECOL6 (+1)	19,0
YHGF_ECOLI	9,7	OMPT_ECOLI [2]	6,2	PPID_ECOL6 (+1)	18,8
YRAP_ECO57 (+2)	9,5	RPOD_ECOLI	6,1	MDTF_ECOLI	18,7
WZZE_ECO57 (+1)	9,5	CYDA_ECOL6 (+1)	6,1	DHNA_ECOLI	18,4
QMCA_ECO57	9,5	XERC_ECO24 (+19)	6,0	FHUA_ECOLI	18,3
SYV_ECO57 (+1)	9,5	CAN_ECOLI	6,0	YFHM_ECOLI	17,9
GADC_ECO57 (+1)	9,1	PGPC_ECOLI	6,0	BAMA_ECO24 (+17)	17,5
MCP2_ECOLI	9,1	YHES_ECO57 (+1)	6,0	LPTD_ECOLI [5]	17,4
LPOA_ECOLI	8,9	ASMA_ECOLI	6,0	ATMA_ECO57 (+1)	16,0
YEAG_ECO57 (+2)	8,5	OMPW_ECOLI	6,0	RNE_ECOLI	15,0
FTSH_ECO57 (+1)	8,4	SULA_ECO24 (+21)	6,0	WZZB_ECOLI	14,7
FEPA_ECOLI	8,2	PANC_ECO24 (+8)	6,0	ACRA_ECO57 (+1)	14,7
FTSN_ECOLI	8,0	DEDD_ECOLI	6,0	YBHG_ECO24 (+15)	13,9
TATB_ECO57 (+4)	8,0	CYCA_ECO57 (+2)	6,0	PBPB_ECOLI	13,9
PA1_ECO57 (+1)	8,0	TOP1_ECOLI	6,0	ODO2_ECO57 (+1)	13,9
PARC_ECO57 (+1)	8,0	RPOE_ECO57 (+2)	6,0	COPA_ECOLI	13,9
SEQA_ECOL6 (+1)	8,0	YEBT_ECOLI	6,0	DLD_ECOLI	13,3
CYDD_ECOLI	8,0	AMPN_ECOLI	6,0	HEMX_ECOLI	12,7
SDHB_ECOLI	8,0	SYK2_ECO57 (+2)	6,0	ATPG_ECO27 (+18)	12,7
ZNUC_ECO57 (+5)	7,8	DEGS_ECO57 (+1)	6,0	GYRA_ECOLI	12,7
LEP_ECOLI	7,8	RSTB_ECOLI	6,0	PNP_ECO24 (+19)	12,5
PUR4_ECOL5 (+2)	7,8	YFIF_ECO57 (+1)	6,0	DACC_ECOLI	12,1
RL19_ECO24 (+20)	7,8	ODO1_ECO57 (+2)	6,0	PHSM_ECOLI	11,9
SPPA_ECOLI	7,8	WBBK_ECOLI	6,0	PPK1_ECO57 (+2)	11,9
TONB_ECOLI	7,8	YHII_ECOLI	6,0	MURG_ECO24 (+11)	11,7
MLAF_ECO57 (+2)	7,8	RNB_ECO24 (+18)	6,0	MUKB_ECO27 (+16)	11,5
PTFBC_ECOLI	7,8	LAMB_ECO24 (+17)	5,8	DHG_ECOLI	11,5
PROP_ECO57 (+1)	7,8	EXBD_ECO57 (+2)	5,8	ODP2_ECOLI	11,3
CYDC_ECOLI	7,8	MREC_ECOLI	5,8	PTGCB_ECO57 (+2)	11,3
OPGH_ECO57 (+2)	7,8	CYSA_ECOL6 (+1)	5,8	PLSB_ECO24 (+19)	11,3
PUR1_ECOLI	7,8	DPO3X_ECOLI	5,8	HLDD_ECO24 [18]	11,3
POTA_ECO57 (+5)	7,5	DEAD_ECO57 (+2)	5,8	UVRA_ECO57 (+2)	11,1
YCEB_ECOLI	7,5	ASNB_ECOLI	5,8	SDHA_ECO57 (+2)	11,1
PSD_ECO24 (+16)	7,5	GCST_ECO24 (+15)	5,8	RECA_ECO24 (+18)	11,0
PTND_ECO57 (+2)	7,5	SYI_ECO24 (+12)	5,8	DLDH_ECO57 (+2)	11,0
YHCB_ECO57 (+2)	7,5	FHUE_ECOLI	5,7		
BTUB_ECOLI	7,5	RADA_ECOLI	5,6		
YHJG_ECOLI	7,5	PHOP_ECO57 (+2)	5,6		
SUCC_ECO24 (+13)	7,5	TOLQ_ECO57 (+1)	5,6		

Figure 34. Co-immunoprecipitation with RecN reveals possible partners or interacting proteins

A- List of proteins with a score of 5 or above. All peptide counts were normalized to the amount of total reads for each sample. Score was calculated by subtracting the amount of reads in the untreated sample from the amount of reads in the MMC treated sample.

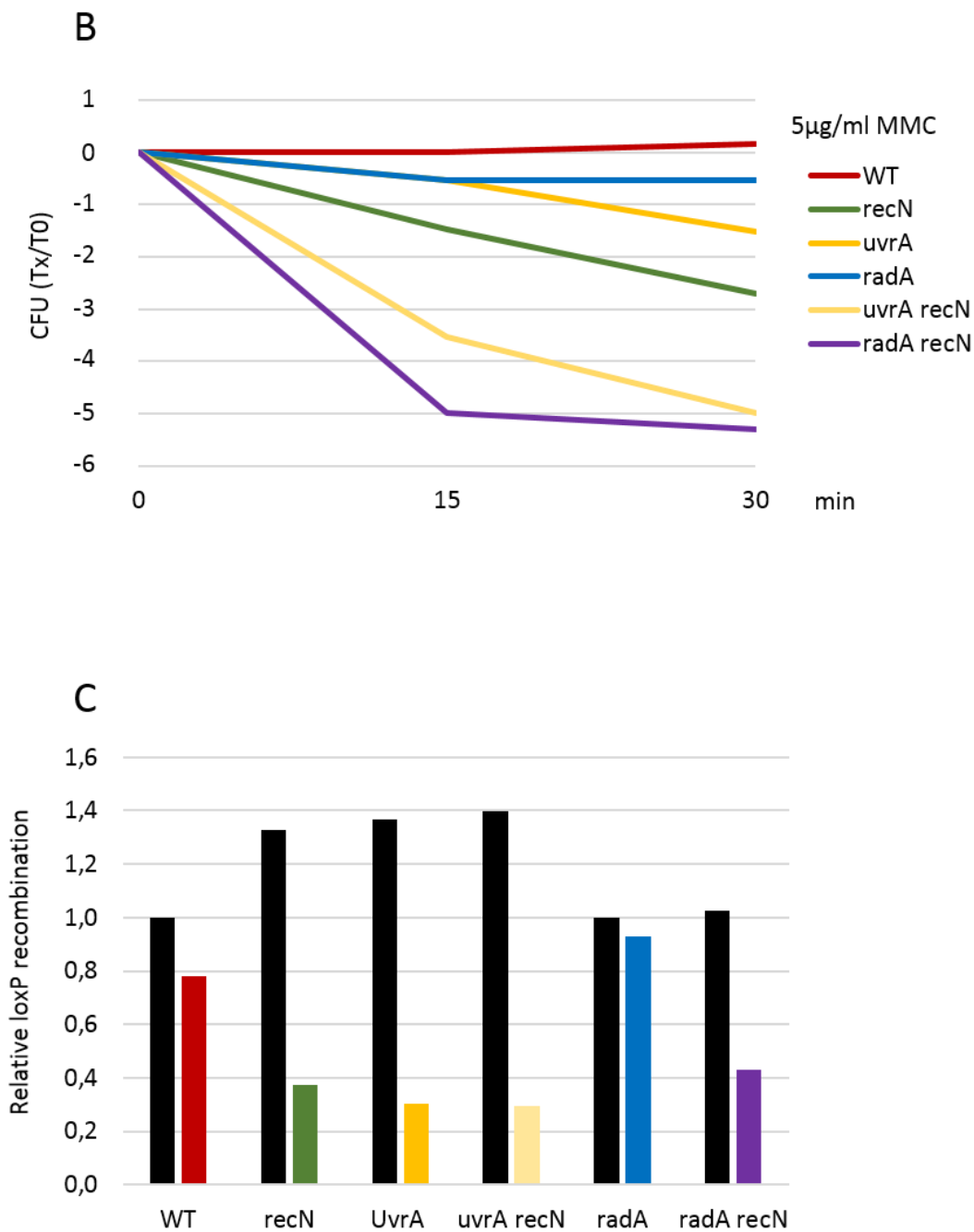


Figure 34. Co-immunoprecipitation with RecN reveals possible partners or interacting proteins

B- Measurement of cell viability after 5µg/ml MMC treatment in various mutants revealed by the Co-IP experiment. C- Measurement of SCIs after 10µg/ml MMC treatment for various mutants revealed by the Co-IP experiment. Results at 30 min are presented. Each sample is normalized to the untreated WT sample.

b) *The SOS response is downregulated in a recN mutant*

We performed an RNAseq experiment in order to test whether the absence of RecN induced a change in expression of other genes, maybe from another DNA damage response pathway. Indeed, in the *recN* mutant, we only observe a 50% loss of SCIs, suggesting that another pathway may also be involved.

The RNAseq experiment was performed in the WT strain and in the *recN* mutant. The cells were treated for 0, 20 or 40min with 10 µg/ml MMC. RNA was extracted and sent to sequencing. We confirmed that MMC induces the SOS response but also found that many of the SOS response genes were downregulated in the *recN* mutant, at 20 and 40 min after MMC addition (figure 35A). To control the specificity of this downregulation, we compared the expression profile in the WT strain treated with MMC and the untreated WT. In the MMC treated sample, we observed a strong change in the expression profile, confirming the effect of MMC on gene expression in the WT strain (figure 35B). We also compared the expression profile between the WT strain treated with MMC and the *recN* mutant treated with MMC. We found that the global gene expression profile in the WT and *recN* mutant treated with MMC is the same, suggesting that it is not an inhibition of expression at the whole genome level or a global loss of transcription that is observed in the *recN* mutant (figure 35C). These controls suggest that the downregulation of gene expression observed in the *recN* mutant is specific to the genes of the SOS response. These results were then validated by RT-qPCR and checked in a *sulA* mutant, confirming that the downregulation of the SOS response genes is specific to the *recN* mutant (figure 35D).

I further thought to investigate whether the Topo IV alteration in the *recN* mutant could also rescue the downregulation of the SOS response as it does for SCIs and viability. Interestingly, expression of the SOS response genes was not restored in the parEts *recN* mutant (figure 35D). This could suggest that the downregulation observed in the *recN* mutant is not exclusively the result of a loss of SCIs. This also suggests that the loss of viability observed in the *recN* mutant is not due to a downregulation of the SOS genes, since Topo IV alteration compensates the loss of viability without restoring SOS gene expression. These observations however did not allow the identification of a gene or a pathway that was significantly upregulated in the absence of RecN.

The down regulation of the SOS response could be linked to RecN's effect on RecA filament formation or RecA dynamics. Indeed, in a *recN* mutant, RecA foci dynamics are altered. In the *recN* mutant, we observe the formation of RecA bundles, structures described by Lesterlin *et al.* in the particular context of a DSB occurring on a sister chromatid that is distant from its homolog (in a WT background). Such bundles monopolize approximately 70% of the RecA protein pool. If RecA is strongly recruited for bundle formation, there may be a shortage of RecA for its function in the SOS induction (Lesterlin *et al.*, 2014). Another hypothesis could be that RecN promotes the stabilization of the RecA filament by keeping sister chromatids together, most likely favoring homology search and strand invasion, thus defining a new modulator of RecA filament dynamics. Studying the effect of RecN on RecA filament stability is quite difficult in the absence of *in vitro* tools. Indeed, *E. coli* RecN has not yet been completely purified which strongly limits the possibility of experiments. To alternatively test these hypotheses, I tried to monitor LexA degradation by WB in a WT strain and a *recN* mutant. If RecN helps stabilize RecA filaments and subsequent SOS induction, LexA, the SOS repressor should be less degraded. Such experiments have been described before, (Mustard and Little, 2000) however, they were more difficult than anticipated, and in my hands, never led to clean conclusions. Alternatively I tried to perform FRAP experiments on the RecA-mcherry foci and RecA-mcherry bundles to test whether the dynamics of the RecA filaments were altered in a *recN* mutant. The resolution of the FRAP laser wasn't good enough the bleach only a small portion of the bundle or the RecA-focus, also rendering the analysis impossible.

Unfortunately, this part of the project was set aside to focus on other aspects, more promising at the time. However, I believe there may be some interesting leads to follow up from these results. There has been encouraging effort put into the purification of *E. coli* RecN, and our collaborator Mauro Modesti has recently purified soluble RecN. This opens the possibility to a wide variety of *in vitro* studies, often used to study RecA dynamics and RecA filament formation.

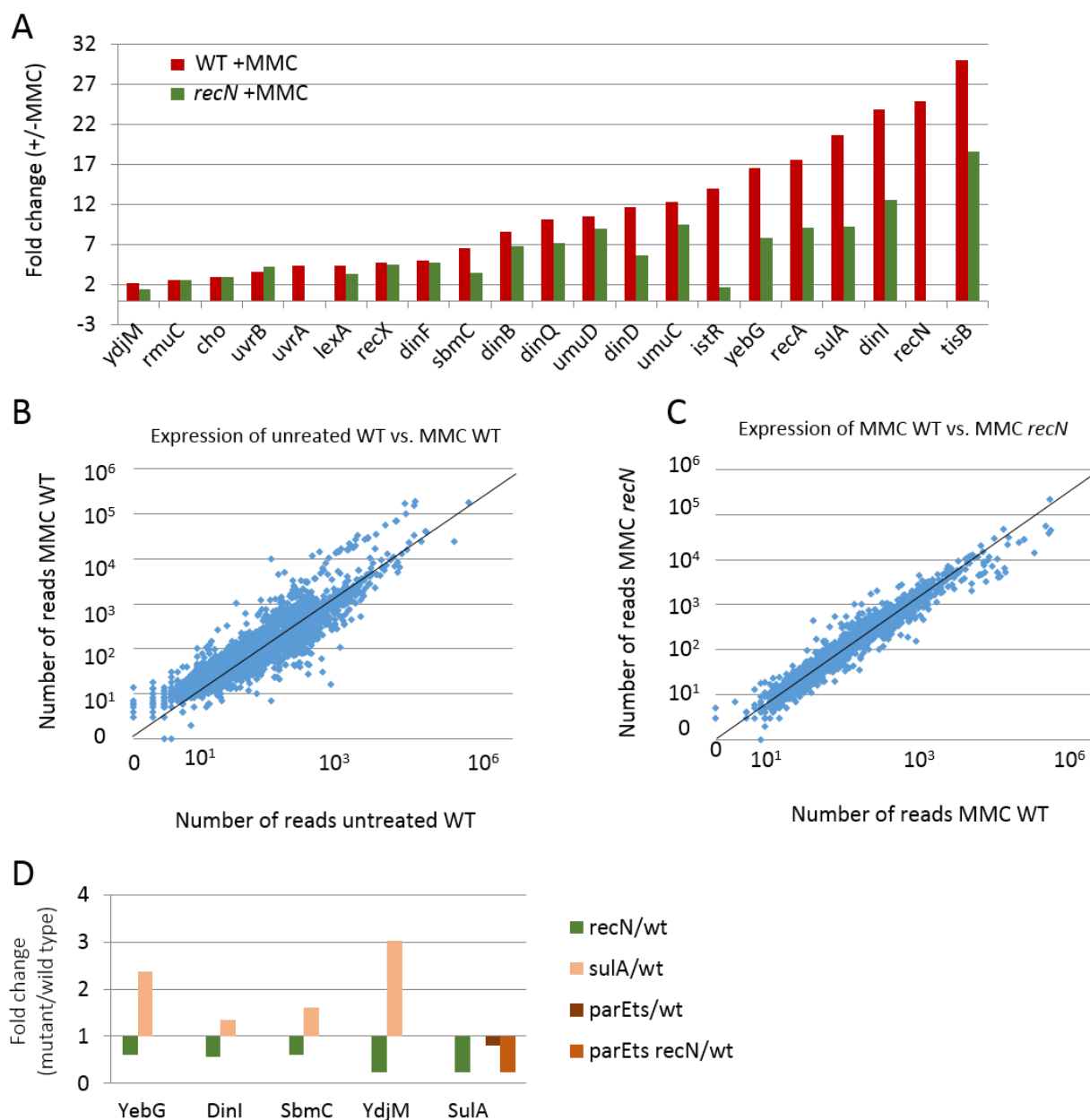


Figure 35. Expression of SOS response genes is downregulated in a *recN* mutant

A- Fold change of gene expression between treated and untreated cells, in the WT (red) and *recN* mutant (green). The number of reads in the MMC treated sample was normalized to the number of reads in the untreated sample for each given gene. B- Comparison of the number of reads between the untreated WT sample and the MMC treated sample. C- Comparison of the number of reads in the MMC treated *recN* mutant and the MMC treated WT strain. D- RT-qPCR validation of the RNAseq experiment. An RT-qPCR was performed in the *sulA*, *recN*, *parEts* and *parEts recN* mutants for various genes of the SOS response. Results are shown as the fold change between gene expression in the mutant over the WT.

c) *Characterization of genes involved in a back-up pathway for RecN*

We used a genetic screen as a different approach to look for possible proteins that can be used in back-up pathways when RecN is deficient. We used a library of plasmids that overexpress *E. coli* genes (approximately 5-10 genes per plasmid (Mossessova et al., 2000)). This library was transformed into a *recN* mutant. Transformed cells were treated for 30 min with 15 µg/ml MMC and plated on LB. Conditions were optimized to plate approximately 40 000 clones. Clones surviving to MMC were selected and growth was verified on LB plates with 1 µg/ml MMC, 2 µg/ml MMC or LB. Fifteen clones grew on either 2µg/ml MMC or 1µg/ml MMC plates, a concentration that kills 100% of *recN* mutant strain but keeps 80% of the WT strain alive. Plasmids from these clones were extracted and sequenced. To test whether survival of the clones is due to overexpression of drug efflux pumps, the clones were also grown on chloramphenicol at different concentrations. Five clones showed growth resistance enhancement to chloramphenicol. We sequenced all of them, and found that they contain at least one gene coding for known or predicted pumps. These clones were discarded.

The overexpressing plasmids of all the other clones were sequenced. Two clones seemed of particular interest because they grew well on 2µg/ml MMC plates. One clone contained the genes comprised in between ArgM and YnjA, and another clone contained the genes comprised between YeeR and DacD. In these two clones, a few genes seemed of particular interest:

SbmC was identified in 1998 by the group of Onhuki. They showed that SbmC (also called Gyrl) can inhibit the supercoiling activity of Gyrase *in vitro* (Nakanishi et al., 2002) . Later, Chatterji and coworkers showed that overexpression of SbmC had no significant effect on the supercoiling state of the DNA *in vivo* suggesting that the inhibition of Gyrase by SbmC is largely dampened *in vivo*. These contradictory observations have not been further studied by other groups. However, Chatterjii and coworkers also showed that overexpression of SbmC can negate the effects of MMC, up to a concentration of 20 µg/ml but has no effect on UV light induced lesions (Chatterji et al., 2003). Although SbmC's role in DNA repair still seems largely unknown, picking up SbmC in the screen was thus quite exciting. Viability and SCIs when overexpressing SbmC in a WT and *recN* background were tested. Surprisingly, overexpressing

SbmC in the WT strain had no consequence on viability. Moreover, overexpression of SbmC in the *recN* mutant did not restore the loss of viability, suggesting that SbmC overexpression cannot compensate for *recN* deletion as observed with the direct inhibition of Gyrase. This observation does not match the results of the overexpression screening. I do not have a valid explanation for this discrepancy (figure 36A). Regarding the SCI profile, the overexpression of SbmC in a WT strain induced a very slight, though significant, increase in SCIs but had absolutely no effect in the *recN* mutant (figure 36B). Deleting *sbmC* in a WT background also increased SCIs but this increase was independent of MMC treatment, meaning it may not be the effect of *sbmC* deletion in response to MMC. Deleting *sbmC* in a *recN* background had no significant effect (figure 36C). Although the described function of SbmC and our experimental data seemed to indicate a possible role for SbmC in DNA damage mediated SCC, we did not manage to reveal an action of SbmC on protection against MMC treatment or on a rescue of the loss of SCIs in a *recN* mutant.

Another interesting protein revealed by the screening was XthA. XthA, also called Exo III is a known Exonuclease of *E. coli*. Despite its name, it mainly exhibits an endonuclease activity. It catalyzes the hydrolysis of an Apurinic or Apyrimidinic DNA 5' to the site of the lost base resulting from the action of glycosylases in the BER pathway (Gossard and Verly, 1978). In 2008, Centore and coworkers from S. Sandler's team showed that XthA mutants have a large increase in the number of RecA-GFP foci. This increase is RecBCD-dependent and *xthA recBCD* double mutants exhibit two fold more double strand breaks than the RecBCD mutant alone. They suggest that there may be a competition between XthA and RecBC for DSB end processing. If XthA degrades the DSB, it will create a 5' ssDNA overhang, which is not a suitable substrate for RecA loading (Centore et al., 2008). They propose that a RecBCD/RecA independent pathway, possibly dependent on RecN, may repair DSBs processed by Exo III.

We therefore decided to test the effect of XthA overexpression on viability and SCIs in a WT strain and *recN* mutant. When overexpressing XthA in a WT strain, we observed no significant effect on cell viability nor SCIs. However, contrary to the screening result, overexpressing XthA in a *recN* mutant rendered the cells more sensitive to MMC although having no effect on SCIs, suggesting that the effect on viability of XthA overexpression in the *recN* mutant may not be linked to sister chromatid cohesion (figure 35D and 35E). Although this observation is

contradictory with our screening results, the sensitivity to MMC of the *recN* XthA OE mutant seems to fit the hypothesis of Centore and coworkers.

Although the results of this screening experiment gave interesting leads, they unfortunately did not allow the clear identification of proteins involved in a back-up pathway in the *recN* mutant. In spite of the disappointing results observed for SbmC deletion, I still consider that this protein, by its ability to inhibit Gyrase (see section 1 of results on Gyrase inhibition) has features that could make it a good alternative pathway to RecN. It remains possible that we did not find the adequate conditions to reveal SbmC influence on DNA repair of ICLs.

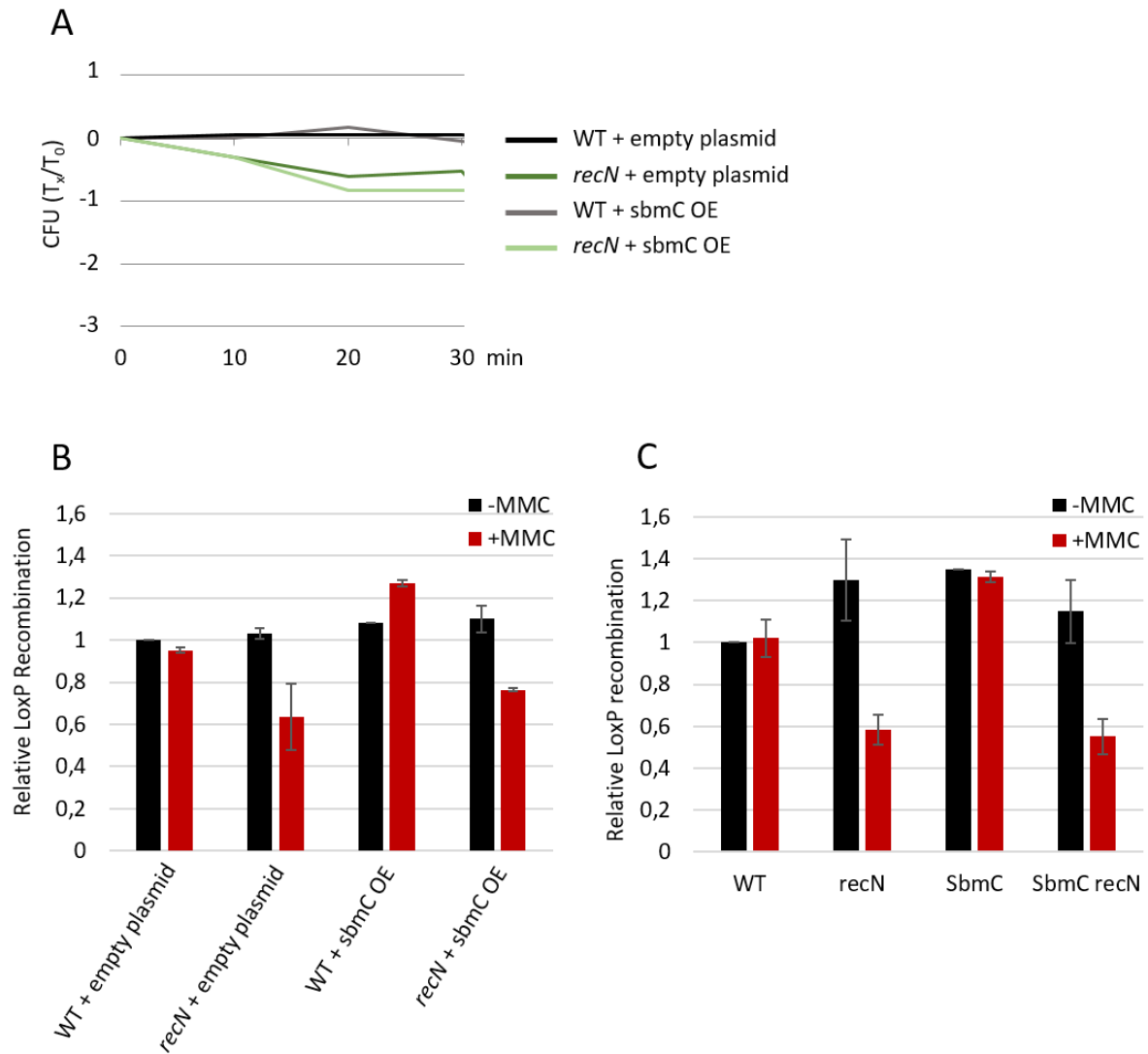


Figure 36. Genetic screen reveals possible RecN partners

A- Influence of SbmC overexpression in a WT strain and *recN* mutant. Cell viability was measured at 0, 10, 20, 30 min after 15 $\mu\text{g}/\text{ml}$ MMC addition. B- Relative *loxP* expression when SbmC is overexpressed in a WT strain or *recN* mutant. Cells were treated for 10, 20, 30 or 40 min with 10 $\mu\text{g}/\text{ml}$ MMC. Results at 30 min are shown. C- Relative *loxP* recombination in an *sbmC* and *sbmC recN* mutant. Cells were treated for 10, 20, 30 or 40 min with 10 $\mu\text{g}/\text{ml}$ MMC. Results at 30 min are shown.

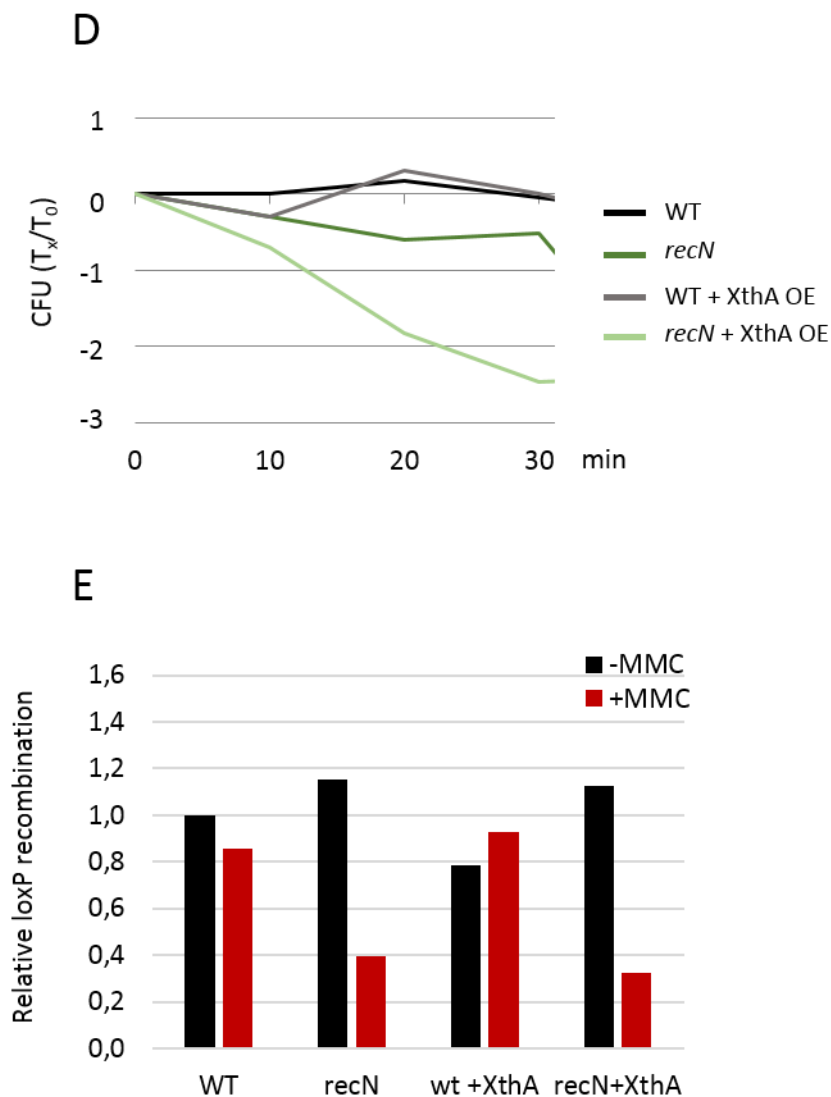


Figure 36. Genetic screen reveals possible *RecN* partners

D- Influence of XthA overexpression in a WT strain and *recN* mutant. Cell viability was measured at 0, 10, 20 and 30 min after 15 $\mu\text{g/ml}$ MMC addition E- Relative loxP expression when XthA is overexpressed in a WT strain or *recN* mutant. Cells were treated for 10, 20, 30 or 40 min with 15 $\mu\text{g/ml}$ MMC. Results at 30 min are shown.

d) *iPOND reveals protein profile at undamaged and damaged forks*

iPond (Immunoprecipitation of nascent DNA) is a new method developed to immunoprecipitate proteins bound to incorporated EdU in DNA. EdU is a thymidine analog incorporated at the replication fork in the nascent DNA. After fixation and permeabilisation of the cells, a click chemistry reaction between EdU and biotin allows immunoprecipitation of the biotin-EdU complex and pull down of all the associated proteins (Dungrawala and Cortez, 2015). This method was used to pull down and identify proteins that are recruited at active and damaged replication forks in Eukaryotes (Sirbu et al., 2011). We used iPOND to identify proteins that may be recruited at the replication fork when cells are facing a replicative DSB induced by MMC, in our model organism, *E. coli*. We also performed the experiment with a thymidine chase, allowing the identification of proteins that are recruited further away from the fork.

In the first experiment, I added EdU for 5 min and then performed a thymidine chase for 15 min. Proteins were crosslinked and pulled down by a streptavidin-biotin interaction. As observed in the co-IP experiment, over 100 proteins were sequenced. We used the normalized peptide count ratios to rank the proteins. As shown in figure 37A, the proteins enriched near the replication fork mainly corresponded to nucleoid-associated proteins (SeqA, MukB...) or topology associated proteins (Gyrase, Topo IV...). This confirmed that the experiment worked and was well adapted to the *E. coli* cell model. Surprisingly, most transcription related proteins were depleted near the replication fork and were only detected at a distance of 1 Mbp or more from the replicating fork. For instance, RNA polymerase was strongly depleted near the replication fork, so was Fis, Hfq or elongation factors G and Tu. This particular protein profile has never been observed before and suggests that transcription may be inhibited by the replication fork apparatus or environment. This inhibition of transcription may be specific, to avoid transcription/replication collisions. Another hypothesis is that the amount of proteins recruited near the replication fork (polymerases, SeqA, Gyrase, Topo IV...) renders it impossible for transcription factors to bind properly, due to steric occupation. An RT-qPCR of genes near the fork in synchronized cells could confirm this observation, and performing another iPond experiment with shorter or more controlled EdU incorporation kinetics should be done.

When performing the experiment with MMC, the profile of the proteins enriched at the replication fork in the presence of MMC-induced DNA damage was comforting as we detected high amounts of RecN, UvrD or RecA for instance (figure 37B). In fact, RecN was one of the most highly enriched proteins. This confirms that RecN is strongly induced and recruited at or near the break, as is RecA. Surprisingly, RadA was depleted near the replication fork, although it had been identified by mass spectrometry in the RecN Co-IP experiment. Proteins that were depleted in the presence of DNA damage corresponded to nucleoid associated proteins, transcription factors, or, interestingly, Gyrase.

When performing the thymidine chase for 15 min and then adding MMC for 15 min, we pulled down RecN with the chased EdU (figure 37C), strengthening the hypothesis that RecN is possibly recruited at the DSB near the replication fork but is also present on a large portion of the nucleoid, even as far as 1 Mbp from the break. This is consistent with the whole nucleoid compaction phenotypes we observe and the high amount of RecN protein that is produced in response to DNA damage.

These experiments will be pursued with mutant strains and iTRAQ will be used to improve quantification.

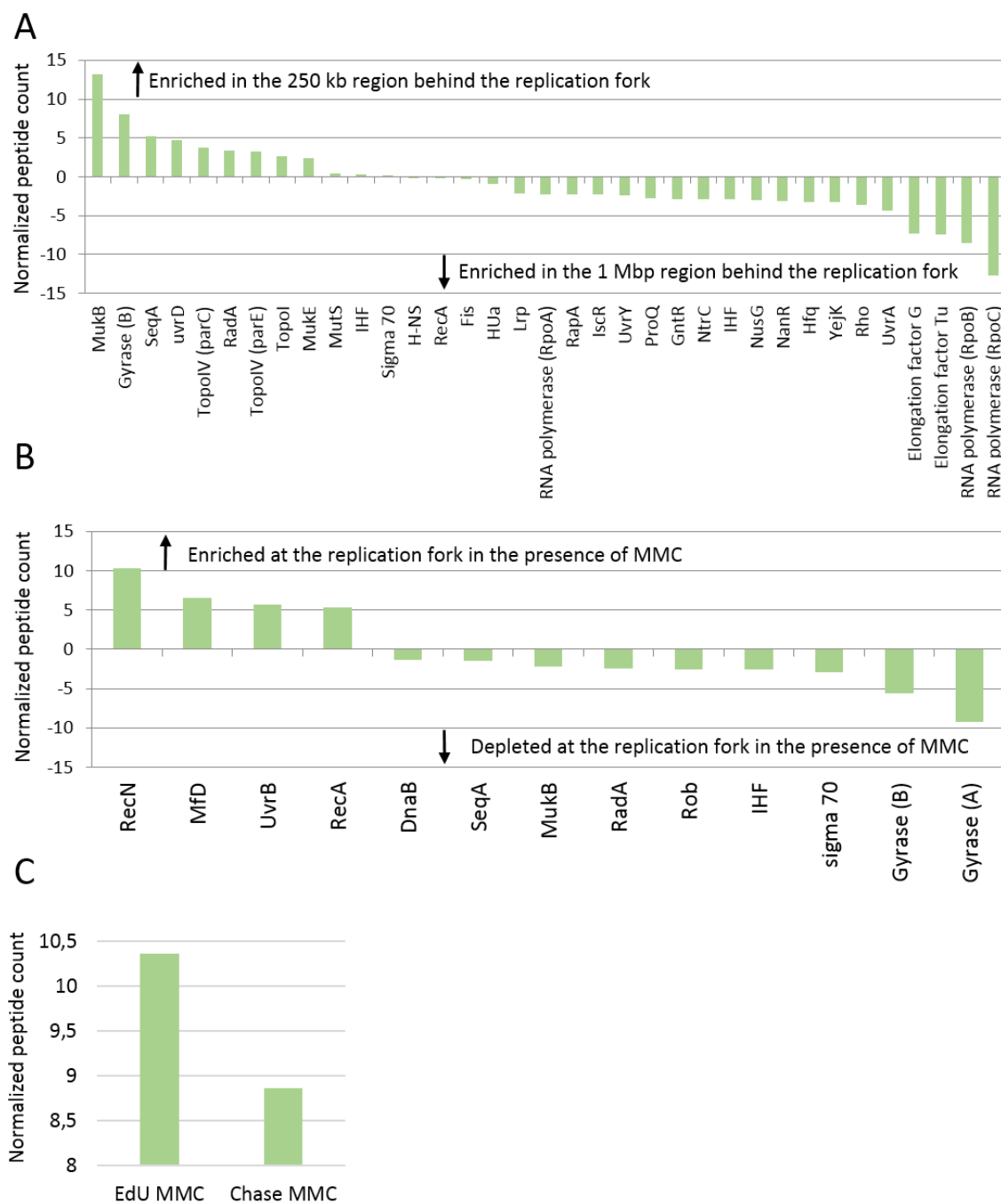


Figure 37. Immunoprecipitation of EdU crosslinked proteins

A- Proteins recruited near the replication fork differ from the proteins recruited at over 1 Mbp from the fork. EdU was incorporated for 5 min and thymidine chase was performed for 15min B- Edu pull down in the presence of an MMC induced double strand break reveals proteins recruited at the damaged replication fork. EdU was incorporated for 5 min and 10 $\mu\text{g/ml}$ MMC were added for 15min C- RecN is strongly recruited at the DSB near the replication fork but also at a distance going up to 1Mbp from the damaged fork. EdU was incorporated for 5min, chased for 15 min with fresh thymidine and 10 $\mu\text{g/ml}$ MMC was added for an extra 15min.

III. Discussion

A. Sister chromatid cohesion and homology search

We have shown that during DNA repair in *E. coli*, sister chromatids are kept together by an SOS-induced protein, RecN. Indeed, upon MMC treatment, in the absence of RecN, sister chromatid cohesion is decreased. Moreover, RecN induces global chromosome rearrangements such as nucleoid compaction and the merging of previously segregated sister chromatids. *recN* mutants are very sensitive to MMC, suggesting that RecN's action on nucleoid dynamics and sister chromatid cohesion is important for DNA repair and subsequent cell survival (figure 38). Interestingly several problems appearing in the absence of RecN can be rescued by Topo IV alteration suggesting that RecN plays a structuring role on sister chromatids as catenanes do during unperturbed cell cycles.

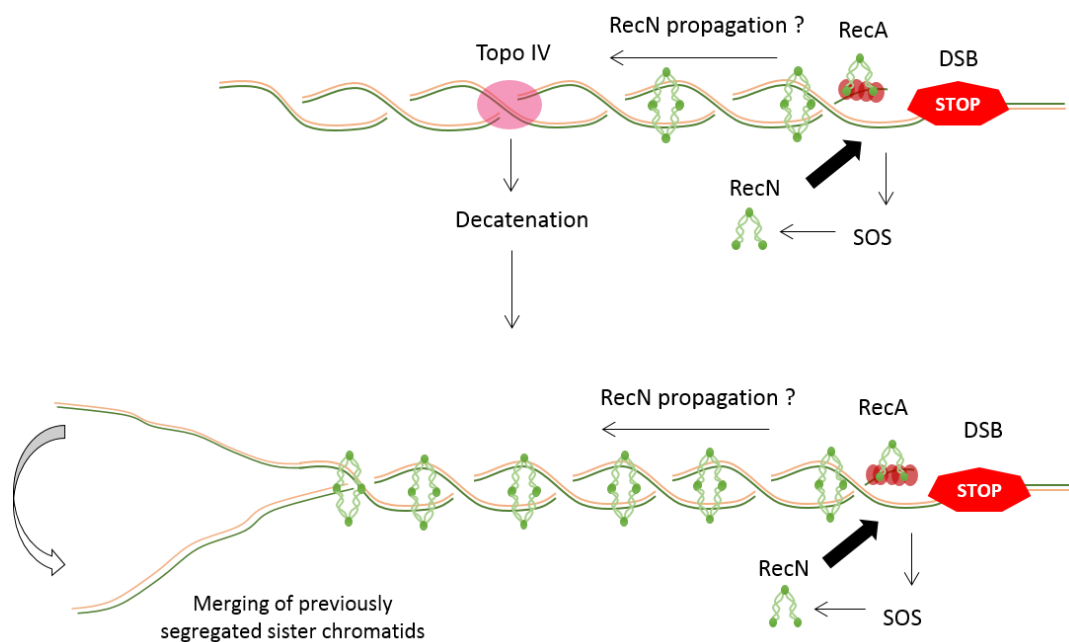


Figure 38. Model for RecN action on sister chromatid cohesion and nucleoid merging

RecA binds the ssDNA extension created at the DSB and induces the SOS response, including RecN. RecN binds to RecA and then propagates along the DNA, keeping sister chromatids in close contact. RecN propagation on a large portion of the nucleoid induces merging of previously segregated sister chromatids and a whole nucleoid compaction.

1. Importance of RecN for homology search

The repair of DSBs by homologous recombination may require the presence of an intact homologue in order to repair without the loss of genetic information. The mechanism by which RecA filaments find and identify the correct homologous sequence amongst the ocean of non-homologous DNA is still debated. The latest models describe a 3D sampling of the DNA by RecA nucleofilament, with a combination of short distance “sliding” and long distance “hopping” (Forget and Kowalczykowski, 2012) . Although this system may be very efficient, the presence of the intact homologous sequence in close vicinity of the damaged region in response to a DSB would avoid extensive sampling and enhance the efficiency and kinetics of the process. This is in good agreement with the results I obtained with microfluidics experiments. Indeed, when the MMC is washed after 10 min (conditions that are not lethal for the *recN* mutant), the WT cells manage to resume a regular cell division pattern in under 3h. However, in the *recN* mutant, most cells do not resume cell division, even 3h after MMC is washed. Cells do not die, but they keep filamenting. This suggests that the presence of RecN strongly enhances the kinetics of repair, possibly by facilitating the early RecA-driven homology search. Moreover, the few cells that do manage to divide in the *recN* mutant show an asymmetrical division. After division, one new born cell resumes extensive filamentation whereas the other is capable of performing another cell division. This could mean that in the absence of RecN, one chromosome may go through a round of DNA repair whereas the other may not have time due to reduced repair kinetics. This would lead to a new cell with a chromosome still damaged. RecN may also serve to stabilize the recombination products and ensure the accuracy of the HR reaction. In fact, it was very recently demonstrated that RecN can actually stimulate RecA D-loop formation *in vitro*, in *D. radiodurans* (Uranga et al., 2017). This function of RecN may be complementary to, or a consequence of, its function on sister chromatid cohesion.

2. RecN's influence on RecA filament formation

The importance of RecN for homology search and RecA filament formation was further studied by observing RecA-mcherry foci in live cells, in a WT strain and in the *recN* mutant. Interestingly, we observed a substantial change in RecA foci shapes and dynamics. In the WT cells, RecA formed bright fluorescent foci on the nucleoids and at the poles. These structures have been previously observed and described in *E. coli* (Renzette et al., 2005) but also in *B. subtilis* for instance (Simmons et al., 2007). In the *recN* mutant, these RecA structures were strongly altered. We observed elongated filaments, resembling the RecA bundles described by Lesterlin *et al.* in 2014 (Lesterlin et al., 2014). Such bundles form in the particular context of a single, I-SceI-induced double strand break occurring on a chromatid that has already segregated from its homolog. They proposed that these structures are RecA filaments performing homology search on the distant homologous chromosome. The fact that we observe such RecA bundles in the *recN* mutant strongly suggests that RecA performs a longer scale homology search when the sister chromatid is not kept close by RecN when the break occurs (figure 39).

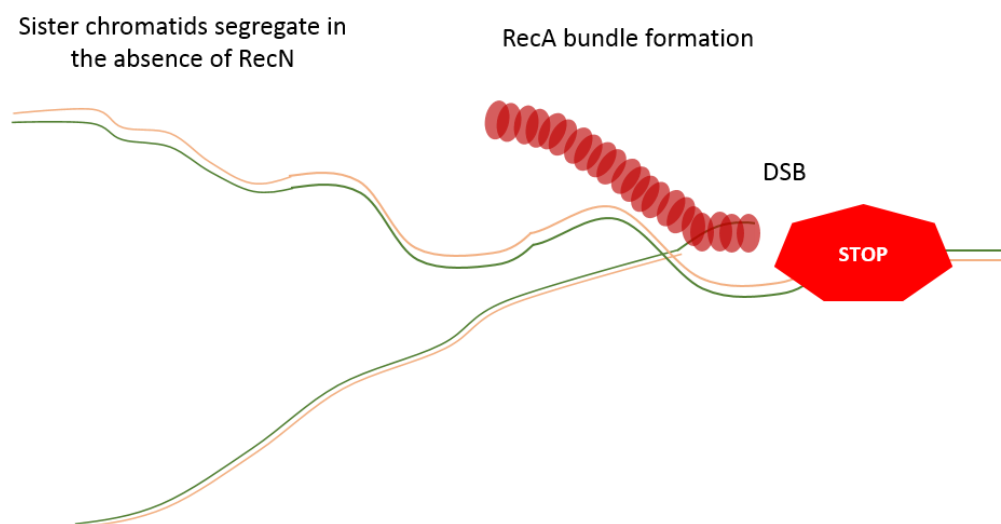


Figure 39. Model for RecA bundle formation in the absence of RecN

In a *recN* mutant, sister chromatids segregate prematurely, before RecA nucleofilament can find the homologous strand for repair by HR.

RecA forms a bundle-like structure in order to find the unbroken homologous strand. Bundle formation may also be the consequence of poor control of filament elongation in the absence of RecN.

It is also possible to imagine that RecN is actually a modulator of RecA filament dynamics and that the occurrence of the RecA bundles is not the result of homology search but rather the unfortunate consequence of poorly controlled elongation of the filament. This could be in good agreement with the interaction we observed between RecN and RecA and the effect of *recN* deletion on the SOS induction. Indeed, an RNAseq experiment showed that the expression of the SOS genes was downregulated in a *recN* mutant. By influencing RecA dynamics, RecN may favour the correct binding of RecA to ssDNA and subsequent SOS induction. It could be interesting to observe the RecA bundles with an I-SceI DSB system to see whether RecN has an effect on RecA dynamics when the sister chromatid is already distant. Testing the SOS induction in these conditions could also shed light on the cause of its downregulation in the *recN* mutant.

B. RecN's influence on chromosome dynamics

1. RecN induces a whole nucleoid compaction

We observed whole nucleoid dynamics thanks to HU-mcherry labelling and timelapse fluorescence microscopy. When the cells are treated with MMC, the nucleoids undergo a large compaction, consistent with previous observations (Odsbu and Skarstad, 2014; Shechter et al., 2013). In the *recN* mutant, the nucleoids do not compact. Nucleoids decondense as the cells filament. To date, it remains unclear why and how the nucleoids compact in this manner.

Nucleoid compaction could favour a three dimensional conformation that would be favourable to the 3D homology search of RecA by bringing closer to each other distant regions. In this compacted state, RecA would only perform homology search on very short distances, hence the observation of RecA-foci rather than bundle structures. We inserted two distinct fluorescent foci on the same replicore, spaced by approximately 200 kb and observed a specific pairing of homologous *loci* but not an increased proximity of the distant loci. This suggests that RecN promotes the ordered realignment of homologous sequences rather than a random compaction. Our previously stated hypothesis is that RecN multimerizes along the

chromosome, progressively realigning the segregated sister chromatids. But why would RecN engage in such a large scale rearrangement if the DSB is at the replication fork, where sister chromatids are originally cohesive thanks to topological links?

Co-Immunoprecipitation experiments revealed the potential role of UvrA and the NER pathway in response to MMC (these observations will be further discussed below). *In vitro*, DSBs can occur during NER after a double incision by UvrC, on both sides of the MMC-induced ICL (Peng et al., 2010). Considering that MMC is inserted all over the DNA, multiple DSBs may be occurring over the genome. RecN would thus be recruited to these various DSB sites, maybe keeping the DNA ends together. This function of RecN has been previously proposed from the observation of enhanced ligation efficiency between linear DNAs in the presence of purified RecN from *B. subtilis* (Sanchez et al., 2008) and *D. radiodurans* (Pellegrino et al., 2012) (figure 40).

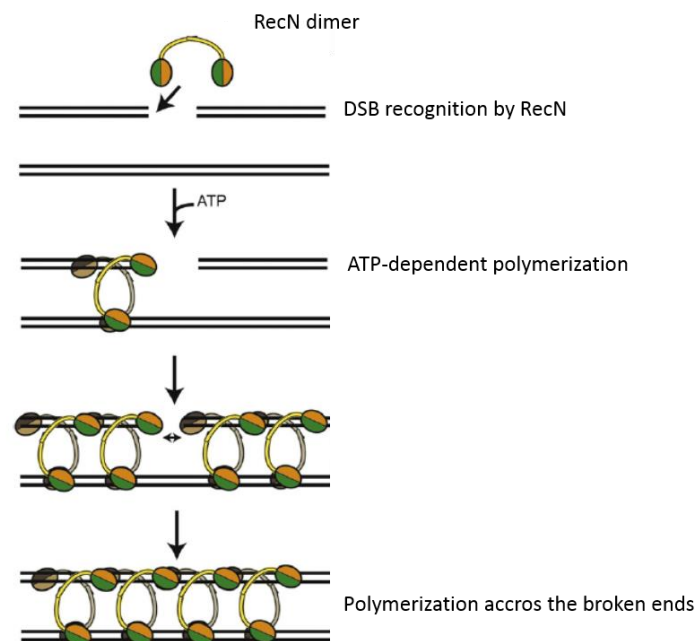


Figure 40. Model for DSB recognition in *D. radiodurans*

DSB recognition occurs through the head domains. Head-head interactions lead to RecN polymerization. RecN molecules on either side of the break keep the broken DNA ends together.

RecN may also be helping D-loop formation by RecA for repair of the DSBs at sites of NER. This could explain the massive induction of RecN, and the several RecA-mcherry foci we observe in WT strains, which would correspond to several RecA-dependent repair sites occurring over the chromosome. We can question how this could fit with the merging of distant sister chromatids. Indeed, RecN is an SMC-like protein that is only 1/3 of the size of Eukaryotic SMC proteins. It is therefore difficult to imagine that RecN could entrap the DNA as Cohesins do, let alone bring distant homologous chromosomes together. An *in vitro* model with *D. radiodurans* RecN suggests that RecN may form head to tail interactions, nucleating at the break and multimerizing along the DNA (Pellegrino et al., 2012) (figure 41). RecN may bind via RecA, at the site of the break, somehow maintaining the DNA ends together and keeping the sister chromatids close when they are already in a cohesive state. RecN could then slide along the DNA as Cohesins do (Ivanov and Nasmyth, 2005) , or multimerize on a certain portion around the break by head to tail interactions, subsequently promoting the merging of distant homologs.

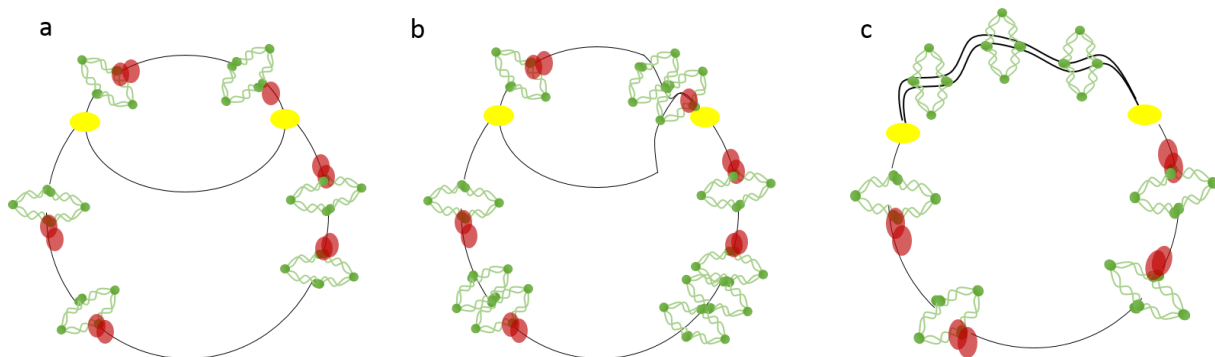


Figure 41. Model for RecN binding at sites of NER induced double strand breaks

- a- RecN (green) binds via RecA (red) at DSBs created by the NER pathway, maybe also performing end-joining of the broken ends
- b- RecN propagates and polymerizes out of its binding site
- c- RecN gradually promotes global nucleoid compaction and merging of previously segregated sister chromatids

2. Could the MMC-induced genome compaction favour protein diffusion?

Hoping to gain more insight into the structure of the compacted nucleoid form, we performed FRAP on HU-GFP stained nucleoids in WT cells and in the *recN* mutant. HU was used as a proxy of chromatin dynamics. In the WT strain, the diffusion of the HU protein was substantially increased when the nucleoids were in the compacted form. This increase was dependent on RecN. This suggests that this RecN-dependent compacted form is enhancing protein diffusion and that we are not observing the aspecific effect of MMC on DNA.

These observations lead us to consider models proposed by the Minsky group. Studies performed in *E.coli* under starving conditions, found that the nucleoid aggregates into crystal-like structures and that these structures are dependent on the unspecific DNA binding protein, Dps. These results suggest that under stressful conditions, the chromosome is capable of assembling into ordered structures, helping it to protect against damage and a stressful environment (Minsky, 2003). *In vitro* studies and computational simulations have established that scanning of the DNA during homology search must be accelerated and facilitated in order to be carried out in an appropriate time frame. This is mediated by the co-aggregation of the presynaptic filaments (here RecA-ssDNA) and the dsDNA target into a linear array (Levin-Zaidman et al., 2000). In this conformation, homology search is performed through a one-dimensional slide that is enforced by the parallel organization of the assembly rather than scanning the genome through three-dimensional random encounters (Minsky, 2003). It was proposed that reactions such as blunt end ligation, which do not require the specific homolog, could be enhanced by a simple increase in DNA concentration, and thus, a random DNA compaction. On the other hand, reactions that depend upon homologous search and recombination are likely to be facilitated by a dynamic ordered crystal-like structure in which 1D sliding is promoted (Minsky, 2003).

To further understand the diffusion of the proteins on the DNA, *in silico* studies were conducted. They established that protein diffusion relies on 3D diffusion but also 1D sliding (similar to the process used by RecA). It is dependent on several factors including the structural fluctuation of DNA that may enhance collisions between proteins and increase their diffusion.

Proteins with a low affinity for DNA are capable of hopping along the DNA, thus increasing their sliding speed (Ando and Skolnick, 2014).

Hu *et al.* also showed that after dissociation of a protein (during the 3D diffusion), the probability of associating with any given locus of the chromosome is equal when DNA is randomly organized. In this non-structured conformation, search would thus be random and time consuming. However, in other more structured DNA conformations, the probability of re-associating near the dissociation point is stronger and may avoid “unorganised” and “random” hopping all over the chromosome. Search can proceed in an orderly and progressive manner. The biocrystals formed under stressful conditions may accelerate homology search by promoting an organised association and dissociation scan (Hu *et al.*, 2006).

In the FRAP experiments I performed, the protein observed is HU, which is a DNA binding protein. HU may follow these 3D hopping and 1D sliding mechanisms for diffusion along the DNA. We can thus hypothesize that under MMC treatment, in a RecN-dependent manner, the chromosome is rearranged into an ordered structure, resembling the biocrystal structures, that may favour protein diffusion and recruitment to the break (Levin-Zaidman *et al.*, 2000). This nucleoid compaction could also favour a three dimensional conformation that would be favourable to the 3D homology search of RecA by bringing closer to each other distant regions. In this compacted state, RecA would only perform homology search on very short distances, hence the observation of RecA-foci rather than bundle structures in the fluorescence microscopy experiments (figure 42).

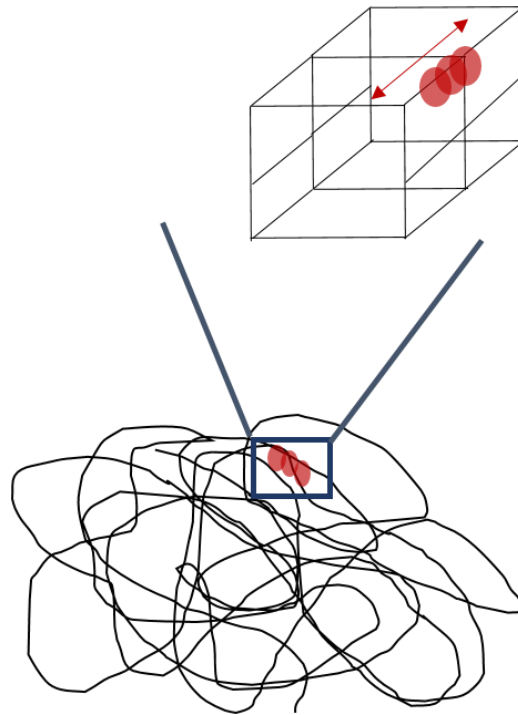


Figure 42. An ordered chromosomal structure may facilitate homology search

The macroscopic compaction state of the nucleoid facilitates 3D homology search.

At a local level, the chromosome may adopt a biocrystal-like structure facilitating 1D diffusion by RecA (red)

Inspired from Mirny et al. 2009

3. RecN's influence on damaged DNA mobility

Further experiments on foci dynamics in WT cells and in the *recN* mutant revealed that the Mean Square displacement slope (MSD slope) of the tagged fluorescent focus was greater in the WT strain than in the *recN* mutant when treated with MMC. Considering RecN holds sister chromatids together, we could have expected an increase in foci mobility in the absence of RecN. However, this observation seems to be in good agreement with the model proposed by R. Rothstein (Miné-Hattab and Rothstein, 2012). He suggests that upon DNA damage, the broken DNA ends are more mobile, in order to explore a greater portion of the nucleoid during homology search. We can thus imagine that although RecN acts to keep sister chromatids

cohesive in response to DNA damage, possibly reducing the mobility of the chromatids on a large scale, it may, at a local level, favor the general mobility of the chromosome to promote homology search. Unpublished results from the laboratory suggest that in an unperturbed *E. coli* cell cycle, the mobility of cohesive loci is reduced compared to segregated loci. In the case of damaged chromosomes it might be different. Replacing topological links by RecN might be a way to enhance mobility of cohesive sister chromatids. In fact, recent work in *Saccharomyces cerevisiae* described similar observations. Zeocin treatment increases foci dynamics and even a single DSB induced at a given locus can lead to an increase of foci mobility over the genome. Further computational simulations linked this increase of chromatin mobility to an increase of chromatin rigidity, which is consistent with our observations and RecN's action on sister chromatid cohesion (Herbert et al., 2017). Such chromatin mobility changes linked to homologous recombination are also reminiscent of meiosis events where paired homologs perform many coordinated movements with the purpose to eliminate unwanted connections (Kozul et al., 2008, 2009). We can propose that RecN favors the diffusion of proteins and maybe their recruitment to the break. In this structured, rigid conformation, loci mobility would be increased in a RecN dependent manner possibly favoring homology search driven by RecA, or limiting unwanted chromosome exchanges. It would therefore be interesting to measure genome rearrangements generated by a MMC treatment in the presence or absence of RecN.

These observations confirm the role of chromosomal morphology in preserving and restoring the integrity of the genome during DNA damage and RecN's central action in this process.

C. Interplay between RecN and the Nucleotide Excision Repair pathway

As mentioned above, co-immunoprecipitation experiments revealed a possible interaction between the NER proteins and RecN. Interestingly, epistatic analysis revealed an intriguing synergy between RecN and UvrA. Briefly, we observed that a *uvrA* mutant is sensitive to MMC, confirming an involvement of the NER in removing MMC induced ICLs. Interestingly,

combining a *uvrA* and a *recN* mutation lead to total death after 40 min of MMC treatment. This could suggest that UvrA and RecN are acting in two alternative pathways.

However, the sister chromatid cohesion analysis suggests a rather different model. SCIs are strongly decreased in a *uvrA* mutant, more than the *recN* mutant alone. The double *uvrA recN* mutant has the same profile as the *uvrA* mutant alone. A preliminary hypothesis for these observations could be that the RecN-dependant SCC observed in response to MMC mainly results from RecN's action on breaks arising from the NER pathway.

The *recN* mutant only shows a loss of 50% of SCIs suggesting that another protein is involved in keeping the sister chromatids together. This protein could be UvrA but it seems unlikely that UvrA is capable of performing cohesion alone and I favour the hypothesis of another protein, acting in a different pathway, that would be capable of creating cohesion.

The intriguing discrepancy between the viability tests and the SCI assay could reflect the existence of another function of RecN, acting independently of UvrA which is important for viability and DNA repair but not for sister chromatid cohesion. This function could be end joining of the two ends of the DSB (figure 43).

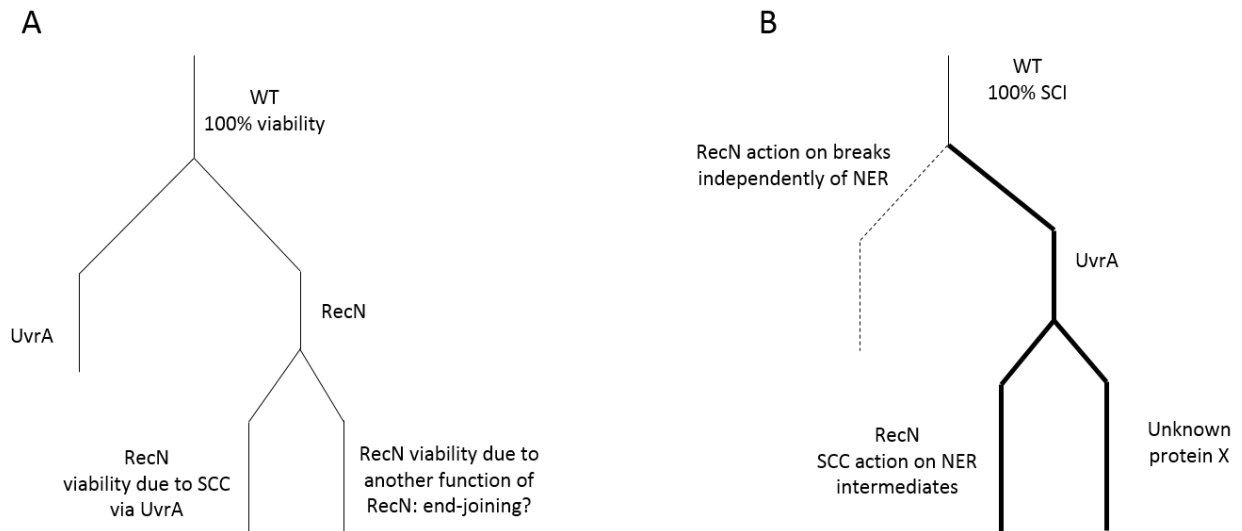


Figure 43. Putative viability and SCC pathway for *recN* and *uvrA* mutants

A- Cell viability measurements suggest RecN and UvrA are acting in different pathways. B- SCIs profile reveal that RecN's action on SCC is mainly dependent on UvrA.

Interestingly, a paper published in 1985 described that the induction of RecA and UmuC was decreased in a *uvrA* mutant, resembling the observation we made with the RNAseq experiment in the *recN* mutant (Yamamoto et al., 1985).

Considering the novelty of these results and the small set of mutants tested in these assays for the moment, strong conclusions should not be inferred from these data.

D. Impact of the supercoiling density on DNA repair

In Eukaryotes and Prokaryotes, Homologous Recombination is the essential process for the repair of highly deleterious double strand breaks. During HR, the presence of the undamaged homologous sister chromatid is required in order to avoid the loss of genetic information. In Eukaryotes, this sister chromatid cohesion is ensured during the whole cell cycle by the action of different SMC complexes. In *E. coli*, sister chromatid cohesion results from topological

linking between sister chromatids. These links are called precatenanes and are removed upon the action of Topoisomerase IV. We showed that during the repair of a DSB induced by MMC, sister chromatid cohesion was conserved thanks to the action of RecN, an SMC-like protein induced by the SOS response. When inhibiting Topo IV in a *recN* mutant, SCIs are preserved and so is viability. Maintaining topological links between sister chromatids seems sufficient to restore the loss of SCIs and viability of the *recN* mutant. Similar observations were made with a Gyrase^{ts} mutant. Identifying SbmC, a gyrase inhibitor, in a screening experiment thus seemed quite promising. However, overexpression of SbmC did not enhance protection against MMC treatment. Moreover, when Topoisomerase IV was inhibited in cells expressing RecN (the simple Topo IV^{ts} mutant), SCIs were maintained but viability was impaired in comparison to the WT strain. This suggests that Topoisomerase IV may be playing a role in the repair of MMC induced DSBs possibly by maintaining a topological homeostasis that is favourable for DNA repair. Although the direct implication in the resolution of HJ intermediates of Topoisomerase III has been suggested (Lopez et al., 2005), little work has been done on the importance of DNA supercoiling for DNA repair and the resolution of repair intermediates. However, one could imagine that the supercoiling state and the supercoiling density of the nucleoid can affect the capacity of the incoming DNA strand to invade the intact homolog. Indeed, it was shown that the extent to which the D-loop can migrate is determined by the supercoiling state of the DNA (Wright et al., 2018). In a Topo IV^{ts} mutant, RecN may block the diffusion or the removal of excess precatenanes. The DNA would thus be in a highly catenated state which would be deleterious to strand invasion and branch migration. Interestingly, the Gyrase^{ts} mutant is also highly supercoiled but viability is not affected. We can thus hypothesize that it is the excess of precatenanes in the Topo IV mutant rather than the global supercoiling density that is deleterious to DNA repair (figure 44).

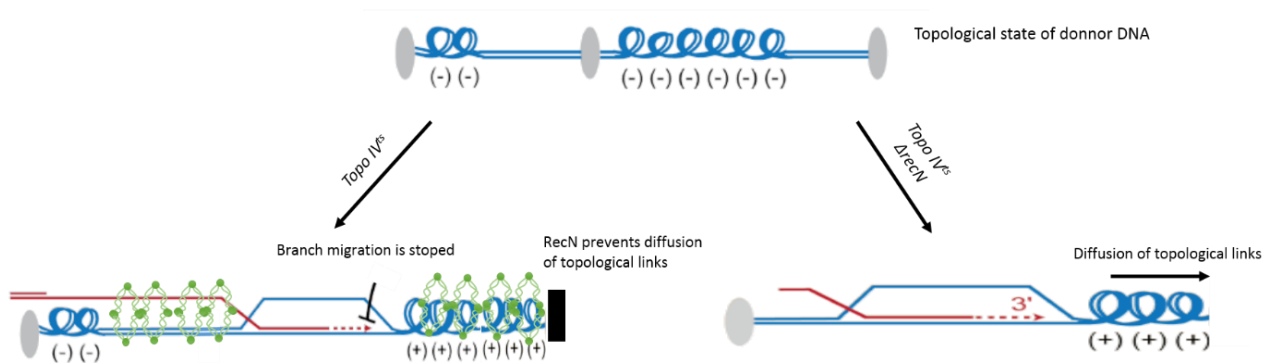


Figure 44. Excessive catenation may impede branch migration

In the Topo IV^{ts} mutant, Topoisomerase IV does not remove precatenation links and RecN prevents their diffusion. Branch migration is inhibited and viability is impaired.

In the Topo IV^{ts} *recN* mutant, Topoisomerase IV does not remove precatenation links, in the absence of RecN, precatenanes may diffuse. Branch migration can proceed and viability is maintained.

To test this hypothesis, the supercoiling density on the whole nucleoid of a Topo IV^{ts} mutant relative to a WT strain or a *recN* mutant could be measured by psoralen intercalation. Psoralen crosslinks DNA but preferentially binds negatively supercoiled DNA. The frequency of psoralen intercalation can give a measure of the nucleoid supercoiling density (Lal et al., 2016; Sinden et al., 1980). A more recent method has permitted visualization of DNA intertwining in budding yeast. By using site-specific recombination, topologically intertwined DNA is excised as catenated circles whereas topologically free sister chromatids are excised as two free DNA circles. The two products can be distinguished by gel electrophoresis.

It could also be interesting to test whether DNA repair is more or less efficient depending on the different regions of the chromosome. Indeed, some regions, called SNAPS, are highly cohesive due to SeqA binding. Although repair may be enhanced due to prolonged sister chromatid cohesion in these regions, it may also be impaired by an excess of DNA precatenanes and topological constraints.

E. Is transcription repressed by cohesion?

In order to identify possible new partners of RecN and in a more general interest of identifying proteins that may be recruited to DSBs induced at the replication fork, I used a new method called iPOND. iPOND allows the purification of proteins on newly synthesized forks by performing an EdU pull down. By adding a thymidine chase with fresh medium, we can also identify proteins at a larger distance from the fork.

The protein profile obtained after a 5 min EdU incorporation (it is estimated that EdU has incorporated over 250-350 kb) revealed the presence of nucleoid associated proteins and topoisomerases such as Topoisomerase IV, MukB or SeqA. This is in good agreement with the current knowledge on these proteins. Interestingly, Gyrase was also identified behind the replication fork. Our experiments do not allow us to know whether Gyrase also binds on the whole chromosome or not but to our knowledge, this is one of the first observations of Gyrase acting behind the replication fork. When performing a 15 min thymidine chase (it is estimated that EdU has incorporated over 1Mbp), the protein profile is substantially changed. Proteins that were pulled down correspond to transcription factors, RNA polymerases and proteins associated to translation, such as RpoB, RpoC or Hfq. The absence of translation factors in the 300kb region behind the fork may be due a repression of transcription in this region since translation is coupled to transcription.

1. What mechanisms are responsible for transcription repression?

This exclusion of transcription related proteins behind the replication fork could be the mere consequence of “overcrowding” by other proteins relative to replication. Indeed, proteins such as SeqA, MukB or Topoisomerase IV act behind the replication fork to manage replication. However, Eukaryotic RNA polymerases are capable of overcoming the crowded nucleosomal environment and are even capable of displacing histones *in vitro* (Bintu et al., 2011).

A second hypothesis is that when the replication fork goes forward, it “kicks off” the transcription-associated proteins (and associated translation machinery). As the proteins are cleared, they may preferably bind to other regions of the chromosome. However, the fact that they don’t re-associate immediately behind the replication fork is surprising. One explanation could be that a physical barrier formed behind the replication fork by sister chromatid cohesion prevents re-association of the transcription machinery. Indeed, the two sister chromatids are bound by precatenation links, creating a supercoiled environment. Considering that transcription itself creates positive and negative supercoils (Liu and Wang, 1987) it may be in conflict with replication associated precatenanes (figure 45).

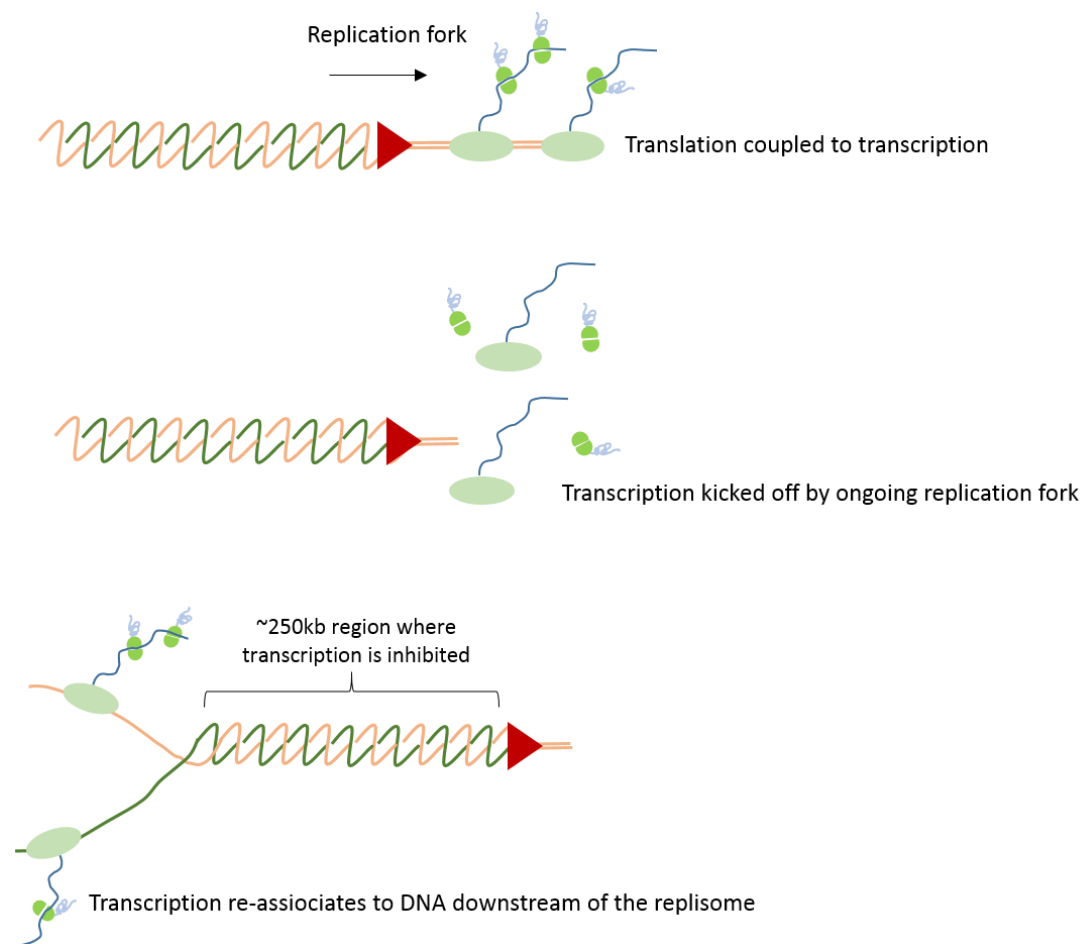


Figure 45. Model for transcription repression behind the replication fork

As the replication fork moves forward, it may kick off the transcription machinery and translation proteins. Proteins bind on the newly synthesized DNA at a distance of over 250 kb from the fork due to repression by sister chromatid cohesion.

Such a hypothesis would need to be further investigated. If sister chromatid cohesion is repressing transcription near the replication fork, the transcription pattern of a Topo IV^{ts} mutant should be altered. This could be tested by performing a whole transcriptome analysis by RNAseq in a Topo IV^{ts} mutant or by simply testing gene transcription by RT-qPCR.

2. Why is there a transcription repression?

The “raison d’être” of such a transcription repression behind the fork should be discussed.

One reason could be to avoid transcription/replication interferences. By avoiding transcription near the replisome, the chances of conflicts between RNA polymerases and the replicative DNA polymerase is decreased. However, the chances of such conflicts seem quite low since the elongation rate of DNA polymerase is ~1kb/sec (Hirose et al., 1983) and the elongation rate of RNA polymerase is ~50 nucleotides/sec (Gotta et al., 1991), thus making it difficult for RNA polymerase to “catch up” with the DNA polymerase.

A more probable hypothesis could be that repressing transcription behind the fork decreases the risk of transcription problems linked to DNA damage. Indeed, as presented in the introduction, most DNA damage occurs at the replication fork, and often leads to DSBs. In the event of a DSB, part of the DNA is degraded (up to 250 kb) by RecBCD (Wiktor et al., 2018), and gene transcription could thus be impeded which would be highly detrimental. In *Saccharomyces cerevisiae*, it was shown that a double strand break causes transcriptional inhibition and mutants defective for resection fail to inhibit transcription (Manfrini et al., 2015). We can therefore imagine that by inhibiting transcription around the replication fork (the most susceptible zone to undergo a DSB) in a controlled manner, the cell could avoid un-programmed loss of transcription of essential genes. Interestingly, our iPOND results show that some of these transcription factors were also depleted around the fork in MMC treated cells, confirming a possible inhibition of transcription around the DSB.

F. Concluding remarks

Altogether, the work accomplished during my PhD has demonstrated the importance of sister chromatid cohesion for DNA repair in *E.coli*. More specifically, I have shown the importance of RecN, an SMC-like protein that is induced by the SOS response. RecN prevents sister chromatid segregation upon DNA damage and mediates a whole chromosome rearrangement. RecN is a highly conserved protein among Prokaryotes which strengthens the importance of sister chromatid cohesion for DNA repair, possibly by enhancing the efficiency of homology search and subsequent homologous recombination. The complementary results obtained recently give rise to new questions and suggest a more complicated mechanism or maybe a dual function of RecN's action. This paves the way for new experiments, more discussions, more papers and maybe a new PhD project...!

IV. Material & Methods

Most methods used during my thesis are described in the material and methods chapter of my publication. In the following chapter, I have described additional methods required for the supplementary results of the publication and the complementary results performed after my paper was published.

A. Strains

The strains and plasmids used during my thesis are listed below. All strains are derived from an MG1655 or MG1556 (delta Lac MluI). Construction of microscopy strains was done using lamda red recombination using the pGBKDparS-pMT1 plasmid as a matrix. Construction of *lacloxP* strains was done using the pGBKDlaclox plasmid as a matrix.

Strain	Genotype	Reference
MG1655		lab stock
MG1656	MG1655 Δ lacMlul	Espeli et al., 2001
Ori-1 inter SC	MG1656 Ori-1 lacZ::loxP-20bp-loxP frt-cat-frt	Lesterlin et al., 2012
Ori-3 inter SC	MG1656 Ori-3 lacZ::loxP-20bp-loxP frt-cat-frt	Lesterlin et al., 2012
Ter-4 inter SC	MG1656 Ter-6 lacZ::loxP-20bp-loxP frt-cat-frt	Lesterlin et al., 2012
EG01	MG1656 Ori-1 lacZ::loxP-20bp-loxP	Lesterlin et al., 2012
EG02	MG1656 Ori-3 lacZ::loxP-20bp-loxP	Lesterlin et al., 2012
EG04	MG1656 Ter-4 lacZ::loxP-20bp-loxP	Lesterlin et al., 2012
MG1655 Ori-1 ::parS pMT1-frt-cat-frt	MG1655 Ori-1 ::parS pMT1-frt-cat-frt	Gift from Michele Valens
EV01	MG1656 Ori-1 ::parS pMT1 frt-cat-frt	this work
EV02	MG1656 Ori-3 ::parS pMT1 frt-cat-frt	this work
EV03	MG1656 left-1:: parS pMT1 frt-cat-frt	this work
EV04	MG1656 Ter-4:: parS pMT1 frt-cat-frt	this work
EV05	DY330 recN::frt-cat-frt	this work
EV06	MG1655 recN::frt-cat-frt	this work
EV07	EG01 recN::frt-cat-frt	this work
EV08	EG02 recN::frt-cat-frt	this work
EV09	EG04 recN::frt-cat-frt	this work
EV10	EG02 recA::frt-cat-frt	this work
EG55	EG02 recA::cat	Lesterlin et al., 2012
JJC123	lexA Ind- malB::Cm	Bénédicte Michel
CP01	EG02 lexAind- malB::Cm	this work
CP02	EG02 pGE51_recA(wt)	this work
CP03	EG02 pGE51_recA(Q300A)	this work
EV11	EG02 recX::frt-kan-frt	this work
EV12	EG02 sbmC::frt-kan-frt	this work
EV13	EG02 yebG::frt-kan-frt	this work
EV14	EG02 yafN::frt-kan-frt	this work
EV15	EG02 yafO::frt-kan-frt	this work
EV16	EG02 ydjM::frt-kan-frt	this work
EV17	EG02 cho::frt-kan-frt	this work
EV18	EG02 yfgJ::frt-kan-frt	this work
EV19	EG02 rmuC::frt-kan-frt	this work
EV20	EG02 dnaT::frt-kan-frt	this work
EV21	EG02 yjbJ::frt-kan-frt	this work
EV22	EG02 bssS::frt-kan-frt	this work
EV23	EG02 mug::frt-kan-frt	this work
EV24	EG02 yhbS::frt-kan-frt	this work
EV25	EG02 dinG::frt-kan-frt	this work
EV26	EG02 yjtD::frt-kan-frt	this work
EV27	EG02 eco::frt-kan-frt	this work
EG28	EG02 dnaC::Tc	this work
EV32	EG15 recN::frt-cat-frt	this work
JC777	recBC::Tn10 Tet	Benedicte Michel
EV33	MG1655 recBC::Tn10 Tet	this work
EV34	EV33 recN::frt-cat-frt	this work
JJC2301	recO1504::Tn5 zfh208::Tn10	this work

EV35	MG1655 recO1504::Tn5 kan	Benedicte Michel
EV36	EV35 recN::frt-cat-frt	this work
EV37	EG02 parEts::Tc	this work
EV38	EV08 parEts::tc	Benedicte Michel
TS4366	recA441 lexA51 malB::Tn9 (CmR)	this work
JJC396	sfiA::kan	this work
CP04	EG02 sfiA::kan	this work
CP05	CP04 lexA51 malB::Tn9	this work
CP06	CP05 recA::Tc	Adriana Bellone
EV39	EG02 pZA31RecN	Benedicte Michel
EV40	EG08 pZA31RecN	this work
EV41	EG02 pZA31	this work
EV42	EG08 pZA31	this work
EV43	EV01 parS pMT1::frt	this work
EV44	EV02 parS pMT1::frt	this work
EV45	EV03 parS pMT1::frt	this work
EV46	EV04 parS pMT1::frt	this work
EV47	EV43 recN::frt-cat-frt	this work
EV48	EV44 recN::frt-cat-frt	this work
EV49	EV45 recN::frt-cat-frt	this work
EV50	EV46 recN::frt-cat-frt	this work
SS6264	hupA100::gfp-901 (kan)	this work
SS6279	hupA100::mcherry (kan)	Espeli et al., 2012
EV53	MG1655 hupA100::gfp-901 (kan)	this work
EV54	MG1655 hupA100::mcherry (kan)	this work
EV55	EV06 hupA100::gfp-901 (kan)	Marceau et al., 2011
EV55	EV06 hupA100::mcherry (kan)	Marceau et al., 2012
EV56	EV44 hupA100::mcherry (kan)	this work
EV57	EV48 hupA100::mcherry (kan)	this work
JJC5795	MG1655 DlacZ ::recA (R28A)-mcherry CmR, recAo1403	this work
EV58	JJC5795 recN::frt-cat-frt	this work
EV59	MG1655 parEts::tc	this work
EV60	EV59 recN::frt-cat-frt	this work
EV61	EV59 recA::frt-cat-frt	Benedicte Michel
EV62	MG1655 recA::frt-Tc-frt	this work
EV63	EG02 topB::frt-kat-frt	this work
EV64	EV63 recN::frt-cat-frt	this work
ALO545	dnaA46ts tna300::TN10	this work
EV65	MG1655 dnaAts::Tc	this work
EV66	EV06 dnaAts::Tc	this work
JJC5980	ytfj::lscel (NM) lscel gene at araB (arabinose inducible) linked to a TN10 at leuO::Kan	this work
JJC573	ytfj::lscel site ::frt-cat-frt	Kirsten Skarstad
EV67	EG02 ytfj::lscel site ::frt-cat-frt	this work
EV68	EV67 lscel gene at araB (arabinose inducible) linked to a TN10 at leuO::Kan	this work
EV69	EV08 ytfj::lscel site ::frt-cat-frt	Benedicte Michel
EV70	EV69 lscel gene at araB (arabinose inducible) linked to a TN10 at leuO::Kan	Benedicte Michel
EV71	JJC5980 recN::frt-cat-frt	this work
EV72	JJC5980 recA::frt-cat-frt	this work

EV35	MG1655 recO1504::Tn5 kan	Benedicte Michel
EV36	EV35 recN::frt-cat-frt	this work
EV37	EG02 parEts::Tc	this work
EV38	EV08 parEts::tc	Benedicte Michel
TS4366	recA441 lexA51 malB::Tn9 (CmR)	this work
JJC396	sfiA::kan	this work
CP04	EG02 sfiA::kan	this work
CP05	CP04 lexA51 malB::Tn9	this work
CP06	CP05 recA::Tc	Adriana Bellone
EV39	EG02 pZA31RecN	Benedicte Michel
EV40	EG08 pZA31RecN	this work
EV41	EG02 pZA31	this work
EV42	EG08 pZA31	this work
EV43	EV01 parS pMT1::frt	this work
EV44	EV02 parS pMT1::frt	this work
EV45	EV03 parS pMT1::frt	this work
EV46	EV04 parS pMT1::frt	this work
EV47	EV43 recN::frt-cat-frt	this work
EV48	EV44 recN::frt-cat-frt	this work
EV49	EV45 recN::frt-cat-frt	this work
EV50	EV46 recN::frt-cat-frt	this work
SS6264	hupA100::gfp-901 (kan)	this work
SS6279	hupA100::mcherry (kan)	Espeli et al., 2012
EV53	MG1655 hupA100::gfp-901 (kan)	this work
EV54	MG1655 hupA100::mcherry (kan)	this work
EV55	EV06 hupA100::gfp-901 (kan)	Marceau et al., 2011
EV55	EV06 hupA100::mcherry (kan)	Marceau et al., 2012
EV56	EV44 hupA100::mcherry (kan)	this work
EV57	EV48 hupA100::mcherry (kan)	this work
JJC5795	MG1655 DlacZ ::recA (R28A)-mcherry CmR, recAo1403	this work
EV58	JJC5795 recN::frt-cat-frt	this work
EV59	MG1655 parEts::tc	this work
EV60	EV59 recN::frt-cat-frt	this work
EV61	EV59 recA::frt-cat-frt	Benedicte Michel
EV62	MG1655 recA::frt-Tc-frt	this work
EV63	EG02 topB::frt-kat-frt	this work
EV64	EV63 recN::frt-cat-frt	this work
ALO545	dnaA46ts tna300::TN10	this work
EV65	MG1655 dnaAts::Tc	this work
EV66	EV06 dnaAts::Tc	this work
JJC5980	ytfj::lscel (NM) lscel gene at araB (arabinose inducible) linked to a TN10 at leuO::Kan	this work
JJC573	ytfj::lscel site ::frt-cat-frt	Kirsten Skarstad
EV67	EG02 ytfj::lscel site ::frt-cat-frt	this work
EV68	EV67 lscel gene at araB (arabinose inducible) linked to a TN10 at leuO::Kan	this work
EV69	EV08 ytfj::lscel site ::frt-cat-frt	Benedicte Michel
EV70	EV69 lscel gene at araB (arabinose inducible) linked to a TN10 at leuO::Kan	Benedicte Michel
EV71	JJC5980 recN::frt-cat-frt	this work
EV72	JJC5980 recA::frt-cat-frt	this work

B. Ori/ter quantification by qPCR assay on *dnaA*ts strains

An overnight culture was diluted 1:200 in minimum medium A supplemented with 0.2% casamino acids and 0.25% glucose. Cells were grown at 30°C until OD₆₀₀~0.2 and immediately placed at 42°C for inactivation of DnaA. At the same time, 10µg/ml of MMC was added or not. 1,5ml of cells was flash frozen at each time point and genomic DNA was extracted as described above. qPCR was performed on a MyiQ Biorad lightcycler qPCR machine. Results are expressed as the difference between ori Ct and ter Ct.

C. Cell viability assay

An overnight culture was diluted 1:200 in LB and grown at 30°C because of the thermosensitivity of the Gyrase^{ts} mutants. At OD~0.2, cultures were put at 40°C for 20 min and then 15 µg/ml MMC was added. Viability was measured by serial dilution every 10 minutes for 40 min. For each dilution, 2 µl drops were plated on LB and plates were incubated ON at 30°C. Colonies were counted the next day.

D. Construction of microscopy strains

To integrate the *parS* sequence in the chromosome of the MG1655 strain, we used a vector derived from pKD4 (Datsenko and Wanner, 2000) called pGBKD3-*parS* pMT1 (Espéli et al., 2012). All the tags were inserted in intergenic regions of non-essential genes (Espéli et al., 2008). The expression of the ParB–YFP fusion protein is driven by the pFH2973 plasmid (Espéli et al., 2012).

E. FRAP (Fluorescence Recovery After Photobleaching)

An overnight culture was diluted 1:200 in minimum medium A 1X supplemented with 0.25% glucose and 0.2% casminoacids and grown at 37°C to OD₆₀₀~0.2. Cells were pelleted and resuspended in 50 µl of fresh medium. 1% agarose pads were made with VWR geneframes,

supplemented with 10 µg/ml MMC or not. 5µl of cells were deposited on the agarose pad and FRAP experiment was performed using a confocal spinning disk (X1 Yokogawa) on a Nikon Ti microscope at 100 x magnification, using an EMCCD camera controlled by metamorph software. For each condition small Regions of Interest (ROI) were defined on the HU-GFP stained nucleoid and fluorescence was acquired using the FRAP module of metamorph software. Analysis was done with imageJ and Excel. The half-life of fluorescence recovery was defined for each ROI and averaged.

F. Foci dynamics

An overnight culture was diluted 1:200 in minimum medium A 1X supplemented with 0.25% glucose and 0.2% casminoacids and grown at 37°C to OD₆₀₀~0.2. Cells were pelleted and resuspended in 50 µl of fresh medium. 1% agarose pads were made with VWR geneframes, supplemented with 10 µg/ml MMC or not. 5 µl of cells were deposited on the agarose pad and timelapse was performed using a confocal spinning disk (X1 Yokogawa) on a Nikon Ti microscope at 100X magnification, using an EMCCD camera controlled by metamorph software. One image was acquired every 10 seconds for 20 min.

Analysis was done with the Mosaic plugin from imageJ. Radius was set at 3, cutoff at 0 and percentile at 0.1. Linkage range and displacement were set at 3. The histograms plot the MSD slope of approximately 500 foci per strain and per condition.

G. RNAseq

An overnight culture of an MG1655 wild type strain and an MG1655 *recN* strain were diluted 1:200 in 30 ml minimum medium A 1X supplemented with 0.2% casaminoacids and 0.25% glucose and grown to OD₆₀₀ ~0.2 at 37°C. Cells were treated with 10 µg/ml MMC or not, for 20 min or 40 min. At each time point, 30 ml of cells were immediately pelleted and RNA was extracted using the ThermoFisher RNA extraction kit. TE buffer, lysis buffer and Ethanol volumes were doubled considering the large volume of cells. RNA was quantified using the nanodrop from thermofisher. Samples were centrifuged, washed in 70% ethanol and speedvaced for 10 min at 40°C. Pellets were resuspended in 10 µl RNase free water from

Invitrogen and quality of RNAs was controlled using RNA nano chips from Agilent and the bioanalyzer. The concentration of each sample and the RNA Integrity Number (RIN) was validated for each sample and RNA was sent to the illumina platform for sequencing.

The results are shown as an induction fold i.e. a number of reads in the treated sample versus the untreated sample.

H. RecN Co-immunoprecipitation

An overnight culture of MG1655 wild type strain and a strain carrying the RecN protein tagged with a flag peptide were diluted 1:200 in 100 ml Minimum Media A 1X supplemented with 0.2% casamino acids and 0.25% glucose. The cells were grown to an $OD_{600} \sim 0.2$. 100 ml of culture was then treated with 10 $\mu\text{g}/\text{ml}$ MMC for 30 min and pelleted at 4°C for 10 min. Cells were washed 3 times with ice cold 1X PBS. Pellets were resuspended in 300 μl of lysis buffer (100mM NaCl; 10mM Tris-HCl pH7.8; 10mM EDTA; 20% sucrose; 1mg/ml lysozyme +1 complete tablet/10ml Complete protease inhibitor mixture EDTA-free (Roche)) and sonicated for 25 cycles for 30" ON and 30" OFF using a bioruptor sonicator from Diagenode. Cells were pelleted and the supernatant was incubated ON at 4°C with an anti-flag antibody (Sigma F3165) (1:300) or anti-RecA antibody (abcam 63797) (1:300).

The next day, 100 μl of magnetic anti-proteinA beads were placed on the dynamag magnetic rack and beads were separated from the buffer. 350 μl of the antibody-lysate mix was added to the 100 μl of beads and incubated for 2h at RT. Lysate was then placed on the dynamag and washed three times with 1X PBS. Elution was performed with 100 μl of an SDS buffer (2% SDS, 100 mM Tris-HCl, 10% glycerol and 0.5mM EDTA).

After elution, proteins were concentrated using a Pal nanosep column (3 kDa cut off or more depending on the size of the proteins of interest). Centrifugation was carried out at 13000g for 12-15 min. Final volume left is $\sim 40 \mu\text{l}$.

Western blot was done on RecNflag and MG1655 samples using an anti-flag antibody 1:500 (sigma) for the RecN-flag and RecA IP.

Western blot was done on RecNflag and MG1655 samples using an anti-RecA antibody 1:1000 (Abcam) for the RecA and RecNflag IP.

I. iPond

An overnight culture was diluted 1:200 in minimum medium A 1X supplemented with 0.25% glucose and 0.2% casminoacids and grown at 37°C to OD ~0.2. Cells were incubated with 10µM EdU (stock 10mM) for 5min [100µl of EdU stock at 10mM].

When performing the chase, cells were washed once with 10 µM fresh thymidine (stock 10mM) and chased with 10 µM (stock 10mM) thymidine in minimum medium A 1X supplemented with 0.25% glucose and 0.2% casminoacids for 15 min.

After the chase, 10 µg/ml MMC was added to the culture or not. At the end of each timepoint, cultures were crosslinked with 2% formaldehyde from sigma (37% stock) for 15 min.

Crosslinking was quenched with 0.125% glycine for 5 min. Cultures were then washed 3 times in cold PBS. Pellets can be frozen at -80°C and the rest of the experiment can be carried out later.

Pellets were resuspended in 2 ml of fresh lysozyme (4mg/ml PBS1X) and incubated at RT for 20 min. One wash was done with 0.5% BSA in PBS 1X and one wash is done with PBS1X.

Pellets were then resuspended in the click solution: 2ml of fresh sodium-L-ascorbate at 10 mM (sigma); 1µl of biotin TEG and 40µl CuSO₄ (stock at 100 mM). Reaction was carried out at RT for 2h, in the dark. Pellets were then washed twice with 2 ml of 0.5% BSA and twice with PBS. Cells were resuspended in 400 µl of fresh COLD lysis buffer [100mM NaCl; 10mM Tris pH7.8; 10mM EDTA; 20% sucrose; 1mg/ml lysozyme + 1 tablet of complete] and sonication was performed in a bioruptor from diagenode for 25 cycles (30" ON and 30" OFF). Cells were then centrifuged at 13000 rpm for 3 min at 4°C. 50 µl were set aside for input and immediately boiled for 30 min in 5x laemmli. Inputs can be stored at -20°C. The remaining 350 µl were transferred to low bind eppendorfs. 50 µl of ademtech beads per sample were washed in the same volume of lysis buffer. Samples were then incubated with the beads for 15-20 h in the dark, at RT. The next day, beads + sample were put on the magnetic rack for 10-15 min, at 4°C to separate beads from proteins. Do not centrifuge as it may favor unspecific binding to the beads. The beads were then washed once with 1ml lysis buffer, once with 1ml 500mM NaCl, and twice with 1X PBS 0.02% tween. Crosslinking was reversed and elution was done in 1% SDS, 10mM Tris-HCL, 1mM EDTA for 30 min at 95°C. Supernatants can be stored at -80°C.

Coomassie gel was done with a precast gradient gel from biorad, with a very short migration as to not separate all protein bands and mass spectrometry was done by the imagif platform.

J. Gene overexpression bank

An overnight culture of an MG1655 *recN* was transformed with a library of pBR322 plasmids overexpressing all the genes of the genome. As a negative control, MG1655 *recN* was also transformed with the pBR322 #inc3, empty vector. Enough plates were plated to obtain 40 000 clones. Clones were harvested and a CFU was performed after a 30 min treatment of 15 µg/ml MMC. 100 µl of culture were plated at a 10⁻³ dilution on 10 kanamycin plates to optimize the amount of clones obtained. Approximately 30 clones grew on kanamycin plates after a 30 min MMC treatment. Clones were verified on kanamycin, MMC 1 µg/ml or MMC 2 µg/ml plates. Of the 30 clones originally obtained, only five grew again on MMC at 1 µg/ml or MMC at 2 µg/ml. Resistance to chloramphenicol was tested to check whether the resistance to MMC wasn't due to overexpression of efflux pumps. This test discarded two extra clones. Clones were sent for sequencing to identify the genes contained on the plasmid and extra viability and laclox assays were performed on the validated clones.

K. Construction of *recA-mcherry* fusion

The strain JC13509 {Citation} carries a RecA-GFP fusion inserted at the *recA* chromosomal locus. In addition to the C-terminal fusion with GFP, this RecA-GFP allele carries two mutations, a *recAo1403* operator mutation (T to A) that increases two-fold the basal level of *recA* transcription and a *recA4155* mutation (R28A) that prevents the formation of DNA-independent polar RecA-GFP foci 1. In a first step, the *ssb* gene from the plasmid pKD3-*ssb-mcherry* was replaced by the *recAo1403* 4155 gene. For this purpose, the *recAo1403* 4155 was amplified from JC13509 using the following oligonucleotides: 5' AAC CCA CTC GTG CAC GGC GGG AAT GCT TCA GCG GCG A 3' and 5' TTC ATG TTC GAA TGA TGC TCC CAA AAT CTT CGT TAG TTT CTG C 3' and the PCR products were cleaved with ApaLI and BstBI. The restriction product was cloned into pKD3-*ssb-mcherry* restricted with ClaI and ApaLI, producing the plasmid pKD3-RecA-mcherry. In a second step, the *recA-mcherry* CmR region of pKD3-RecA-mcherry

was amplified using the following oligonucleotides, which contain homology regions with the chromosomal *lacI* and *lacZ* sequences: 3'-GCA GCT GGC ACG ACA GGT TTC CCG ACT GGA AAG CGG GCA GTG AGG CGG GAA TGC TTC AGC GGC GA 5' and 3'TCA TCA TAT TTA ATC AGC GAC TGA TCC ACC CAG TCC CAG ACG AAG ATG AAT ATC CTC CTT AGT TCC TA- 5'. The PCR product was used to electroporate MG1655 [pKD46] as described (Datsenko and Wanner, 2000) creating a *recA-mcherry* fusion gene inserted into the *lac* operon under the control of its own promoter *recAo1403* (strain JJC5789). The presence of the correct insertion was verified by PCR and by sequencing. The presence of polar foci was unexpected since the RecA-mcherry allele carries the R28A mutation that prevents RecA-GFP polar foci formation (Renzette et al., 2005). We demonstrated that an increased number of polar foci is the consequence of co-expression of RecA-mCherry and wild type RecA.

L. Construction of LoxP strains

The wild type strain was *E. coli* K12 MG1655 (Δ *lacMI*). The LacloxP cassette was constructed by the integration of a double stranded oligonucleotide 5'-

CGTAATAACTTCGTATAATGTATGCTATACGAAGTTATGGATCCCCGGGTACCGAGCTCATAACTTCG TATAATGTATGCTATACGAAGTTATCCTA-3" into the *Cl*I restriction site of the *lacZ* gene. The LacloxP cassette was integrated in the chromosome, using a vector derived from pKD4 called pGBKD3-Laclox (Lesterlin et al., 2012). These vectors contained the LacloxP cassettes adjacent to the chloramphenicol resistance gene. Laclox::Cm was inserted into the intergenic regions of non-essential genes using the standard 'lambda red' technique (Datsenko and Wanner, 2000). Expression of the Cre recombinase was driven by a pSC101 carrying the arabinose-inducible Cre gene derived from pFX465, kindly given by FX Barre. The lacloxP::Cm cassettes inserted at the different chromosome sites were then moved into different strain backgrounds by using P1 transductions.

M. LoxP recombination assays

LoxP recombination assays were performed as described in Vickridge et al. from Methods in Molecular Biology (Vickridge et al., 2017).

The experiments with the Gyrase^{ts} and Topo IV^{ts} mutants were performed as described in Vickridge *et al.* 2017, except that the strains were incubated for 20 min at 40°C before 10 µg/ml MMC and 0.1% arabinose addition.

N. Published article in Methods in Molecular Biology: The Bacterial Nucleoid

The *loxP/Cre* recombination assay was the object of an article published in The Methods in Molecular Biology book in 2017.

Revealing Sister Chromatid Interactions with the *loxP*/Cre recombination assay

Elise Vickridge, Charlène Planchenault and Olivier Espéli

CIRB, Collège de France, UMR CNRS 7241, 11 place Marcelin Berthelot, 75005 Paris, France

Published in 2017

Running title: *LoxP*/Cre recombination assay

Abstract

Site specific recombination methods have been used in several occasions to probe chromosome structure. Site specific recombinases only recognize DNA in an adequate structure. These properties have been used to reveal different DNA structuring features. The supercoiling density of *E. coli* plasmids has been measured *in vivo* and *in vitro* according to the recombination frequency of λ Int/Xis recombinase on attL/R sites (Bliska and Cozzarelli, 1987). Biases in λ Int/Xis mediated recombination also revealed macrodomain structures in the *E. coli* chromosome (Valens et al., 2004). Tn3/ λ Int recombination has been used to monitor supercoiling microdomains (Deng et al., 2004; Staczek and Higgins, 1998) in *S. typhimurium*. In yeast, the *loxP*/Cre recombination system has allowed to measure interactions between homologous and ectopic loci (Burgess and Kleckner, 1999). Here we describe a simple assay based on the *loxP*/Cre recombination system that reveals interactions between sister chromatids and allows to follow segregation of loci in a quantitative manner (Lesterlin et al., 2012). This method can be used to study sister chromatid interactions in a normal cell cycle, in response to genotoxic stress or in various mutants.

1. Introduction

Two consecutive *loxP* sites, spaced by only 20bp are cloned at a given site on the chromosome. In our original set-up they were cloned into an ectopic *lacZ* gene, thus preventing its transcription. The plated colonies are white. When the two sister chromatids are in very close proximity, the *loxP* sites from each sister chromatid will be able to recombine with one another, once Cre is induced with 0.1% arabinose. The products formed by this recombination are a 1*loxP* site on one sister chromatid and 3*loxP* sites on the other sister chromatid. These three *loxP* sites on one sister chromatid will recombine together, eventually leading to a 1 *loxP* site. When there is only one *loxP* site in the *lacZ* gene, the open reading frame of *lacZ* is reconstituted and the colonies become blue when plated on Xgal. The frequency of recombination which is directly linked to the proximity

between sister chromatids can be assessed by a white/blue colony count. In this chapter, we also present a new method to immediately analyze recombination products formed in the minutes following Cre recombination with a semi quantitative PCR and a Bioanalyzer. The amount of 1 *loxP* product versus the total amount of DNA gives the recombination frequency and thus, the amount of sister chromatid interactions (Figure 1).

2.Material

Store all reagents as indicated on the product. The bioanalyzer reagents must be equilibrated at room temperature for at least an hour before use.

2.1 Plasmids, strains and primers

Strains:

MG1655 (*E. coli* K12)

MG1656 (*E. coli* K12 Δ lac *Mlu*I)

Plasmids:

pGBKD3-LacloxP (Lesterlin et al., 2012)

pGBKD3-Lacloxrif (Espéli et al., 2012)

pCre (Lesterlin et al., 2012)

Primers for insertion of *loxP* sites onto the chromosome:

LacloxP-ins-Forward: [50nt of homology upstream of insertion site - GAT TGT GTA GGC TGG AGC TGC]

LacloxP-ins-Reverse: [50nt of homology downstream of insertion site - GG TCT GCT ATG TGG TGC TAT CT]

Primers for analysis of *loxP* recombination products by PCR:

LacloxP-Forward: CTTCTGCTTCAATCAGCGTGCCGTC

LacloxP-Reverse: GATCAGGATATGTGGCGGATGAGCGG

2.2 Reagents: stock solutions

All solutions must be prepared using ultrapure water (by purifying deionized water, to attain a sensitivity of 18 M Ω -cm at 25 °C)

Prepare the following buffers and stock solutions. Unless otherwise specified, filter solutions using a 0.2 μ m low protein binding non-pyrogenic membrane.

20% (w/v) Arabinose in H₂O

40% Glycerol in H₂O

20% Glucose in H₂O

20 mg/ml Xgal (5-bromo-4-chloro-3-indolyl- β -D-galactopyranoside) in dimethylformamide

20% Casaminoacids in H₂O

100 mg/ml Spectinomycin in H₂O

30 mg/ml Chloramphenicol in absolute Ethanol

1M MgSO₄

2M MgCl₂
Dimethyl Sulfoxide (DMSO)
10X Minimum Medium A: 0.26M KH₂PO₄, 0.06M K₂HPO₄, 0.01M tri sodium citrate, 2mM MgSO₄,
0.04M (NH₄)₂ SO₄
Transformation and Storage Solution (TSS): LB, 10 % PEG 6000, 10mM MgSO₄, 10 mM MgCl₂, 5%
DMSO
LB Broth (Lennox Broth)
Select agar
10X TBE: 1M Tris, 1M Borate, 0.02M EDTA
1.7% Agarose (molecular grade) in 1X TBE

DNA Ladder 100bp DNA

2.3 Medium

For *LoxP* recombination assays in *Escherichia coli* and related bacteria, grow cells in 1X Minimum Medium A supplemented with 0.2% casaminoacids and 0.25 % glycerol. pCre transformation and measure of recombination can be performed in Minimum Medium A supplemented with 0.2% glucose, 0.25% casaminoacids, 40 µg/ml Xgal and 100 µg/ml spectinomycin or on LB agar plates supplemented with 40 µg/ml Xgal and 100 µg/ml spectinomycin.

2.4 Genomic DNA extractions

Liquid nitrogen
Genomic DNA extraction kit

2.4 Genomic DNA and PCR product quantification

DNA quantification using a Nanodrop (ThermoScientific)

2.5 PCR

Primers for strain constructions (see section 2.1)

Insertion of *LacloxP* and *LacloxP-rif* cassettes on the chromosome:

Four 50µl of reactions were assembled using 1ng of plasmid DNA as matrix (pGBKD3-LacloxP or pGBKD3-LacloxP-rif), primers LacloxP-ins-Forward and LacloxP-ins-Reverse (20 µM), dNTPs (10µM each), Mg²⁺ plus buffer and TaKaRa Ex Taq (see Note 1).

Amplification of *loxP* sites:

50µl of reaction was assembled using 1µL of genomic DNA at 2ng/µl, primers LacloxP-Forward and LacloxP-Reverse (20 µM), dNTPs (10µM each) and Mg²⁺ plus buffer and TaKaRa Ex Taq.

2.6 PCR product verification on agarose gel

1.7% agarose gel electrophoresis in 1X TBE

2.6 Detection of *loxP* recombination events by bioanalyzer

Agilent DNA 1000 kit

3. Methods

3.1 Strain constructions

The *LacloxP* cassette that allows measuring of intermolecular recombination was constructed by the integration of a double stranded oligonucleotide 5'CGTAATAACTTCGTATAATGTATGCTATACGAAGTTATGGATCCCCGGGTACCGAGCTCATAACTTCGTATAA TGTATGCTATACGAAGTTATCCTA-3' into the *Clal* restriction site of the *lacZ* gene of the pGBKD3-*lacZ* plasmid. We called this plasmid pGBKD3-*LacloxP* (Lesterlin et al., 2012). For the control of intramolecular recombination, a rifampicin resistance gene (*rif*) and its promoter were introduced between the 2 *loxP* sites by cloning into the *BamHI* site of pGBKD3-*Laclox*. We called this plasmid pGBKD3-*Laclox-rif* (Lesterlin et al., 2012). The pGBKD3-*LacloxP* or pGBKD3-*Laclox-rif* were used as matrices to insert the intermolecular and intramolecular cassettes inside intergenic regions of non-essential genes of the DY330 strain with the standard 'lambda red' method (Datsenko and Wanner, 2000). These vectors contained the *LacloxP* or the *LacloxP-rif* cassettes adjacent to the chloramphenicol resistance gene. The *LacloxP::Cm* or the *LacloxP-rif::Cm* cassettes were then P1 transduced into the genome of MG1656 strain. Expression of the Cre recombinase was driven by an arabinose-inducible promoter on a plasmid (pFX465) derived from pSC101, we called this plasmid pCre (Lesterlin et al., 2012). pCre also contains a PLac promoter antisense to *cre* that can be used to further repress Cre expression with IPTG in some conditions (see Note 2).

3.2 Measuring *LoxP* recombination as a function of the number of Lac⁺ colonies on plate

Day 1:

Transformation of the pCre plasmid in the MG1656-*lacloxP* and MG1656 *LacloxP-rif* strains.

1. Inoculate 100ml of LB with 1ml of overnight culture of MG1656 *LacloxP* and MG1656 *LacloxP-rif* at 37°C. Let the cells grow to an OD_{600nm}≈0.5-0.6.
2. Centrifuge at 6000 rpm, 10 min at 4°C.
3. Resuspend the pellet in a 1/10 volume of cold TSS.
4. Leave the cells for 10 min on ice.
5. Mix 100 µl of cells with 2 to 4 ng of pCre plasmid.
6. Leave the cells with the plasmid for 10 min on ice.
7. Induce a heat shock at 37°C for 3min or 42°C for 90 sec.
8. Leave the sample on ice for 30 sec and add 900 µl of LB.
9. Incubate for 60 min at 37°C.
10. Plate 100µl of the transformation on LB supplemented with 40µg/ml Xgal and 100µg/ml spectinomycin.
11. Incubate over night at 37°C (see Note 3).

Day 2

1. Select a white colony and streak on a fresh plate of Minimum Medium A supplemented with 0.2% glucose, 0.25% casaminoacids, 40µg/ml Xgal and 100 µg/ml spectinomycin.

Day 3

1. Prepare three different 1.5 ml cultures from three different white colonies in Minimum Medium A supplemented with 0.2% glucose, 0.25% casaminoacids and 100µg/ml spectinomycin final concentration for both the intramolecular strain and the intermolecular strain.
2. Incubate overnight at 37°C.

Day 4

1. Dilute the overnight cultures at 1/200 in minimum medium A supplemented with 0.2% casaminoacids and 0.2% glycerol at 37°C, under shaking. Use a 100ml Erlenmeyer and 25ml of medium. (see Notes 4).
2. At $OD_{600nm} \approx 0.2$ take two 100 µl aliquots of each culture; dilute them at a convenient dilution to obtain about 200 colonies per 100 µl plating. This is the non-induced recombination frequency reference. Add 0.1% arabinose to each culture (see Note 5 and 6).
This step is crucial because recombination occurs as soon as the arabinose is added; specific care must be taken for the timing.
3. For each time-point 5, 10, 15, 20 min for intermolecular recombination and between 3, 5, 10 min for intramolecular recombination (see Notes 7 and 8), dilute samples 1/100 in minimum medium A, casaminoacids and glycerol in order to dilute the arabinose and stop Cre induction. We observed that Cre recombination dramatically dropped down in the minutes following arrest of induction (Lesterlin et al., 2012) (see Note 9)
4. Then, dilute each sample at a convenient dilution to obtain about 200 colonies per 100 µl plating (see Note 10).
5. Plate two times 100 µl of each sample on LB plates supplemented with 40 µg/ml Xgal and 100µg/ml spectinomycin.
6. Incubate at 37°C overnight.
7. Count the number of white and blue colonies for each plate and each sample.
8. Quantification of recombination: (number of blue colonies/number of white colonies INTER)/ (number of blue colonies/number of white colonies INTRA). The intramolecular recombination rate serves as normalization for Cre recombination efficiency *per se*, which depends on the locus considered, growth conditions and the genetic background.

3.3 LacloxP assay by PCR method

This alternative method relies on quantification of the *loxP* recombination products by combining a PCR amplification of the *loxP* products with their quantification on an Agilent Bioanalyzer. This method significantly facilitates interpretation of the results when working with mutants whose viability is

affected or with drugs that affect the cell cycle. In addition we observed higher reproducibility of the results with the PCR-Bioanalyzer method than with the plating method.

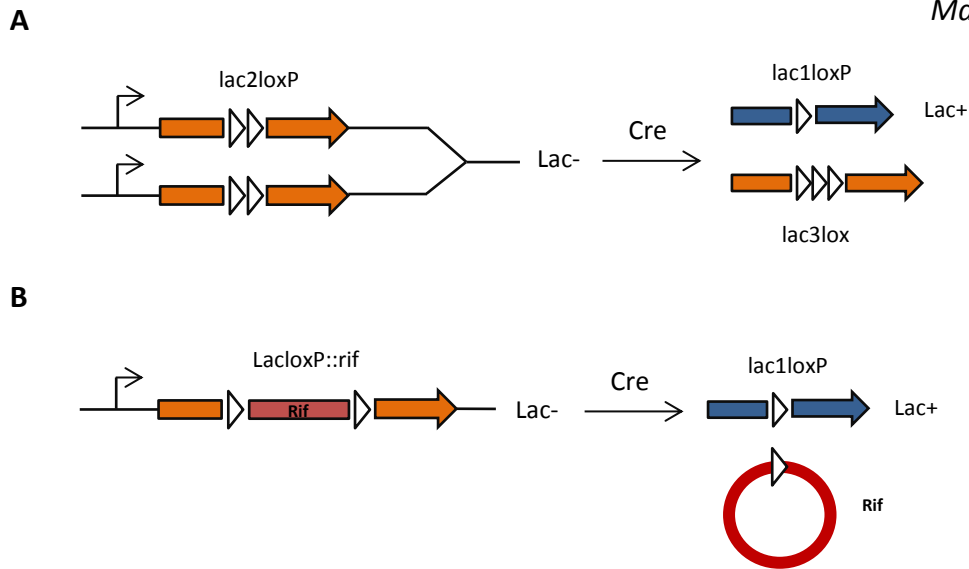
For growth conditions and Cre induction, see section 3.2 Day 3 and Day 4 (1-2)

1. Before Cre induction and at chosen time-points after induction, take 1.5 ml of the given samples and flash freeze them immediately in liquid nitrogen in a 2 ml test tubes. Frozen samples may be stored at -20°C for several weeks.
2. Gently thaw samples and centrifuge them for 3 min at 9000 rpm. Remove the supernatant and proceed to genomic DNA extraction according to manufacturer instructions. Elute DNA in 100 µl of elution buffer.(see Note 11)
3. Quantify DNA with the Thermo Fisher Scientific Nanodrop. Expected DNA concentration is between 20 and 80 ng/µl.
4. Dilute all samples to 2 ng/µl in molecular grade water.
5. Perform a PCR on each sample using Ex Taq enzyme from TaKaRa. Use 1µl of diluted sample for each 50µl reaction. Tm=58°C, 28 cycles. Elongation step is 30 seconds
6. Verify the PCR products with a 1.7% agarose gel in TBE 1X (see Note 12). Migration should be done at no more than 10V/cm for 1 hour in order to reveal the *loxP* recombination products.
7. Take out the DNA 1000 agilent kit from 4°C about one hour before use to equilibrate reagents to room temperature.
8. Load chip with amplified PCR products according to the manufacturer protocol (see note 13).
9. Bioanalyzer software automatically performs DNA intensity peak calling and quantification. Typical results are described on figure 2A and 2B. Results are then expressed as a frequency of recombination by the following formula: (Amount of 1*loxP* + 3*loxP* products (in ng/ml))/(amount of 1*loxP*+2*loxP*+3*loxP* products (in ng/ml)).

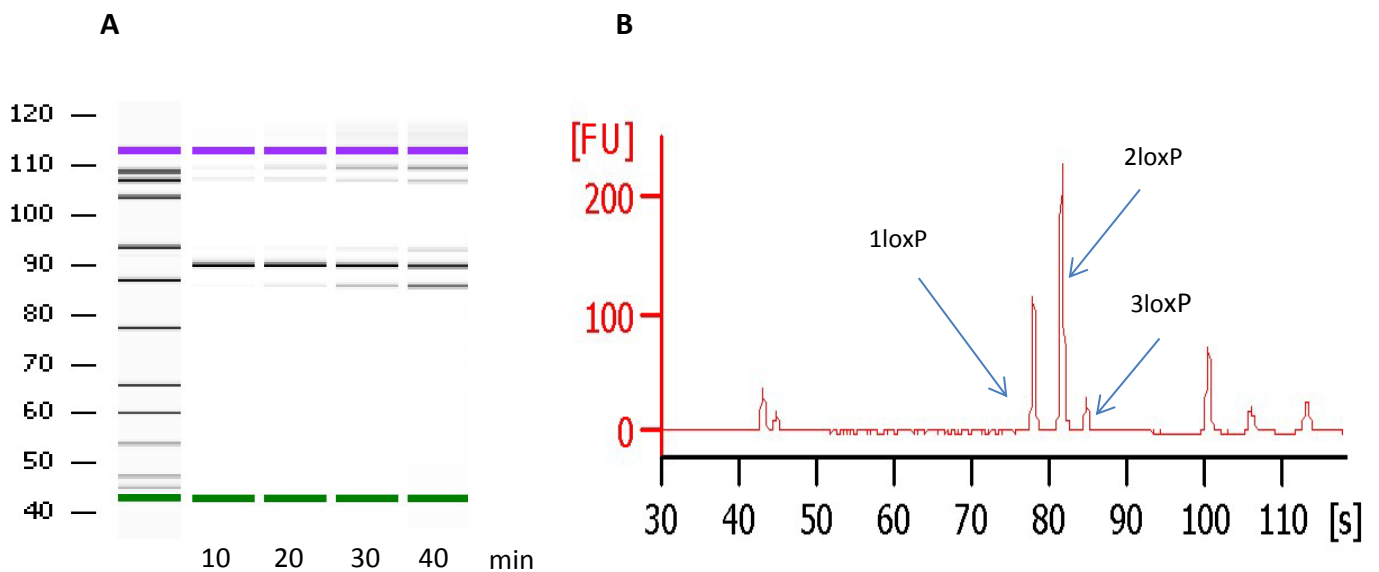
Notes

1. We noticed that many Taq polymerases failed to properly amplify two and three successive *loxP* sites. The best results were obtained with TaKaRa Ex Taq in Mg²⁺ plus buffer.
2. In some genetic backgrounds or growth conditions a high level of Cre recombination of the Laclox-rif cassette can be observed immediately after pCre transformation even in the absence of induction. If required, IPTG 20 µg/ml can be used to further repress Cre expression.
3. Strains with the pCre plasmid cannot be stored at -80°C. The pCre plasmid must be transformed fresh before each experiment.
4. The induction of pCre by arabinose in LB medium rapidly produces a high level of recombination. 100% of recombination products are observed in less than 10 min. We noticed that such a short time window does not allow obtaining highly reproducible results. We recommend performing the experiments in minimum media A or M9 supplemented with casaminoacids 0.2% and glycerol 0.2% or succinate 0.2% as a carbon source. Avoid glucose to assure the proper induction of the arabinose promoter.
5. A residual Cre recombination can be observed in some cases even in the absence of induction. This background recombination should be kept below 5% and must be subtracted from the recombination samples before analysis.

6. Growth conditions are critical for reproducibility. We recommend the systematic usage of 100ml erlenmeyers, with 8ml of culture for your experiment. Best results were obtained when growth was carried in a water bath shaker (250 rpm).
7. Timing is very important when adding the arabinose and the drug. Indeed, recombination occurs very quickly after arabinose induction and a bias can occur between samples if not timed properly.
8. The Cre induction length should be adjusted according to the growth conditions and the genetic background. Recombination frequency is linear as a function of time between 5% and 70%. We recommend using appropriate time points for your experiments depending on the chosen conditions. Recombination frequency is strongly affected by temperature. Intra molecular normalization is required for each temperature change.
9. When doing the experiment on plate, recombination rates are higher than with the PCR method. Time points for kinetics must be shorter than with the PCR method. We do not yet fully understand this observation. Our current hypothesis is that a significant part of the recombination reaction initiated during the induction period only gives rise to resolved recombination products after this induction period and therefore could remain undetected by the PCR method (Lesterlin et al., 2012).
10. When using the plate method, samples have to be diluted at 1/100e directly for each time point to stop the induction of Cre as quickly as possible. When using drugs affecting cell viability, make sure to calibrate dilutions for plating in order to have a countable amount of bacteria on plate
11. Variation between experiments can be observed when changing genomic extraction kits. We suggest you always use the same supplier for your experiments.
12. TBE 1X rather than TAE 0.5X should be used for the agarose gel verification for a better separation of the *loxP* products.
13. The DNA 1000 Agilent chip is sensitive. It is important to avoid the amplification of non-specific products by PCR. The T_m and the number of cycles of the PCR are important factors allowing optimization of this step. When using the piko PCR machine from Thermo Scientific, optimal T_m is 58°C and 28 cycles are enough. These parameters may need changing and optimization if using a different PCR machine.

**Figure 1**

A) The intermolecular loxP recombination reaction occurs between two close sister chromatids. The frequency of sister chromatid interactions can be assessed by a blue/white colony count or by a semi-quantitative PCR by amplifying the recombination products. **B)** The intramolecular loxP recombination frequency is measured by the loss of the rifampicin resistance gene by recombination of the two loxP sites spaced by 1kb.

**Figure 2**

A) Typical Electrophoresis run of a wild type strain upon Cre induction by arabinose. Cells were treated for 10, 20, 30 or 40 min with 0.1% arabinose and analyzed with an agilent bioanalyzer. **B)** Typical electropherogram of a wild type strain upon Cre induction by arabinose. The result after 40 min of Cre induction is shown. The results are shown as Fluorescence Units (FU) in function of the time of elution.

V. Résumé de thèse en français

Dans toutes les cellules, Eucaryotes, comme Procaryotes, le maintien de l'intégrité du génome est essentiel à la survie des cellules afin de correctement transmettre l'information génétique aux prochaines générations.

Lorsqu'une cassure survient sur une des molécules d'ADN, l'information génétique de la cellule peut être compromise, ce qui est extrêmement délétère, voire mortel. La réparation de telles cassures se fait principalement par recombinaison homologue (RH) entre la molécule lésée et son homologue intact (Pâques and Haber, 1999). *Escherichia coli* (*E.coli*) est un organisme modèle largement utilisé car il permet d'aborder des questions complexes et fondamentales tout en étant simple à manipuler. Son utilisation a d'ailleurs permis de grandes avancées en termes de recherche sur la réparation de l'ADN et les processus de recombinaison homologue. Chez *E.coli*, lorsqu'une cassure survient sur une des molécules d'ADN, RecA, la protéine centrale de la réponse SOS, se charge sur l'extrémité simple brin créée par l'hélicase RecBC et permet l'induction de la réponse SOS. La réponse SOS est un ensemble de plus de 100 protéines impliquées dans la réparation de l'ADN chez *E. coli* (Kreuzer, 2013). Ensemble, ces protéines vont orchestrer les différentes étapes de la réparation de la cassure, notamment via le processus de recombinaison homologue (RH). Ce processus est une étape essentielle à la réparation d'une cassure double brin survenant sur une des deux molécules d'ADN. En effet, la molécule d'ADN lésée se sert de sa chromatide sœur homologue comme matrice afin de réparer la lésion sans perdre d'information génétique, ce qui serait extrêmement délétère pour la survie de la cellule (Kowalczykowski et al., 1994). La proximité de la chromatide sœur homologue est alors essentielle à l'efficacité de la réaction de RH. En effet, une recherche extensive de la région homologue intacte semble chronophage et donc néfaste à l'efficacité de la réparation. Chez les Eucaryotes, des complexes multi-protéiques appelés Cohésines maintiennent les chromatides sœurs ensemble derrière la fourche de réplication. Certaines Cohésines telles que le complexe SMC5/SMC6 sont essentielles à la survie lorsque les cellules sont irradiées par des rayons γ et il a été montré que ces Cohésines pourraient être impliquées dans la réparation de l'ADN (Lehmann et al., 1995; Lindroos et al., 2006). Chez *E.coli*, qui ne possède pas de telles cohésines, une étape de cohésion des chromatides sœurs existe mais elle est assurée par des liens topologiques. En effet, lors d'un cycle de réplication normal, les

chromatides sœurs nouvellement répliquées restent liées entre elles, derrière la fourche de réplication, grâce à des liens topologiques appelés précatéranes. Ces précatéranes sont ensuite éliminées par la Topoisomérase IV permettant ainsi la ségrégation des deux chromatides (Wang et al., 2008). Ces précatéranes peuvent s'étendre sur une distance allant jusqu'à 1 Mpb derrière la fourche de réplication et définissent la phase dite de cohésion des chromatides sœurs.

Mon projet de thèse s'intéresse à cette étape de cohésion des chromatides sœurs pour la réparation de cassures survenant sur l'ADN et pour la recombinaison homologue chez *E.coli*. Elle s'articule autour de différents axes. i) La cohésion des chromatides sœurs chez *E.coli* est-elle modifiée lors de cassures à l'ADN ? ii) Quel est le rôle de la réponse SOS et quelles protéines de la réparation de l'ADN sont impliquées dans ce processus ? iii) L'altération des Topoisomérases influence-t-elle la réparation de l'ADN ? iv) Quel est l'impact des différentes drogues chimiothérapeutiques sur la cohésion des chromatides et la réparation de l'ADN ?

Grâce à une technique de biologie moléculaire reposant sur la recombinaison site spécifique entre sites *loxP* portés par deux chromatides sœurs homologues, j'ai montré que l'étape de cohésion des chromatides sœurs est prolongée lorsque l'ADN est endommagé par des lésions liées à la Mitomycine C (MMC). Lors d'un traitement par la MMC, la ségrégation des chromatides sœurs est inhibée de façon dépendante de la réponse SOS et j'ai montré plus particulièrement que la protéine RecN est largement impliquée dans ce processus. RecN appartient au régulon SOS et possède une structure de type SMC (Maintient de la Structure des Chromosomes). Chez *E. coli* il a été montré qu'elle est importante pour la survie à un traitement MMC, à une coupure site spécifique *IscI* et aux radiations ionisantes (Picksley et al., 1984). Elle n'a pas encore été purifiée chez *E.coli* mais chez *D. radiodurans* des études *in vitro* montrent que RecN serait capable de liguer deux extrémités d'ADN et présenterait une structure similaire à celles d'une Cohésine Eucaryote, bien qu'étant plus petite (Pellegrino et al., 2012). Chez *B.subtilis*, une fonction similaire a été décrite. RecN pourrait protéger les extrémités de la cassure double brin et les maintenir proches, facilitant l'accès de la cassure à RecA et aux autres protéines de la réparation de l'ADN (Sanchez et al., 2006). En revanche, j'ai montré que les cassures de type gap simple brin, comme celles créées par l'AZT ou l'hydroxyurée n'induisent pas une prolongation de l'étape de cohésion des chromatides sœurs

et leur réparation est indépendante de RecN. RecN semble donc être une protéine spécifique de la réparation des cassures double brin.

Il a été démontré que l'inhibition de la Topoisomérase IV prolonge la phase de cohésion des chromatides sœurs en inhibant leur ségrégation (Lesterlin et al., 2012). Dans le but de tester l'influence d'une inhibition de la Topo IV sur la cohésion des chromatides sœurs en réponse à des dommages à l'ADN, j'ai réalisé des expériences de recombinaison *loxP* et des tests de viabilité. J'ai observé que la perte de cohésion observée dans un mutant *recN* peut être compensée par une inhibition de la Topoisomérase IV, suggérant que l'action principale de RecN est de maintenir des liens entre les chromatides sœurs lors de la réparation d'une cassure. Le maintien de proximité entre chromatides sœurs, assuré par les liens topologiques, se traduit par une compensation de la perte de viabilité du mutant *recN*. Ceci suggère que maintenir les chromatides sœurs proches est favorable à la survie à un traitement à la MMC et donc à la réparation de l'ADN.

L'observation par microscopie confocale de la dynamique de foci fluorescents marqués sur le nucléoïde a permis de mettre en évidence un second rôle de RecN. En effet, lorsque deux chromatides sœurs ont déjà été ségrégués, elles sont capables de se réappairer après un traitement à la MMC. Ce réappariement est dépendant de RecN et s'accompagne d'une compaction globale des nucléoïdes, démontrant que RecN est capable d'empêcher la ségrégation de chromatides sœurs déjà cohésives mais aussi d'induire le rapprochement et le réappariement de chromatides sœurs préalablement ségrégués. Ce rapprochement pourrait néanmoins être la conséquence d'une compaction globale et aspécifique du nucléoïde en réponse à la MMC, semblable à l'action d'une condensine. Afin de distinguer entre une possible fonction de condensine ou de cohésine de RecN, j'ai inséré deux sites *parS* distincts, reconnus par deux fluorophores différents à une distance de 188 kb sur le même réplichore. Lorsque les cellules sont traitées à la MMC, la distance entre les deux foci fluorescents ne décroît pas, bien que l'on observe un rapprochement des chromatides sœurs ségrégués. Ceci semble suggérer que RecN est capable de médier le rapprochement des chromatides sœurs sans induire une compaction globale et aspécifique du nucléoïde, comme c'est le cas avec certains antibiotiques comme le chloramphénicol.

Un RNAseq mené dans une souche sauvage et une souche *recN* a permis de mettre en évidence une influence de RecN sur l'induction de la réponse SOS. En effet, en l'absence de RecN, l'induction de nombreux gènes de la réponse SOS est réduite. Cette réduction est spécifique des gènes de la réponse SOS étant donné que l'expression des autres gènes n'est pas affectée par la délétion de *recN*. L'influence de RecN sur la réponse SOS pourrait être liée à une influence de RecN sur RecA étant donné que RecA est la protéine centrale d'induction de la réponse SOS. En 2013, le groupe de Hishida a montré une potentielle interaction entre RecN et RecA (Keyamura et al., 2013). Afin d'approfondir cette observation j'ai décidé de regarder la dynamique et la formation des foci RecA en microscopie à haute résolution dans un mutant *recN*. Dans une souche sauvage, RecA forme plusieurs foci sur l'ADN lorsque les cellules sont traitées à la MMC. En revanche, dans un mutant *recN*, RecA forme des structures de type « bundle » décrites en 2013 par Lesterlin *et al.* Ce type de filaments de RecA se forme dans un contexte particulier, lorsqu'une cassure double brin survient sur une chromatide sœur déjà ségréguée, dans le but de la réappairier avec son homologue. La formation de ces filaments en l'absence de RecN pourrait résulter d'une recherche de l'homologue intacte, étant donné que les deux chromatides ne sont plus maintenues proches par RecN. D'autres expériences ont permis de conclure que RecN nécessite RecA pour se charger sur l'ADN, définissant RecA comme un loader de RecN.

L'ensemble de ces travaux ont mené à une publication dans Nature Communications en 2017 (Vickridge et al., 2017).

La recherche d'éventuels partenaires et l'étude d'aspects plus mécanistiques sur le chargement de RecN ont fait l'objet de la suite de ma thèse.

Afin d'aborder ces questions, différentes approches ont été mises en œuvre. La surexpression de différents gènes dans un mutant *recN*, et la sélection des clones capables de pousser après un traitement à la MMC a permis l'identification de plusieurs gènes dont la surexpression pourrait compenser la perte de viabilité de *recN*. Une étude plus poussée de ces gènes, (*sbmC*, *xthA* ou encore *dacD*) n'ont cependant pas permis de mettre en évidence une potentielle interaction ou synergie avec RecN.

Deux approches de biochimie différentes, la co-immunoprécipitation avec RecN et l'IPOND (immunoprecipitation of proteins on nascent DNA) ont révélé une possible interaction entre

RecN et UvrA, UvrB, UvrC et RadA. Les protéines Uvr font partie de la voie de réparation par NER (réparation par excision de nucléotides), impliquée lors de dommages par MMC pour éliminer les liens convalents entre les deux molécules d'ADN créés par la MMC. RadA est une protéine impliquée dans le processus de recombinaison homologue. Il a été montré que RadA est capable, même en l'absence de RecA, de promouvoir l'extension de branche lors de la recombinaison homologue (Cooper and Lovett, 2016). Des expériences préliminaires ont montré que la cohésion entre chromatides sœurs révélée par recombinaison *loxP* est réduite dans un mutant *uvrA*. Le double mutant *uvrA recN* possède un phénotype semblable à celui du simple mutant *uvrA* suggérant que RecN agirait principalement via un mécanisme lié à UvrA. Lors de l'excision de MMC par la voie du NER, il arrive que UvrC, l'endonuclease qui excise la lésion, fasse une double incision, créant ainsi une cassure double brin (Peng et al., 2010; Weng et al., 2010). Il est possible d'envisager que RecN soit recruté à ces cassures doubles brins, pour éventuellement maintenir les extrémités de la cassure ensemble et favoriser la réparation par recombinaison homologue. Ces résultats, encore préliminaire devront faire l'objet d'une étude plus poussée.

L'ensemble de mes travaux de thèse a permis de démontrer l'importance de la cohésion des chromatides sœurs pour la réparation de l'ADN chez *E. coli*. Plus particulièrement, j'ai montré l'importance de RecN, une protéine de type SMC, induite par la réponse SOS. RecN empêche la ségrégation des chromatides sœurs lors de cassures à l'ADN et permet un réarrangement global des nucleoids endommagés. RecN est une protéine très conservée chez les Procaryotes ce qui renforce son importance pour la cohésion des chromatides sœurs et la réparation de l'ADN, possiblement en favorisant la recherche de la séquence homologue. Les résultats complémentaires obtenus soulèvent des questions intéressantes et des mécanismes complexes qui feront l'objet, je n'en doute pas, de nouvelles recherches.

VI. Bibliography

- Aertsen, A., Van Houdt, R., Vanoirbeek, K., and Michiels, C.W. (2004). An SOS response induced by high pressure in *Escherichia coli*. *J. Bacteriol.* *186*, 6133–6141.
- Anderson, D.G., and Kowalczykowski, S.C. (1997). The recombination hot spot *chi* is a regulatory element that switches the polarity of DNA degradation by the RecBCD enzyme. *Genes Dev.* *11*, 571–581.
- Ando, T., and Skolnick, J. (2014). Sliding of Proteins Non-specifically Bound to DNA: Brownian Dynamics Studies with Coarse-Grained Protein and DNA Models. *PLoS Comput. Biol.* *10*.
- Arenson, T.A., Tsodikov, O.V., and Cox, M.M. (1999). Quantitative analysis of the kinetics of end-dependent disassembly of RecA filaments from ssDNA. *J. Mol. Biol.* *288*, 391–401.
- Au, K.G., Welsh, K., and Modrich, P. (1992). Initiation of methyl-directed mismatch repair. *J. Biol. Chem.* *267*, 12142–12148.
- Badrinarayanan, A., Le, T.B.K., and Laub, M.T. (2015). Rapid pairing and re-segregation of distant homologous loci enables double-strand break repair in bacteria. *J. Cell Biol.* *210*, 385–400.
- Baharoglu, Z., and Mazel, D. (2014). SOS, the formidable strategy of bacteria against aggressions. *FEMS Microbiol. Rev.* *38*, 1126–1145.
- Bailone, A., Bäckman, A., Sommer, S., Célérier, J., Bagdasarian, M.M., Bagdasarian, M., and Devoret, R. (1988). PsiB polypeptide prevents activation of RecA protein in *Escherichia coli*. *Mol. Gen. Genet. MGG* *214*, 389–395.
- Balakrishnan, L., and Bambara, R.A. (2013). Okazaki fragment metabolism. *Cold Spring Harb. Perspect. Biol.* *5*.
- Banda, S., Cao, N., and Tse-Dinh, Y.-C. (2017). Distinct Mechanism Evolved for Mycobacterial RNA Polymerase and Topoisomerase I Protein-Protein Interaction. *J. Mol. Biol.* *429*, 2931–2942.
- Barker, S., Weinfeld, M., and Murray, D. (2005). DNA-protein crosslinks: their induction, repair, and biological consequences. *Mutat. Res.* *589*, 111–135.
- Bates, D., and Kleckner, N. (2005). Chromosome and replisome dynamics in *E. coli*: loss of sister cohesion triggers global chromosome movement and mediates chromosome segregation. *Cell* *121*, 899–911.
- Beam, C.E., Saveson, C.J., and Lovett, S.T. (2002). Role for *radA/sms* in recombination intermediate processing in *Escherichia coli*. *J. Bacteriol.* *184*, 6836–6844.
- Bennett, R.J., Dunderdale, H.J., and West, S.C. (1993). Resolution of Holliday junctions by RuvC resolvase: cleavage specificity and DNA distortion. *Cell* *74*, 1021–1031.
- Berg, O.G., and von Hippel, P.H. (1988). Selection of DNA binding sites by regulatory proteins. II. The binding specificity of cyclic AMP receptor protein to recognition sites. *J. Mol. Biol.* *200*, 709–723.

- Berghuis, B.A., Raducanu, V.-S., Elshenawy, M.M., Jergic, S., Depken, M., Dixon, N.E., Hamdan, S.M., and Dekker, N.H. (2018). What is all this fuss about Tus? Comparison of recent findings from biophysical and biochemical experiments. *Crit. Rev. Biochem. Mol. Biol.* *53*, 49–63.
- Bermejo, R., Branzei, D., and Foiani, M. (2008). Cohesion by topology: sister chromatids interlocked by DNA. *Genes Dev.* *22*, 2297–2301.
- Bernhardt, T.G., and de Boer, P.A.J. (2005). SlmA, a nucleoid-associated, FtsZ binding protein required for blocking septal ring assembly over Chromosomes in *E. coli*. *Mol. Cell* *18*, 555–564.
- Bichara, M., Meier, M., Wagner, J., Cordonnier, A., and Lambert, I.B. (2011). Postreplication repair mechanisms in the presence of DNA adducts in *Escherichia coli*. *Mutat. Res.* *727*, 104–122.
- Bintu, L., Kopaczynska, M., Hodges, C., Lubkowska, L., Kashlev, M., and Bustamante, C. (2011). The elongation rate of RNA polymerase determines the fate of transcribed nucleosomes. *Nat. Struct. Mol. Biol.* *18*, 1394–1399.
- Bird, R.E., Louarn, J., Martuscelli, J., and Caro, L. (1972). Origin and sequence of chromosome replication in *Escherichia coli*. *J. Mol. Biol.* *70*, 549–566.
- Bliska, J.B., and Cozzarelli, N.R. (1987). Use of site-specific recombination as a probe of DNA structure and metabolism in vivo. *J. Mol. Biol.* *194*, 205–218.
- Breen, A.P., and Murphy, J.A. (1995). Reactions of oxyl radicals with DNA. *Free Radic. Biol. Med.* *18*, 1033–1077.
- Brent, R., and Ptashne, M. (1981). Mechanism of action of the *lexA* gene product. *Proc. Natl. Acad. Sci. U. S. A.* *78*, 4204–4208.
- Brutlag, D., and Kornberg, A. (1972). Enzymatic synthesis of deoxyribonucleic acid. 36. A proofreading function for the 3' leads to 5' exonuclease activity in deoxyribonucleic acid polymerases. *J. Biol. Chem.* *247*, 241–248.
- Burgess, S.M., and Kleckner, N. (1999). Collisions between yeast chromosomal loci in vivo are governed by three layers of organization. *Genes Dev.* *13*, 1871–1883.
- Campbell, J.L., and Kleckner, N. (1990). *E. coli* *oriC* and the *dnaA* gene promoter are sequestered from dam methyltransferase following the passage of the chromosomal replication fork. *Cell* *62*, 967–979.
- Cardenas, P.P., Gándara, C., and Alonso, J.C. (2014). DNA double strand break end-processing and RecA induce RecN expression levels in *Bacillus subtilis*. *DNA Repair* *14*, 1–8.
- Cebrián, J., Castán, A., Martínez, V., Kadomatsu-Hermosa, M.J., Parra, C., Fernández-Nestosa, M.J., Schaerer, C., Hernández, P., Krimer, D.B., and Schwartzman, J.B. (2015). Direct Evidence for the Formation of Precatenanes during DNA Replication. *J. Biol. Chem.* *290*, 13725–13735.
- Centore, R.C., Lestini, R., and Sandler, S.J. (2008). XthA (Exonuclease III) regulates loading of RecA onto DNA substrates in log phase *Escherichia coli* cells. *Mol. Microbiol.* *67*, 88–101.
- Chae, Y.K., Anker, J.F., Carneiro, B.A., Chandra, S., Kaplan, J., Kalyan, A., Santa-Maria, C.A., Plataniias, L.C., and Giles, F.J. (2016). Genomic landscape of DNA repair genes in cancer. *Oncotarget* *7*, 23312–23321.

- Champoux, J.J., Young, L.S., and Been, M.D. (1979). Studies on the regulation and specificity of the DNA-untwisting enzyme. *Cold Spring Harb. Symp. Quant. Biol.* *43 Pt 1*, 53–58.
- Chatterjee, N., and Walker, G.C. (2017). Mechanisms of DNA damage, repair, and mutagenesis. *Environ. Mol. Mutagen.* *58*, 235–263.
- Chatterji, M., Sengupta, S., and Nagaraja, V. (2003). Chromosomally encoded gyrase inhibitor Gyrl protects *Escherichia coli* against DNA-damaging agents. *Arch. Microbiol.* *180*, 339–346.
- Chen, Z., Yang, H., and Pavletich, N.P. (2008). Mechanism of homologous recombination from the RecA-ssDNA/dsDNA structures. *Nature* *453*, 489–484.
- Churchill, J.J., Anderson, D.G., and Kowalczykowski, S.C. (1999). The RecBC enzyme loads RecA protein onto ssDNA asymmetrically and independently of χ , resulting in constitutive recombination activation. *Genes Dev.* *13*, 901–911.
- Ciosk, R., Shirayama, M., Shevchenko, A., Tanaka, T., Toth, A., Shevchenko, A., and Nasmyth, K. (2000). Cohesin's binding to chromosomes depends on a separate complex consisting of Scc2 and Scc4 proteins. *Mol. Cell* *5*, 243–254.
- Cobbe, N., and Heck, M.M. (2000). Review: SMCs in the world of chromosome biology- from prokaryotes to higher eukaryotes. *J. Struct. Biol.* *129*, 123–143.
- Cole, R.S. (1973). Repair of DNA containing interstrand crosslinks in *Escherichia coli*: sequential excision and recombination. *Proc. Natl. Acad. Sci. U. S. A.* *70*, 1064–1068.
- Cooper, D.L., and Lovett, S.T. (2011). Toxicity and tolerance mechanisms for azidothymidine, a replication gap-promoting agent, in *Escherichia coli*. *DNA Repair* *10*, 260–270.
- Cooper, D.L., and Lovett, S.T. (2016). Recombinational branch migration by the RadA/Sms paralog of RecA in *Escherichia coli*. *ELife* *5*.
- Cooper, D.N., and Youssoufian, H. (1988). The CpG dinucleotide and human genetic disease. *Hum. Genet.* *78*, 151–155.
- Cooper, D.L., Lahue, R.S., and Modrich, P. (1993). Methyl-directed mismatch repair is bidirectional. *J. Biol. Chem.* *268*, 11823–11829.
- Cooper, D.L., Boyle, D.C., and Lovett, S.T. (2015). Genetic analysis of *Escherichia coli* RadA: functional motifs and genetic interactions. *Mol. Microbiol.* *95*, 769–779.
- Courcelle, J., Khodursky, A., Peter, B., Brown, P.O., and Hanawalt, P.C. (2001). Comparative gene expression profiles following UV exposure in wild-type and SOS-deficient *Escherichia coli*. *Genetics* *158*, 41–64.
- Cunningham, R.P., Saporito, S.M., Spitzer, S.G., and Weiss, B. (1986). Endonuclease IV (nfo) mutant of *Escherichia coli*. *J. Bacteriol.* *168*, 1120–1127.
- Datsenko, K.A., and Wanner, B.L. (2000). One-step inactivation of chromosomal genes in *Escherichia coli* K-12 using PCR products. *Proc. Natl. Acad. Sci. U. S. A.* *97*, 6640–6645.
- Davies, B.W., Kohanski, M.A., Simmons, L.A., Winkler, J.A., Collins, J.J., and Walker, G.C. (2009). Hydroxyurea induces hydroxyl radical-mediated cell death in *Escherichia coli*. *Mol. Cell* *36*, 845–860.

De Mot, R., Schoofs, G., and Vanderleyden, J. (1994). A putative regulatory gene downstream of *recA* is conserved in gram-negative and gram-positive bacteria. *Nucleic Acids Res.* *22*, 1313–1314.

De Vlaminck, I., van Loenhout, M.T.J., Zweifel, L., den Blanken, J., Hooning, K., Hage, S., Kerssemakers, J., and Dekker, C. (2012). Mechanism of homology recognition in DNA recombination from dual-molecule experiments. *Mol. Cell* *46*, 616–624.

Deng, S., Stein, R.A., and Higgins, N.P. (2004). Transcription-induced barriers to supercoil diffusion in the *Salmonella typhimurium* chromosome. *Proc. Natl. Acad. Sci. U. S. A.* *101*, 3398–3403.

Dianov, G., and Lindahl, T. (1994). Reconstitution of the DNA base excision-repair pathway. *Curr. Biol. CB* *4*, 1069–1076.

Dillingham, M.S., Spies, M., and Kowalczykowski, S.C. (2003). RecBCD enzyme is a bipolar DNA helicase. *Nature* *423*, 893–897.

Dion, V., Kalck, V., Horigome, C., Towbin, B.D., and Gasser, S.M. (2012). Increased mobility of double-strand breaks requires Mec1, Rad9 and the homologous recombination machinery. *Nat. Cell Biol.* *14*, 502–509.

Drake, J.W., Charlesworth, B., Charlesworth, D., and Crow, J.F. (1998). Rates of spontaneous mutation. *Genetics* *148*, 1667–1686.

Drees, J.C., Lusetti, S.L., Chitteni-Pattu, S., Inman, R.B., and Cox, M.M. (2004). A RecA filament capping mechanism for RecX protein. *Mol. Cell* *15*, 789–798.

Drees, J.C., Chitteni-Pattu, S., McCaslin, D.R., Inman, R.B., and Cox, M.M. (2006). Inhibition of RecA protein function by the RdgC protein from *Escherichia coli*. *J. Biol. Chem.* *281*, 4708–4717.

Drolet, M., Phoenix, P., Menzel, R., Massé, E., Liu, L.F., and Crouch, R.J. (1995). Overexpression of RNase H partially complements the growth defect of an *Escherichia coli* delta *topA* mutant: R-loop formation is a major problem in the absence of DNA topoisomerase I. *Proc. Natl. Acad. Sci. U. S. A.* *92*, 3526–3530.

Dubuisson, J.G., Dyess, D.L., and Gaubatz, J.W. (2002). Resveratrol modulates human mammary epithelial cell O-acetyltransferase, sulfotransferase, and kinase activation of the heterocyclic amine carcinogen N-hydroxy-PhIP. *Cancer Lett.* *182*, 27–32.

Dungrawala, H., and Cortez, D. (2015). Purification of proteins on newly synthesized DNA using iPOND. *Methods Mol. Biol. Clifton NJ* *1228*, 123–131.

Egelman, E.H., and Stasiak, A. (1986). Structure of helical RecA-DNA complexes. Complexes formed in the presence of ATP-gamma-S or ATP. *J. Mol. Biol.* *191*, 677–697.

Espeli, O., Levine, C., Hassing, H., and Marians, K.J. (2003). Temporal regulation of topoisomerase IV activity in *E. coli*. *Mol. Cell* *11*, 189–201.

Espéli, O., Borne, R., Dupaigne, P., Thiel, A., Gigant, E., Mercier, R., and Boccard, F. (2012). A MatP-divisome interaction coordinates chromosome segregation with cell division in *E. coli*. *EMBO J.* *31*, 3198–3211.

Espeli Olivier, Mercier Romain, and Boccard Frédéric (2008). DNA dynamics vary according to macrodomain topography in the *E. coli* chromosome. *Mol. Microbiol.* *68*, 1418–1427.

- Ferreira, E., Giménez, R., Cañas, M.A., Aguilera, L., Aguilar, J., Badia, J., and Baldomà, L. (2015). Glyceraldehyde-3-phosphate dehydrogenase is required for efficient repair of cytotoxic DNA lesions in *Escherichia coli*. *Int. J. Biochem. Cell Biol.* *60*, 202–212.
- Fersht, A.R., and Knill-Jones, J.W. (1983). Fidelity of replication of bacteriophage phi X174 DNA in vitro and in vivo. *J. Mol. Biol.* *165*, 633–654.
- Finch, P.W., Chambers, P., and Emmerson, P.T. (1985). Identification of the *Escherichia coli* recN gene product as a major SOS protein. *J. Bacteriol.* *164*, 653–658.
- Flores, M.-J., Bierne, H., Ehrlich, S.D., and Michel, B. (2001). Impairment of lagging strand synthesis triggers the formation of a RuvABC substrate at replication forks. *EMBO J.* *20*, 619–629.
- Flores, M.J., Bidnenko, V., and Michel, B. (2004). The DNA repair helicase UvrD is essential for replication fork reversal in replication mutants. *EMBO Rep.* *5*, 983–988.
- Forget, A.L., and Kowalczykowski, S.C. (2012). Single-molecule imaging of DNA pairing by RecA reveals a three-dimensional homology search. *Nature* *482*, 423–427.
- Fuchs, R.P. (2016). Tolerance of lesions in *E. coli*: Chronological competition between Translesion Synthesis and Damage Avoidance. *DNA Repair* *44*, 51–58.
- Fuchs, R.P., and Fujii, S. (2013). Translesion DNA synthesis and mutagenesis in prokaryotes. *Cold Spring Harb. Perspect. Biol.* *5*, a012682.
- Fujii, S., Isogawa, A., and Fuchs, R.P. (2006). RecFOR proteins are essential for Pol V-mediated translesion synthesis and mutagenesis. *EMBO J.* *25*, 5754–5763.
- Funayama, T., Narumi, I., Kikuchi, M., Kitayama, S., Watanabe, H., and Yamamoto, K. (1999). Identification and disruption analysis of the recN gene in the extremely radioresistant bacterium *Deinococcus radiodurans*. *Mutat. Res.* *435*, 151–161.
- Galletto, R., Amitani, I., Baskin, R.J., and Kowalczykowski, S.C. (2006). Direct observation of individual RecA filaments assembling on single DNA molecules. *Nature* *443*, 875–878.
- Gellert, M., Mizuuchi, K., O’Dea, M.H., and Nash, H.A. (1976). DNA gyrase: an enzyme that introduces superhelical turns into DNA. *Proc. Natl. Acad. Sci. U. S. A.* *73*, 3872–3876.
- Giese, K.C., Michalowski, C.B., and Little, J.W. (2008). RecA-dependent cleavage of LexA dimers. *J. Mol. Biol.* *377*, 148–161.
- Gligoris, T.G., Scheinost, J.C., Bürmann, F., Petela, N., Chan, K.-L., Uluocak, P., Beckouët, F., Gruber, S., Nasmyth, K., and Löwe, J. (2014). Closing the cohesin ring: structure and function of its Smc3-kleisin interface. *Science* *346*, 963–967.
- Godoy, V.G., Jarosz, D.F., Walker, F.L., Simmons, L.A., and Walker, G.C. (2006). Y-family DNA polymerases respond to DNA damage-independent inhibition of replication fork progression. *EMBO J.* *25*, 868–879.
- Gossard, F., and Verly, W.G. (1978). Properties of the main endonuclease specific for apurinic sites of *Escherichia coli* (endonuclease VI). Mechanism of apurinic site excision from DNA. *Eur. J. Biochem.* *82*, 321–332.

- Gotta, S.L., Miller, O.L., and French, S.L. (1991). rRNA transcription rate in *Escherichia coli*. *J. Bacteriol.* *173*, 6647–6649.
- Graham, J.E., Marians, K.J., and Kowalczykowski, S.C. (2017). Independent and Stochastic Action of DNA Polymerases in the Replisome. *Cell* *169*, 1201–1213.e17.
- Graumann, P.L., and Knust, T. (2009). Dynamics of the bacterial SMC complex and SMC-like proteins involved in DNA repair. *Chromosome Res. Int. J. Mol. Supramol. Evol. Asp. Chromosome Biol.* *17*, 265–275.
- Grilley, M., Griffith, J., and Modrich, P. (1993). Bidirectional excision in methyl-directed mismatch repair. *J. Biol. Chem.* *268*, 11830–11837.
- Gruber, S., Haering, C.H., and Nasmyth, K. (2003). Chromosomal Cohesin Forms a Ring. *Cell* *112*, 765–777.
- Gruber, S., Arumugam, P., Katou, Y., Kuglitsch, D., Helmhart, W., Shirahige, K., and Nasmyth, K. (2006). Evidence that loading of cohesin onto chromosomes involves opening of its SMC hinge. *Cell* *127*, 523–537.
- Haering, C.H., Löwe, J., Hochwagen, A., and Nasmyth, K. (2002). Molecular architecture of SMC proteins and the yeast cohesin complex. *Mol. Cell* *9*, 773–788.
- Hanada, K., Budzowska, M., Modesti, M., Maas, A., Wyman, C., Essers, J., and Kanaar, R. (2006). The structure-specific endonuclease Mus81-Eme1 promotes conversion of interstrand DNA crosslinks into double-strand breaks. *EMBO J.* *25*, 4921–4932.
- Handa, N., Yang, L., Dillingham, M.S., Kobayashi, I., Wigley, D.B., and Kowalczykowski, S.C. (2012). Molecular determinants responsible for recognition of the single-stranded DNA regulatory sequence, χ , by RecBCD enzyme. *Proc. Natl. Acad. Sci.* *109*, 8901–8906.
- Hegde, M.L., Theriot, C.A., Das, A., Hegde, P.M., Guo, Z., Gary, R.K., Hazra, T.K., Shen, B., and Mitra, S. (2008). Physical and functional interaction between human oxidized base-specific DNA glycosylase NEIL1 and flap endonuclease 1. *J. Biol. Chem.* *283*, 27028–27037.
- Heller, R.C., and Marians, K.J. (2006). Replication fork reactivation downstream of a blocked nascent leading strand. *Nature* *439*, 557–562.
- Henestrosa, A.R.F. de, Ogi, T., Aoyagi, S., Chafin, D., Hayes, J.J., Ohmori, H., and Woodgate, R. (2000). Identification of additional genes belonging to the LexA regulon in *Escherichia coli*. *Mol. Microbiol.* *35*, 1560–1572.
- Henle, E.S., and Linn, S. (1997). Formation, prevention, and repair of DNA damage by iron/hydrogen peroxide. *J. Biol. Chem.* *272*, 19095–19098.
- Herbert, S., Brion, A., Arbona, J.-M., Lelek, M., Veillet, A., Lelandais, B., Parmar, J., Fernández, F.G., Almayrac, E., Khalil, Y., et al. (2017). Chromatin stiffening underlies enhanced locus mobility after DNA damage in budding yeast. *EMBO J.* *36*, 2595–2608.
- Hiasa, H., Yousef, D.O., and Marians, K.J. (1996). DNA strand cleavage is required for replication fork arrest by a frozen topoisomerase-quinolone-DNA ternary complex. *J. Biol. Chem.* *271*, 26424–26429.
- Hill, T.M. (1992). Arrest of bacterial DNA replication. *Annu. Rev. Microbiol.* *46*, 603–633.

- Hill, T.M., Henson, J.M., and Kuempel, P.L. (1987). The terminus region of the *Escherichia coli* chromosome contains two separate loci that exhibit polar inhibition of replication. *Proc. Natl. Acad. Sci. U. S. A.* *84*, 1754–1758.
- Hirose, S., Hiraga, S., and Okazaki, T. (1983). Initiation site of deoxyribonucleotide polymerization at the replication origin of the *Escherichia coli* chromosome. *Mol. Gen. Genet.* *MGG 189*, 422–431.
- Horii, Z., and Clark, A.J. (1973). Genetic analysis of the *recF* pathway to genetic recombination in *Escherichia coli* K12: isolation and characterization of mutants. *J. Mol. Biol.* *80*, 327–344.
- Horii, T., Ogawa, T., Nakatani, T., Hase, T., Matsubara, H., and Ogawa, H. (1981). Regulation of SOS functions: purification of *E. coli* LexA protein and determination of its specific site cleaved by the RecA protein. *Cell* *27*, 515–522.
- Horiuchi, T., Fujimura, Y., Nishitani, H., Kobayashi, T., and Hidaka, M. (1994). The DNA replication fork blocked at the Ter site may be an entrance for the RecBCD enzyme into duplex DNA. *J. Bacteriol.* *176*, 4656–4663.
- Howard, M.T., Neece, S.H., Matson, S.W., and Kreuzer, K.N. (1994). Disruption of a topoisomerase-DNA cleavage complex by a DNA helicase. *Proc. Natl. Acad. Sci. U. S. A.* *91*, 12031–12035.
- Hu, T., Grosberg, A.Y., and Shklovskii, B.I. (2006). How Proteins Search for Their Specific Sites on DNA: The Role of DNA Conformation. *Biophys. J.* *90*, 2731–2744.
- Huisman, O., D’Ari, R., and Gottesman, S. (1984). Cell-division control in *Escherichia coli*: specific induction of the SOS function SfiA protein is sufficient to block septation. *Proc. Natl. Acad. Sci. U. S. A.* *81*, 4490–4494.
- Inoue, J., Honda, M., Ikawa, S., Shibata, T., and Mikawa, T. (2008). The process of displacing the single-stranded DNA-binding protein from single-stranded DNA by RecO and RecR proteins. *Nucleic Acids Res.* *36*, 94–109.
- Ivanov, D., and Nasmyth, K. (2005). A topological interaction between cohesin rings and a circular minichromosome. *Cell* *122*, 849–860.
- Jain, S.K., Cox, M.M., and Inman, R.B. (1994). On the role of ATP hydrolysis in RecA protein-mediated DNA strand exchange. III. Unidirectional branch migration and extensive hybrid DNA formation. *J. Biol. Chem.* *269*, 20653–20661.
- Jameson, K.H., and Wilkinson, A.J. (2017). Control of Initiation of DNA Replication in *Bacillus subtilis* and *Escherichia coli*. *Genes* *8*.
- Jia, L., Kropachev, K., Ding, S., Van Houten, B., Geacintov, N.E., and Broyde, S. (2009). Exploring damage recognition models in prokaryotic nucleotide excision repair with a benzo[a]pyrene-derived lesion in UvrB. *Biochemistry (Mosc.)* *48*, 8948–8957.
- Joshi, M.C., Bourniquel, A., Fisher, J., Ho, B.T., Magnan, D., Kleckner, N., and Bates, D. (2011). *Escherichia coli* sister chromosome separation includes an abrupt global transition with concomitant release of late-splitting intersister snaps. *Proc. Natl. Acad. Sci. U. S. A.* *108*, 2765–2770.
- Joshi, M.C., Magnan, D., Montminy, T.P., Lies, M., Stepankiw, N., and Bates, D. (2013). Regulation of sister chromosome cohesion by the replication fork tracking protein SeqA. *PLoS Genet.* *9*, e1003673.

- Kaguni, J.M. (2011). Replication initiation at the Escherichia coli chromosomal origin. *Curr. Opin. Chem. Biol.* *15*, 606–613.
- Kamada, K., Horiuchi, T., Ohsumi, K., Shimamoto, N., and Morikawa, K. (1996). Structure of a replication-terminator protein complexed with DNA. *Nature* *383*, 598–603.
- Kato, J., Nishimura, Y., Imamura, R., Niki, H., Hiraga, S., and Suzuki, H. (1990). New topoisomerase essential for chromosome segregation in E. coli. *Cell* *63*, 393–404.
- Kegel, A., and Sjögren, C. (2010). The Smc5/6 Complex: More Than Repair? *Cold Spring Harb. Symp. Quant. Biol.* *75*, 179–187.
- Keyamura, K., Sakaguchi, C., Kubota, Y., Niki, H., and Hishida, T. (2013). RecA protein recruits structural maintenance of chromosomes (SMC)-like RecN protein to DNA double-strand breaks. *J. Biol. Chem.* *288*, 29229–29237.
- Khodursky, A.B., Peter, B.J., Schmid, M.B., DeRisi, J., Botstein, D., Brown, P.O., and Cozzarelli, N.R. (2000). Analysis of topoisomerase function in bacterial replication fork movement: Use of DNA microarrays. *Proc. Natl. Acad. Sci. U. S. A.* *97*, 9419–9424.
- Kidane, D., Sanchez, H., Alonso, J.C., and Graumann, P.L. (2004). Visualization of DNA double-strand break repair in live bacteria reveals dynamic recruitment of Bacillus subtilis RecF, RecO and RecN proteins to distinct sites on the nucleoids. *Mol. Microbiol.* *52*, 1627–1639.
- Kitagawa, R., Ozaki, T., Moriya, S., and Ogawa, T. (1998). Negative control of replication initiation by a novel chromosomal locus exhibiting exceptional affinity for Escherichia coli DnaA protein. *Genes Dev.* *12*, 3032–3043.
- Knight, K.L., Aoki, K.H., Ujita, E.L., and McEntee, K. (1984). Identification of the amino acid substitutions in two mutant forms of the recA protein from Escherichia coli: recA441 and recA629. *J. Biol. Chem.* *259*, 11279–11283.
- Kogoma, T. (1997). Stable DNA replication: interplay between DNA replication, homologous recombination, and transcription. *Microbiol. Mol. Biol. Rev.* *MMBR* *61*, 212–238.
- Kogoma, T., Cadwell, G.W., Barnard, K.G., and Asai, T. (1996). The DNA replication priming protein, PriA, is required for homologous recombination and double-strand break repair. *J. Bacteriol.* *178*, 1258–1264.
- Kosa, J.L., Zdraveski, Z.Z., Currier, S., Marinus, M.G., and Essigmann, J.M. (2004). RecN and RecG are required for Escherichia coli survival of Bleomycin-induced damage. *Mutat. Res.* *554*, 149–157.
- Koszul, R., Kim, K.P., Prentiss, M., Kleckner, N., and Kameoka, S. (2008). Meiotic chromosomes move by linkage to dynamic actin cables with transduction of force through the nuclear envelope. *Cell* *133*, 1188–1201.
- Koszul, R., Kameoka, S., and Weiner, B.M. (2009). Real-time imaging of meiotic chromosomes in Saccharomyces cerevisiae. *Methods Mol. Biol. Clifton NJ* *558*, 81–89.
- Kowalczykowski, S.C., Dixon, D.A., Eggleston, A.K., Lauder, S.D., and Rehrauer, W.M. (1994). Biochemistry of homologous recombination in Escherichia coli. *Microbiol. Rev.* *58*, 401–465.

- Kozubek, S., Ogievetskaya, M.M., Krasavin, E.A., Drasil, V., and Soska, J. (1990). Investigation of the SOS response of *Escherichia coli* after gamma-irradiation by means of the SOS chromotest. *Mutat. Res.* *230*, 1–7.
- Kreuzer, K.N. (2013). DNA damage responses in prokaryotes: regulating gene expression, modulating growth patterns, and manipulating replication forks. *Cold Spring Harb. Perspect. Biol.* *5*, a012674.
- Kuraoka, I., Kobertz, W.R., Ariza, R.R., Biggerstaff, M., Essigmann, J.M., and Wood, R.D. (2000). Repair of an interstrand DNA cross-link initiated by ERCC1-XPF repair/recombination nuclease. *J. Biol. Chem.* *275*, 26632–26636.
- Kuzminov, A. (1995). Collapse and repair of replication forks in *Escherichia coli*. *Mol. Microbiol.* *16*, 373–384.
- Kuzminov, A. (2001). Single-strand interruptions in replicating chromosomes cause double-strand breaks. *Proc. Natl. Acad. Sci. U. S. A.* *98*, 8241–8246.
- Lahue, R.S., Au, K.G., and Modrich, P. (1989). DNA mismatch correction in a defined system. *Science* *245*, 160–164.
- Lal, A., Dhar, A., Trostel, A., Kouzine, F., Seshasayee, A.S.N., and Adhya, S. (2016). Genome scale patterns of supercoiling in a bacterial chromosome. *Nat. Commun.* *7*.
- Lee, A.J., Sharma, R., Hobbs, J.K., and Wälti, C. (2017). Cooperative RecA clustering: the key to efficient homology searching. *Nucleic Acids Res.* *45*, 11743–11751.
- Lehmann, A.R., Walicka, M., Griffiths, D.J., Murray, J.M., Watts, F.Z., McCreedy, S., and Carr, A.M. (1995). The *rad18* gene of *Schizosaccharomyces pombe* defines a new subgroup of the SMC superfamily involved in DNA repair. *Mol. Cell. Biol.* *15*, 7067–7080.
- Lengronne, A., Katou, Y., Mori, S., Yokobayashi, S., Kelly, G.P., Itoh, T., Watanabe, Y., Shirahige, K., and Uhlmann, F. (2004). Cohesin relocation from sites of chromosomal loading to places of convergent transcription. *Nature* *430*, 573–578.
- Lesterlin, C., Gigant, E., Boccard, F., and Espéli, O. (2012). Sister chromatid interactions in bacteria revealed by a site-specific recombination assay. *EMBO J.* *31*, 3468–3479.
- Lesterlin, C., Ball, G., Schermelleh, L., and Sherratt, D.J. (2014). RecA bundles mediate homology pairing between distant sisters during DNA break repair. *Nature* *506*, 249–253.
- Levin-Zaidman, S., Frenkiel-Krispin, D., Shimoni, E., Sabanay, I., Wolf, S.G., and Minsky, A. (2000). Ordered intracellular RecA–DNA assemblies: A potential site of in vivo RecA-mediated activities. *Proc. Natl. Acad. Sci. U. S. A.* *97*, 6791–6796.
- Lewis, L.K., Harlow, G.R., Gregg-Jolly, L.A., and Mount, D.W. (1994). Identification of High Affinity Binding Sites for LexA which Define New DNA Damage-inducible Genes in *Escherichia coli*. *J. Mol. Biol.* *241*, 507–523.
- Lin, J.J., and Sancar, A. (1992). Active site of (A)BC excinuclease. I. Evidence for 5' incision by UvrC through a catalytic site involving Asp399, Asp438, Asp466, and His538 residues. *J. Biol. Chem.* *267*, 17688–17692.

- Lin, L.L., and Little, J.W. (1988). Isolation and characterization of noncleavable (Ind⁻) mutants of the LexA repressor of *Escherichia coli* K-12. *J. Bacteriol.* *170*, 2163–2173.
- Lin, Z., Kong, H., Nei, M., and Ma, H. (2006). Origins and evolution of the recA/RAD51 gene family: evidence for ancient gene duplication and endosymbiotic gene transfer. *Proc. Natl. Acad. Sci. U. S. A.* *103*, 10328–10333.
- Lindahl, T. (1974). An N-glycosidase from *Escherichia coli* that releases free uracil from DNA containing deaminated cytosine residues. *Proc. Natl. Acad. Sci. U. S. A.* *71*, 3649–3653.
- Lindroos, H.B., Ström, L., Itoh, T., Katou, Y., Shirahige, K., and Sjögren, C. (2006). Chromosomal association of the Smc5/6 complex reveals that it functions in differently regulated pathways. *Mol. Cell* *22*, 755–767.
- Little, J.W. (1984). Autodigestion of lexA and phage lambda repressors. *Proc. Natl. Acad. Sci. U. S. A.* *81*, 1375–1379.
- Little, J.W. (1991). Mechanism of specific LexA cleavage: autodigestion and the role of RecA coprotease. *Biochimie* *73*, 411–421.
- Little, J.W., Edmiston, S.H., Pacelli, L.Z., and Mount, D.W. (1980). Cleavage of the *Escherichia coli* lexA protein by the recA protease. *Proc. Natl. Acad. Sci. U. S. A.* *77*, 3225–3229.
- Liu, L.F., and Wang, J.C. (1987). Supercoiling of the DNA template during transcription. *Proc. Natl. Acad. Sci. U. S. A.* *84*, 7024–7027.
- Livneh, Z., and Lehman, I.R. (1982). Recombinational bypass of pyrimidine dimers promoted by the recA protein of *Escherichia coli*. *Proc. Natl. Acad. Sci. U. S. A.* *79*, 3171–3175.
- Lloyd, R.G., and Sharples, G.J. (1993). Dissociation of synthetic Holliday junctions by *E. coli* RecG protein. *EMBO J.* *12*, 17–22.
- Lloyd, R.G., Benson, F.E., and Shurvinton, C.E. (1984). Effect of ruv mutations on recombination and DNA repair in *Escherichia coli* K12. *Mol. Gen. Genet. MGG* *194*, 303–309.
- Loeb, L.A., and Kunkel, T.A. (1982). Fidelity of DNA synthesis. *Annu. Rev. Biochem.* *51*, 429–457.
- Lopez, C.R., Yang, S., Deibler, R.W., Ray, S.A., Pennington, J.M., Digate, R.J., Hastings, P.J., Rosenberg, S.M., and Zechiedrich, E.L. (2005). A role for topoisomerase III in a recombination pathway alternative to RuvABC. *Mol. Microbiol.* *58*, 80–101.
- Lovett, S.T., and Clark, A.J. (1984). Genetic analysis of the recJ gene of *Escherichia coli* K-12. *J. Bacteriol.* *157*, 190–196.
- Lovett, S.T., and Kolodner, R.D. (1989). Identification and purification of a single-stranded-DNA-specific exonuclease encoded by the recJ gene of *Escherichia coli*. *Proc. Natl. Acad. Sci. U. S. A.* *86*, 2627–2631.
- Lu, A.L., Clark, S., and Modrich, P. (1983). Methyl-directed repair of DNA base-pair mismatches in vitro. *Proc. Natl. Acad. Sci. U. S. A.* *80*, 4639–4643.

- Luo, Y., Pfuetzner, R.A., Mosimann, S., Paetzel, M., Frey, E.A., Cherney, M., Kim, B., Little, J.W., and Strynadka, N.C. (2001). Crystal structure of LexA: a conformational switch for regulation of self-cleavage. *Cell* 106, 585–594.
- Lusetti, S.L., Drees, J.C., Stohl, E.A., Seifert, H.S., and Cox, M.M. (2004). The DinI and RecX proteins are competing modulators of RecA function. *J. Biol. Chem.* 279, 55073–55079.
- Maki, H., Horiuchi, T., and Kornberg, A. (1985). The polymerase subunit of DNA polymerase III of *Escherichia coli*. I. Amplification of the *dnaE* gene product and polymerase activity of the alpha subunit. *J. Biol. Chem.* 260, 12982–12986.
- Makowska-Grzyska, M., and Kaguni, J.M. (2010). Primase directs the release of DnaC from DnaB. *Mol. Cell* 37, 90–101.
- Mamber, S.W., Brookshire, K.W., and Forenza, S. (1990). Induction of the SOS response in *Escherichia coli* by azidothymidine and dideoxynucleosides. *Antimicrob. Agents Chemother.* 34, 1237–1243.
- Manfrini, N., Clerici, M., Wery, M., Colombo, C.V., Descrimes, M., Morillon, A., Fagagna, F. d'Adda di, and Longhese, M.P. (2015). Resection is responsible for loss of transcription around a double-strand break in *Saccharomyces cerevisiae*. *ELife* 4, e08942.
- Marians, K.J. (2000). PriA-directed replication fork restart in *Escherichia coli*. *Trends Biochem. Sci.* 25, 185–189.
- Mariezcurrentena, A., and Uhlmann, F. (2017). Observation of DNA intertwining along authentic budding yeast chromosomes. *Genes Dev.* 31, 2151–2161.
- Martel, M., Balleydier, A., Sauriol, A., and Drolet, M. (2015). Constitutive stable DNA replication in *Escherichia coli* cells lacking type 1A topoisomerase activity. *DNA Repair* 35, 37–47.
- Massé, E., and Drolet, M. (1999). *Escherichia coli* DNA topoisomerase I inhibits R-loop formation by relaxing transcription-induced negative supercoiling. *J. Biol. Chem.* 274, 16659–16664.
- Mazin, A.V., and Kowalczykowski, S.C. (1996). The Specificity of the Secondary DNA Binding Site of RecA Protein Defines its Role in DNA Strand Exchange. *Proc. Natl. Acad. Sci. U. S. A.* 93, 10673–10678.
- McGlynn, P., and Lloyd, R.G. (2000). Modulation of RNA polymerase by (p)ppGpp reveals a RecG-dependent mechanism for replication fork progression. *Cell* 101, 35–45.
- McGlynn, P., and Lloyd, R.G. (2001). Rescue of stalled replication forks by RecG: simultaneous translocation on the leading and lagging strand templates supports an active DNA unwinding model of fork reversal and Holliday junction formation. *Proc. Natl. Acad. Sci. U. S. A.* 98, 8227–8234.
- McHenry, C.S., and Crow, W. (1979). DNA polymerase III of *Escherichia coli*. Purification and identification of subunits. *J. Biol. Chem.* 254, 1748–1753.
- Meddows, T.R., Savory, A.P., Grove, J.I., Moore, T., and Lloyd, R.G. (2005). RecN protein and transcription factor DksA combine to promote faithful recombinational repair of DNA double-strand breaks. *Mol. Microbiol.* 57, 97–110.
- Mellon, I., and Hanawalt, P.C. (1989). Induction of the *Escherichia coli* lactose operon selectively increases repair of its transcribed DNA strand. *Nature* 342, 95–98.

- Mendelsohn, M.L., Moore, D.H., and Lohman, P.H. (1992). International Commission for Protection Against Environmental Mutagens and Carcinogens. A method for comparing and combining short-term genotoxicity test data: results and interpretation. *Mutat. Res.* 266, 43–60.
- Menetski, J.P., Bear, D.G., and Kowalczykowski, S.C. (1990). Stable DNA heteroduplex formation catalyzed by the *Escherichia coli* RecA protein in the absence of ATP hydrolysis. *Proc. Natl. Acad. Sci. U. S. A.* 87, 21–25.
- Mercier, R., Petit, M.-A., Schbath, S., Robin, S., El Karoui, M., Boccard, F., and Espéli, O. (2008). The MatP/matS site-specific system organizes the terminus region of the *E. coli* chromosome into a macrodomain. *Cell* 135, 475–485.
- Mertens, K., and Samuel, J.E. (2012). Defense Mechanisms Against Oxidative Stress in *Coxiella burnetii*: Adaptation to a Unique Intracellular Niche. In *Coxiella Burnetii: Recent Advances and New Perspectives in Research of the Q Fever Bacterium*, (Springer, Dordrecht), pp. 39–63.
- Michaelis, C., Ciosk, R., and Nasmyth, K. (1997). Cohesins: chromosomal proteins that prevent premature separation of sister chromatids. *Cell* 91, 35–45.
- Michel, B., Ehrlich, S.D., and Uzest, M. (1997). DNA double-strand breaks caused by replication arrest. *EMBO J.* 16, 430–438.
- Michel, B., Flores, M.J., Viguera, E., Grompone, G., Seigneur, M., and Bidnenko, V. (2001). Rescue of arrested replication forks by homologous recombination. *Proc. Natl. Acad. Sci. U. S. A.* 98, 8181–8188.
- Miné-Hattab, J., and Rothstein, R. (2012). Increased chromosome mobility facilitates homology search during recombination. *Nat. Cell Biol.* 14, 510–517.
- Minsky, A. (2003). Structural aspects of DNA repair: the role of restricted diffusion. *Mol. Microbiol.* 50, 367–376.
- Moolenaar, G.F., van Sluis, C.A., Backendorf, C., and van de Putte, P. (1987). Regulation of the *Escherichia coli* excision repair gene *uvrC*. Overlap between the *uvrC* structural gene and the region coding for a 24 kD protein. *Nucleic Acids Res.* 15, 4273–4289.
- Moolenaar, G.F., van Rossum-Fikkert, S., van Kesteren, M., and Goosen, N. (2002). Cho, a second endonuclease involved in *Escherichia coli* nucleotide excision repair. *Proc. Natl. Acad. Sci. U. S. A.* 99, 1467–1472.
- Moore, T., McGlynn, P., Ngo, H.-P., Sharples, G.J., and Lloyd, R.G. (2003). The RdgC protein of *Escherichia coli* binds DNA and counters a toxic effect of RecFOR in strains lacking the replication restart protein PriA. *EMBO J.* 22, 735–745.
- Morimatsu, K., and Kowalczykowski, S.C. (2003). RecFOR proteins load RecA protein onto gapped DNA to accelerate DNA strand exchange: a universal step of recombinational repair. *Mol. Cell* 11, 1337–1347.
- Mossessova, E., Levine, C., Peng, H., Nurse, P., Bahng, S., and Marians, K.J. (2000). Mutational analysis of *Escherichia coli* topoisomerase IV. I. Selection of dominant-negative *parE* alleles. *J. Biol. Chem.* 275, 4099–4103.

- Mount, D.W. (1977). A mutant of *Escherichia coli* showing constitutive expression of the lysogenic induction and error-prone DNA repair pathways. *Proc. Natl. Acad. Sci. U. S. A.* *74*, 300–304.
- Mukherjee, A., Cao, C., and Lutkenhaus, J. (1998). Inhibition of FtsZ polymerization by Sula, an inhibitor of septation in *Escherichia coli*. *Proc. Natl. Acad. Sci. U. S. A.* *95*, 2885–2890.
- Müller, B., Koller, T., and Stasiak, A. (1990). Characterization of the DNA binding activity of stable RecA-DNA complexes. Interaction between the two DNA binding sites within RecA helical filaments. *J. Mol. Biol.* *212*, 97–112.
- Mustard, J.A., and Little, J.W. (2000). Analysis of *Escherichia coli* RecA Interactions with LexA, λ CI, and UmuD by Site-Directed Mutagenesis of recA. *J. Bacteriol.* *182*, 1659–1670.
- Nagashima, K., Kubota, Y., Shibata, T., Sakaguchi, C., Shinagawa, H., and Hishida, T. (2006). Degradation of *Escherichia coli* RecN aggregates by ClpXP protease and its implications for DNA damage tolerance. *J. Biol. Chem.* *281*, 30941–30946.
- Naiman, K., Pagès, V., and Fuchs, R.P. (2016). A defect in homologous recombination leads to increased translesion synthesis in *E. coli*. *Nucleic Acids Res.* *44*, 7691–7699.
- Nakai, Y., Nelson, W.G., and De Marzo, A.M. (2007). The dietary charred meat carcinogen 2-amino-1-methyl-6-phenylimidazo[4,5-b]pyridine acts as both a tumor initiator and promoter in the rat ventral prostate. *Cancer Res.* *67*, 1378–1384.
- Nakanishi, A., Imajoh-Ohmi, S., and Hanaoka, F. (2002). Characterization of the interaction between DNA gyrase inhibitor and DNA gyrase of *Escherichia coli*. *J. Biol. Chem.* *277*, 8949–8954.
- Nasmyth, K., and Schleiffer, A. (2004). From a single double helix to paired double helices and back. *Philos. Trans. R. Soc. Lond. B. Biol. Sci.* *359*, 99–108.
- Neher, S.B., Villén, J., Oakes, E.C., Bakalarski, C.E., Sauer, R.T., Gygi, S.P., and Baker, T.A. (2006). Proteomic profiling of ClpXP substrates after DNA damage reveals extensive instability within SOS regulon. *Mol. Cell* *22*, 193–204.
- Neylon, C., Kralicek, A.V., Hill, T.M., and Dixon, N.E. (2005). Replication termination in *Escherichia coli*: structure and antihelicase activity of the Tus-Ter complex. *Microbiol. Mol. Biol. Rev. MMBR* *69*, 501–526.
- Nicolas, E., Upton, A.L., Uphoff, S., Henry, O., Badrinarayanan, A., and Sherratt, D. (2014). The SMC complex MukBEF recruits topoisomerase IV to the origin of replication region in live *Escherichia coli*. *MBio* *5*, e01001-01013.
- Nishinaka, T., Ito, Y., Yokoyama, S., and Shibata, T. (1997). An extended DNA structure through deoxyribose-base stacking induced by RecA protein. *Proc. Natl. Acad. Sci.* *94*, 6623–6628.
- Nitiss, J.L., Liu, Y.X., and Hsiung, Y. (1993). A temperature sensitive topoisomerase II allele confers temperature dependent drug resistance on amsacrine and etoposide: a genetic system for determining the targets of topoisomerase II inhibitors. *Cancer Res.* *53*, 89–93.
- Nolivos, S., Upton, A.L., Badrinarayanan, A., Müller, J., Zawadzka, K., Wiktor, J., Gill, A., Arciszewska, L., Nicolas, E., and Sherratt, D. (2016). MatP regulates the coordinated action of topoisomerase IV and MukBEF in chromosome segregation. *Nat. Commun.* *7*.

Noll, D.M., Mason, T.M., and Miller, P.S. (2006). Formation and repair of interstrand cross-links in DNA. *Chem. Rev.* *106*, 277–301.

Nurse, P., Levine, C., Hassing, H., and Marians, K.J. (2003). Topoisomerase III can serve as the cellular decatenase in *Escherichia coli*. *J. Biol. Chem.* *278*, 8653–8660.

O'Donnell, M., Langston, L., and Stillman, B. (2013). Principles and concepts of DNA replication in bacteria, archaea, and eukarya. *Cold Spring Harb. Perspect. Biol.* *5*.

Odsbu, I., and Skarstad, K. (2014). DNA compaction in the early part of the SOS response is dependent on RecN and RecA. *Microbiol. Read. Engl.* *160*, 872–882.

O'Reilly, E.K., and Kreuzer, K.N. (2004). Isolation of SOS constitutive mutants of *Escherichia coli*. *J. Bacteriol.* *186*, 7149–7160.

Orren, D.K., and Sancar, A. (1989). The (A)BC excinuclease of *Escherichia coli* has only the UvrB and UvrC subunits in the incision complex. *Proc. Natl. Acad. Sci. U. S. A.* *86*, 5237–5241.

Orren, D.K., Selby, C.P., Hearst, J.E., and Sancar, A. (1992). Post-incision steps of nucleotide excision repair in *Escherichia coli*. Disassembly of the UvrBC-DNA complex by helicase II and DNA polymerase I. *J. Biol. Chem.* *267*, 780–788.

Palecek, J.J., and Gruber, S. (2015). Kite Proteins: a Superfamily of SMC/Kleisin Partners Conserved Across Bacteria, Archaea, and Eukaryotes. *Structure* *23*, 2183–2190.

Pandey, M., Elshenawy, M.M., Jergic, S., Takahashi, M., Dixon, N.E., Hamdan, S.M., and Patel, S.S. (2015). Two mechanisms coordinate replication termination by the *Escherichia coli* Tus-Ter complex. *Nucleic Acids Res.* *43*, 5924–5935.

Pâques, F., and Haber, J.E. (1999). Multiple pathways of recombination induced by double-strand breaks in *Saccharomyces cerevisiae*. *Microbiol. Mol. Biol. Rev. MMBR* *63*, 349–404.

Pebbernard, S., McDonald, W.H., Pavlova, Y., Yates, J.R., and Boddy, M.N. (2004). Nse1, Nse2, and a Novel Subunit of the Smc5-Smc6 Complex, Nse3, Play a Crucial Role in Meiosis. *Mol. Biol. Cell* *15*, 4866–4876.

Pellegrino, S., Radzimanowski, J., de Sanctis, D., Erba, E.B., McSweeney, S., and Timmins, J. (2012a). Structural and Functional Characterization of an SMC-like Protein RecN: New Insights into Double-Strand Break Repair. *Structure* *20*, 2076–2089.

Pellegrino, S., de Sanctis, D., McSweeney, S., and Timmins, J. (2012b). Expression, purification and preliminary structural analysis of the coiled-coil domain of *Deinococcus radiodurans* RecN. *Acta Crystallograph. Sect. F Struct. Biol. Cryst. Commun.* *68*, 218–221.

Peng, X., Ghosh, A.K., Van Houten, B., and Greenberg, M.M. (2010). Nucleotide Excision Repair of a DNA Interstrand Cross-Link Produces Single and Double Strand Breaks. *Biochemistry (Mosc.)* *49*, 11–19.

Peter, B.J., Ullsperger, C., Hiasa, H., Marians, K.J., and Cozzarelli, N.R. (1998). The structure of supercoiled intermediates in DNA replication. *Cell* *94*, 819–827.

Petrova, V., Chitteni-Pattu, S., Drees, J.C., Inman, R.B., and Cox, M.M. (2009). An SOS inhibitor that binds to free RecA protein: the PsiB protein. *Mol. Cell* *36*, 121–130.

- Picksley, S.M., Attfield, P.V., and Lloyd, R.G. (1984). Repair of DNA double-strand breaks in *Escherichia coli* K12 requires a functional recN product. *Mol. Gen. Genet.* *MGG* *195*, 267–274.
- Postow, L., Peter, B.J., and Cozzarelli, N.R. (1999). Knot what we thought before: the twisted story of replication. *BioEssays News Rev. Mol. Cell. Dev. Biol.* *21*, 805–808.
- Potts, P.R., Porteus, M.H., and Yu, H. (2006). Human SMC5/6 complex promotes sister chromatid homologous recombination by recruiting the SMC1/3 cohesin complex to double-strand breaks. *EMBO J.* *25*, 3377–3388.
- Pugh, B.F., and Cox, M.M. (1987). Stable binding of recA protein to duplex DNA. Unraveling a paradox. *J. Biol. Chem.* *262*, 1326–1336.
- Pukkila, P.J., Peterson, J., Herman, G., Modrich, P., and Meselson, M. (1983). Effects of high levels of DNA adenine methylation on methyl-directed mismatch repair in *Escherichia coli*. *Genetics* *104*, 571–582.
- Radman, M. (1975). SOS repair hypothesis: phenomenology of an inducible DNA repair which is accompanied by mutagenesis. *Basic Life Sci.* *5A*, 355–367.
- Ragunathan, K., Liu, C., and Ha, T. (2012). RecA filament sliding on DNA facilitates homology search. *ELife* *1*.
- Ramilo, C., Gu, L., Guo, S., Zhang, X., Patrick, S.M., Turchi, J.J., and Li, G.-M. (2002). Partial reconstitution of human DNA mismatch repair in vitro: characterization of the role of human replication protein A. *Mol. Cell. Biol.* *22*, 2037–2046.
- Register, J.C., and Griffith, J. (1985). The direction of RecA protein assembly onto single strand DNA is the same as the direction of strand assimilation during strand exchange. *J. Biol. Chem.* *260*, 12308–12312.
- Renzette, N., Gumlaw, N., Nordman, J.T., Krieger, M., Yeh, S.-P., Long, E., Centore, R., Boonsombat, R., and Sandler, S.J. (2005). Localization of RecA in *Escherichia coli* K-12 using RecA-GFP. *Mol. Microbiol.* *57*, 1074–1085.
- Reyes, E.D., Patidar, P.L., Uranga, L.A., Bortoletto, A.S., and Lusetti, S.L. (2010). RecN is a cohesin-like protein that stimulates intermolecular DNA interactions in vitro. *J. Biol. Chem.* *285*, 16521–16529.
- Reyes-Lamothe, R., Sherratt, D.J., and Leake, M.C. (2010). Stoichiometry and architecture of active DNA replication machinery in *Escherichia coli*. *Science* *328*, 498–501.
- Reyes-Lamothe, R., Nicolas, E., and Sherratt, D.J. (2012). Chromosome replication and segregation in bacteria. *Annu. Rev. Genet.* *46*, 121–143.
- Rodríguez-Beltrán, J., Rodríguez-Rojas, A., Guelfo, J.R., Couce, A., and Blázquez, J. (2012). The *Escherichia coli* SOS Gene *dinF* Protects against Oxidative Stress and Bile Salts. *PLOS ONE* *7*, e34791.
- Rossi, M.J., Mazina, O.M., Bugreev, D.V., and Mazin, A.V. (2011). The RecA/RAD51 protein drives migration of Holliday junctions via polymerization on DNA. *Proc. Natl. Acad. Sci. U. S. A.* *108*, 6432–6437.
- Rostas, K., Morton, S.J., Picksley, S.M., and Lloyd, R.G. (1987). Nucleotide sequence and LexA regulation of the *Escherichia coli* recN gene. *Nucleic Acids Res.* *15*, 5041–5049.

- Rudolph, C.J., Upton, A.L., and Lloyd, R.G. (2009). Replication fork collisions cause pathological chromosomal amplification in cells lacking RecG DNA translocase. *Mol. Microbiol.* *74*, 940–955.
- Rudolph, C.J., Upton, A.L., Stockum, A., Nieduszynski, C.A., and Lloyd, R.G. (2013). Avoiding chromosome pathology when replication forks collide. *Nature* *500*.
- Rupp, W.D., and Howard-Flanders, P. (1968). Discontinuities in the DNA synthesized in an excision-defective strain of *Escherichia coli* following ultraviolet irradiation. *J. Mol. Biol.* *31*, 291–304.
- Rybicki, B.A., Neslund-Dudas, C., Bock, C.H., Nock, N.L., Rundle, A., Jankowski, M., Levin, A.M., Beebe-Dimmer, J., Savera, A.T., Takahashi, S., et al. (2011). Red wine consumption is inversely associated with 2-amino-1-methyl-6-phenylimidazo[4,5-b]pyridine-DNA adduct levels in prostate. *Cancer Prev. Res. Phila. Pa* *4*, 1636–1644.
- Sajesh, B.V., Lichtensztejn, Z., and McManus, K.J. (2013). Sister chromatid cohesion defects are associated with chromosome instability in Hodgkin lymphoma cells. *BMC Cancer* *13*, 391.
- Sakai, A., and Cox, M.M. (2009). RecFOR and RecOR as distinct RecA loading pathways. *J. Biol. Chem.* *284*, 3264–3272.
- Sancar, A., Wharton, R.P., Seltzer, S., Kacinski, B.M., Clarke, N.D., and Rupp, W.D. (1981a). Identification of the *uvrA* gene product. *J. Mol. Biol.* *148*, 45–62.
- Sancar, A., Clarke, N.D., Griswold, J., Kennedy, W.J., and Rupp, W.D. (1981b). Identification of the *uvrB* gene product. *J. Mol. Biol.* *148*, 63–76.
- Sancar, A., Kacinski, B.M., Mott, D.L., and Rupp, W.D. (1981c). Identification of the *uvrC* gene product. *Proc. Natl. Acad. Sci. U. S. A.* *78*, 5450–5454.
- Sanchez, H., and Alonso, J.C. (2005). *Bacillus subtilis* RecN binds and protects 3'-single-stranded DNA extensions in the presence of ATP. *Nucleic Acids Res.* *33*, 2343–2350.
- Sanchez, H., Kidane, D., Castillo Cozar, M., Graumann, P.L., and Alonso, J.C. (2006). Recruitment of *Bacillus subtilis* RecN to DNA Double-Strand Breaks in the Absence of DNA End Processing. *J. Bacteriol.* *188*, 353–360.
- Sanchez, H., Cardenas, P.P., Yoshimura, S.H., Takeyasu, K., and Alonso, J.C. (2008). Dynamic structures of *Bacillus subtilis* RecN–DNA complexes. *Nucleic Acids Res.* *36*, 110–120.
- Sargentini, N.J., and Smith, K.C. (1983). Characterization of an *Escherichia coli* mutant (*radB101*) sensitive to gamma and uv radiation, and methyl methanesulfonate. *Radiat. Res.* *93*, 461–478.
- Sawitzke, J.A., and Stahl, F.W. (1992). Phage lambda has an analog of *Escherichia coli* *recO*, *recR* and *recF* genes. *Genetics* *130*, 7–16.
- Sayyed, H.E., Chat, L.L., Lebailly, E., Vickridge, E., Pages, C., Cornet, F., Lagomarsino, M.C., and Espéli, O. (2016). Mapping Topoisomerase IV Binding and Activity Sites on the *E. coli* Genome. *PLOS Genet.* *12*, e1006025.
- Scheuermann, R., Tam, S., Burgers, P.M., Lu, C., and Echols, H. (1983). Identification of the epsilon-subunit of *Escherichia coli* DNA polymerase III holoenzyme as the *dnaQ* gene product: a fidelity subunit for DNA replication. *Proc. Natl. Acad. Sci. U. S. A.* *80*, 7085–7089.

- Schleiffer, A., Kaitna, S., Maurer-Stroh, S., Glotzer, M., Nasmyth, K., and Eisenhaber, F. (2003). Kleisins: A Superfamily of Bacterial and Eukaryotic SMC Protein Partners. *Mol. Cell* *11*, 571–575.
- Schulte-Frohlinde, D. (1994). Radiation-Induced Formation of DNA Double-Strand Breaks in Plasmids and *E. coli*. In *Chromosomal Alterations*, (Springer, Berlin, Heidelberg), pp. 1–9.
- Sczepanski, J.T., Jacobs, A.C., Van Houten, B., and Greenberg, M.M. (2009). Double Strand Break Formation During Nucleotide Excision Repair of a DNA Interstrand Cross-link. *Biochemistry (Mosc.)* *48*, 7565–7567.
- Seigneur, M., Bidnenko, V., Ehrlich, S.D., and Michel, B. (1998). RuvAB acts at arrested replication forks. *Cell* *95*, 419–430.
- Seigneur, M., Ehrlich, S.D., and Michel, B. (2000). RuvABC-dependent double-strand breaks in dnaBts mutants require recA. *Mol. Microbiol.* *38*, 565–574.
- Selby, C.P., and Sancar, A. (1993). Molecular mechanism of transcription-repair coupling. *Science* *260*, 53–58.
- Selby, C.P., and Sancar, A. (1995). Structure and function of transcription-repair coupling factor. II. Catalytic properties. *J. Biol. Chem.* *270*, 4890–4895.
- Setlow, R.B., and Carrier, W.L. (1964). The disappearance of thymine dimers from dna: an error-correcting mechanism. *Proc. Natl. Acad. Sci. U. S. A.* *51*, 226–231.
- Shan, Q., and Cox, M.M. (1997). RecA Filament Dynamics during DNA Strand Exchange Reactions. *J. Biol. Chem.* *272*, 11063–11073.
- Shechter, N., Zaltzman, L., Weiner, A., Brumfeld, V., Shimoni, E., Fridmann-Sirkis, Y., and Minsky, A. (2013). Stress-induced Condensation of Bacterial Genomes Results in Re-pairing of Sister Chromosomes. *J. Biol. Chem.* *288*, 25659–25667.
- Simmons, L.A., Grossman, A.D., and Walker, G.C. (2007). Replication is required for the RecA localization response to DNA damage in *Bacillus subtilis*. *Proc. Natl. Acad. Sci. U. S. A.* *104*, 1360–1365.
- Simmons, L.A., Davies, B.W., Grossman, A.D., and Walker, G.C. (2008). β -Clamp directs localization of mismatch repair in *Bacillus subtilis*. *Mol. Cell* *29*, 291–301.
- Simmons, L.A., Goranov, A.I., Kobayashi, H., Davies, B.W., Yuan, D.S., Grossman, A.D., and Walker, G.C. (2009). Comparison of responses to double-strand breaks between *Escherichia coli* and *Bacillus subtilis* reveals different requirements for SOS induction. *J. Bacteriol.* *191*, 1152–1161.
- Sinden, R.R., Carlson, J.O., and Pettijohn, D.E. (1980). Torsional tension in the DNA double helix measured with trimethylpsoralen in living *E. coli* cells: analogous measurements in insect and human cells. *Cell* *21*, 773–783.
- Singleton, M.R., Scaife, S., and Wigley, D.B. (2001). Structural analysis of DNA replication fork reversal by RecG. *Cell* *107*, 79–89.
- Sirbu, B.M., Couch, F.B., Feigerle, J.T., Bhaskara, S., Hiebert, S.W., and Cortez, D. (2011). Analysis of protein dynamics at active, stalled, and collapsed replication forks. *Genes Dev.* *25*, 1320–1327.

- Sjögren, C., and Nasmyth, K. (2001). Sister chromatid cohesion is required for postreplicative double-strand break repair in *Saccharomyces cerevisiae*. *Curr. Biol. CB* 11, 991–995.
- Skaar, E.P., Lazio, M.P., and Seifert, H.S. (2002). Roles of the *recJ* and *recN* genes in homologous recombination and DNA repair pathways of *Neisseria gonorrhoeae*. *J. Bacteriol.* 184, 919–927.
- Slater, S., Wold, S., Lu, M., Boye, E., Skarstad, K., and Kleckner, N. (1995). *E. coli* SeqA protein binds *oriC* in two different methyl-modulated reactions appropriate to its roles in DNA replication initiation and origin sequestration. *Cell* 82, 927–936.
- Slilaty, S.N., and Little, J.W. (1987). Lysine-156 and serine-119 are required for LexA repressor cleavage: a possible mechanism. *Proc. Natl. Acad. Sci. U. S. A.* 84, 3987–3991.
- Slupska, M.M., Chiang, J.H., Luther, W.M., Stewart, J.L., Amii, L., Conrad, A., and Miller, J.H. (2000). Genes involved in the determination of the rate of inversions at short inverted repeats. *Genes Cells Devoted Mol. Cell. Mech.* 5, 425–437.
- Sneeden, J.L., and Loeb, L.A. (2004). Mutations in the R2 subunit of ribonucleotide reductase that confer resistance to hydroxyurea. *J. Biol. Chem.* 279, 40723–40728.
- Staczek, P., and Higgins, N.P. (1998). Gyrase and Topo IV modulate chromosome domain size in vivo. *Mol. Microbiol.* 29, 1435–1448.
- Story, R.M., and Steitz, T.A. (1992). Structure of the *recA* protein-ADP complex. *Nature* 355, 374–376.
- Stouf, M., Meile, J.-C., and Cornet, F. (2013). FtsK actively segregates sister chromosomes in *Escherichia coli*. *Proc. Natl. Acad. Sci. U. S. A.* 110, 11157–11162.
- Stracy, M., Jaciuk, M., Uphoff, S., Kapanidis, A.N., Nowotny, M., Sherratt, D.J., and Zawadzki, P. (2016). Single-molecule imaging of UvrA and UvrB recruitment to DNA lesions in living *Escherichia coli*. *Nat. Commun.* 7, 12568.
- Strecker, J., Gupta, G.D., Zhang, W., Bashkurov, M., Landry, M.-C., Pelletier, L., and Durocher, D. (2016). DNA damage signalling targets the kinetochore to promote chromatin mobility. *Nat. Cell Biol.* 18, 281–290.
- Ström, L., and Sjögren, C. (2007). Chromosome segregation and double-strand break repair - a complex connection. *Curr. Opin. Cell Biol.* 19, 344–349.
- Ström, L., Lindroos, H.B., Shirahige, K., and Sjögren, C. (2004). Postreplicative recruitment of cohesin to double-strand breaks is required for DNA repair. *Mol. Cell* 16, 1003–1015.
- Su, S.S., and Modrich, P. (1986). *Escherichia coli* mutS-encoded protein binds to mismatched DNA base pairs. *Proc. Natl. Acad. Sci. U. S. A.* 83, 5057–5061.
- Sunako Yumi, Onogi Toshinari, and Hiraga Sota (2002). Sister chromosome cohesion of *Escherichia coli*. *Mol. Microbiol.* 42, 1233–1241.
- Suski, C., and Marians, K.J. (2008). Resolution of Converging Replication Forks by RecQ and Topoisomerase III. *Mol. Cell* 30, 779–789.

- Swanson, R.L., Morey, N.J., Doetsch, P.W., and Jinks-Robertson, S. (1999). Overlapping specificities of base excision repair, nucleotide excision repair, recombination, and translesion synthesis pathways for DNA base damage in *Saccharomyces cerevisiae*. *Mol. Cell. Biol.* *19*, 2929–2935.
- Tanaka, T., Fuchs, J., Loidl, J., and Nasmyth, K. (2000). Cohesin ensures bipolar attachment of microtubules to sister centromeres and resists their precocious separation. *Nat. Cell Biol.* *2*, 492–499.
- Taylor, A.F., and Smith, G.R. (1985). Substrate specificity of the DNA unwinding activity of the RecBC enzyme of *Escherichia coli*. *J. Mol. Biol.* *185*, 431–443.
- Taylor, A.F., and Smith, G.R. (2003). RecBCD enzyme is a DNA helicase with fast and slow motors of opposite polarity. *Nature* *423*, 889–893.
- Timson, J. (1975). Hydroxyurea. *Mutat. Res.* *32*, 115–132.
- Tiwari, P.B., Chapagain, P.P., Banda, S., Darici, Y., Üren, A., and Tse-Dinh, Y.-C. (2016). Characterization of molecular interactions between *Escherichia coli* RNA polymerase and topoisomerase I by molecular simulations. *FEBS Lett.* *590*, 2844–2851.
- Trewick, S.C., Henshaw, T.F., Hausinger, R.P., Lindahl, T., and Sedgwick, B. (2002). Oxidative demethylation by *Escherichia coli* AlkB directly reverts DNA base damage. *Nature* *419*, 174–178.
- Truglio, J.J., Karakas, E., Rhau, B., Wang, H., DellaVecchia, M.J., Van Houten, B., and Kisker, C. (2006). Structural basis for DNA recognition and processing by UvrB. *Nat. Struct. Mol. Biol.* *13*, 360–364.
- Tsaneva, I.R., Illing, G., Lloyd, R.G., and West, S.C. (1992). Purification and properties of the RuvA and RuvB proteins of *Escherichia coli*. *Mol. Gen. Genet.* *MGG 235*, 1–10.
- Uhlmann, F., and Nasmyth, K. (1998). Cohesion between sister chromatids must be established during DNA replication. *Curr. Biol.* *CB 8*, 1095–1101.
- Uhlmann, F., Wernic, D., Poupart, M.A., Koonin, E.V., and Nasmyth, K. (2000). Cleavage of cohesin by the CD clan protease separin triggers anaphase in yeast. *Cell* *103*, 375–386.
- Unal, E., Heidinger-Pauli, J.M., and Koshland, D. (2007). DNA double-strand breaks trigger genome-wide sister-chromatid cohesion through Eco1 (Ctf7). *Science* *317*, 245–248.
- Unoson, C., and Wagner, E.G.H. (2008). A small SOS-induced toxin is targeted against the inner membrane in *Escherichia coli*. *Mol. Microbiol.* *70*, 258–270.
- Uphoff, S., Reyes-Lamothe, R., Garza de Leon, F., Sherratt, D.J., and Kapanidis, A.N. (2013). Single-molecule DNA repair in live bacteria. *Proc. Natl. Acad. Sci. U. S. A.* *110*, 8063–8068.
- Uranga, L.A., Balise, V.D., Benally, C.V., Grey, A., and Lusetti, S.L. (2011). The *Escherichia coli* DinD protein modulates RecA activity by inhibiting postsynaptic RecA filaments. *J. Biol. Chem.* *286*, 29480–29491.
- Uranga, L.A., Reyes, E.D., Patidar, P.L., Redman, L.N., and Lusetti, S.L. (2017). The cohesin-like RecN protein stimulates RecA-mediated recombinational repair of DNA double-strand breaks. *Nat. Commun.* *8*.

- Valens, M., Penaud, S., Rossignol, M., Cornet, F., and Boccard, F. (2004). Macrodome organization of the *Escherichia coli* chromosome. *EMBO J.* *23*, 4330–4341.
- Van Houten, B., Eisen, J.A., and Hanawalt, P.C. (2002). A cut above: discovery of an alternative excision repair pathway in bacteria. *Proc. Natl. Acad. Sci. U. S. A.* *99*, 2581–2583.
- Verhoeven, E.E., van Kesteren, M., Moolenaar, G.F., Visse, R., and Goosen, N. (2000). Catalytic sites for 3' and 5' incision of *Escherichia coli* nucleotide excision repair are both located in UvrC. *J. Biol. Chem.* *275*, 5120–5123.
- Verhoeven, E.E.A., Wyman, C., Moolenaar, G.F., and Goosen, N. (2002). The presence of two UvrB subunits in the UvrAB complex ensures damage detection in both DNA strands. *EMBO J.* *21*, 4196–4205.
- Vickridge, E., Planchenault, C., Cockram, C., Junceda, I.G., and Espéli, O. (2017). Management of *E. coli* sister chromatid cohesion in response to genotoxic stress. *Nat. Commun.* *8*.
- Volkert, M.R., and Hartke, M.A. (1984). Suppression of *Escherichia coli* recF mutations by recA-linked srfA mutations. *J. Bacteriol.* *157*, 498–506.
- Wagner, R., and Meselson, M. (2005). Repair tracts in mismatched DNA heteroduplexes. 1976. *DNA Repair* *4*, 126-130; discussion 103-104, 131.
- Walker, G.C. (1984). Mutagenesis and inducible responses to deoxyribonucleic acid damage in *Escherichia coli*. *Microbiol. Rev.* *48*, 60–93.
- Wang, J.C. (2002). Cellular roles of DNA topoisomerases: a molecular perspective. *Nat. Rev. Mol. Cell Biol.* *3*, 430–440.
- Wang, G., and Maier, R.J. (2008). Critical role of RecN in recombinational DNA repair and survival of *Helicobacter pylori*. *Infect. Immun.* *76*, 153–160.
- Wang, T.C., and Smith, K.C. (1986). recA (Srf) suppression of recF deficiency in the postreplication repair of UV-irradiated *Escherichia coli* K-12. *J. Bacteriol.* *168*, 940–946.
- Wang, T.C., and Smith, K.C. (1988). Different effects of recJ and recN mutations on the postreplication repair of UV-damaged DNA in *Escherichia coli* K-12. *J. Bacteriol.* *170*, 2555–2559.
- Wang, H., Lu, M., Tang, M., Van Houten, B., Ross, J.B.A., Weinfeld, M., and Le, X.C. (2009). DNA wrapping is required for DNA damage recognition in the *Escherichia coli* DNA nucleotide excision repair pathway. *Proc. Natl. Acad. Sci. U. S. A.* *106*, 12849–12854.
- Wang, X., Reyes-Lamothe, R., and Sherratt, D.J. (2008). Modulation of *Escherichia coli* sister chromosome cohesion by topoisomerase IV. *Genes Dev.* *22*, 2426–2433.
- Weel-Sneve, R., Kristiansen, K.I., Odsbu, I., Dalhus, B., Booth, J., Rognes, T., Skarstad, K., and Bjørås, M. (2013). Single transmembrane peptide DinQ modulates membrane-dependent activities. *PLoS Genet.* *9*, e1003260.
- Weng, M., Zheng, Y., Jasti, V.P., Champeil, E., Tomasz, M., Wang, Y., Basu, A.K., and Tang, M. (2010). Repair of mitomycin C mono- and interstrand cross-linked DNA adducts by UvrABC: a new model. *Nucleic Acids Res.* *38*, 6976–6984.

- Wiktor, J., van der Does, M., Büller, L., Sherratt, D.J., and Dekker, C. (2018). Direct observation of end resection by RecBCD during double-stranded DNA break repair in vivo. *Nucleic Acids Res.* *46*, 1821–1833.
- Wood, R.D. (2010). Mammalian nucleotide excision repair proteins and interstrand crosslink repair. *Environ. Mol. Mutagen.* *51*, 520–526.
- Wright, W.D., Shah, S.S., and Heyer, W.-D. (2018). Homologous recombination and the repair of DNA Double-Strand Breaks. *J. Biol. Chem.*
- Wu, H.-Y., Lu, C.-H., and Li, H.-W. (2017). RecA-SSB Interaction Modulates RecA Nucleoprotein Filament Formation on SSB-Wrapped DNA. *Sci. Rep.* *7*, 11876.
- Yamaguchi, M., Dao, V., and Modrich, P. (1998). MutS and MutL activate DNA helicase II in a mismatch-dependent manner. *J. Biol. Chem.* *273*, 9197–9201.
- Yamamoto, K., Higashikawa, T., Ohta, K., and Oda, Y. (1985). A loss of *uvrA* function decreases the induction of the SOS functions *recA* and *umuC* by mitomycin C in *Escherichia coli*. *Mutat. Res.* *149*, 297–302.
- Yasuda, T., Morimatsu, K., Horii, T., Nagata, T., and Ohmori, H. (1998). Inhibition of *Escherichia coli* RecA coprotease activities by DinI. *EMBO J.* *17*, 3207–3216.
- Yeeles, J.T.P., and Marians, K.J. (2011). The *Escherichia coli* replisome is inherently DNA damage tolerant. *Science* *334*, 235–238.
- Zechiedrich, E.L., Khodursky, A.B., and Cozzarelli, N.R. (1997). Topoisomerase IV, not gyrase, decatenates products of site-specific recombination in *Escherichia coli*. *Genes Dev.* *11*, 2580–2592.
- Zechiedrich, E.L., Khodursky, A.B., Bachellier, S., Schneider, R., Chen, D., Lilley, D.M., and Cozzarelli, N.R. (2000). Roles of topoisomerases in maintaining steady-state DNA supercoiling in *Escherichia coli*. *J. Biol. Chem.* *275*, 8103–8113.
- Zhu, Q., Pongpech, P., and DiGate, R.J. (2001a). Type I topoisomerase activity is required for proper chromosomal segregation in *Escherichia coli*. *Proc. Natl. Acad. Sci. U. S. A.* *98*, 9766–9771.

VII. Annex

Annex 1. During my PhD, I got the opportunity to participate in Hafez El Sayyed's article, published in Plos Genetics in 2016.


Hafez's PhD consisted in mapping the Topoisomerase IV binding sites and cutting sites on the *E.coli* chromosome. Interestingly, one observation that he made was that Topo IV cleavage at the *dif* site was impaired in a *matP* mutant. Complementary experiments lead to the conclusion that MatP may be important for targeting Topo IV to *dif*. It was hypothesized that the activity of Topo IV at *dif* could be specific to post-replication decatenation events linked to circular chromosomes. Cleavage was completely lost in a strain with a linear chromosome suggesting that Topo IV's activity is only required at *dif* with circular chromosomes. To test whether the phenotypes associated with *matP* deletion were also dependent on the circularity of the chromosome, I constructed *matP* mutants in a strain with a circular chromosome and in a strain where the chromosome is linearized. I then observed the nucleoids by microscopy and DAPI staining in the different backgrounds. I found that the phenotypes associated with *matP* deletion were suppressed by the linearization of the chromosome, also confirming that cleavage of Topo IV at *dif* is specific to circular chromosomes.

RESEARCH ARTICLE

Mapping Topoisomerase IV Binding and Activity Sites on the *E. coli* Genome

Hafez El Sayyed^{1,2} , Ludovic Le Chat¹ , Elise Lebailly³, Elise Vickridge^{1,2}, Carine Pages³, Francois Cornet³, Marco Cosentino Lagomarsino⁴, Olivier Espéli^{1*}

1 Center for Interdisciplinary Research in Biology (CIRB), Collège de France, UMR-CNRS 7241, Paris, France, **2** Université Paris–Saclay, Gif-sur-Yvette, France, **3** Laboratoire de Microbiologie et de Génétique Moléculaires (LMGM), CNRS-Université Toulouse III, Toulouse, France, **4** UMR 7238, Computational and quantitative biology, Institut de biologie Paris Seine, Paris, France

 These authors contributed equally to this work.

* olivier.espeli@college-de-france.fr



 OPEN ACCESS

Citation: El Sayyed H, Le Chat L, Lebailly E, Vickridge E, Pages C, Cornet F, et al. (2016) Mapping Topoisomerase IV Binding and Activity Sites on the *E. coli* Genome. PLoS Genet 12(5): e1006025. doi:10.1371/journal.pgen.1006025

Editor: Patrick H. Viollier, University of Geneva Medical School, SWITZERLAND

Received: December 11, 2015

Accepted: April 11, 2016

Published: May 12, 2016

Copyright: © 2016 El Sayyed et al. This is an open access article distributed under the terms of the [Creative Commons Attribution License](https://creativecommons.org/licenses/by/4.0/), which permits unrestricted use, distribution, and reproduction in any medium, provided the original author and source are credited.

Data Availability Statement: Sequencing data are available on the GEO NCBI server with the accession number GSE75641.

Funding: This work was supported by grants from Agence Nationale de la Recherche, ANR sisters (ANR-10-JCJC-1204-0), and ANR Magisbac (ANR-14-CE10-0007). The funders had no role in study design, data collection and analysis, decision to publish, or preparation of the manuscript.

Competing Interests: The authors have declared that no competing interests exist.

Abstract

Catenation links between sister chromatids are formed progressively during DNA replication and are involved in the establishment of sister chromatid cohesion. Topo IV is a bacterial type II topoisomerase involved in the removal of catenation links both behind replication forks and after replication during the final separation of sister chromosomes. We have investigated the global DNA-binding and catalytic activity of Topo IV in *E. coli* using genomic and molecular biology approaches. ChIP-seq revealed that Topo IV interaction with the *E. coli* chromosome is controlled by DNA replication. During replication, Topo IV has access to most of the genome but only selects a few hundred specific sites for its activity. Local chromatin and gene expression context influence site selection. Moreover strong DNA-binding and catalytic activities are found at the chromosome dimer resolution site, *dif*, located opposite the origin of replication. We reveal a physical and functional interaction between Topo IV and the XerCD recombinases acting at the *dif* site. This interaction is modulated by MatP, a protein involved in the organization of the Ter macrodomain. These results show that Topo IV, XerCD/*dif* and MatP are part of a network dedicated to the final step of chromosome management during the cell cycle.

Author Summary

DNA topoisomerases are ubiquitous enzymes that solve the topological problems associated with replication, transcription and recombination. Type II Topoisomerases play a major role in the management of newly replicated DNA. They contribute to the condensation and segregation of chromosomes to the future daughter cells and are essential for the optimal transmission of genetic information. In most bacteria, including the model organism *Escherichia coli*, these tasks are performed by two enzymes, DNA gyrase and DNA Topoisomerase IV (Topo IV). The distribution of the roles between these enzymes during the cell cycle is not yet completely understood. In the present study we use genomic and molecular biology methods to decipher the regulation of Topo IV during the cell cycle.

Here we present data that strongly suggest the interaction of Topo IV with the chromosome is controlled by DNA replication and chromatin factors responsible for its loading to specific regions of the chromosome. In addition, our observations reveal, that by sharing several key factors, the DNA management processes ensuring accuracy of the late steps of chromosome segregation are all interconnected.

Introduction

DNA replication of a circular bacterial chromosome involves strong DNA topology constraints that are modulated by the activity of DNA topoisomerases [1]. Our current understanding of these topological modifications comes from extensive studies on replicating plasmids [2, 3]. These studies suggest that positive supercoils are formed ahead of the replication fork, while precatenanes are formed on newly replicated sister strands. At the end of a replication round, unresolved precatenanes accumulate in the region of replication termination and are converted to catenanes between the replicated sister chromosomes. Neither precatenanes or catenanes have been directly observed on chromosomes but their presence is generally accepted and failure to resolve them leads to chromosome segregation defects and cell death [4].

Topo IV is a type II topoisomerase formed by two dimers of the ParC and ParE subunits and is the main decatenase in *Escherichia coli* [5]. *in vitro*, its activity is 100 fold stronger on catenated circles than that of DNA gyrase [6]. Topo IV activity is dependent on the topology of the DNA substrate; Topo IV activity is strongest on positively supercoiled DNA and has a marked preference for L-braids, which it relaxes completely and processively. Topo IV can also unlink R-braids but only when they supercoil to form L-plectonemes [7–9]. *In vivo*, DNA gyrase appears to have multiple targets on the *E. coli* chromosome [10–12], whereas Topo IV cleavage sites seem to occur less frequently [11]. Interestingly, Topoisomerase IV activity is not essential for replication itself [13] but is critical for chromosome segregation [14]. The pattern of sister chromatid separation has been shown to vary upon Topo IV alteration, leading to the view that precatenanes mediate sister chromatid cohesion by accumulating for several hundred kilobases behind the replication forks keeping the newly replicated DNA together [13, 15]. The regulation of Topo IV and perhaps the accessibility of the protein to chromosome dimers was proposed to be an important factor controlling chromosome segregation [15, 16]. Topo IV activity can be modulated by a number of proteins including MukB and SeqA. MukB, is an SMC-related protein in *E. coli* and is reported to bind to the C-terminus of Topo IV [17] to enhance Topo IV unlinking activities [18, 19]. MukB also appears to be important in favoring the formation of Topo IV foci (clusters) near the origin of replication [20]. SeqA, a protein involved in the control of replication initiation, and Topo IV also interact [21]. These interactions may play a role in sister chromatid segregation at the late segregating SNAP regions near the origin of replication of the chromosome [16].

Beside its role in the resolution of precatenanes, Topo IV is mostly required in the post-replicative (G2) phase of the cell cycle for the resolution of catenation links. Indeed, *Espeli et al.* showed that Topo IV activity is mostly observed during the G2 phase, suggesting that a number of catenation links persist after replication [22]. Recent cell biology experiments revealed that in G2, the terminal region (*ter*) opposite *oriC* segregates following a specific pattern [23–25]. Sister *ter* regions remain associated from the moment of their replication to the onset of cell division. This sister-chromosome association is mediated by the Ter macrodomain organizing protein, MatP [26]. At the onset of cell division, the FtsK DNA-translocase processes this region, releasing the MatP-mediated association. This process ends at the *dif* site, when the

dimeric forms of the sister chromosomes are resolved by the XerC and XerD recombinases. A functional interaction between the MatP/FtsK/XerCD-*dif* system and Topo IV has long been suspected. FtsK interacts with Topo IV, enhancing its decatenation activity *in vitro* [27, 28] and the *dif* region has been reported as a preferential site of Topo IV cleavage [29]. This functional interaction has been poorly documented to date and is therefore remains elusive.

In this study we have used genomic and molecular biology methods to characterize Topo IV regulation during the *Escherichia coli* cell cycle on a genome-wide scale. The present work revealed that Topo IV requires DNA replication to load on the chromosome. In addition, we have identified two binding patterns: i) regions where Topo IV binds DNA but is not engaged in a cleavage reaction; ii) numerous sites where Topo IV cleavage is frequent. We show that Topo IV-mediated removal of precatenanes is influenced by both local chromatin structure and gene expression. We also demonstrate that at the *dif* site, Topo IV cleavage and binding are enhanced by the presence of the XerCD recombinase and the MatP chromosome-structuring factor. The enhancement of Topo IV activity at *dif* promotes decatenation of fully replicated chromosomes and through interaction with other DNA management processes, this decatenation ensures accurate separation of the sister chromosomes.

Results

Topoisomerase IV binding on the *E. coli* chromosome

To identify Topo IV binding, we performed ChIP-seq experiments in ParE and ParC Flag tagged strains. The C-terminus fusions of ParE and ParC replaced the wild-type (WT) alleles without any observable phenotypes (S1 Fig). We performed three independent experiments, two ParE-flag IPs and one ParC-flag IP, with reproducible patterns identified in all three experiments. A Pearson correlation of 0.8, 0.9 and 0.7 was observed for ParC-ParE1, ParE1-ParE2 and ParC-ParE2 respectively. A map of enriched regions observed in each experiment is represented on Fig 1A (red circles). Four of the highly-enriched sites are illustrated at a higher magnification in Fig 1A—right panels. Interestingly one of these sites corresponds to the *dif* site (position 1.58Mb), which has previously been identified as a strong Topoisomerase IV cleavage site in the presence of norfloxacin [29]. We also observed strong enrichment over rRNA operons, tRNA and IS sequences. To address the significance of the enrichment at rRNA, tRNA and IS, we monitored these sites in ChIP-seq experiments performed in the same conditions with a MatP-flag strain and mock IP performed with strain that did not contain any flag tagged protein. Both MatP and Mock IP presented significant signals on rRNA, tRNA and IS loci (S2 Fig). This observation suggested that Topo IV enrichment at rRNA, tRNAs and IS was an artifact of the ChIP-Seq technique. By contrast no enrichment was observed at the *dif* site in the MatP and mock-IP experiments (S2 Fig), we therefore considered *dif* to be a genuine Topo IV binding site and compared every enriched region (>2 fold) with the *dif* IP. We filtered the raw data for regions presenting the highest Pearson correlation with the *dif* signal (>0.7). This procedure discarded many highly enriched regions (Fig 1A orange circles). We identified 19 sites throughout the chromosome where Topo IV IP/input signal suggested a specific binding for at least two of the experiments (Fig 1A, outer circle histogram, S1 Table). Most Topo IV binding sites span a 200 bp region. These sites frequently overlapped intergenic regions, with their mid-points located inside the intergenic region, and did not correlate with any identifiable consensus sequence. In addition to *dif*, which exhibited a 10-fold enrichment, three other sites were strongly enriched. These sites corresponded to positions 1.25Mb (9.4x), 1.85Mb (31x) and 2.56Mb (19x) on the chromosome (Fig 1A, right panels). Beside these specific sites, Topo IV IP showed non-specific enrichment in the *oriC* proximal half of the chromosome. This bias was not a consequence of locus copy number, as the enrichment remained after copy number normalization (Fig 1B). We

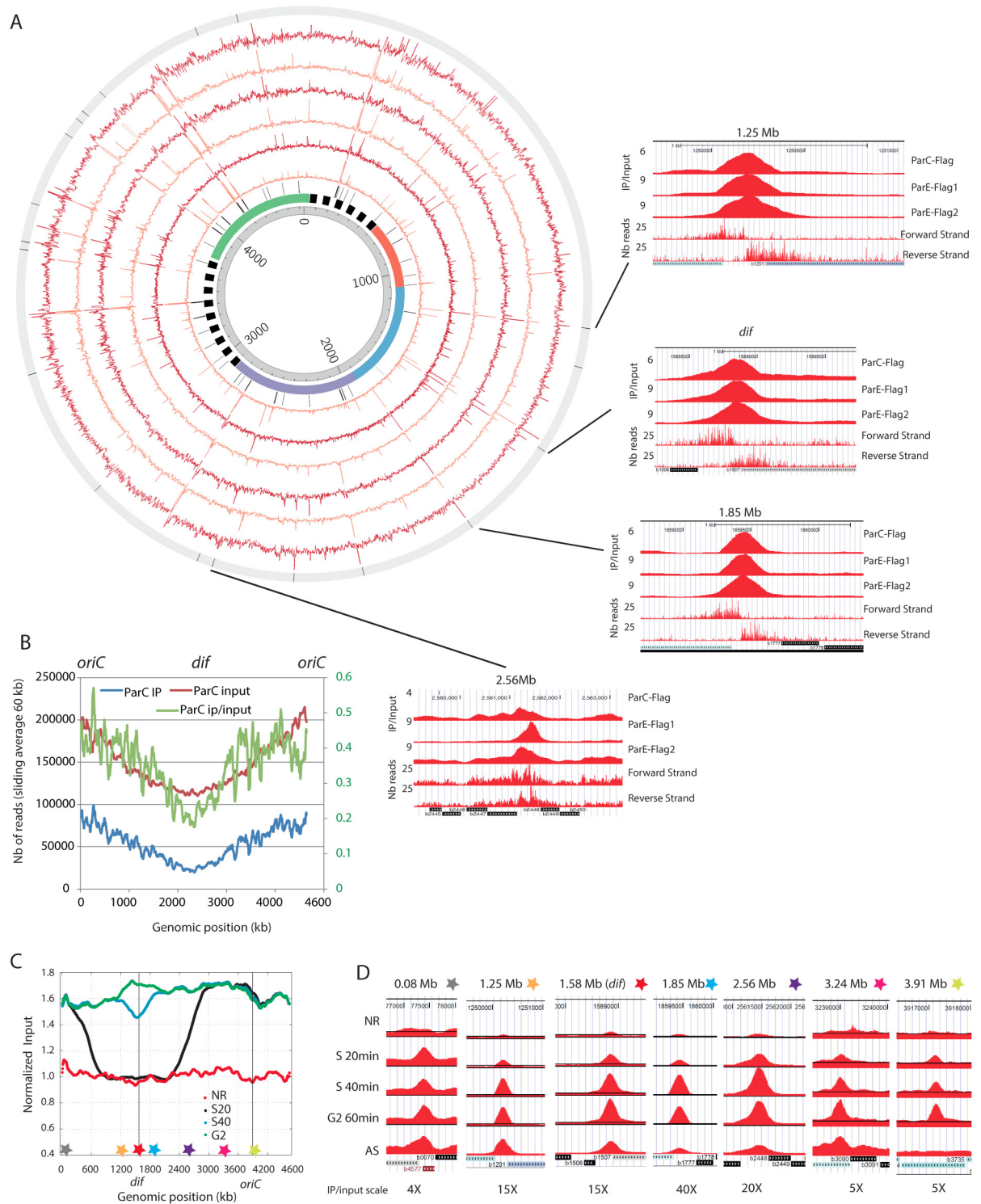


Fig 1. Topo IV binding pattern of replicating chromosome. A) Circos plot of the ChIP-seq experiments for ParC-flag and ParE-flag. The IP / input ratio over the entire *E. coli* genome is presented for three independent experiments, one IP on the *parC-flag* strain and two IPs on the *parE-flag* strain. From the center to the outside, circles represent: genomic coordinates, macrodomain map, position of tRNA genes and ribosomal operons, ParE-Flag 1 ChIP-seq (untreated data, orange), ParE-Flag 1 ChIP-seq (filtered data, red), ParE-Flag 2 ChIP-seq (untreated data, orange), ParE-Flag 2 ChIP-seq (filtered data, red), ParC-Flag ChIP-seq (untreated data, orange), ParC-Flag ChIP-seq (filtered data, red), position of the 19 validated Topo IV binding sites. The right panels represent magnifications for four specific Topo IV binding sites, position 1.25 Mb, position 1.58 Mb (*dif*), position 1.85 Mb and position 2.56Mb. The three first rows correspond to filtered IP/Input ratio for ParC-Flag, ParE-Flag1 and ParE-Flag2 IPs, the

fourth and fifth rows correspond respectively to the forward and reverse raw read numbers of the *parC-flag* experiment. The position and orientation of genes are illustrated at the bottom of each panel. B) Sliding averages of the IP (blue, left Y axis), Input (red, left Y axis) and IP/input (green, right Y axis) data for the *parC-flag* experiment over 60 kb regions along the genome. To facilitate the reading, *oriC* is positioned at 0 and 4.639 Mb. C) Analysis of Topo IV binding during the bacterial cell cycle. Marker frequency analysis was used to demonstrate the synchrony of the population at each time point. Stars represent the position of the selected Topo IV sites. D) IP/input ratio for 7 regions presenting specific Topo IV enrichment during S and G2 phases. For each genomic position the maximum scale is set to the maximum IP/Input ratio observed.

doi:10.1371/journal.pgen.1006025.g001

used MatP-Flag IP [30] and a control IP in a strain that does not contain a Flag tagged gene to differentiate non-specific Topo IV binding from experimental noise (S3A Fig). In addition, Topo IV enrichment was also observed in GC rich regions of the chromosomes (S3B Fig). Importantly, the *ori/ter* bias was not a result of the GC% bias along the chromosome since it was still explicit after GC% normalization (S3C Fig). More precisely, the Topo IV binding pattern closely followed gene dosage for a ~3Mb region centered on *oriC* (S3D and S3E Fig and S1 Text). In the complementary ter-proximal region, gene dosage (input reads) was higher than the ChIP-seq profile, suggesting that the nonspecific Topo IV binding was lower or lasts for a shorter time in the cell cycle (since these data are population-averaged). The Terminus region that is depleted in Topo IV binding (1.6Mb) surpassed, by far, the size of the Ter macrodomain (800kb).

Topo IV binding is influenced by replication

The influence of Topo IV on sister chromatid interactions [15] prompted the question of how Topo IV would follow replication forks and bind to the newly replicated sister chromatids throughout the cell cycle. We performed ChIP-seq experiments in *E. coli dnaC2* strains under conditions suitable for cell cycle synchronization of the entire population. Synchronization was achieved through a double temperature shift, as described previously [15]. Using these conditions, in each cell, S phase is initiated on one chromosome, lasts for 40–45 min and is followed by a G2 phase (20 min) (S4 Fig). We analyzed ParE binding before the initiation of replication, in S phase 20 min (S20) and 40 min (S40) after the initiation of replication and in G2 phase. The synchronization of replication in the population was monitored by marker frequency analysis of the Input DNA (Fig 1C). The profile observed for bacteria that did not replicate at non-permissive temperature was strictly flat, but the S20 replication profile presented two sharp changes of the marker frequency slope around positions 500kb and 2700kb. This suggested that each replication fork had crossed approximately 1000 to 1300 kb in 20 min. The S40 replication profile demonstrated that most cells had finished replication, with the unreplicated region being limited to 300 kb around *dif* in no more than 20% of the bacteria. In G2 phase the marker frequency was flat. We used flow cytometry to demonstrate that at G2, the amount of DNA in each bacterium was double compared to that of the G1 bacteria, indicating that cytokinesis has not yet occurred (S4 Fig). We analyzed Topo IV binding at specific binding sites (Fig 1D). Binding at these sites was strongly impaired in the absence of replication. Binding at every site started in the S20 sample and was maximal in the S40 or G2 samples, without showing any marked decrease, even in the *oriC*-proximal region. These observations suggest that Topo IV binds to specific sites during S phase. However, since enrichment was observed for non-replicated loci and was maintained for a long time after replication, it was not compatible with a model of Topo IV migration with the replication forks. Synchronization experiments with a higher temporal resolution are required to clarify this observation.

Only certain Topo IV binding sites correspond to Topo IV cleavage sites

To measure Topo IV cleavage at the binding sites, we took advantage of the fact that norfloxacin covalently links Topoisomerase II to the gate segment of DNA and prevent its relegation

[31]. We first monitored Topo IV activity on the Topo IV enriched regions (1.2, 1.8, 2.5, 3.2 Mb and *dif*) by incubating bacteria with norfloxacin for 10 minutes before genomic extraction and performing Southern blot analysis to detect the cleaved DNA products [10, 29]. This revealed cleavage fragments induced by both DNA Gyrase and Topo IV poisoning in the WT strain, but only Topo IV cleavage in a *nalR* strain where DNA Gyrase is resistant to norfloxacin. Among the 5 tested sites, only two displayed clear Topo IV cleavage at the expected position (Fig 2A). As expected, the *dif* site exhibited strong cleavage. Moreover cleavage was also observed at position 2.56 Mb. However the 1.2, 1.8 and 3.2 Mb sites did not show any Topo IV mediated cleavage in the presence of norfloxacin.

Topo IV presents hundreds of cleavage sites on the chromosome

The above result prompted us to investigate Topo IV cleavage at the genome-wide scale. We performed IPs in the presence of norfloxacin as a crosslinking agent instead of formaldehyde. Following this step, all downstream steps of the protocol were identical to that of the ChIP-Seq assay. We referred to this method as NorflIP. The NorflIP profile differed from the ChIP-seq profile (Fig 2B). Regions immunoprecipitated with Topo IV-norfloxacin cross-links were frequently observed (Fig 2C orange circle). Similarly to the ChIP-seq experiments, the NorflIP profile revealed strong enrichment over the rRNA operons and IS sequences but not at the tRNA genes (S5A Fig). We used a Southern blot cleavage assay to demonstrate that these signal did not correspond to Topo IV cleavages (S5B Fig). The NorflIP peaks correspond to a ~170 bp forward and reverse enrichment signal separated by a 130 bp segment, which is not enriched. This pattern is the consequence of the covalent binding of Topo IV to the 5' bases at the cleavage site. After Proteinase K treatment the cleaving tyrosine residue bound to the 5' extremity resulted in poor ligation efficiency and infrequent sequencing of the cleaved extremities. (S6A and S6B Fig) This observation confirmed that we were observing genuine Topoisomerase cleavage sites. We used this pattern to define an automatic peak calling procedure (S6C Fig) that identified between 134 and 458 peaks in the three NorflIP experiments, two experiments performed with ParC-Flag and one with ParE-Flag (Fig 2C purple circles and Fig 2D). We observed a total of 571 possible sites in the three experiments with about half of the sites common to at least two experiments and approximately 88 sites common to all three experiments (S1 Table). We analyzed sequencing reads for the three experiments around the *dif*, 0.2 Mb and 1.92Mb positions. It revealed abrupt depletions of forward and reverse reads in a 100bp center region suggesting that it corresponds to the site of cleavage. We extrapolated this result for every peak to estimate the cleavage positioning of Topo IV (~150bp downstream of the center of the forward peak, S6D Fig) We manually validated 172 sites that were common to ParC-1 and ParE-1 experiments (S1 Table) for further analysis.

Characteristics of Topo IV cleavage sites

The Topo IV cleavage at the *dif* site was the most enriched of the chromosome (~ 30 fold), fourteen sites were enriched from 5 to 10 fold and other positions were enriched from 2 to 5 fold (Fig 2E). Most NorflIP sites did not correspond to significant peaks in the ChIP-seq experiment (Fig 2E). We also did not observe any cleavage for the majority of the strong binding sites observed by ChIP-seq. This is illustrated for the binding site at 1.85 Mb (Fig 2E). We verified several Topo IV cleavage sites by Southern blot, a significant cleaved DNA fragment was observed at the expected size for each of them (Fig 2F). Southern blotting experiments following DNA cleavage in the presence of norfloxacin on synchronized cultures revealed that, like its binding, Topo IV cleavage is coordinated with DNA replication. In good agreement with

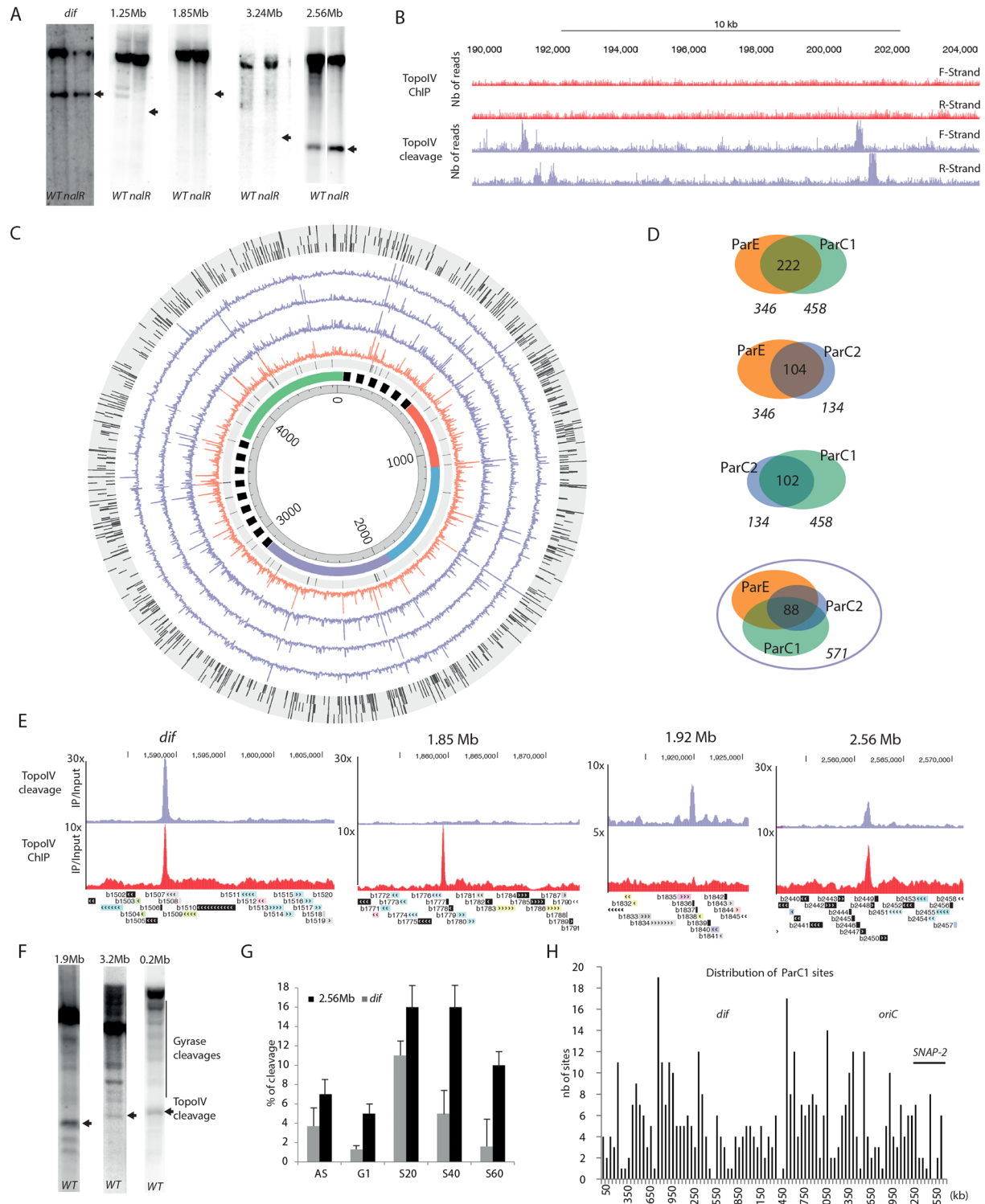


Fig 2. Topo IV cleavage at the Topo IV binding sites. A) Norfloxacin mediated DNA cleavage revealed by Southern blot with a radiolabeled probe near the *dif* site, the 1.25 Mb, 1.85 Mb, 2.56 Mb and the 3.24 Mb site. The size of the expected fragment generated by Topo IV cleavage is marked by an arrow. Topo IV cleavage can be differentiated from gyrase cleavages because of their presence in a *nalR* strain. B) Genome browser image of a 15kb region representative of Topo IV cleavage frequency (purple). These cleavage sites are not correlated with Topo IV enrichment in the ChIP-seq experiments described in Fig 1 (red). C) Circos plot of the NorfIIP experiments. From the center to the outside, circles represent: genomic coordinates, macrodomain map, position of

tRNA genes and ribosomal operons, ParC-Flag 1 NorfIIP (untreated data, orange), ParC-Flag 1 NorfIIP (filtered data, purple), ParE-Flag NorfIIP (filtered data, purple), ParC-Flag 2 NorfIIP (filtered data, purple), validated TopoIV sites present in the ParC-Flag 1, ParE-Flag and ParC-Flag 2 experiments. For visualization purpose, the maximum scale of NorfIIP data has been fixed to an IP/input ratio of 10. D) Peak calling procedure, dedicated to DNA cleavage mediated by TopoIV in the presence of norfloxacin (S6 Fig), revealed 571 sites in total, in three experiments. Venn diagrams of common Topo IV cleavage sites in two experiments. About 200 common sites are observed in each pair of experiments. E) Genome browser zooms on the *dif*, 1.85, 1.92 and 2.56 Mb regions for Topo IV cleavage (purple) and Topo IV binding revealed by ChIP-seq (red). F) DNA cleavage mediated by TopoIV in the presence of norfloxacin revealed by Southern blot with a radiolabeled probe at 0.02, 1.92 Mb and the 3.2 Mb sites. G) Cleavage experiments performed on synchronized cultures, revealed a replication dependency (AS asynchronous, NR not replicating, S20 20 min after the initiation of replication (IR), S40 40 min after IR, S60 60 min after IR. H) Distribution of the ParC-Flag 1 NorfIIP validated sites on the genome by 50 kb bins.

doi:10.1371/journal.pgen.1006025.g002

ChIP-seq experiments, increased cleavage was observed as soon as 20 minutes after initiation of replication for the *dif* and 2.56 Mb sites (Fig 2G).

Genomic distribution of Topo IV cleavage sites

The general genomic distribution of Topo IV cleavage sites was not homogeneous; a few regions had a large number of sites clustered together, while the 1.2Mb– 2.5 Mb region contained a low density of sites (Fig 2H). We further analyzed the distribution of cleavage sites in the terminus and the *oriC* regions. In the terminus region, the average distance of consecutive cleavage sites was long (around 30 kb in the 1.5–2.5 Mb region) compared to 8 kb in the 0.8–1.5 Mb or the 2.5–3.1 Mb regions (S7A Fig). The *oriC* region displays a mixed distribution (S7B Fig), a high density of sites near *oriC* flanked by two depleted regions, including the SNAP2 region [16]. At the gene scale, the mid-point of Topo IV cleavage signal can be localized inside genes (82%) or intergenic regions (16%) but it presents a bias toward the 5' or 3' gene extremities (S7C Fig). Since the cleavage signal spans approximately 200bp, nearly 50% of the sites overlapped, at least partly, with intergenic regions that account for only 11% of the genome. Finally, we did not identify any robust consensus between sets of Topo IV cleavage sites. The only sequence traits that we identified are a bias for GC dinucleotides near the center of the sites (S7D Fig) and an increased spacing of GATC motifs around cleavage sites (S7E Fig).

Targeting of Topo IV cleavage activity is influenced by local environment

The bias in the distribution of cleavage sites (Fig 2H) was very similar to the Topo IV binding bias revealed by ChIP-seq (Fig 1C). NorfIIP and ChIP-seq data were compared on Fig 3A. Despite the lack of corresponding ChIP-seq enrichment at the position of most highly enriched NorfIIP sites, a number of consistencies were observed between these two data sets. Overall the NorfIIP and ChIP-seq datasets had a Pearson correlation of 0.3 and the averaged data (1 kb bin) revealed a Pearson correlation of 0.5. First a small amount of local enrichment in the ChIP-seq experiments was frequently observed in the regions containing many cleavage sites (Fig 3A and 3C). This led us to consider that trapped Topo IV engaged in the cleavage reaction could contribute to a small amount of local enrichment in the ChIP-seq experiments. Second, both Topo IV cleavages and binding sites were rare in highly expressed regions (Fig 3A), only one of the 172 manually validated Topo IV cleavage site overlapped a highly expressed region. However cleavages sites were more frequently, than expected for a random distribution, observed in their vicinity (Fig 3C and S8 Fig). Thirty percent (50/172) of the Topo IV sites are less than 2 kb away from the next highly expressed transcription unit (Fig 3).

We explored correlations between the localization of Topo IV cleavages and binding sites of various NAPs thanks to the Nust database and tools [32]. A significant correlation was only observed for Fis binding sites (Fig 3B). Sixty eight genes present both Fis binding [33] and Topo IV cleavage (P value 2×10^{-03}). Thirty-three of the 172 manually validated cleavage sites

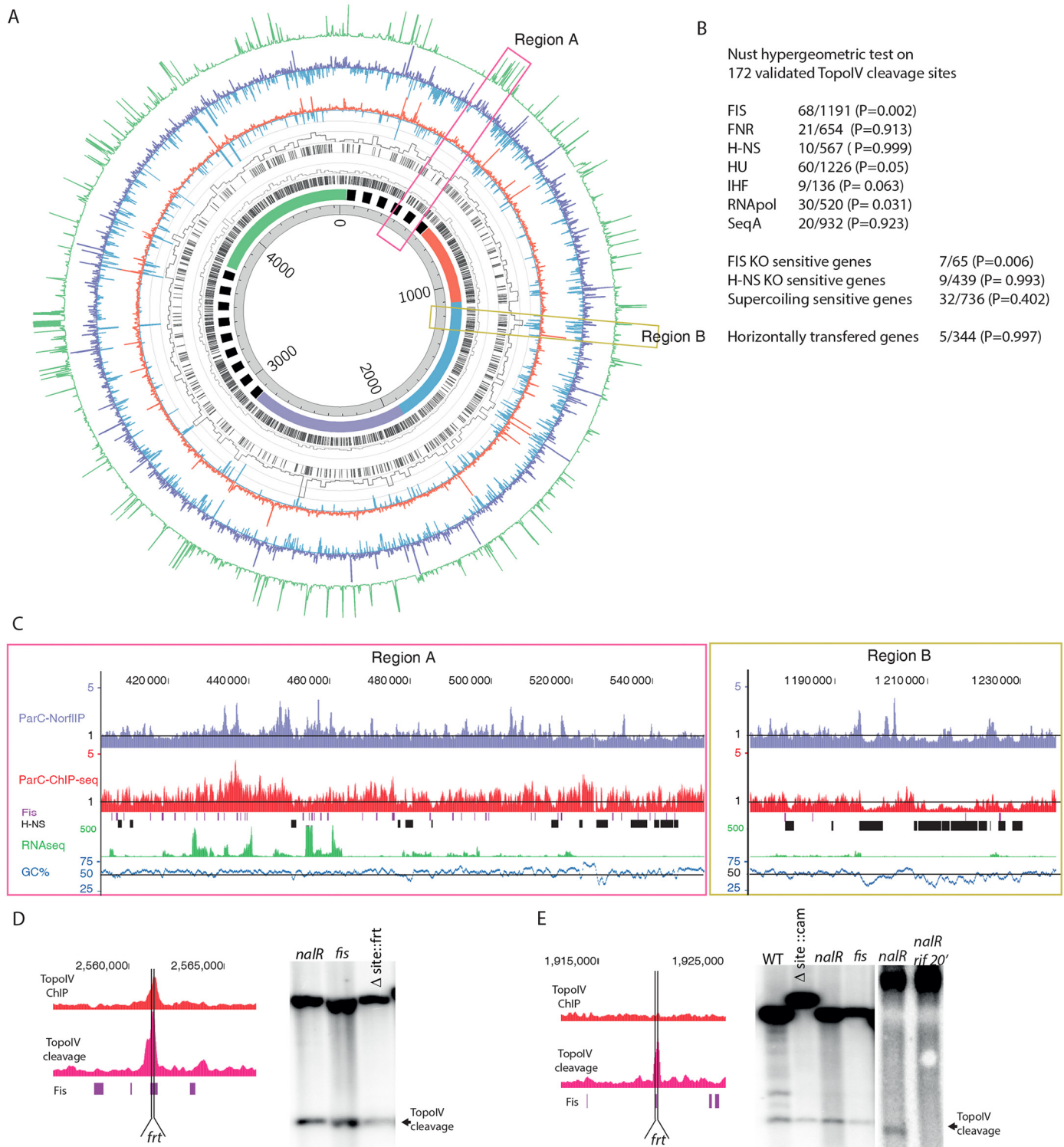


Fig 3. Targeting Topo IV cleavage sites along the *E. coli* genome. A) Circos plot of the ParC-Flag ChIPseq and ParC-Flag 1 NorfIIP experiments. From the center to the outside, circles represent: genomic coordinates, macrodomain map, Fis binding sites in mid exponential phase, % of bases bound by Fis per 20 kb windows of genomic DNA, H-NS binding sites in mid exponential phase, % of bases bound by H-NS per 20 kb windows of genomic DNA [33], ParC-Flag ChIP-seq (depleted regions blue, IP/input <1), ParC-Flag ChIP-seq (enriched regions red, IP/input >1), ParC-Flag 1 NorfIIP (depleted regions blue, IP/input <1), ParC-Flag 1 NorfIIP (enriched regions red, IP/input >1), gene expression data (RNA-seq results performed in the ChIP-seq and NorfIIP conditions). For visualization purpose, the maximum scale of RNAseq data has been fixed to 500 reads which

approximately corresponds to the 400 transcription units that were the most expressed (the distribution of read counts scaled from 0 to 30 000). B) Correlation between the localization of Topo IV cleavages and chromatin markers. The NUST [32] hypergeometric test was used to compare Topo IV and chromatin markers localization. The set of 172 validated Topo IV cleavage sites was used. The number of common localizations over the total number of chromatin marker localization is indicated. The P value of a Fisher's exact test is indicated. C) Genome browser magnifications of the panel A's pink and yellows regions. Mid log phase Fis and H-NS binding sites are respectively indicated with burgundy and black boxes [33]. D) Magnification of the 2.56 Mb Topo IV binding and cleavage site that overlaps a Fis binding site. The position of the deleted Topo IV site is marked by vertical lines (*frt*). Southern blot analysis of Topo IV cleavage at the 2.56 Mb locus, in the *nalR* strain, the *nalR* strain with a deletion of the Topo IV cleavage and binding site and the deletion of *fis*. E) Same as D for the 1.92 Mb Topo IV cleavage site. Southern blot analysis of Topo IV cleavage at the 1.92 Mb locus, in the WT, the *nalR* strain, the *nalR* strain with a deletion of the Topo IV cleavage and Fis binding site and the *nalR* strain with *fis* deletion. The cleavage was also analyzed following a 20 min treatment with rifampicin (*rif*).

doi:10.1371/journal.pgen.1006025.g003

overlapped at least partially with a Fis binding site, 80 of them are located less than 400 bp away from a Fis binding site. At the genome scale this correlation is difficult to observe (Fig 3A), but close examination clearly revealed overlapping Topo IV cleavages and Fis binding sites (Fig 3C). Fis binding sites are more numerous than Topo IV cleavage sites, therefore a large number of them do not present enrichment for Topo IV (Fig 3C). By contrast, Topo IV peaks are excluded from H-NS rich regions (Fig 3A, 3B and 3C). Only one of the 172 manually validated Topo IV cleavage site overlapped with an H-NS binding site. As observed for highly expressed regions Topo IV cleavage sites were frequently observed at the border of H-NS rich regions (Fig 3C). Moreover H-NS rich regions contain less Topo IV than the rest of the chromosome (Fig 3A–3D and S9A Fig). H-NS rich regions correspond to an AT rich segment of the chromosome (Fig 3C and 3D). Indeed background level of Topo IV binding and cleavage were significantly reduced in AT rich regions (S9B Fig). In rare occasions binding of H-NS has been observed in regions with a regular AT content (Fig 3C), notably Topo IV binding and cleavage were also reduced in these regions. This observation suggested that H-NS itself rather than AT content limits the accessibility of Topo IV to DNA. This observation was confirmed by the identification of Topo IV cleavage in regions with an AT content ranging from 20 to 80% (S9C and S9D Fig).

We performed Southern blot analysis of Topo IV cleavage on representative sites to test whether gene expression and chromatin factors influenced Topo IV site selection. First, we observed that the exact deletion of cleavage sites at position 1.92 Mb and 2.56 Mb did not abolish Topo IV cleavage activity (Fig 3D and 3E). Second, since these loci also contain a Fis binding site overlapping Topo IV cleavage signal, we deleted the *fis* gene. However, deletion of the *fis* gene did not modify Topo IV cleavage (Fig 3D and 3E). Finally we performed cleavage assays in the presence of rifampicin to inhibit transcription. To limit the pleiotropic effects of rifampicin addition we performed the experiment with a 20 min pulse of rifampicin. Rifampicin treatment abolished Topo IV cleavage (Fig 3E). These results suggest that gene expression rather than chromatin factors influences Topo IV targeting.

XerC targets Topo IV to the *dif* site

Our analysis confirms that the *dif* region is a hot spot for Topo IV activity [29]. Indeed, ChIP-seq and NorfIIP show that Topo IV binds to and cleaves frequently in the immediate proximity of *dif*. We measured DNA cleavage by Topo IV in the presence of norfloxacin in various mutants affecting the structure of *dif* or genes implicated in chromosome dimer resolution. Southern blot was used to measure Topo IV cleavage (Fig 4A). We observed that exact deletion of *dif* totally abolished Topo IV cleavage. Interestingly, the deletion of the XerC-binding sequence (XerC box) of *dif* was also sufficient to abolish cleavage, while the deletion of the XerD box only had a weak effect. Deletion of the *xerC* and *xerD* genes abolished Topo IV cleavage at *dif*. However, cleavage was restored when the catalytically inactive mutants XerC K172A or XerC K172Q were substituted for XerC (Fig 4B). This suggests that the role of XerCD/*dif* in

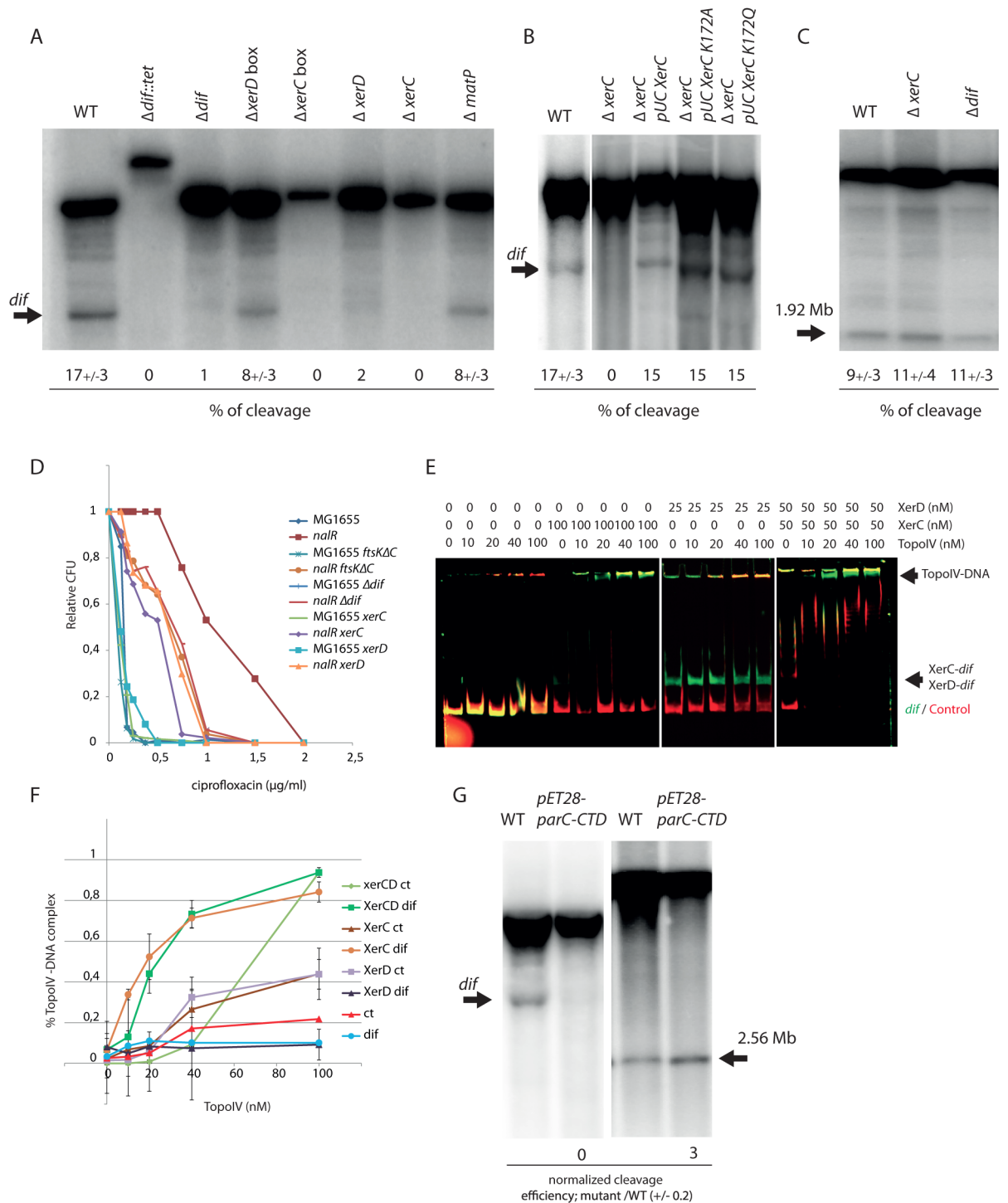


Fig 4. Determinants of Topo IV activity at *dif*. A) Southern blot analysis of the Topo IV cleavage at the *dif* site. Genomic DNA extracted from WT, $\Delta dif::Tc$, Δdif , $\Delta xerD$ box, $\Delta xerC$ box, $\Delta xerD$, and $\Delta xerC$ strains was digested by *Pst*I; the size of the fragment generated by Topo IV cleavage at *dif* is marked by an arrow. The average percentage of cleavage observed in two independent experiments is presented. B) Southern blot analysis of the Topo IV cleavage at the *dif* site. Genomic DNA extracted from WT, $\Delta xerC$, $\Delta xerC$ pUCxerC, $\Delta xerC$ pUCxerCK172A, $\Delta xerC$ pUCxerCK172Q strains was digested with *Pst*I; the size of the cleaved fragment in *dif* is marked by an arrow. C) Topo IV cleavage at the 1.9Mb site in the WT, $\Delta xerC$ and Δdif . D) Plating of *parEts*, *parEts* *xerC*, *parEts* *xerD* and *parEts* *recN* mutants at 30 and 37°C. E) Colony Forming Unit (CFU) analysis of the WT and *nalR* strains deleted for the *dif* site, the *xerC*, *xerD* genes or the C-terminal domain of FtsK in the presence of ciprofloxacin. F) EMSA on a 250 bp CY3 probe containing *dif* (green) and a 250 bp CY5 control probe (red). The amount of Topo IV, XerC or XerD proteins present

in each line is indicated above the gel. G) Quantification of Topo IV EMSA presented in C, data are an average of three experiments. H) Southern blot analysis of Topo IV cleavage at *dif* and position 1.92Mb in a strain overexpressing the C-terminal domain of ParC.

doi:10.1371/journal.pgen.1006025.g004

the control of Topo IV activity is structural and independent of XerCD catalysis. Deletion of *dif* or *xerC* did not significantly alter cleavage at any of the other tested Topo IV cleavage sites (Fig 4C). This suggests that influence of XerC on Topo IV is specific to *dif*.

To evaluate the role of XerCD-mediated Topo IV cleavage at *dif*, we attempted to construct *parEts xerC*, *parEts xerD* and *parCts xerC* double mutants. We could not obtain *parCts xerC* mutants by P1 transduction at any tested temperature. We obtained *parEts xerC* and *parEts xerD* mutants at 30°C. The *parEts xerC* double mutant presented a growth defect phenotype at 30°C and did not grow at temperature above 35°C (Fig 4D). The *parEts xerD* mutant presented a slight growth defect at 37°C compared to *parEts* or *xerD* mutants. None of the *parEts* mutant grew above 42°C. Next, we used quinolone sensitivity as a reporter of Topo IV activity. To this aim, we introduced mutants of the FtsK/Xer system into a *gyrA^{nalR}* (*nalR*) strain; Topo IV is the primary target of quinolones in such strains. The absence of XerC, XerD, the C-terminal activating domain of FtsK or *dif* exacerbated the sensitivity of the *nalR* strain to ciprofloxacin (Fig 4D). We therefore concluded that the impairment of Topo IV was more detrimental to the cell when the FtsK/Xer system was inactivated. Among partners of the FtsK/Xer system the absence of XerC was significantly the most detrimental, suggesting a specific role for XerC in this process.

The above results suggest an interaction between Topo IV and the XerCD/*dif* complex. We therefore attempted to detect this interaction directly *in vitro* (Fig 4E and 4F). We performed EMSA with two fluorescently labeled linear probes, one containing *dif* and the other containing a control DNA not targeted by Topo IV in our genomic assays. Topo IV alone bound poorly to both probes (Kd > 100nM). Binding was strongly enhanced when XerC or both XerC and XerD were added to the reaction mix. In contrast, Topo IV binding to *dif* was slightly inhibited in the presence of XerD alone. These results were consistent with the observation that deletion of the XerC box but not of the XerD box inhibited Topo IV cleavage at *dif* and pointed to a specific role for XerC in Topo IV targeting. The control fragment showed that these effects are specific to *dif*. Topo IV-XerC/*dif* complexes were stable and resisted a challenge by increasing amount of XerD (S10A Fig). The positive influence of XerCD on TopoIV binding was also observed on a negatively supercoiled plasmid containing *dif*. In the presence of XerCD (50nM), a delay in the plasmid migration was observed with 40nM of TopoIV. By contrast, 200 nM was required in the absence of XerCD (S10B Fig). The Southern blot cleavage assay showed that overexpression of the ParC C-terminal domain (pET28parC-CTD) strongly reduced cleavage at *dif* but enhanced cleavage at the Topo IV site located at 2.56Mb. This suggested that, as observed for MukB [17], Topo IV might interact with XerC through its C-terminal domain (Fig 4G).

Topo IV activity at *dif* depends on dynamics of the *ter* region and chromosome circularity

We assayed the effects of the reported Topo IV modulators and proteins involved in chromosome segregation the activity of Topo IV at *dif*. MukB has previously been shown to influence the activity of Topo IV [17, 18]. We measured Topo IV cleavage in a *mukB* mutant at *dif* and at position 2.56 Mb, cleavage was reduced at *dif* but no significant effect was observed at position 2.56Mb (Fig 5A). We did not detect any effect of a *seqA* deletion on Topo IV cleavage at either position (Fig 5B). We next assayed the effect of MatP, which is required for compaction and

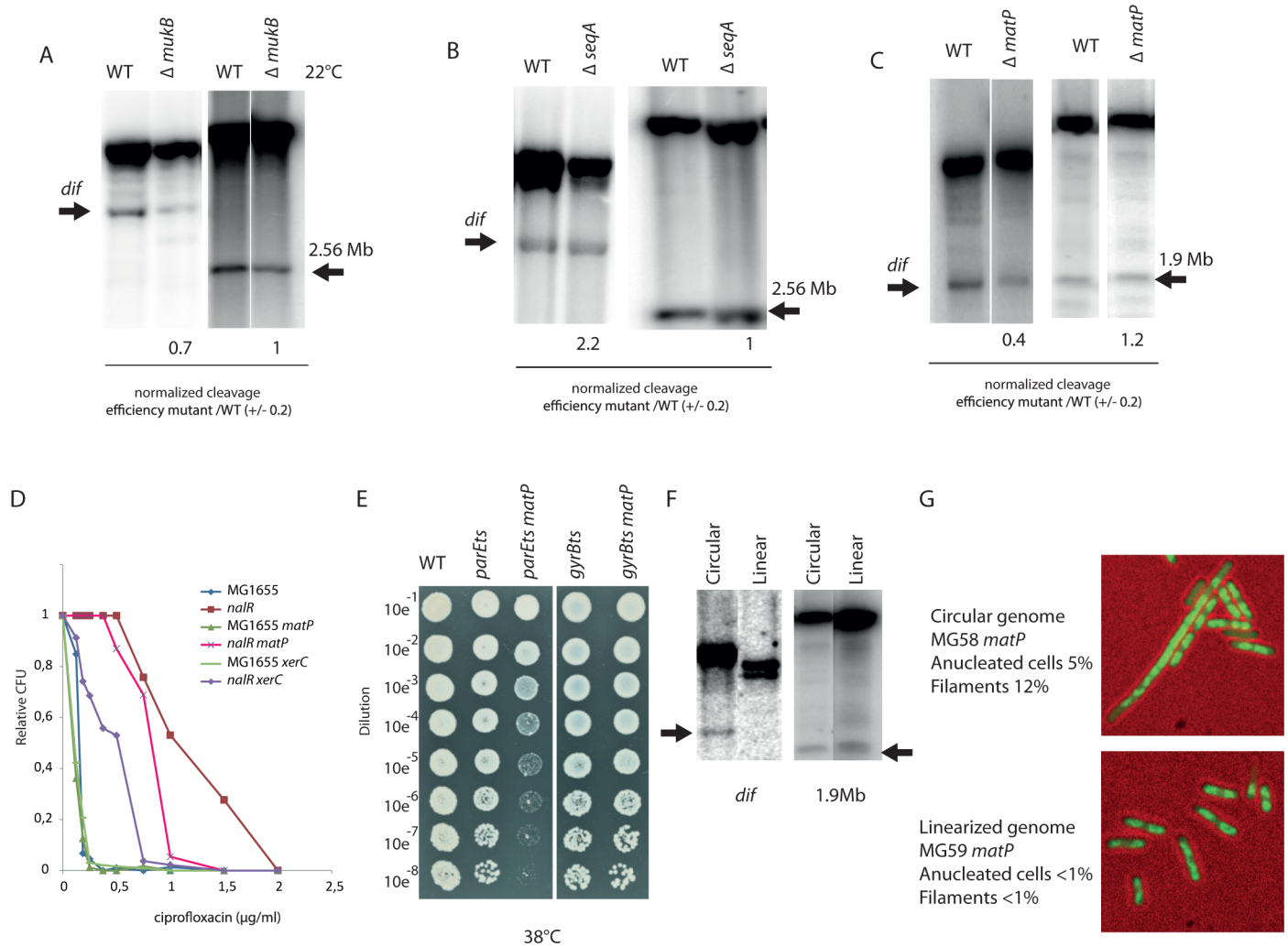


Fig 5. Role of the *dif* site for the management of circular chromosomes. A) Southern blot analysis of Topo IV cleavage at the *dif* and 2.56 Mb sites in the *mukB* mutant grown in minimal medium at 22°C. B) Southern blot analysis of Topo IV cleavage at the *dif* and 2.56 Mb sites in the *seqA* mutant grown in minimal medium at 37°C. C) Southern blot analysis of Topo IV cleavage at the *dif* and 1.9 Mb sites in the *matP* mutant grown in LB at 37°C. D) Colony Forming Unit (CFU) analysis of the WT and *nalR* strains deleted for the *dif* site, the *xerC* and *matP* genes in the presence of ciprofloxacin. E) Colony Forming Unit (CFU) analysis of the WT, *parEts* and *gyrBts* strains deleted for the *matP* at a semi permissive temperature (38°C). F) Southern blot analysis of the Topo IV cleavage at the *dif* and 1.9Mb sites in cells with a circular or linearized chromosome. G) Phenotypes observed during exponential growth in LB in the *matP* mutant strains with circular or linear chromosome (DNA is labeled with DAPI, green). Scale bar is 5µm.

doi:10.1371/journal.pgen.1006025.g005

intracellular positioning of the *ter* region as well as for its progressive segregation pattern ending at *dif* [25, 26]. The Topo IV cleavage at *dif* was significantly impaired in the *matP* mutant (Fig 5C). The Topo IV cleavage site at position 1.9Mb is included in the Ter macrodomain, but cleavage at this site was almost unchanged in the absence of MatP (Fig 5C). Introduction of a *matP* deletion into the *nalR* strain yielded an increase in ciprofloxacin sensitivity (Fig 5D). We also constructed a *parEts matP* double mutant. Growth of this strain was significantly altered compared to the *parEts* parental strain at an intermediate temperature (Fig 5E). Such a synergistic effect was not found when combining the *matP* deletion with a *gyrBts* mutation. Taken together, these results led us to consider that MatP itself or the folding of the Ter macrodomain might be important for Topo IV targeting at *dif*.

Since the FtsK/Xer/*dif* system is dedicated to post-replicative events that are specific to a circular chromosome, it was tempting to postulate that the activity of Topo IV at *dif* is also dedicated to post-replicative decatenation events and is strictly required for circular chromosomes. To address this question, we used *E. coli* strains harboring linear chromosomes [34]. In this strain, expression of TelN from the N15 phage promotes linearization of the chromosome at the *tos* site inserted a 6kb away from *dif*. Indeed, chromosome linearization suppresses the phenotypes associated with *dif* deletion [34]. We analyzed cleavage at the *dif* site by Topo IV in the context of a linearized chromosome. Cleavage was completely abolished; showing that Topo IV activity at *dif* is not required on linear chromosomes. This effect was specific to the *dif* site, since cleavage at the 1.9Mb site remained unchanged after chromosome linearization (Fig 5F). We next assayed if the phenotypes associated with *matP* deletion, i.e., formation of elongated cells with non-partitioned nucleoids [26], depend on chromosome circularity. Strikingly, most of the phenotypes observed in the *matP* mutant were suppressed by linearization of the chromosome (Fig 5G). Interestingly, the frequency of cleavage at *dif* sites inserted far (300 kb) from the normal position of *dif* or in a plasmid were significantly reduced compared to the WT situation (S11 Fig) confirming that Topo IV cleavage at *dif* is specific to circular chromosomes.

Discussion

Specific Topo IV binding and cleavage sites on the chromosome

Whole genome analysis of Topo IV binding by ChIP-seq revealed approximately 10 Topo IV binding sites across the *E. coli* genome. Among them, only 5 sites were strongly enriched in every experiment and these were mapped to positions 1.25, 1.58 (*dif*), 1.85, 2.56 and 3.24 Mb. We did not identify any consensus sequence that could explain specific binding to these sites. Band shift experiments at the *dif* site and the 1.25 Mb site revealed that Topo IV binding is not sequence-dependent.

This led us to favor models involving exogenous local determinants for Topo IV binding as it is the case for the *dif* site in the presence of XerC. Because XerC is only known to bind to *dif*, we could speculate that other chromatin factors might be involved in Topo IV targeting. Topo IV and Fis binding sites [33] overlap more frequently than expected (Nust P value $10e-03$ [32]). Topo IV and Fis binding sites overlap at the positions 1.25 and 2.56 Mb; it is therefore possible that Fis plays a role in defining some Topo IV binding sites. However our EMSA, cleavage and ChIP experiments did not show any cooperative binding of Topo IV with Fis. In spite of its colocalization with Topo IV, Fis does not contribute in defining Topo IV binding or cleavage sites. Nevertheless, the role of the chromatin in Topo IV localization was also illustrated by the strong negative correlation observed for the Topo IV and H-NS bound regions. H-NS rich regions were significantly less enriched for nonspecific Topo IV binding than the rest of the chromosome.

Topo IV mediated DNA cleavage sites

We postulated that loci where Topo IV is catalytically-active could be identified by DNA cleavage mediated by the quinolone drug norfloxacin. We designed a new ChIP-seq strategy that consisted of capturing DNA-norfloxacin-Topo IV complexes. We called it NorfIIP. Three independent experiments show that Topo IV was trapped to a large number of loci (300 to 600) with most of these loci observed in two out of three experiments. A hundred of these loci were identified in all three experiments. *Dif* presented a strong signal in the NorfIIP as in the ChIP-seq but this is not the case for most of the other ChIP-seq peaks. NorfIIP peaks presented a characteristic pattern suggesting that they are genuine DNA-norfloxacin-Topo IV complexes. Considering that norfloxacin does not alter Topo IV specificity, our results suggest that for Topo IV the genome is divided into five categories: i) Loci where Topo IV binds strongly but remains inactive

for most of the cell cycle; ii) Loci where Topo IV is highly active but does not reside for very long time; iii) Loci where we observed both binding and activity (*dif* and 2.56 Mb); iv) regions where Topo IV interacts non-specifically with the DNA and where topological activity is not stimulated; v) regions where non-specific interactions are restricted (the Ter domain, chromatin rich regions (tsEPODs [35], H-NS rich regions). Detection of norfloxacin-mediated genomic cleavage by pulse field electrophoresis has previously revealed that when Topo IV is the only target of norfloxacin the average fragment size is 300–400 kb while it drops to 20 kb when Gyrase is the target [11]. This suggests that, for each cell, no more than 10 to 20 Topo IV cleavages are formed in 10 min of norfloxacin treatment. To fit this observation with our data, only a small fraction (10–20 out of 600) of the detected Topo IV cleavage sites would actually be used in each cell. This might explain why Topo IV cleavage sites were hardly distinguishable from background in the CHIP-seq assay (Fig 3). This is in good agreement with the estimation that the catalytic cycle only provokes a short pause (1.8 sec) in Topo IV dynamics [36]. The mechanism responsible for the choice of specific Topo IV cleavage sites is yet to be determined. As indicated by our findings that deletion of the cleavage site resulted in the formation of a new site or sites in the vicinity, cleavage is not directly sequence-related. We observed several biases that might be involved in determination of cleavage sites (GC di-nucleotide skew, GATC spacing, positioning near gene ends or intergenic regions, proximity with highly expressed genes and Fis binding regions). Interestingly inhibition of transcription with rifampicin inhibits Topo IV cleavage (Fig 3). This raises the possibility that transcription, that can be stochastic, may influence stochastic determination of Topo IV activity sites. The influence of transcription could be direct, if RNA polymerase pushes Topo IV to a suitable place, or indirect if the diffusion of topological constraints results in their accumulation near barriers imposed by gene expression [37, 38]. This accumulation could then, in turn, signal for the recruitment of Topo IV.

Replication influences Topo IV binding and activity

Synchronization experiments revealed that, like Topo IV binding at specific sites, Topo IV cleavage activity is enhanced by chromosome replication. Enrichment was the highest in late S phase or G2 phase; it seems to persist after the passage of the replication fork at a defined locus. Enrichment in asynchronous cultures was significantly reduced compared to S40 or G2 synchronized cultures suggesting that Topo IV is not bound to the chromosome for the entire cell cycle. Unfortunately our experiments did not have the time resolution to determine at what point of the cell cycle Topo IV leaves the chromosome and if it would leave the chromosome during a regular cell cycle. The role of DNA replication of Topo IV dynamics has recently been observed by a very different approach [36]. The authors propose that Topo IV accumulates in the *oriC* proximal part of the chromosome in a MukB and DNA replication dependent process. These observations are in good agreement with our data and suggest that Topo IV is loaded on DNA at the time of replication, accumulate towards the origin of replication and remains bound to the DNA until a yet unidentified event triggers its release. Formation of positive supercoils and precatenanes ahead and behind of the replication forks respectively, could be the reason for Topo IV recruitment. One could hypothesize that MukB is used as a DNA topology sensor that is responsible for redistribution of Topo IV. However we only detected a modest effect of *mukB* deletion on Topo IV cleavage at *dif* (Fig 5). Putative events responsible for Topo IV release could be, among others, complete decatenation of the chromosome, SNAPs release, or stripping by other proteins such as FtsK.

Non-specific Topo IV binding

Non-specific Topo IV binding presents a very peculiar pattern; it is significantly higher in the *oriC* proximal 3Mb than in the 1.6Mb surrounding *dif*. This pattern is not simply explained by

the influence of replication (S3 Fig). Interestingly, ChIP-seq and ChIP-on-Chip experiments have already revealed a similar bias for DNA gyrase [12] and SeqA [39]. The CbpA protein has been shown to present an inverse binding bias [40], with enrichment in the terminal region and a reduction in the *oriC* proximal domain. The HU regulon has also presented a similar bias [41]. The terminus domain defined by these biases always comprises the Ter macrodomain but it extends frequently beyond the extreme *matS* sites. The role of MatP in the definition of these biases has not yet been tested. The group of G. Mushelishvili proposed a topological model to interpret the DNA gyrase and HU regulon biases, suggesting that HU coordinates the global genomic supercoiling by regulating the spatial distribution of RNA polymerase in the nucleoid [41]. Topo IV could benefit from such a supercoiling gradient to load on the chromosome. Interestingly, the strongest Topo IV binding and cleavage sites are localized inside the Terminus depleted domain. One possibility could be that these sites minimize Topo IV binding to adjacent nonspecific sequences. Alternatively one can propose that a regional reduction of non-specific binding creates a selective advantage for optimal loading on to specific sites.

Dif and the control of decatenation

Dif was the strongest Topo IV cleavage site detected by NorfIP, it was also detected in the ChIP-seq assays. We have used Southern blot to analyze the determinants involved in this activity. The binding of XerC on the *xerC* box of *dif* and the region downstream of the *xerC* box are essential. *In vitro*, XerC also strongly favors binding of Topo IV at *dif*. Interestingly XerD and the *xerD* box did not improve Topo IV binding or cleavage. We propose that XerC works as a scaffold for Topo IV, simultaneously stimulating its binding and its activity. Topo IV activity at *dif* is also dependent on the circularity of the chromosome, suggesting that when topological constraints can be evacuated through chromosome ends, Topoisomerase IV does not catalyze strand passage at *dif*. This suggests that topological complexity is directly responsible for Topo IV activity. Topo IV cleavage activity at *dif* is not influenced by SeqA or FtsK, which are two known Topo IV partners. Interestingly, *mukB* and *matP* deletion mutants slightly reduced this activity. The synergistic effect observed when a *matP* deletion is combined with a *parEts* mutation suggests that MatP indeed influences Topo IV activity. The phenotypes of the *matP* mutant are rescued by the linearization of the chromosome. A similar rescue has been observed for the *dif* mutant [34]. Therefore it is likely that a significant part of the problems that cells encounter in the absence of *matP* corresponds to failure in chromosome topology management, either decatenation or chromosome dimer resolution [25]. In conclusion, we propose that genomic regulation of Topo IV consists of: (1) Topo IV loading during replication, (2) Topo IV binding to specific sites that may serve as reservoirs, (3) Topo IV activation to remove precatenanes or positive supercoils in a dozen of stochastically chosen loci (4) XerC and MatP ensuring the loading of Topo IV at the *dif* site for faithful decatenation of fully replicated chromosomes.

Materials and Methods

ChIP-seq assay

ParE-flag and ParC-flag C-terminus fusions were constructed by lambda red recombination [42]. Cultures were grown in LB or Minimal medium A supplemented with succinate (0.2%) and casamino acids (0.2%). Cells were fixed with fresh Formaldehyde (final concentration 1%) at an OD_{600nm} 0.2–0.4. Sonication was performed with a Bioruptor Pro (Diagenode). Immunoprecipitations were performed as previously described²⁶. Libraries were prepared according to Illumina's instructions accompanying the DNA Sample Kit (FC-104-5001). Briefly, DNA was

end-repaired using a combination of T4 DNA polymerase, *E. coli* DNA Pol I large fragment (Klenow polymerase) and T4 polynucleotide kinase. The blunt, phosphorylated ends were treated with Klenow fragment (3' to 5' exo minus) and dATP to yield a protruding 3- 'A' base for ligation of Illumina's adapters which have a single 'T' base overhang at the 3' end. After adapter ligation DNA was PCR amplified with Illumina primers for 15 cycles and library fragments of ~250 bp (insert plus adaptor and PCR primer sequences) were band isolated from an agarose gel. The purified DNA was captured on an Illumina flow cell for cluster generation. Libraries were sequenced on the Genome Analyzer following the manufacturer's protocols.

Norflip assay

Norfloxacin (final concentration 2 μ M) was added to the cultures at OD_{600nm} 0.2 LB for 10 min before harvesting. Sonication and immunoprecipitation were performed as described for the ChIP-seq assay.

Analysis of sequencing results

Sequencing results were processed by the IMAGIF facility. Base calls were performed using CASAVA version 1.8.2. ChIP-seq and NorfIP reads were aligned to the *E. coli* NC_000913 genome using BWA 0.6.2. A custom made pipeline for the analysis of sequencing data was developed with Matlab (available on request). Briefly, the number of reads for the input and IP data was smoothed over a 200bp window. Forward and reverse signals were added, reads were normalized to the total number of reads in each experiment, strong non-specific signals observed in unrelated experiments were removed, data were exported to the UCSC genome browser for visualization and comparisons. The strongest peaks observed with NorfIP experiments (*dif* and 1.9 Mb) present a characteristic shape (S6 Fig) that allows the automatic detection of lower amplitude peaks but preserves the characteristic shape. We measured Pearson correlation coefficient with the *dif* and the 1.9 Mb site for 600bp sliding windows over the entire genome. Peaks with a Pearson correlation above 0.72 were considered as putative Topo IV cleavage sites. Sequencing data are available on the GEO Repository (<http://www.ncbi.nlm.nih.gov/geo/>) with the accession number GSE75641. Data were plotted with the Circos tool [43] and UCSC Archaeal Genome Browser [44].

Southern blot

Cleavage of DNA by Topo IV in the presence of Norfloxacin was monitored by Southern blot as previously described [10]. DNA was extracted from *E. coli* culture grown in minimal medium supplemented with glucose 0.2% and casaminoacids 0.2%. Norfloxacin (final concentration 10 μ M) was added to the cultures at OD 0.2 for 10 min before harvesting. DNA was transferred by neutral blotting on nitrocellulose membranes. For synchronization experiments a flash freeze step in liquid nitrogen is included before harvesting. Quantification was performed with Image J software.

EMSA

Experiments were conducted using Cy3-coupled probes harboring the *dif* site and a Cy5-coupled dye as control. Reactions were carried out in EMSA reaction buffer (1mM spermidine, 30mM potassium glutamate, 10mM DTT, 6mM magnesium chloride, 10% glycerol, pH 7.4). Reactions were incubated for 15 min at RT, loaded on 4% native PAGE gel at 25 volts and then run at 125 volts for 2 hours. Gels were then visualized using a Typhoon FLA 5000 scanner (GE healthcare Life Science). EMSA of plasmids were performed with unlabeled supercoiled

plasmid in the same reaction buffer. Electrophoresis was performed in a 0.8% agarose gel in 0.5x TAE buffer at 4°C for 80 min at 150V. DNA labeling was performed with SYBR green.

Supporting Information

S1 Fig. A) Measure of the colony formation unit (CFU) of the WT, *nalR*, ParC-Flag, ParC-Flag *nalR* and ParE-Flag *nalR* strains. Culture were grown until OD 0.2 and treated for 40 minutes with norfloxacin 2 μ M and plated on LB plates. **B)** Measure of the growth rate of the *nalR*, ParC-Flag *nalR* and ParE-Flag *nalR* strains. **C)** Southern blot analysis of Topo IV mediated cleavage in the presence of norfloxacin at the 1.9 Mb site in the WT, *nalR* and ParC-Flag *nalR* and ParE-Flag *nalR* strains.

(PDF)

S2 Fig. Genome browser magnifications illustrating common non-specific signal observed over rRNA operons, tRNA and IS sequences. ParE-Flag ChIP-seq is represented in red, MatP-Flag ChIP-seq is represented in blue, Mock IP with a strain that did not contain Flag tagged proteins is represented in black. Genes, ribosomal operons and tRNA are represented below ChIPseq signals

(PDF)

S3 Fig. A) Analysis of the Topo IV nonspecific binding. Normalized enrichment (Average number of reads in a 1kb sliding window divided by the total amount of reads) of each flag immuno-precipitation experiment was plotted as a function of the genomic position. Left panel a 100 kb region near *oriC* (positions 4.26 to 4.36 Mb) is represented. Right panel a 100 kb region around *dif* (positions 1.55 to 1.65 Mb) is represented. **B)** Scatter plot of the average GC content according to *parC-flag* IP/Input. 60 kb sliding windows were used for GC content and IP/Input. **C)** Average IP/Input values were normalized for GC content. **D)** Null model I, a Topo IV comet follows replication forks. Illustration of the Topo IV binding kinetics under null model I described in [S1 Text](#). The x axis in the plots represents the chromosome coordinates, going between 0 (*ori*) and L (*ter*). The y axis represents cell cycle time. The shaded areas are the positions of the Topo IV comets (also sketched as red lines on a circular representation of the chromosome), and the numbers represent the number of bound regions per replichore. **Left panel:** case of non-overlapping rounds. **Right panel:** case of overlapping rounds, in the case where the B period starts after the termination of replication within the same cell cycle. **E)** Topo IV binding bias, shown by the specific Input/IP values (each normalized by total reads). This bias is not compatible with a model where Topo IV binding follows replication and persists for a characteristic period of time (purple trace).

(PDF)

S4 Fig. Flow cytometry analysis of the synchronization experiment. Samples were fixed in ethanol at different time points: after 1h30 at 40°C (G1), 20 min after downshift to 30°C (S20), 40 min after downshift to 30°C (S40), 60 min after downshift to 30°C (G2) and in stationary phase.

(PDF)

S5 Fig. A) Genome browser magnifications illustrating common non specific signal observed over rRNA operon, IS sequences in the NorflIP and ChIP-seq experiments. ParE-Flag NorflIP is represented in purple, MatP-Flag ChIP-seq is represented in blue, Mock IP with a strain that did not contained Flag tagged proteins is represented in black. Genomic localization are the same as in [S2 Fig B\)](#) Southern blot cleavage assays performed in WT and *nalR* strains at the *insH* locus, ribosomal operon A and ribosomal operon B. TopoIV did not present any cleavage

in this regions confirming the artefactual nature of the corresponding signals in the NorflIP experiments. Arrows indicated the position on the corresponding bottom map. (PDF)

S6 Fig. A) Snapshots of the ChIP-seq and NorflIP experiments at the position 1.85 and 1.92 Mb. Topo IV binding to position 1.85 Mb was only revealed by the ChIP-seq experiment in the presence of formaldehyde. Topo IV cleavage at position 1.92 Mb was only revealed by the NorflIP experiment. NorflIP peaks present a characteristic shape illustrated on the 1.92Mb with a large 200 bp empty region in between the forward and reverse signal (arrow). **B)** Snapshot of the ChIP-seq and NorflIP experiments at the *dif* position. Topo IV binding (ChIP-seq) and cleavage (NorflIP) were detected at the *dif* position. **C)** Description of the NorflIP peak calling procedure. Forward and reverse reads from the Flag immunoprecipitation were smoothed over 200 bp, and then subtracted from each other. The *dif* and 1.9Mb signals observed on a 2kb window were used as a probe to test the entire genome with 100 bp sliding intervals. Pearson coefficient between the *dif* and 1.9 Mb signals and each interval were measured. Pearson coefficients above 0.72 were considered as putative Topo IV peaks. The initial list of Topo IV sites (S1 Table) corresponds to sites presenting a Pearson correlation above 0.72 in comparison with *dif* and 1.9Mb. IP/input ratio was measured. 172 peaks with Pearson coefficient above 0.72 and an IP/input ratio >2 were manually validated as Topo IV sites (S1 Table). **D)** Analysis of reads orientation in the NorflIP experiment at position 0.2Mb. Forward and reverse read peaks are about 200 bp large, a 100 nucleotides gap is observed in between the peaks. For the analysis of Topo IV cleavage site distribution we estimated that the center of the 100 nucleotides gap corresponds to the position of Topo IV cleavage. (PDF)

S7 Fig. A) Measure of the distance between two adjacent Topo IV cleavage sites in the *dif* region (A) and the region containing *oriC* and SNAP2 (B). For this analysis the 571 Topo IV cleavage sites observed in the 3 experiments were pooled. **C)** Distribution of the Topo IV cleavages inside genes and intergenic regions. The gene sizes were normalized to 1. **D)** RSAT analysis of the NorflIP peak calling results (<http://www.rsat.eu/>; Thomas-Chollier M, Defrance M, Medina-Rivera A, Sand O, Herrmann C, Thieffry D, van Helden J. (2011) RSAT 2011: regulatory sequence analysis tools. Nucleic Acids Res. 2011 Jul;39. Analysis of the dinucleotide bias in 172 manually validated NorflIP Topo IV cleavage sites. In average GC dinucleotides are enriched near the middle of the ChIP signal. **E)** GATC spacing around Topo IV peaks detected with the NorflIP experiment. Average distances between two consecutive GATC are measured around (+/- 20 GATC sites) 172 validated Topo IV cleavage sites and 172 random sequences. (PDF)

S8 Fig. A) Box plot of the distribution of distance between TopoIV cleavages and the closest highly expressed transcription unit (T.U.). For this analysis the 571 Topo IV cleavage sites observed in the 3 experiments were pooled. T.U. expression was determined by RNAseq. An arbitrary threshold was set to 500 reads, it corresponds to the 10% of the T.U. the most expressed. The distribution of a random set of cleavage sites was used as control. The two distributions are statistically different according to Anova test. The median distance is 8.5 kb for the TopoIV cleavage set and 12.3 kb for the random set. **B)** Genome browser zoom on the region 1.92 Mb were TopoIV cleavages were observed in a region with a number of highly expressed T.U. **C)** Distribution of 458 Topo IV cleavages (black) and random sites (grey) in between two consecutive highly expressed T. U. Topo IV cleavages are slightly more frequent near the TU than in the middle of the region. (PDF)

S9 Fig. **A)** Distribution of ParE-Flag 1 ChIP-seq enrichment in the region overlapping or not a H-NS binding site. **B)** Box plot of the distribution of GC% in the regions depleted for Topo IV (IP/input <0.6) or enriched for Topo IV (IP/input >1.2) or enriched for H-NS. **C)** Distribution of the GC% in 172 validated Topo IV cleavage sites as function of NorfIIP IP/input signal. **D)** Measure of the GC% in the 172 validated cleavage sites. GC % was measured in sliding windows of 20 bp and color coded.

(PDF)

S10 Fig. **A)** Analysis of the robustness of the Topo IV-XerC-*dif* complex in the presence of increasing amounts of XerD protein. EMSA were performed with prebound Topo IV and XerC on *dif* and subsequent addition of XerD for 10 minutes before loading on the gel. **B)** Analysis of Topo IV binding to negatively supercoiled plasmid by EMSA on agarose gel. Topo IV from 10, 50, 100, 200 nM was added to the pFC24 (*dif*) plasmid in the presence of XerCD (25 or 50 nM).

(PDF)

S11 Fig. **A)** Southern Blot analysis of Topo IV cleavage in the *nalR* strain at *dif* and an ectopic *dif* site located at 1.3Mb on the genomic map. **B)** Southern Blot analysis of Topo IV cleavage on a plasmid (pFC25) carrying the *dif* region (10 kb around *dif*) + *or-dif*

(PDF)

S1 Table. **Sheet 1)** Validated ChIP-seq sites. **Sheet 2)** NorfIIP sites observed in the ParC-Flag 1 NorfIIP, ParE-Flag NorfIIP and ParC-Flag 2 NorfIIP. **Sheet 3)** Common NorfIIP sites for the different experiments. **Sheet 4)** Manually Validated Topo IV cleavages.

(XLSX)

S1 Text. Model to test the correlation between TopoIV binding and the progression of replication. To test if ParC and ParE ChIP-seq biases were related to chromosome replication we constructed *in silico* models The result of this null model is that in all cases (overlapping or non-overlapping rounds) the observed mean occupancy should follow the dosage. Hence the occupancy gap observed in [S3E Fig](#) in the Ter region (when occupancy is normalized by dosage) has to be interpreted as a sign that this model does not apply, at least in this region.

(DOCX)

Acknowledgments

We thank D. Sherratt, K. Mariani, D. Grainger, J. Berger, P. Rousseau and F.X. Barre for the generous gift of proteins and plasmids. We thank Marie Franquin, Jorgelindo Da Veiga Moreira and Estelle Mignot for preliminary experiments. We thank Stephane Marcand for Southern blot tips. We thank Charlotte Cockram for careful reading of the manuscript. We thank Ivan Junier and Thibault Lepage for technical help with Circos. We thank the IMAGIF genomic facility for deep sequencing.

Author Contributions

Conceived and designed the experiments: HES LLC EL FC OE. Performed the experiments: HES LLC EL EV CP. Analyzed the data: HES LLC EL FC MCL OE. Wrote the paper: FC MCL OE. Conceived and analyzed models: MCL OE.

References

1. Khodursky A. B. et al. Analysis of topoisomerase function in bacterial replication fork movement: use of DNA microarrays. *Proc. Natl. Acad. Sci. U. S. A.* 97, 9419–9424 (2000). PMID: [10944214](#)

2. Peter B. J., Ullsperger C., Hiasa H., Marians K. J. & Cozzarelli N. R. The structure of supercoiled intermediates in DNA replication. *Cell* 94, 819–827 (1998). PMID: [9753328](#)
3. Martínez-Robles M. L. et al. Interplay of DNA supercoiling and catenation during the segregation of sister duplexes. *Nucleic Acids Res.* 37, 5126–5137 (2009). doi: [10.1093/nar/gkp530](#) PMID: [19553196](#)
4. Wang X., Montero Llopis P. & Rudner D. Z. Organization and segregation of bacterial chromosomes. *Nat. Rev. Genet.* 14, 191–203 (2013). doi: [10.1038/nrg3375](#) PMID: [23400100](#)
5. Zechiedrich E. L., Khodursky A. B. & Cozzarelli N. R. Topoisomerase IV, not gyrase, decatenates products of site-specific recombination in *Escherichia coli*. *Genes Dev.* 11, 2580–2592 (1997). PMID: [9334322](#)
6. Peng H. & Marians K. J. Decatenation activity of topoisomerase IV during oriC and pBR322 DNA replication in vitro. *Proc. Natl. Acad. Sci. U. S. A.* 90, 8571–8575 (1993). PMID: [8104339](#)
7. Charvin G., Bensimon D. & Croquette V. Single-molecule study of DNA unlinking by eukaryotic and prokaryotic type-II topoisomerases. *Proc. Natl. Acad. Sci. U. S. A.* 100, 9820–9825 (2003). PMID: [12902541](#)
8. Crisona N. J., Strick T. R., Bensimon D., Croquette V. & Cozzarelli N. R. Preferential relaxation of positively supercoiled DNA by *E. coli* topoisomerase IV in single-molecule and ensemble measurements. *Genes Dev.* 14, 2881–2892 (2000). PMID: [11090135](#)
9. Neuman K. C., Charvin G., Bensimon D. & Croquette V. Mechanisms of chiral discrimination by topoisomerase IV. *Proc. Natl. Acad. Sci. U. S. A.* 106, 6986–6991 (2009). doi: [10.1073/pnas.0900574106](#) PMID: [19359479](#)
10. Espéli O. & Boccard F. In vivo cleavage of *Escherichia coli* BIME-2 repeats by DNA gyrase: genetic characterization of the target and identification of the cut site. *Mol. Microbiol.* 26, 767–777 (1997). PMID: [9427406](#)
11. Hsu Y.-H., Chung M.-W. & Li T.-K. Distribution of gyrase and topoisomerase IV on bacterial nucleoid: implications for nucleoid organization. *Nucleic Acids Res.* 34, 3128–3138 (2006). PMID: [16757578](#)
12. Jeong K. S., Ahn J. & Khodursky A. B. Spatial patterns of transcriptional activity in the chromosome of *Escherichia coli*. *Genome Biol.* 5, R86 (2004). PMID: [15535862](#)
13. Wang X., Reyes-Lamothe R. & Sherratt D. J. Modulation of *Escherichia coli* sister chromosome cohesion by topoisomerase IV. *Genes Dev.* 22, 2426–2433 (2008). doi: [10.1101/gad.487508](#) PMID: [18765793](#)
14. Kato J. et al. New topoisomerase essential for chromosome segregation in *E. coli*. *Cell* 63, 393–404 (1990). PMID: [2170028](#)
15. Lesterlin C., Gigant E., Boccard F. & Espéli O. Sister chromatid interactions in bacteria revealed by a site-specific recombination assay. *EMBO J.* 31, 3468–3479 (2012). doi: [10.1038/emboj.2012.194](#) PMID: [22820946](#)
16. Joshi M. C. et al. Regulation of sister chromosome cohesion by the replication fork tracking protein SeqA. *PLoS Genet.* 9, e1003673 (2013). doi: [10.1371/journal.pgen.1003673](#) PMID: [23990792](#)
17. Vos S. M., Stewart N. K., Oakley M. G. & Berger J. M. Structural basis for the MukB-topoisomerase IV interaction and its functional implications in vivo. *EMBO J.* 32, 2950–2962 (2013). doi: [10.1038/emboj.2013.218](#) PMID: [24097060](#)
18. Hayama R., Bahng S., Karasu M. E. & Marians K. J. The MukB-ParC interaction affects the intramolecular, not intermolecular, activities of topoisomerase IV. *J. Biol. Chem.* 288, 7653–7661 (2013). doi: [10.1074/jbc.M112.418087](#) PMID: [23349462](#)
19. Li Y. et al. *Escherichia coli* condensin MukB stimulates topoisomerase IV activity by a direct physical interaction. *Proc. Natl. Acad. Sci. U. S. A.* 107, 18832–18837 (2010). doi: [10.1073/pnas.1008678107](#) PMID: [20921377](#)
20. Nicolas E. et al. The SMC complex MukBEF recruits topoisomerase IV to the origin of replication region in live *Escherichia coli*. *mBio* 5, e01001–01013 (2014). doi: [10.1128/mBio.01001-13](#) PMID: [24520061](#)
21. Kang S., Han J. S., Park J. H., Skarstad K. & Hwang D. S. SeqA protein stimulates the relaxing and decatenating activities of topoisomerase IV. *J. Biol. Chem.* 278, 48779–48785 (2003). PMID: [14512422](#)
22. Espeli O., Levine C., Hassing H. & Marians K. J. Temporal regulation of topoisomerase IV activity in *E. coli*. *Mol. Cell* 11, 189–201 (2003). PMID: [12535532](#)
23. Espeli O., Mercier R. & Boccard F. DNA dynamics vary according to macrodomain topography in the *E. coli* chromosome. *Mol. Microbiol.* 68, 1418–1427 (2008). doi: [10.1111/j.1365-2958.2008.06239.x](#) PMID: [18410497](#)
24. Li Y., Youngren B., Sergueev K. & Austin S. Segregation of the *Escherichia coli* chromosome terminus. *Mol. Microbiol.* 50, 825–834 (2003). PMID: [14617144](#)

25. Stouf M., Meile J.-C. & Cornet F. FtsK actively segregates sister chromosomes in *Escherichia coli*. *Proc. Natl. Acad. Sci. U. S. A.* 110, 11157–11162 (2013). doi: [10.1073/pnas.1304080110](https://doi.org/10.1073/pnas.1304080110) PMID: [23781109](https://pubmed.ncbi.nlm.nih.gov/23781109/)
26. Mercier R. et al. The MatP/matS site-specific system organizes the terminus region of the *E. coli* chromosome into a macrodomain. *Cell* 135, 475–485 (2008). doi: [10.1016/j.cell.2008.08.031](https://doi.org/10.1016/j.cell.2008.08.031) PMID: [18984159](https://pubmed.ncbi.nlm.nih.gov/18984159/)
27. Bigot S. & Marians K. J. DNA chirality-dependent stimulation of topoisomerase IV activity by the C-terminal AAA+ domain of FtsK. *Nucleic Acids Res.* 38, 3031–3040 (2010). doi: [10.1093/nar/gkp1243](https://doi.org/10.1093/nar/gkp1243) PMID: [20081205](https://pubmed.ncbi.nlm.nih.gov/20081205/)
28. Espeli O., Lee C. & Marians K. J. A physical and functional interaction between *Escherichia coli* FtsK and topoisomerase IV. *J. Biol. Chem.* 278, 44639–44644 (2003). PMID: [12939258](https://pubmed.ncbi.nlm.nih.gov/12939258/)
29. Hojgaard A., Szerlong H., Tabor C. & Kuempel P. Norfloxacin-induced DNA cleavage occurs at the dif resolvase locus in *Escherichia coli* and is the result of interaction with topoisomerase IV. *Mol. Microbiol.* 33, 1027–1036 (1999). PMID: [10476036](https://pubmed.ncbi.nlm.nih.gov/10476036/)
30. Dupaigne P. et al. Molecular basis for a protein-mediated DNA-bridging mechanism that functions in condensation of the *E. coli* chromosome. *Mol. Cell* 48, 560–571 (2012). doi: [10.1016/j.molcel.2012.09.009](https://doi.org/10.1016/j.molcel.2012.09.009) PMID: [23084832](https://pubmed.ncbi.nlm.nih.gov/23084832/)
31. Morais Cabral J. H. et al. Crystal structure of the breakage-reunion domain of DNA gyrase. *Nature* 388, 903–906 (1997). PMID: [9278055](https://pubmed.ncbi.nlm.nih.gov/9278055/)
32. Scolari V. F., Zarei M., Osella M. & Lagomarsino M. C. NuST: analysis of the interplay between nucleoid organization and gene expression. *Bioinforma. Oxf. Engl.* 28, 1643–1644 (2012).
33. Kahramanoglou C. et al. Direct and indirect effects of H-NS and Fis on global gene expression control in *Escherichia coli*. *Nucleic Acids Res.* 39, 2073–2091 (2011). doi: [10.1093/nar/gkq934](https://doi.org/10.1093/nar/gkq934) PMID: [21097887](https://pubmed.ncbi.nlm.nih.gov/21097887/)
34. Cui T. et al. *Escherichia coli* with a linear genome. *EMBO Rep.* 8, 181–187 (2007). PMID: [17218953](https://pubmed.ncbi.nlm.nih.gov/17218953/)
35. Vora T., Hottes A. K. & Tavazoie S. Protein occupancy landscape of a bacterial genome. *Mol. Cell* 35, 247–253 (2009). doi: [10.1016/j.molcel.2009.06.035](https://doi.org/10.1016/j.molcel.2009.06.035) PMID: [19647521](https://pubmed.ncbi.nlm.nih.gov/19647521/)
36. Zawadzki P. et al. The Localization and Action of Topoisomerase IV in *Escherichia coli* Chromosome Segregation Is Coordinated by the SMC Complex, MukBEF. *Cell Rep.* 13, 2587–2596 (2015). doi: [10.1016/j.celrep.2015.11.034](https://doi.org/10.1016/j.celrep.2015.11.034) PMID: [26686641](https://pubmed.ncbi.nlm.nih.gov/26686641/)
37. Deng S., Stein R. A. & Higgins N. P. Organization of supercoil domains and their reorganization by transcription. *Mol. Microbiol.* 57, 1511–1521 (2005). PMID: [16135220](https://pubmed.ncbi.nlm.nih.gov/16135220/)
38. Le T. B. K., Imakaev M. V., Mirny L. A. & Laub M. T. High-resolution mapping of the spatial organization of a bacterial chromosome. *Science* 342, 731–734 (2013). doi: [10.1126/science.1242059](https://doi.org/10.1126/science.1242059) PMID: [24158908](https://pubmed.ncbi.nlm.nih.gov/24158908/)
39. Waldminghaus T., Weigel C. & Skarstad K. Replication fork movement and methylation govern SeqA binding to the *Escherichia coli* chromosome. *Nucleic Acids Res.* 40, 5465–5476 (2012). doi: [10.1093/nar/gks187](https://doi.org/10.1093/nar/gks187) PMID: [22373925](https://pubmed.ncbi.nlm.nih.gov/22373925/)
40. Chintakayala K. et al. *E. coli* Fis protein insulates the *cbpA* gene from uncontrolled transcription. *PLoS Genet.* 9, e1003152 (2013). doi: [10.1371/journal.pgen.1003152](https://doi.org/10.1371/journal.pgen.1003152) PMID: [23341772](https://pubmed.ncbi.nlm.nih.gov/23341772/)
41. Berger M. et al. Coordination of genomic structure and transcription by the main bacterial nucleoid-associated protein HU. *EMBO Rep.* 11, 59–64 (2010). doi: [10.1038/embor.2009.232](https://doi.org/10.1038/embor.2009.232) PMID: [20010798](https://pubmed.ncbi.nlm.nih.gov/20010798/)
42. Datsenko K. A. & Wanner B. L. One-step inactivation of chromosomal genes in *Escherichia coli* K-12 using PCR products. *Proc. Natl. Acad. Sci. U. S. A.* 97, 6640–6645 (2000). PMID: [10829079](https://pubmed.ncbi.nlm.nih.gov/10829079/)
43. Krzywinski M. et al. Circos: An information aesthetic for comparative genomics. *Genome Res.* 19, 1639–1645 (2009). doi: [10.1101/gr.092759.109](https://doi.org/10.1101/gr.092759.109) PMID: [19541911](https://pubmed.ncbi.nlm.nih.gov/19541911/)
44. Chan P. P., Holmes A. D., Smith A. M., Tran D. & Lowe T. M. The UCSC Archaeal Genome Browser: 2012 update. *Nucleic Acids Res.* 40, D646–652 (2012). doi: [10.1093/nar/gkr990](https://doi.org/10.1093/nar/gkr990) PMID: [22080555](https://pubmed.ncbi.nlm.nih.gov/22080555/)

